

# **Metabolic mapping** of high-fit and low-fit individuals for human physiological health

**Joëlle J.E. Janssen**

# Propositions

1. Quantification of physiological health states in humans is key for monitoring the effect of lifestyle interventions. (*this thesis*)
2. PBMC metabolic function is a promising biomarker for human physiological health. (*this thesis*)
3. Statistically significant and scientifically meaningful are not the same.
4. Lifestyle medicine is the best basis of chronic disease management.
5. The future of food is personalized.
6. The only incentive to jog that counts are smiling joggers.
7. The most important function of taking 10.000 steps a day is clearing one's mind.

Propositions belonging to the thesis, entitled  
**“Metabolic mapping of high-fit and low-fit individuals  
for human physiological health”**

Joëlle J.E. Janssen  
Wageningen, 12 October 2022

## Thesis committee

### Promotors

Prof. Dr Jaap Keijer  
Professor of Human and Animal Physiology  
Wageningen University & Research

Prof. Dr Huub F.J. Savelkoul  
Professor of Cell Biology and Immunology  
Wageningen University & Research

### Co-promotors

Dr Vincent C.J. de Boer  
Assistant Professor, Human and Animal Physiology  
Wageningen University & Research

Prof. Dr R.J. Joost van Neerven  
Special Professor, Cell Biology and Immunology  
Wageningen University & Research

### Other members

Prof. Dr Renger F. Witkamp, Wageningen University & Research, the Netherlands  
Dr Jan van den Bossche, Amsterdam UMC, the Netherlands  
Dr Suzan Wopereis, TNO, Netherlands Organization for Applied Scientific Research, Zeist  
Prof. Dr Francisca Serra Vich, University of the Balearic Islands, Palma, Spain

This research was conducted under the auspices of the Graduate School Wageningen  
Institute of Animal Sciences.

# **Metabolic mapping**

of high-fit and low-fit individuals  
for human physiological health

Joëlle J. E. Janssen

## **Thesis**

submitted in fulfilment of the requirements for the degree of doctor

at Wageningen University

by the authority of the Rector Magnificus,

Prof. Dr A.P.J. Mol,

in the presence of the

Thesis Committee appointed by the Academic Board

to be defended in public

on Wednesday 12 October 2022

at 1.30 p.m. in the Omnia Auditorium

Joëlle J.E. Janssen

**Metabolic mapping of high-fit and low-fit individuals for human physiological health**

284 pages.

PhD thesis, Wageningen University, Wageningen, the Netherlands (2022)

With references, with summary in English

**ISBN** 978-94-6447-305-6

**DOI** <https://doi.org/10.18174/573397>

## Table of contents

<b>Chapter 1</b>	General Introduction	7
<b>Chapter 2</b>	Muscle mitochondrial capacity in high- and low-fitness females using near-infrared spectroscopy	31
<b>Chapter 3</b>	Novel standardized method for extracellular flux analysis of oxidative and glycolytic metabolism in peripheral blood mononuclear cells	49
<b>Chapter 4</b>	Extracellular flux analyses reveal differences in mitochondrial PBMC metabolism between high-fit and low-fit females	83
<b>Chapter 5</b>	Single and joined behaviour of circulating biomarkers in high-fit and low-fit healthy females	113
<b>Chapter 6</b>	Mito-nuclear communication and its regulation by B-vitamins	163
<b>Chapter 7</b>	The effect of a single bout of exercise on vitamin B2 status is not different between high-fit and low-fit females	213
<b>Chapter 8</b>	General Discussion	233
	Summary of main findings	267
	Acknowledgements	271
	About the author	279
	- Curriculum vitae	279
	- List of publications	281
	- Education and training activities	283



# 1

## General Introduction





## Human physiological health

The World Health Organization (WHO) defines health as ‘a state of complete, physical, mental, and social well-being and not merely the absence of disease or infirmity’, a definition that has not been changed since it was adopted in 1948 (1). While this definition covers health, it is also a definition that is impractical, especially because it does not define the word *complete* and considers only one state of health. On the other hand, given the fact that there are numerous disease-inducing pathways and conditions, a negative definition of health as ‘the nonexistence of any kind of pathology’ is also impractical (2). Health can also be addressed in a positive and describing fashion that considers physical and mental fitness coupled to normal physiological function (3). This has the advantage of stressing that health is more than a physiological state and accurately includes mental and societal aspects, yet this broadness makes it also difficult to address health and quantify health status. For this reason, specialists from various fields often address different aspects of health and focus on disease, i.e. the absence of health. These specialists generally operate from the perspective of specific disorders: physicians treat physiological disorders, i.e., diseases, psychologists and psychiatrists treat mental disorders, and a wide range of professionals deal with social problems. This makes sense, as different aspects of health are important for wellbeing and patient treatment, but for the development and improvement of scientific concepts and tools it is necessary to reduce complexity, for example by focusing on one aspect of health. In this thesis, I therefore focus on metabolism as a key aspect of human physiological health, aiming to develop concepts and tools that will allow for defining metabolic health and offer ways to improve this. I will go beyond the negative definition of health as absence of disease, but rather consider health as a continuum from a healthy state to a disease state, including different states of health and the transition from health to disease. For a difference in health states one can consider healthy individuals of high and low levels physical activity, since high physical activity levels are associated improved health outcomes, such as improved immune system functioning (4), and reduced risk for development of later life disease (5,6).

Human physiological health is based on a complex network of interactions between molecules, mechanisms, pathways, and processes that result in a crosstalk between cells, tissues, organs, and systems (2). Biochemical and physiological mechanisms act as a buffering system to maintain homeostasis during continuously external perturbations, such as food intake, exercise, infections, or cold temperature (3). A healthy organism can maintain physiological homeostasis during such changing circumstances, which means that it can mount a protective response, reduce the

potential for harm, and restore its equilibrium when confronted with physiological stress (3). In case this coping strategy is not successful, the organism develops physiological damage, which results in reduced and later impaired physiological health, that could ultimately lead to disease development (2,3). On the other hand, reinforcement of these intrinsic, self-regulating mechanisms increases physiological resilience and robustness, and contributes to health improvement. Quantification of these dynamic states of human physiology is therefore needed to measure and monitor health improvements. In this thesis I will define and analyse several physiological parameters that are related to healthy metabolic physiologies, which will contribute to a better understanding of physiological health and transition from health to disease states.

## Assessment of human physiological health

Health optimization strategies aim to achieve or improve health. However, biomarkers that assess 'health' are poorly applicable to measure health improvements and are rather exclusively suitable to establish an unhealthy state. The levels of classical clinical diagnostic biomarkers such as levels of blood glucose, triglycerides, c-reactive protein (CRP), and interleukin 6 (IL6) are clinically used as indicators of an unhealthy state, with levels above a certain threshold indicative of an increased risk for cardiometabolic or inflammation-related disease (7–9). From this cut-off level upward, these biomarkers can reflect ranges of disease progression. However, the transition from a healthy to less healthy state is mostly not considered or not even studied. In summary, these classical clinical diagnostic biomarkers have been studied extensively for detecting differences between health and disease, but are very limited in detecting differences between optimal health, health, and the different steps in the trajectory towards disease, i.e. they are not yet suited to monitor the continuum of health to disease. Since differences in health states may be distinct and are likely more subtle than differences between health and disease, biomarkers that measure health states could differ and require another level of sensitivity than disease biomarkers (10–12). Health biomarkers (or health state biomarkers) should thus allow the detection of relevant physiological differences between healthy individuals. Such physiological differences may not come to the surface by detecting individual levels of classical clinical diagnostic biomarkers, which are mostly circulating bioactive molecules with a short lifetime and acute signaling roles. Instead, they may potentially be encapsulated in functional parameters in cells or tissues, which have a longer lifespan and may imprint these subtle differences. In addition, linking individual levels of circulating bioactive compounds to underlying physiological processes and studying these processes

relative to each other may also give more insight in factors that contribute to physiological health. In theory, classical clinical diagnostic biomarkers could be imagined as ‘the tip of the iceberg’, whereas the relevant health differences are most likely below the surface, and can be revealed by diving deeper into dynamic physiological processes on the tissue and cellular level (Figure 1). Thus, to monitor the progression from health to optimized health conditions in humans and vice versa, biomarkers that respond to physiological differences in healthy individuals are needed. Such biomarkers are good candidates to act as a future health biomarker that can be implemented to monitor health promotion strategies.

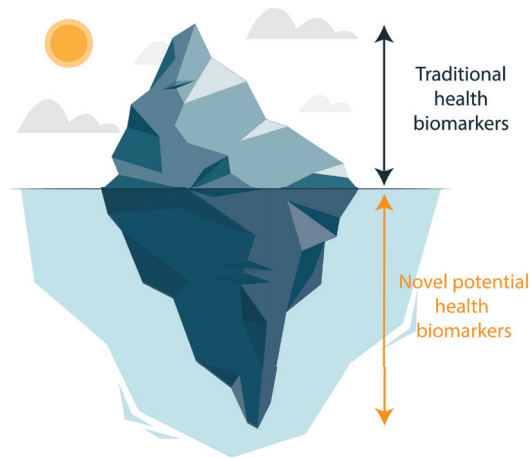


Figure 1: Graphical illustration of the concept of physiological health assessment that is studied in this thesis.

## Metabolic parameters as potential health biomarkers

Metabolism is a fundamental process in all living organisms and is required to perform all physiological functions and maintain life. It manifests as a complex metabolic network that includes metabolic pathways, which are complex sequences of controlled biochemical reactions involving enzymes, substrates, products, and cofactors, which generate energy and supply building blocks (13). Energy is generated via catabolism of macronutrients (carbohydrates, lipids, and proteins) and consumed during anabolic reactions to promote cellular functions, such as muscle contraction (14), nerve impulse propagation (15), ion signaling (16), and synthesis of biochemical compounds (17). At the cellular level, metabolic reactions

use energy in the form of adenosine triphosphate (ATP). ATP is the energy currency of a cell and provides readily releasable energy via hydrolysis to adenosine diphosphate (ADP) and inorganic phosphate (Pi). ATP is mostly synthesized via cytosolic glycolysis coupled to mitochondrial oxidative phosphorylation (OXPHOS) (Figure 2). During cellular respiration, glucose is catabolized by glycolysis into pyruvate simultaneously generating 2 moles of ATP per mole of glucose. Pyruvate is then shuttled into the mitochondria, generating a further 30 moles of ATP per mole of glucose. In more detail, pyruvate is converted to acetyl-coenzyme A (CoA), which enters the tricarboxylic acid (TCA) cycle and undergoes complete oxidation to carbon dioxide ( $\text{CO}_2$ ), yielding reduced nicotinamide adenine dinucleotide (NADH) and hydroquinone flavin adenine dinucleotide ( $\text{FADH}_2$ ). NADH and  $\text{FADH}_2$  feed the electron transport complexes of the mitochondrial inner membrane, principally consisting of four multi-protein electron transport complexes (complex I - IV, CI – CIV) that compose the electron transport system (ETS). Together with  $\text{F}_1\text{F}_0$ -ATP synthase (complex V, CV), the ETS forms the OXPHOS system. The function of the ETS is to generate an electrochemical gradient over the mitochondrial inner membrane by pumping protons from the mitochondrial matrix to the intermembrane space, which is needed to generate ATP via CV. To perform this function, the ETS takes up electrons from NADH at CI or from succinate, with  $\text{FADH}_2$  as an intermediate, at CII, which are transferred to CIII via ubiquinone. Cytochrome C transfers the electrons from CIII to CIV where they react with oxygen to form water. Oxygen is thus the final electron acceptor, and the use of oxygen ( $\text{O}_2$ ) by the OXPHOS system can be quantified as a proxy for mitochondrial ATP production (18). During certain conditions, including limited or absent oxygen availability and specific cellular conditions, such as rapid cell proliferation, cytosolic ATP can also be produced via glycolysis alone. Glycolytic metabolism produces much less ATP (2 ATP versus 32 ATP per glucose for oxidative metabolism) and provides lactate as energy containing 'waste product'. Lactate is then transported out of the cell, resulting in extracellular acidification. Energy metabolism thus provides several readily measurable metabolites ( $\text{CO}_2$ ,  $\text{O}_2$  and acid efflux) that can be used for functional characterization of cells in the context of health physiology.

## Quantification of cellular energy metabolism

Measurement of cellular oxygen consumption as a proxy for mitochondrial respiration is well established (19,20). Classically, Clark-type electrodes have been used to measure oxygen consumption in real-time (19,20). Development of the Oroboros respirometric system improved the sensitivity and precision of oxygen consumption rate measurements, and enabled the sequential addition of

mitochondrial substrates, modulators, and inhibitors to probe multiple parameters of respiration (18). More recently, it has become possible to measure oxygen consumption rate in a multi-well format using extracellular flux (XF) analysis, which strongly increases the number of samples and conditions to be analyzed (21). XF analysis measures the oxygen consumption rate (OCR) and extracellular acidification rate (ECAR) as a proxy for mitochondrial and glycolytic ATP production, respectively (21) (**Figure 2**). OCR and ECAR are simultaneously measured in culture plates using fluorescent sensors in a Seahorse XF analyzer (21). The multi-well

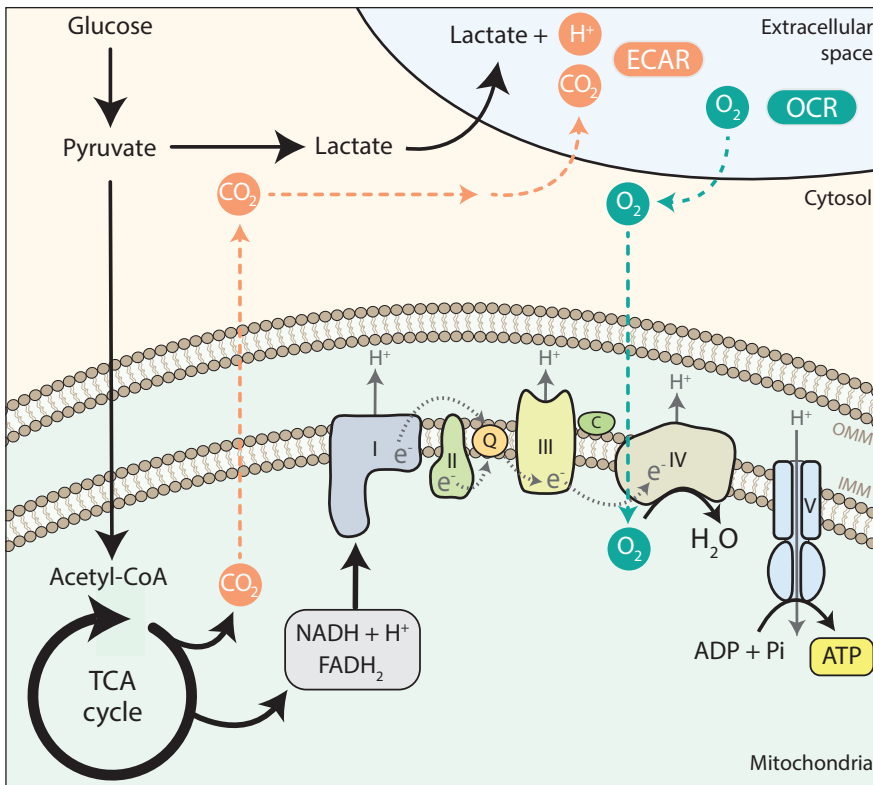


**Figure 2: Schematic overview of cellular energy metabolism and quantification of mitochondrial respiration and glycolysis.** Abbreviations: TCA cycle = tricarboxylic acid cycle, NADH = reduced form of nicotinamide adenine dinucleotide (NAD), FADH<sub>2</sub> = hydroquinone form flavin adenine dinucleotide (FAD), Q = coenzyme Q, C = cytochrome C, CO<sub>2</sub> = carbon dioxide, O<sub>2</sub> = oxygen, H<sub>2</sub>O = water, ADP = adenosine diphosphate, Pi = inorganic phosphate, ATP = adenosine triphosphate, OMM = outer mitochondrial membrane, IMM = inner mitochondrial membrane, OCR = oxygen consumption rate, ECAR = extracellular acidification rate.

format allows the addition of multiple injections sequentially or in parallel to probe multiple parameters of mitochondrial respiration and glycolysis, which enables the assessment of metabolic flexibility and capacity on top of steady-state basal metabolic rate, metabolic parameters that could be useful for the characterization of human physiological health. Thus, the ability to concomitantly measure OCR and ECAR in a high-throughput manner has enabled a technology to generate a comprehensive overview of cellular bioenergetics and identify changes that are associated with alterations in cell physiology or pathophysiology.

## Beyond energy metabolism: the role of mitochondria in biosynthesis and cellular signaling

Mitochondria are dynamic cellular organelles central to cellular metabolism. They are not only critical for sustainable cellular energy metabolism, but also function in other cellular processes, including macromolecule biosynthesis and intracellular signaling (22). Mitochondria generate metabolic building blocks that are used for the biosynthesis of macromolecules, such as DNA, RNA, lipids, proteins, heme, and iron-sulfur (FeS) clusters (22). Furthermore, they play a role in redox signaling by compartmentalization of redox equivalents (22) and by generating, sequestering, and interconverting reactive oxygen species (ROS) (23). ROS are highly reactive biomolecules such as superoxide ( $O_2^-$ ) and hydrogen peroxide ( $H_2O_2$ ) that can react with DNA, lipids, and proteins. They can be generated in the mitochondrial ETS, during mitochondrial substrate oxidation, or via the activity of enzymes such as nicotinamide adenine dinucleotide phosphate (NADPH) oxidase in the cytosol (23). While some ROS are highly damaging, such as  $O_2^-$ , others also have the properties of a signaling molecule, such as  $H_2O_2$ .  $H_2O_2$  at physiological levels can serve as an alarm to notify the cell that the extracellular environment is changing, and can trigger redox signaling events, such as cell proliferation, cell differentiation, cell repair, and immune signaling (24). Cellular homeostasis is maintained through antioxidant systems that detoxify ROS. Usually, mitochondrial generated  $O_2^-$  is rapidly converted by superoxide dismutases to  $H_2O_2$ . Various antioxidant systems then play a role in subsequent  $H_2O_2$  homeostasis, including the glutathione (GSH) antioxidant system (24). GSH can react with  $H_2O_2$  to form glutathione disulfide (GSSG) and water ( $H_2O$ ), protecting the cell from oxidative damage. The balance between ROS production and detoxification determines redox homeostasis (23). Antioxidant systems require NADPH for regeneration, and the ratio between NADPH and  $NADP^+$  determines the cellular redox state (22). In addition to regulating redox signaling, mitochondria orchestrate other cellular signaling routes. They can initiate cell death by releasing mitochondrial

cytochrome C (25) and can instruct nuclear signaling routes involved in cell death decisions and immune signaling (26). Considering the multidisciplinary role of mitochondria in cellular metabolism, bioenergetics, biosynthesis, and intracellular signaling, it is of great interest to study mitochondrial function as a biomarker for physiological health.

## The link between mitochondrial function and aerobic fitness

Regular physical activity, especially regular aerobic exercise, is associated with an increase in mitochondrial mass, function, and quality in skeletal muscles (27,28). Together with other physiological adaptations, such as an increase in stroke volume and increased vascularization and oxygen extraction in skeletal muscle, these factors contribute to increased aerobic fitness (29). Aerobic fitness refers to the capacity of the circulatory and respiratory systems to take up oxygen from the atmosphere and supply it to skeletal muscle mitochondria for ATP production (30). It is measured as whole-body maximal or peak oxygen consumption ( $\dot{V}O_{2\text{max}}$  or  $\dot{V}O_{2\text{peak}}$ ) that is assessed using an incremental exercise test (31). Since aerobic fitness quantifies the functional capacity of an individual and is directly related to the integrated function of numerous physiological systems, aerobic fitness is considered a reflection of total body health (29). Studying the link between mitochondrial function parameters and levels of aerobic fitness in healthy individuals is therefore of great relevance to better characterize human physiological health. A classical method for mitochondrial function analysis is *ex vivo* respirometry in isolated skeletal muscle fibers (32). While the use of permeabilized skeletal muscle fibers has improved the sensitivity and robustness of respirometry, the need for fresh tissue, the limited amount of available tissue, the heterogeneity of skeletal muscle tissue (33,34), the requirement for technical expertise, and the invasiveness of tissue sampling pose major application limitations. Therefore, less invasive methods that can routinely and robustly assess *in vivo* or *ex vivo* mitochondrial function over time are needed.

## Non-invasive assessment of *in vivo* skeletal muscle mitochondrial capacity using NIRS

A technique that can assess mitochondrial function non-invasively is based on near-infrared (NIR) spectroscopy (NIRS). It can be used to indirectly quantify *in vivo* skeletal muscle mitochondrial capacity (32,35,36). NIRS makes use of the difference in light absorption of oxygenated and deoxygenated haemoglobin ( $O_2Hb$  and  $HHb$ ) and myoglobin ( $O_2Mb$  and  $HMb$ ), respectively the oxygen-binding molecules in blood and myofibrils, in the NIR region to quantify oxygen use (37). In combination with arterial occlusions, NIRS allows for the measurement of muscle oxygen consumption ( $m\dot{V}O_2$ ). Upon blood flow occlusion, there is no supply of fresh, oxygenated blood and the change from  $O_2Hb$  and  $O_2Mb$  to the deoxygenated forms reflects oxygen use under the NIRS probe (38,39) (**Figure 3A**). It is assumed that  $m\dot{V}O_2$  reflects oxygen consumption in mitochondria during aerobic ATP production, hence the rate of  $m\dot{V}O_2$  recovery is used as a proxy for skeletal muscle mitochondrial capacity (40). Using NIRS, it was previously shown that skeletal muscle mitochondrial capacity differed between endurance-trained athletes and untrained, inactive individuals with a large difference in  $\dot{V}O_{2peak}$  (41), yet it is incompletely understood whether NIRS can also detect possible smaller differences in mitochondrial capacity, for example between recreationally active healthy individuals with a smaller difference in aerobic fitness level. Recently, our group showed that NIRS can detect differences in skeletal muscle mitochondrial capacity between recreationally active males with high and low  $\dot{V}O_{2peak}$  (42).

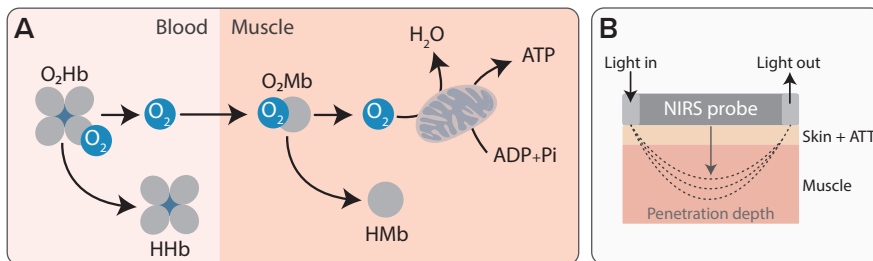


**Figure 3: Schematic representation of the NIRS method.** (A) Oxygen consumption in skeletal muscle mitochondria during blood flow occlusions is used as a reflection for skeletal muscle mitochondrial capacity. (B) Graphical illustration of the penetration depth of the NIRS signal. Abbreviations:  $O_2Hb$  = oxygenated haemoglobin,  $HHb$  = deoxygenated haemoglobin,  $O_2Mb$  = oxygenated myoglobin,  $HMb$  = deoxygenated myoglobin, ADP = adenosine diphosphate, Pi = inorganic phosphate, ATP = adenosine triphosphate, ATT = adipose tissue thickness.

However, it is not known whether these results can be extrapolated to females. It is technically more challenging to use NIRS for determination of skeletal muscle mitochondrial capacity in females, because females typically show higher subcutaneous adipose tissue thickness (ATT) than males (43), which limits the penetration of the NIRS signal into skeletal muscle ([Figure 3B](#)). Indeed, the amount of NIRS signal recovered from skeletal muscle decreases with increased adiposity and subcutaneous ATT (44,45). Although studies in mixed populations have confirmed the application of NIRS in both sexes (32,41,46,47), it is currently not known whether NIRS can detect physiologically relevant differences in skeletal muscle mitochondrial capacity in an exclusively female population with different levels of aerobic fitness, i.e. in the normal physiological range.

## Non-invasive assessment of *ex vivo* PBMC mitochondrial metabolism

In addition to measuring mitochondrial capacity *in vivo* using NIRS, mitochondrial function can be analyzed *ex vivo* using Seahorse XF analysis. Measurement of mitochondrial respiration is an indicator of mitochondrial function, since it reflects the activity of the ETS complexes and ATP synthase and responds to changes in the inner mitochondrial membrane potential, which occurs during alterations in cellular physiology. Seahorse XF analysis can be applied to peripheral blood mononuclear cells (PBMCs). PBMCs are white blood cells that have a single round nucleus and mainly include T- and B-lymphocytes, monocytes, dendritic cells, and natural killer (NK) cells (48,49). The potential of mitochondrial PBMC function as a biomarker has emerged during the past decades (50–56), especially because PBMCs are a readily accessible source of fresh cells from individuals that can be sampled with relative ease, low invasiveness, high viability and over repeated periods in time (57). A further advantage of PBMCs is their acute metabolic response upon immunological stimulation (58), which enables the assessment of metabolic flexibility on top of steady-state metabolic analysis and the determination of metabolic capacity. Using Seahorse XF analysis, several studies have shown defects in mitochondrial PBMC function in patients with cardiovascular disease (54), neurodegenerative disease (55,56), and recently also in patients with coronavirus disease 19 (COVID 19) (52), which supports their potential for monitoring disease progression. However, to evaluate the potential of PBMCs as a health biomarker, studies that compare mitochondrial PBMC function between healthy individuals with a physiologically relevant difference are needed. Yet, these studies are scarce compared to the studies in individuals with disease. Furthermore, to implement PBMC mitochondrial function analysis as a robust

health biomarker, several obstacles must be tackled, that have been previously either been overlooked or only been taken along sparsely. First, normalization of Seahorse XF assay data is critical for accurate and consistent interpretation and comparison of PBMC metabolic analyses. Yet, the current normalization methods are poorly applicable to non-adherent and dynamic cells such as PBMCs. Therefore, a normalization method that reliably measures, compares, and extrapolates PBMC XF assay data must be developed and integrated in the Seahorse XF assay workflow. Second, PBMCs are pooled cells that are not only immunologically, but also metabolically distinct (59,60). Differences or changes in PBMC composition could thus affect the interpretation of PBMC metabolic outcomes, but most studies do not consider the impact of PBMC composition on metabolic PBMC outcomes. For example, recent evidence in healthy individuals has suggested that metabolic PBMC profiles can respond to regular and acute aerobic exercise (61,62). Yet, it is not clear whether these metabolic alterations in PBMCs are primarily related to alterations in cellular metabolism per se, or whether these responses reflect changes in PBMC composition since acute exercise has also been associated with a change in PBMC subsets (63,64). Therefore, to establish the influence of PBMC composition and long- and short-term exercise on PBMC metabolic outcomes, both PBMC metabolism and PBMC composition should be measured at baseline and after a single exercise session in individuals with different regular aerobic exercise activities. This information is essential to evaluate the potential of PBMC metabolism as a health biomarker. Furthermore, a study in female individuals is of particular relevance, since PBMC metabolism was found to differ between males and females (65) and previous studies have been mainly performed in males (66,67).

## Circulating biomarkers in relation to physiological processes to monitor health

In addition to studying metabolic responses at the tissue and cellular level for human physiological health, another opportunity is to explore whether classical clinical diagnostic biomarkers that are mainly used as disease risk indexes could also act as biomarkers that reflect health. Most of these biomarkers have not been examined in healthy individuals for discriminative potential between different health states. Likely, these biomarkers will have difficulty capturing early deviations in the trajectory from a healthy towards an more unhealthy state unless the individual is acutely challenged (68). This is due to the fact that a functional, even suboptimal, homeostasis tends to maintain the levels of circulating bioactive molecules (i.e., hormones, cytokines, metabolites) within a certain range of values

(69). This is particularly true for individual biomarkers. However, the sensitivity may increase if multiple biomarkers are measured simultaneously and their joined responses are evaluated. Measuring multiple biomarkers was a major hurdle some time ago, but the advent of multi-parameter 'omics' approaches now permits simultaneous analysis of many parameters in small blood volumes (70,71). A further improvement may be obtained by physiological grouping of biomarkers in overarching physiological processes that are considered to play a role in determining health state and in disease development. Three major overarching physiological processes are metabolism, inflammation, and oxidative stress (10). By analysing biomarkers grouped in the context of these physiological processes, additional sensitivity and resolution may be obtained. In other words, when considered separately, small changes in the levels of these biomarkers may not stand out as relevant but changes may become more relevant when considering multiple biomarkers that are linked to the same physiological process. Furthermore, this approach enables examination of the behaviour of these biomarkers relative to each other. In this way, small changes in the overall homeostasis that contribute to early deviations from an optimal health state might be captured and could be of relevance to monitor the health to disease trajectory. While this approach is attractive, studying the individual and grouped behaviour of multiple biomarkers in the context of specific physiological processes has hardly been examined in individuals that differ in aerobic fitness level, and it has especially not been studied which biomarkers respond in a corresponding manner. Since most of these biomarkers have a short lifetime and acute signaling function, their levels change in response to a physiological perturbation such as a single exercise session (4,72,73). Importantly, this exercise-induced response can differ between high physically active (regularly exercising) and sedentary individuals, due to the adaptations in many physiological systems in response to regular exercise (73). However, it is not completely clear how exercise performance on the day prior to blood sampling impacts the levels of many of these biomarkers, and whether this impact depends on an individual's aerobic fitness level, while this information is important to evaluate whether standardization of exercise activities prior to blood sampling is required in such studies.

## Regulation of cellular energy metabolism by B-vitamins

The B-vitamins are essential for maintaining healthy physiology (74). The B-vitamins, thiamine (B1), riboflavin (B2), niacin (B3), pantothenate (B5), pyridoxine (B6), biotine (B8/B7), folate (B11/B9) and cobalamin (B12) are structurally unrelated, but are grouped because of their primary function in energy metabolism, with interrelated

and principal roles in mitochondrial and one-carbon metabolism (75,76). They support the biosynthesis of metabolic intermediates that are used for DNA/RNA synthesis, FeS cluster generation, and redox signaling, and they regulate the activity of mitochondrial enzymes to drive ATP generation (75,76). Because B-vitamins are important for energy generation, B-vitamin deficiencies are always associated with various types of fatigue. Although it is well recognized that severe B-vitamin deficiency promotes disease, milder marginal deficiencies have also been shown to impair physiological functions (77). For example, a marginal vitamin B1 (thiamine) deficiency has been linked to fatigue, low appetite, and sleep disturbance (78). Maintaining a balanced cellular pool of B-vitamins is thus important to support metabolism and health. Since B-vitamins are essential nutrients that must be derived from dietary intake, sufficient consumption of foods with B-vitamins is recommended (79). While sufficient intake is important, lifestyle activities may affect the need and use of B-vitamins. For example, it has been suggested that exercise performance could affect the need for B-vitamins in several metabolic reactions, particularly in the mitochondria (80). Exercise increases cellular energy demands to enable skeletal muscle contractions and relaxations, putting a high demand on mitochondrial reactions that are supported by B-vitamins. At the same time, exercise generates ROS as a by-product, which enhances antioxidant defense systems, including those that rely on B-vitamin-derived cofactors (81–83). B-vitamin status may thus change in individuals that perform regular exercise (80), but this is incompletely understood. Of note, mitochondria do not operate in isolation, but active communication exists between mitochondria-derived metabolic signals and the nucleus (26). In view of the essential role of B-vitamins in energy metabolism and mitochondrial function, they also likely play a role in this communication, but an overview is currently lacking.

## The link between vitamin B2 status and exercise

Vitamin B2 (riboflavin) is of special interest in metabolism since this B-vitamin is an essential gatekeeper of mitochondrial ATP production and redox balance. Vitamin B2 is the precursor for the electron carriers flavin mononucleotide (FMN) and flavin adenine dinucleotide (FAD), which are both essential mitochondrial co-enzymes of OXPHOS CI and CII, respectively (84,85). In addition, FAD is an essential cofactor for the antioxidant enzyme glutathione reductase (GR), which catalyzes the conversion of GSSG (oxidized glutathione) to GSH (reduced glutathione) with concomitant reduction of NADPH to NADP<sup>+</sup> (Figure 4) (84,86). The subsequent catalytic activity of the enzyme glutathione peroxidase (GPx) regenerates GSSG from GSH via oxidation of a selenium group and the formation

of  $\text{H}_2\text{O}$  from  $\text{H}_2\text{O}_2$ , thereby clearing ROS and maintaining redox homeostasis (82). In exercise studies, systemic vitamin B2 status is commonly assessed by the erythrocyte glutathione reductase activation coefficient (EGRAC) biomarker (80,87). This coefficient represents the ratio between erythrocyte GR (EGR) activity in the presence and absence of its cofactor FAD (88,89). Higher EGR activity in the presence of FAD compared to the activity in its absence reflects incomplete occupancy of EGR by FAD *in vivo*, resulting in a lower vitamin B2 status that is reflected by a higher EGRAC. Since aerobic exercise puts a high demand on metabolic processes that are essentially dependent on the vitamin B2-derived cofactors FMN and FAD, especially athletes and recreationally active, high aerobically fit individuals, are thought to benefit from an optimal vitamin B2 status (80). However, studies that investigate the link between vitamin B2 status and aerobic fitness level are contradictory (90–94), potentially because the long- and short-term exercise effects on vitamin B2 status could differ (94–96), but this has not yet been investigated. Since these outcomes could influence future dietary recommendations for exercising individuals, additional insight in the link between vitamin B2 status, aerobic fitness level, and exercise is necessary.

## Better understanding of physiological health in females

Males and females differ in body composition (97) and metabolic health (98). Females have proportionally higher levels of adipose tissue than males (97). Males accumulate adipose tissue around the abdomen, while females deposit adipose tissue around the hips and thighs (97). Sex differences have been shown to affect health outcomes (99) and disease risk and development (43,100), but also the response to drug treatment (101) and exercise (102). For example, because the

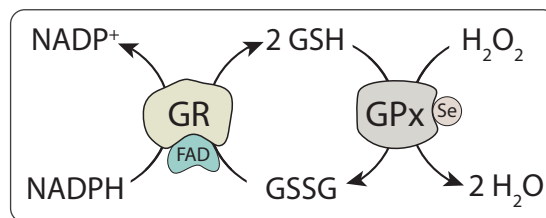


**Figure 4: The glutathione cycle.** NADPH = reduced form of nicotinamide adenine dinucleotide phosphate (NADP<sup>+</sup>), GR = glutathione reductase, GPx = glutathione peroxidase, FAD = flavin adenine dinucleotide, GSSG = oxidized glutathione, GSH = reduced glutathione,  $\text{H}_2\text{O}_2$  = hydrogen peroxide, Se = selenium.

distribution of adipose tissue is a stronger determinant of cardiovascular disease development than total adipose tissue, males have a higher cardiometabolic disease risk than females (103). However, most research has been conducted in males only, and there is a large bias for research in males in a variety of research areas (104,105). Females are underrepresented, but are important to study because they represent 50% of the human population. Therefore, the research in this thesis will be conducted in females.

## Aims and outline of this thesis

The overall aim of this thesis is to study how metabolic measurements in healthy females with high and low levels of aerobic fitness can contribute to a better understanding of human physiological health. This may allow for the quantification of physiological health states and evaluation of the trajectory from health to disease, which may translate into strategies to improve health and prevent disease.

Specific aims of this thesis are:

- 1) To study the link between skeletal muscle mitochondrial capacity and aerobic fitness level.
- 2) To evaluate the potential of PBMC metabolism as a health biomarker, by:
  - a. Developing a normalization method for PBMC metabolic XF analysis.
  - b. Examining the link between PBMC metabolism and aerobic fitness level.
- 3) To explore the relationship between systemic metabolism biomarkers and aerobic fitness level.
- 4) To describe the state-of-the-art on the role of B-vitamins in mitochondrial metabolism and the communication with the nucleus.
- 5) To study the link between vitamin B2 status parameters and aerobic fitness level.

The aim of **Chapter 2** of this thesis was to measure mitochondrial capacity in skeletal muscle using NIRS in high aerobically fit (high-fit) and low aerobically fit (low-fit) females and to study whether NIRS can detect a physiologically relevant difference in a recreationally active population of healthy females. Females show increased adiposity as compared to males, which could hamper the penetration of NIR-light in the muscle and makes NIRS measurements in females more difficult. **Chapter 3** aimed to develop, optimize, and validate a normalization method for XF metabolic analysis of PBMCs. Correct normalization of XF assay data is crucial to reliably measure, compare, and extrapolate XF assay results, but the currently used normalization methods are poorly applicable to PBMCs. This new normalization

method was integrated into the Seahorse XF experimental set-up, providing a standardized workflow for XF analysis of human PBMCs. In [Chapter 4](#), PBMC metabolism and PBMC composition were measured using our new standardized workflow in high-fit and low-fit females at baseline and after a recent bout of exercise. This allowed us to investigate the impact of longer- and short-term exercise on PBMC metabolism and PBMC composition, and to examine the influence of PBMC composition on the interpretation of PBMC metabolic outcomes. These findings improve our understanding on the use of PBMC metabolism as a biomarker in healthy individuals and contribute to the evaluation of its potential as a health biomarker. In [Chapter 5](#), the aim was to measure the levels of multiple systemic biomarkers in serum and plasma of high-fit and low-fit females in a steady-state and after a recent bout of exercise, and analyze the individual and joined responses of these biomarkers in the context of specific physiological processes. These biomarkers have been extensively studied in the context of disease, but it is poorly understood how these biomarkers behave in healthy individuals with a physiological difference in aerobic fitness, and how these biomarkers respond relative to each other. Furthermore, linking each biomarker to a physiological health process may result in functional biomarker categories that could prove to be relevant for characterization of human physiological health. In [Chapter 6](#), I described the role of B-vitamins on mitochondrial metabolite-mediated nuclear signaling routes, also called mito-nuclear communication pathways. These pathways are important in the regulation of (patho)physiology, but an overview of the role of B-vitamins in these signaling routes is currently lacking. As vitamin B2 status may change in individuals that perform regular aerobic exercise, and it is incompletely understood whether these effects are affected by a single exercise session, the aim of [Chapter 7](#) was to measure vitamin B2 status in high-fit and low-fit females and to examine whether parameters of vitamin B2 status change in response to a recent bout of exercise. In the final chapter of this thesis, [Chapter 8](#), I discuss the main findings of this thesis, the implications, and the directions for future research.

## References

1. WHO. Preamble to the Constitution of the World Health Organization as adopted by the International Health Conference. Official Records of the World Health Organization. New York, New York, USA; 1948. (Official Records of the World Health Organization, no. 2, p. 100).
2. Ayres JS. The Biology of Physiological Health. *Cell*. 2020;181(2):250–69.
3. López-Otín C, Kroemer G. Hallmarks of Health. *Cell*. 2021;184(1):33–63.
4. Pedersen BK, Hoffman-Goetz L. Exercise and the immune system: Regulation, integration, and adaptation. *Physiol Rev*. 2000;80(3):1055–81.
5. Blair SN, Kohl HW 3rd, Paffenbarger RSJ, Clark DG, Cooper KH, Gibbons LW, et al. Physical Fitness and All-Cause Mortality: A Prospective Study of Healthy Men and Women. *JAMA*. 1989 Nov 3;262(17):2395–401.
6. Kodama S, Saito K, Tanaka S, Maki M, Yachi Y, Asumi M, et al. Cardiorespiratory fitness as a quantitative predictor of all-cause mortality and cardiovascular events in healthy men and women: a meta-analysis. *JAMA*. 2009 May;301(19):2024–35.
7. Rydén L, Grant PJ, Anker SD, Berne C, Cosentino F, Danchin N, et al. ESC Guidelines on diabetes, pre-diabetes, and cardiovascular diseases developed in collaboration with the EASD: The Task Force on diabetes, pre-diabetes, and cardiovascular diseases of the European Society of Cardiology (ESC) and developed in collaboration. *Eur Heart J*. 2013 Oct 14;34(39):3035–87.
8. Nordestgaard BG, Benn M, Schnohr P, Tybjaerg-Hansen A. Nonfasting Triglycerides and Risk of Myocardial Infarction, Ischemic Heart Disease, and Death in Men and Women. *JAMA*. 2007 Jul 18;298(3):299–308.
9. Wang X, Bao W, Liu J, OuYang Y-Y, Wang D, Rong S, et al. Inflammatory Markers and Risk of Type 2 Diabetes: A systematic review and meta-analysis. *Diabetes Care*. 2012 Dec 1;36(1):166–75.
10. van Ommen B, Keijer J, Heil SG, Kaput J. Challenging homeostasis to define biomarkers for nutrition related health. *Mol Nutr Food Res*. 2009;53(7):795–804.
11. Hoevenaars F, van der Kamp J-W, van den Brink W, Wopereis S. Next Generation Health Claims Based on Resilience: The Example of Whole-Grain Wheat. Vol. 12, *Nutrients*. 2020.
12. Krug S, Kastenmüller G, Stücker F, Rist MJ, Skurk T, Sailer M, et al. The dynamic range of the human metabolome revealed by challenges. *FASEB J*. 2012;26(6):2607–19.
13. Walsh CT, Tu BP, Tang Y. Eight Kinetically Stable but Thermodynamically Activated Molecules that Power Cell Metabolism. *Chem Rev*. 2018 Feb 28;118(4):1460–94.
14. Davies RE. A Molecular Theory of Muscle Contraction: Calcium-Dependent Contractions with Hydrogen Bond Formation Plus ATP-Dependent Extensions of Part of the Myosin-Actin Cross-Bridges. *Nature*. 1963;199(4898):1068–74.
15. Attwell D, Laughlin SB. An energy budget for signaling in the grey matter of the brain. *J Cereb Blood Flow Metab*. 2001 Oct;21(10):1133–45.
16. Schwiebert EM, Zsembery A. Extracellular ATP as a signaling molecule for epithelial cells. *Biochim Biophys Acta - Biomembr*. 2003;1615(1):7–32.
17. G. VHM, C. CL, B. TC. Understanding the Warburg Effect: The Metabolic Requirements of Cell Proliferation. *Science (80- )*. 2009 May 22;324(5930):1029–33.
18. Gnaiger E, Steinlechner-Maran R, Méndez G, Eberl T, Margreiter R. Control of mitochondrial and cellular respiration by oxygen. *J Bioenerg Biomembr*. 1995;27(6):583–96.
19. Clark LCJ. Monitor and control of blood and tissue oxygen tensions. *ASAIO J*. 1956;2(1).
20. Clark Jr. LC, Lyons C. Electrode systems for continuous monitoring in cardiovascular surgery. *Ann N Y Acad Sci*. 1962;102(1):29–45.
21. Ferrick DA, Neilson A, Beeson C. Advances in measuring cellular bioenergetics using extracellular flux. *Drug Discov Today*. 2008;13(5):268–74.
22. Spinelli JB, Haigis MC. The multifaceted contributions of mitochondria to cellular metabolism. *Nat Cell Biol*. 2018;20(7):745–54.
23. Zorov DB, Juhaszova M, Sollott SJ. Mitochondrial Reactive Oxygen Species (ROS) and ROS-Induced ROS Release. *Physiol Rev*. 2014 Jul 1;94(3):909–50.

24. Dröge W. Free Radicals in the Physiological Control of Cell Function. *Physiol Rev.* 2002 Jan 1;82(1):47–95.
25. Garrido C, Galluzzi L, Brunet M, Puig PE, Didelot C, Kroemer G. Mechanisms of cytochrome c release from mitochondria. *Cell Death Differ.* 2006;13(9):1423–33.
26. Quirós PM, Mottis A, Auwerx J. Mitonuclear communication in homeostasis and stress. *Nat Rev Mol Cell Biol.* 2016;17(4):213–26.
27. Tonkonogi M, Sahlin K. Physical exercise and mitochondrial function in human skeletal muscle. *Exerc Sport Sci Rev.* 2002 Jul;30(3):129–37.
28. Huertas JR, Casuso RA, Agustín PH, Cogliati S. Stay Fit, Stay Young: Mitochondria in Movement: The Role of Exercise in the New Mitochondrial Paradigm. *Oxid Med Cell Longev.* 2019;2019:7058350.
29. Ross R, Blair SN, Arena R, Church TS, Després J-P, Franklin BA, et al. Importance of Assessing Cardiorespiratory Fitness in Clinical Practice: A Case for Fitness as a Clinical Vital Sign: A Scientific Statement From the American Heart Association. *Circulation.* 2016 Dec;134(24):e653–99.
30. Caspersen CJ, Powell KE, Christenson GM. Physical activity, exercise, and physical fitness: definitions and distinctions for health-related research. *Public Health Rep.* 1985;100(2):126–31.
31. Fletcher GF, Ades PA, Kligfield P, Arena R, Balady GJ, Bittner VA, et al. Exercise Standards for Testing and Training. *Circulation.* 2013 Aug 20;128(8):873–934.
32. Ryan TE, Brophy P, Lin C-T, Hickner RC, Neufer PD. Assessment of in vivo skeletal muscle mitochondrial respiratory capacity in humans by near-infrared spectroscopy: a comparison with in situ measurements. *J Physiol.* 2014 Aug;592(15):3231–41.
33. Elder GC, Bradbury K, Roberts R. Variability of fiber type distributions within human muscles. *J Appl Physiol.* 1982 Dec;53(6):1473–80.
34. Horwath O, Envall H, Røja J, Emanuelsson EB, Sanz G, Ekblom B, et al. Variability in vastus lateralis fiber type distribution, fiber size, and myonuclear content along and between the legs. *J Appl Physiol.* 2021 May 20;131(1):158–73.
35. Grassi B, Quaresima V. Near-infrared spectroscopy and skeletal muscle oxidative function in vivo in health and disease: a review from an exercise physiology perspective. *J Biomed Opt.* 2016 Jul 1;21(9):1–20.
36. Nagasawa T, Hamaoka T, Sako T, Murakami M, Kime R, Homma T, et al. A practical indicator of muscle oxidative capacity determined by recovery of muscle O<sub>2</sub> consumption using NIR spectroscopy. *Eur J Sport Sci.* 2003 Apr;3(2):1–10.
37. Jöbsis FF. Noninvasive, infrared monitoring of cerebral and myocardial oxygen sufficiency and circulatory parameters. *Science.* 1977 Dec;198(4323):1264–7.
38. De Blasi RA, Almenrader N, Aurisicchio P, Ferrari M. Comparison of two methods of measuring forearm oxygen consumption (VO<sub>2</sub>) by near infrared spectroscopy. *J Biomed Opt.* 1997 Apr;2(2):171–5.
39. Van Beekvelt MC, Colier WN, Wevers RA, Van Engelen BG. Performance of near-infrared spectroscopy in measuring local O<sub>2</sub> consumption and blood flow in skeletal muscle. *J Appl Physiol.* 2001 Feb;90(2):511–9.
40. McMahon S, Jenkins D. Factors Affecting the Rate of Phosphocreatine Resynthesis Following Intense Exercise. *Sport Med.* 2002;32(12):761–84.
41. Brizendine JT, Ryan TE, Larson RD, McCully KK. Skeletal Muscle Metabolism in Endurance Athletes with Near-Infrared Spectroscopy. *Med Sci Sport Exerc.* 2013 May;45(5):869–75.
42. Lagerwaard B, Keijer J, McCully KK, de Boer VCJ, Nieuwenhuizen AG. In vivo assessment of muscle mitochondrial function in healthy, young males in relation to parameters of aerobic fitness. *Eur J Appl Physiol.* 2019;
43. Power ML, Schulkin J. Sex differences in fat storage, fat metabolism, and the health risks from obesity: possible evolutionary origins. *Br J Nutr.* 2008/05/01. 2008;99(5):931–40.
44. Craig JC, Broxterman RM, Wilcox SL, Chen C, Barstow TJ. Effect of adipose tissue thickness, muscle site, and sex on near-infrared spectroscopy derived total-[hemoglobin + myoglobin]. *J Appl Physiol.* 2017 Sep 21;123(6):1571–8.
45. van Beekvelt MC, Borghuis MS, van Engelen BG, Wevers RA, Colier WN. Adipose tissue thickness affects in vivo quantitative near-IR spectroscopy in human skeletal muscle. *Clin Sci (London, England).* 2001 Jul;101(1):21–8.

46. Ryan TE, Brizendine JT, McCully KK, Belardinelli R, Barstow T, Nguyen P, et al. A comparison of exercise type and intensity on the noninvasive assessment of skeletal muscle mitochondrial function using near-infrared spectroscopy. *J Appl Physiol*. 2013 Jan;114(2):230–7.
47. Hamaoka T, McCully KK, Niwayama M, Chance B. The use of muscle near-infrared spectroscopy in sport, health and medical sciences: recent developments. *Philos Trans R Soc A Math Phys Eng Sci*. 2011 Nov;369(1955):4591–604.
48. Kleiveland CR. Peripheral Blood Mononuclear Cells. In: Verhoeckx K, Cotter P, López-Expósito I, Kleiveland C, Lea T, Mackie A, et al., editors. *The Impact of Food Bioactives on Health: in vitro and ex vivo models*. Cham: Springer International Publishing; 2015. p. 161–7.
49. Autissier P, Soulas C, Burdo TH, Williams KC. Evaluation of a 12-color flow cytometry panel to study lymphocyte, monocyte, and dendritic cell subsets in humans. *Cytometry A*. 2010 May;77(5):410–9.
50. DeConne TM, Muñoz ER, Sanjana F, Hobson JC, Martens CR. Cardiometabolic risk factors are associated with immune cell mitochondrial respiration in humans. *Am J Physiol Circ Physiol*. 2020 Jul 17;319:H481–487.
51. Hartman M-L, Shirihai OS, Holbrook M, Xu G, Kocherla M, Shah A, et al. Relation of mitochondrial oxygen consumption in peripheral blood mononuclear cells to vascular function in type 2 diabetes mellitus. *Vasc Med*. 2014 Feb;19(1):67–74.
52. Ajaz S, McPhail MJ, Singh KK, Mujib S, Trovato FM, Napoli S, et al. Mitochondrial metabolic manipulation by SARS-CoV-2 in peripheral blood mononuclear cells of patients with COVID-19. *Am J Physiol Cell Physiol*. 2021 Jan;320(1):C57–65.
53. Ajaz S, McPhail MJ, Gnudi L, Trovato FM, Mujib S, Napoli S, et al. Mitochondrial dysfunction as a mechanistic biomarker in patients with non-alcoholic fatty liver disease (NAFLD). *Mitochondrion*. 2021 Mar;57:119–30.
54. Zhou B, Wang DD, Qiu Y, Airhart S, Liu Y, Stempien-Otero A, et al. Boosting NAD Level Suppresses Inflammatory Activation of PBMC in Heart Failure. *J Clin Invest*. 2020;130(11):6054–63.
55. Maynard S, Hejl AM, Dinh TST, Keijzers G, Hansen ÅM, Desler C, et al. Defective mitochondrial respiration, altered dNTP pools and reduced AP endonuclease 1 activity in peripheral blood mononuclear cells of Alzheimer's disease patients. *Aging (Albany NY)*. 2015;7(10):793–815.
56. Smith AM, Depp C, Ryan BJ, Johnston GI, Alegre-Abarrategui J, Evetts S, et al. Mitochondrial dysfunction and increased glycolysis in prodromal and early Parkinson's blood cells. *Mov Disord*. 2018 Oct 1;33(10):1580–90.
57. Chen H, Schürch CM, Noble K, Kim K, Krutzik PO, O'Donnell E, et al. Functional comparison of PBMCs isolated by Cell Preparation Tubes (CPT) vs. Lymphoprep Tubes. *BMC Immunol*. 2020 Mar;21(1):15.
58. Schmid D, Burmester GR, Tripmacher R, Kuhnke A, Buttgerit F. Bioenergetics of Human Peripheral Blood Mononuclear Cell Metabolism in Quiescent, Activated, and Glucocorticoid-Treated States. *Biosci Rep*. 2000;20(4):289–302.
59. Chacko BK, Kramer PA, Ravi S, Johnson MS, Hardy RW, Ballinger SW, et al. Methods for defining distinct bioenergetic profiles in platelets, lymphocytes, monocytes, and neutrophils, and the oxidative burst from human blood. *Lab Invest*. 2013;93(6):690–700.
60. Rausser S, Trumpff C, McGill MA, Junker A, Wang W, Ho S-H, et al. Mitochondrial phenotypes in purified human immune cell subtypes and cell mixtures. Johnson SC, Akhmanova A, editors. *Elife*. 2021;10:e70899.
61. Liepinsh E, Makarova E, Plakane L, Konrade I, Liepins K, Videja M, et al. Low-intensity exercise stimulates bioenergetics and increases fat oxidation in mitochondria of blood mononuclear cells from sedentary adults. *Physiol Rep*. 2020 Jun;8(12):e14489.
62. Kocher M, McDermott M, Lindsey R, Shikuma CM, Gerschenson M, Chow DC, et al. Short Communication: HIV Patient Systemic Mitochondrial Respiration Improves with Exercise. *AIDS Res Hum Retroviruses*. 2017 Oct;33(10):1035–7.
63. Oshida Y, Yamanouchi K, Hayamizu S, Sato Y. Effect of acute physical exercise on lymphocyte subpopulations in trained and untrained subjects. *Int J Sports Med*. 1988 Apr;9(2):137–40.

64. Shinkai S, Shore S, Shek PN, Shephard RJ. Acute exercise and immune function. Relationship between lymphocyte activity and changes in subset counts. *Int J Sports Med.* 1992 Aug;13(6):452–61.
65. Silaidos C, Pilatus U, Grewal R, Matura S, Lienerth B, Pantel J, et al. Sex-associated differences in mitochondrial function in human peripheral blood mononuclear cells (PBMCs) and brain. *Biol Sex Differ.* 2018;9(1):1–10.
66. Tsai H-H, Chang S-C, Chou C-H, Weng T-P, Hsu C-C, Wang J-S. Exercise Training Alleviates Hypoxia-induced Mitochondrial Dysfunction in the Lymphocytes of Sedentary Males. *Sci Rep.* 2016;6(1):35170.
67. Hedges CP, Woodhead JST, Wang HW, Mitchell CJ, Cameron-Smith D, Hickey AJR, et al. Peripheral blood mononuclear cells do not reflect skeletal muscle mitochondrial function or adaptation to high-intensity interval training in healthy young men. *J Appl Physiol.* 2019;126(2):454–61.
68. Elliott R, Pico C, Dommels Y, Wybranska I, Hesketh J, Keijer J. Nutrigenomic approaches for benefit-risk analysis of foods and food components: defining markers of health. *Br J Nutr.* 2007 Dec;98(6):1095–100.
69. van Ommen B, van der Greef J, Ordovas JM, Daniel H. Phenotypic flexibility as key factor in the human nutrition and health relationship. *Genes Nutr.* 2014;9(5):423.
70. Monteiro MS, Carvalho M, Bastos ML, Guedes de Pinho P. Metabolomics analysis for biomarker discovery: advances and challenges. *Curr Med Chem.* 2013;20(2):257–71.
71. Sara A, O. GA, Peipei P, Thomas K, Brian S, Jennifer van E, et al. Cardiovascular Proteomics: Tools to Develop Novel Biomarkers and Potential Applications. *J Am Coll Cardiol.* 2006 Nov 7;48(9):1733–41.
72. Schraner D, Kastenmüller G, Schönfelder M, Römisch-Margl W, Wackerhage H. Metabolite Concentration Changes in Humans After a Bout of Exercise: a Systematic Review of Exercise Metabolomics Studies. *Sport Med - Open.* 2020;6(1):11.
73. Fischer CP. Interleukin-6 in acute exercise and training: what is the biological relevance? *Exerc Immunol Rev.* 2006;12:6–33.
74. Zempleni J, Suttie JW, Gregory III JF, Stover PJ. Handbook of Vitamins. Fifth. Zempleni J, Suttie JW, Gregory III JF, Stover PJ, editors. Boca Raton, FL: CRC Press Taylor and Francis Group; 2014. 576 p.
75. Depeint F, Bruce WR, Shangari N, Mehta R, O'Brien PJ. Mitochondrial function and toxicity: role of the B vitamin family on mitochondrial energy metabolism. *Chem Biol Interact.* 2006 Oct;163(1–2):94–112.
76. Depeint F, Bruce WR, Shangari N, Mehta R, O'Brien PJ. Mitochondrial function and toxicity: role of B vitamins on the one-carbon transfer pathways. *Chem Biol Interact.* 2006 Oct;163(1–2):113–32.
77. Pietrzik K. Modern Lifestyles, Lower Energy Intake and Micronutrient Status. Softcover. Pietrzik K, Macdonald I, editors. London: Springer-Verlag; 1991. 212 p.
78. Smidt LJ, Cremin FM, Grivetti LE, Clifford AJ. Influence of Thiamin Supplementation on the Health and General Well-being of an Elderly Irish Population With Marginal Thiamin Deficiency. *J Gerontol.* 1991 Jan 1;46(1):M16–22.
79. European Food and Safety Authority. Dietary Reference Values for Nutrients. 2017.
80. Woolf K, Manore MM. B-vitamins and exercise: Does exercise alter requirements? *Int J Sport Nutr Exerc Metab.* 2006;16(5):453–84.
81. He F, Li J, Liu Z, Chuang C-C, Yang W, Zuo L. Redox Mechanism of Reactive Oxygen Species in Exercise. *Front Physiol.* 2016 Nov 7;7:486.
82. Sen CK. Oxidants and antioxidants in exercise. *J Appl Physiol.* 1995;79(3):675–86.
83. Jackson MJ. Control of Reactive Oxygen Species Production in Contracting Skeletal Muscle. *Antioxid Redox Signal.* 2011 Jun 23;15(9):2477–86.
84. Lienhart WD, Gudipati V, MacHeroux P. The human flavoproteome. *Arch Biochem Biophys.* 2013;535(2):150–62.
85. Joosten V, van Berkel WJ. Flavoenzymes. *Curr Opin Chem Biol.* 2007;11(2):195–202.
86. Schulz GE, Schirmer RH, Sachsenheimer W, Pai EF. The structure of the flavoenzyme glutathione reductase. *Nature.* 1978;273(5658):120–4.
87. Turck D, Bresson J, Burlingame B, Dean T, Fairweather-Tait S, Heinonen M, et al. Dietary Reference Values for riboflavin. *EFSA J.* 2017;15(8).

88. Bayoumi RA, Rosalki SB. Evaluation of methods of coenzyme activation of erythrocyte enzymes for detection of deficiency of vitamins B1, B2, and B6. *Clin Chem.* 1976 Mar;22(3):327–35.
89. Sauberlich HE, Judd Jr. JH, Nicholals GE, Broquist HP, Darby WJ. Application of the erythrocyte glutathione reductase assay in evaluating riboflavin nutritional status in a high school student population. *Am J Clin Nutr.* 1972 Aug 1;25(8):756–62.
90. Belko AZ, Obarzanek E, Kalkwarf HJ, Rotter MA, Bogusz S, Miller D, et al. Effects of exercise on riboflavin requirements of young women. *Am J Clin Nutr.* 1983 Apr;37(4):509–17.
91. Winters LR, Yoon JS, Kalkwarf HJ, Davies JC, Berkowitz MG, Haas J, et al. Riboflavin requirements and exercise adaptation in older women. *Am J Clin Nutr.* 1992 Sep;56(3):526–32.
92. Fogelholm M. Micronutrient status in females during a 24-week fitness-type exercise program. *Ann Nutr Metab.* 1992;36(4):209–18.
93. Ohno H, Yahata T, Sato Y, Yamamura K, Taniguchi N. Physical training and fasting erythrocyte activities of free radical scavenging enzyme systems in sedentary men. *Eur J Appl Physiol Occup Physiol.* 1988;57(2):173–6.
94. Evelo CTA, Palmen NGM, Artur Y, Janssen GME. Changes in blood glutathione concentrations, and in erythrocyte glutathione reductase and glutathione S-transferase activity after running training and after participation in contests. *Eur J Appl Physiol Occup Physiol.* 1992;64(4):354–8.
95. Frank T, Kuhl M, Makowski B, Bitsch R, Jahreis G, Hubscher J. Does a 100-km walking affect indicators of vitamin status? *Int J Vitam Nutr Res.* 2000 Sep;70(5):238–50.
96. Ohno H, Sato Y, Yamashita K, Doi R, Arai K, Kondo T, et al. The effect of brief physical exercise on free radical scavenging enzyme systems in human red blood cells. *Can J Physiol Pharmacol.* 1986 Sep;64(9):1263–1265.
97. Wells JCK. Sexual dimorphism of body composition. *Best Pract Res Clin Endocrinol Metab.* 2007;21(3):415–30.
98. Pradhan AD. Sex Differences in the Metabolic Syndrome: Implications for Cardiovascular Health in Women. *Clin Chem.* 2014 Jan 1;60(1):44–52.
99. Regitz-Zagrosek V. Sex and gender differences in health. *EMBO Rep.* 2012 Jul 1;13(7):596–603.
100. Regitz-Zagrosek V, Kararigas G. Mechanistic Pathways of Sex Differences in Cardiovascular Disease. *Physiol Rev.* 2016 Nov 2;97(1):1–37.
101. Soldin OP, Mattison DR. Sex differences in pharmacokinetics and pharmacodynamics. *Clin Pharmacokinet.* 2009;48(3):143–57.
102. Ansdell P, Thomas K, Hicks KM, Hunter SK, Howatson G, Goodall S. Physiological sex differences affect the integrative response to exercise: acute and chronic implications. *Exp Physiol.* 2020 Dec;105(12):2007–21.
103. Gerdtz E, Regitz-Zagrosek V. Sex differences in cardiometabolic disorders. *Nat Med.* 2019;25(11):1657–66.
104. Costello JT, Bieuzen F, Bleakley CM. Where are all the female participants in Sports and Exercise Medicine research? *Eur J Sport Sci.* 2014;14(8):847–51.
105. Clayton JA, Collins FS. Policy: NIH to balance sex in cell and animal studies. *Nature.* 2014;509(7500):282–3.





# 2

## Muscle mitochondrial capacity in high- and low-fitness females using near-infrared spectroscopy

Bart Lagerwaard<sup>1,2</sup>, Joëlle J.E. Janssen<sup>1</sup>, Iris Cuijpers<sup>1</sup>,  
Jaap Keijer<sup>1</sup>, Vincent C.J. de Boer<sup>1</sup>, Arie G. Nieuwenhuizen<sup>1</sup>

<sup>1</sup> *Human and Animal Physiology, Wageningen University and Research,  
P.O. Box 338, 6700 AH, Wageningen, the Netherlands*

<sup>2</sup> *Ti Food and Nutrition, P.O. Box 557, 6700 AN, Wageningen, the Netherlands*

**Physiol Rep.** 2021; May; 9(9):e14838  
doi: 10.14814/phy2.14838

## Abstract

The recovery of muscle oxygen consumption ( $m\dot{V}O_2$ ) after exercise measured using near-infrared (NIR) spectroscopy (NIRS) provides a measure of skeletal muscle mitochondrial capacity. Nevertheless, due to sex differences in factors that can influence scattering and thus penetration depth of the NIRS signal in the tissue, e.g. subcutaneous adipose tissue thickness and intramuscular myoglobin and hemoglobin, it is unknown whether results in males can be extrapolated to a female population. Therefore, the aim of this study was to measure skeletal muscle mitochondrial capacity in females at different levels of aerobic fitness, to test whether NIRS can measure relevant differences in mitochondrial capacity. Mitochondrial capacity was analyzed in the *gastrocnemius* muscle and the wrist flexors of 32 young female adults, equally divided in a relatively high ( $\dot{V}O_{2peak} \geq 47$  mL/kg/min) and relatively low aerobic fitness group ( $\dot{V}O_{2peak} \leq 37$  mL/kg/min).  $m\dot{V}O_2$  recovery was significantly faster in the high-fitness compared to the low-fitness group in the *gastrocnemius*, but not in the wrist flexors ( $P = 0.009$  and  $P = 0.0528$ , respectively). Furthermore,  $\dot{V}O_{2peak}$  was significantly correlated to  $m\dot{V}O_2$  recovery in both *gastrocnemius* ( $R^2 = 0.27$ ,  $P = 0.0051$ ) and wrist flexors ( $R^2 = 0.13$ ,  $P = 0.0393$ ). In conclusion, NIRS measurements can be used to assess differences in mitochondrial capacity within a female population and is correlated to  $\dot{V}O_{2peak}$ . This further supports NIRS assessment of muscle mitochondrial capacity providing additional evidence for NIRS as a promising approach to monitor mitochondrial capacity, also in an exclusively female population.

## Introduction

Regular endurance exercise increases whole-body peak oxygen uptake ( $\dot{V}O_{2\text{peak}}$ ) due to bodily adaptations that increase oxygen transport, delivery and consumption. At the level of the skeletal muscle, maximal oxygen consumption increases due to an increase in muscle mitochondrial mass and function (1). The exact contribution of this increased skeletal muscle oxidative capacity to the improved  $\dot{V}O_{2\text{peak}}$  after regular endurance exercise remains debated. Nevertheless, there appears to be a strong link between mitochondrial mass and  $\dot{V}O_{2\text{peak}}$  (2). Furthermore, skeletal muscle oxidative capacity is suggested to be a determining factor in prolonged strenuous exercise performance (3). Classically, skeletal muscle oxidative or mitochondrial capacity is analyzed *ex vivo*, by measuring oxygen consumption in permeabilized muscle fibers from muscle biopsies. The invasive nature of this technique, the isolation of the tissue from its physiological environment, as well as the infringement of cell integrity by the permeabilization procedure provides a rationale for non-invasive assessment of muscle mitochondrial capacity in an intact system.

A near-infrared spectroscopy (NIRS)-based technique has been developed to assess skeletal muscle mitochondrial capacity *in vivo* (4). Using multiple, transient vascular occlusions after a short bout of exercise it allows for the measurement of post-exercise recovery of  $m\dot{V}O_2$  (5). The underlying assumption is that post-exercise regeneration of readily available energy carriers, i.e., ATP and phosphocreatine (PCr), is directly linked to aerobic metabolism and, therefore, a higher mitochondrial capacity will be associated with a faster recovery to the pre-exercise state (6). NIRS offers advantages over other non-invasive techniques, such as magnetic resonance spectroscopy ( $^{31}\text{P}$ -MRS), due to its higher portability and relatively low-costs, making it more suitable for on-site and routine measurements. However, a limitation of the NIRS technique is the limited penetration depth in the tissue, as the greater the distance the NIR light has to travel to reach muscle tissue, the lower the resolution (7). Therefore, factors that influence the scattering of the signal, such as differences in subcutaneous adipose tissue thickness (ATT), but also skin thickness, skin pigmentation and blood flow (7–9) can affect the NIRS measurement of post-exercise recovery of  $m\dot{V}O_2$ .

In a normally active male population, we previously showed that NIRS is able to detect differences in mitochondrial capacity in the *gastrocnemius* muscle between relatively high- fitness and low-fitness subjects, and this NIRS-derived measure of mitochondrial capacity was correlated to  $\dot{V}O_{2\text{peak}}$  (10). Nevertheless, it is unsure if these results are easily extrapolated to a female population, because of the

forementioned factors that could affect the signal to noise ratio, such as ATT thickness, which can be anticipated to be larger in females, and total hemoglobin and myoglobin, which was shown to be lower in females in the *gastrocnemius* muscle, but not in other muscles, e.g. wrist flexors, compared to males (9). Additionally, it could be that possible sex differences in the relationship between mitochondrial capacity  $\dot{V}O_{2\text{peak}}$  also affect this relationship. For instance, males showed a larger stimulation of mitochondrial biogenesis than females upon sprint interval training (11). Indeed, straightforward extrapolation is warned, as a recent NIRS study showed no correlation between mitochondrial capacity in the *gastrocnemius* muscle and  $\dot{V}O_{2\text{peak}}$  when males and females were combined (12), which contrasted our previous findings in males only (10).

Thus, even though studies in mixed population indicate the application of the technique in both sexes (13–17), it is unknown whether NIRS is able to detect physiologically relevant differences within an exclusively female population, a population also often underrepresented in sports and exercise research (18). Therefore, the aim of this study was to measure skeletal muscle mitochondrial capacity in healthy females at different levels of aerobic fitness to further support the applicability of NIRS assessment of mitochondrial capacity in this population. Mitochondrial capacity was measured in both the frequently activated *gastrocnemius* muscle and the often-undertrained wrist flexors in 32 recreationally active, healthy females divided into a relatively low and a relatively high-fitness group. We hypothesized that high-fitness females will show a higher mitochondrial capacity compared to low-fitness females in both muscles.

## Materials and Methods

### Ethical approval

The study was approved by the medical ethical committee of Wageningen University & Research with reference number NL70136.081.19. All procedures performed were in accordance with the ethical standards of the institutional and/or national research committee and with the 1964 Helsinki declaration and its later amendments or comparable ethical standards (Fortaleza, Brazil 2013). The study is registered in the Dutch trial register (NL7891). Written informed consent was obtained from all individual participants included in the study.

### Subjects

Healthy females between the age of 18–28 years were recruited from the local university and community population. None of the subjects had a history of

cardiovascular, respiratory or metabolic disease. None of the subjects were a regular smoker (> 5 cigarettes per week), used recreational drugs during the study or reported recent use of performance enhancing drugs or supplements. Subjects were non-anaemic (haemoglobin concentration > 12 g/dL), verified by using HemoCue Hb 201 microcuvette (HemoCue AB, Sweden). None of the subjects were pregnant or lactating. 17  $\beta$ -estradiol levels were measured with at Erasmus Medical Centre, the Netherlands using chemiluminescent immunoassay on Lumipulse G1200 analyzer (Fujirebio Inc, Japan). Subjects that used any other monophasic oral contraceptive containing low synthetic estradiol and progesterone were excluded from participation. Test days were planned within the end of the follicular phase until menstruation, based on self-reported occurrence of last menstruation or during final 14 days of pill cycle.

### Pre-experimental screening protocol

Subjects were selected based on  $\dot{V}O_2$ peak, measured using an incremental exercise test on electrically braked bicycle ergometer (Corival CPET, Lode, the Netherlands). Subjects were asked to refrain themselves from vigorous exercise for 48 hours and to have consumed their last meal two hours before this test. Oxygen consumption, carbon dioxide production and air flow were measured using MAX-II metabolic cart (AEI technologies, USA). Exhaled air was continuously sampled from a mixing chamber and heart rate was measured with a strap-on chest heart rate monitor (Polar Electro, Finland). After a 3-minute unloaded cycling warming-up, the protocol started at a workload of 50 W for subjects who exercised < 3 times a week or 75 W for subjects who exercised > 3 times per week and was increased every minute in increments of 15 W. Subjects were instructed to maintain a self-selected pedal rate between 70 – 80 revolutions per minute (RPM). Inability to pedal at a rate above 60 RPM for 10 seconds was considered point of exhaustion and the end of the test. For the test to be valid, two out of three of the following criteria should have been met: 1) A maximal heart rate within 10 beats of the predicted maximum ( $220 - \text{age}$ ), 2) Attainment of a plateau in  $\dot{V}O_2$ , i.e.  $\dot{V}O_2$  failing to increase with 150 mL/min, despite an increase in workload, 3) Achievement of an  $RER \geq 1.1$ .  $\dot{V}O_2$ peak was determined by binning data in 15 seconds intervals. Sixteen relatively high-fitness ( $\dot{V}O_2$ peak  $\geq 47$  mL/kg/min) and sixteen relatively low-fitness subjects ( $\dot{V}O_2$ peak  $\leq 37$  mL/kg/min) were selected to take part in the study, based on chosen cut offs. Main exercise modalities in the high-fitness group were running/athletics (6x), rowing (3x), kickboxing (2x), hockey (1x), swimming (1x), ice skating (1x), climbing (1x) and weightlifting (1x). Main exercise modalities in low-fitness group were aerobics (2x), horseback riding (1x), weightlifting (1x), climbing (1x), walking (1x), dancing (1x), badminton (1x) or no regular exercise (8x). A total of 111 exercise tests were conducted to end up with the desired sample size.

### Experimental protocol

The subjects refrained from heavy physical exercise 48 hours prior to testing and from any exercise and consumption of alcohol 24 hours prior to testing. Maximal Voluntary Contraction (MVC) hand grip strength of the non-dominant and dominant hand was measured using a Jamar Hydraulic Hand Dynamometer (Performance Health, IL, USA). Highest value out of three 5 seconds isometric contractions was set as MVC. Body fat percentage was measured according to the four-site method by Durnin-Womersley using the skinfold measurements of the triceps, biceps, sub scapula and supra iliac, measured using a skinfold caliper (Harpenden, UK). Furthermore, skinfold between NIRS receiver and transmitter was measured on the calf and the forearm.

### NIRS measurements

Deoxyhaemoglobin (HHb) and oxyhaemoglobin ( $O_2Hb$ ) were continuously measured using the continuous wave Oxymon, dual-wavelength NIRS system (760 and 850 nm; Artinis Medical Systems, The Netherlands) at three optode distances 15 mm, 45 mm and 55 mm. Data were collected via bluetooth at 10 Hz using Oxysoft software (Artinis Medical Systems). The NIRS probe was placed longitudinally on the belly of the muscle, identified by palpation by an experienced investigator, on the medial *gastrocnemius* and on the wrist flexors of the non-dominant side. To secure the probe and protect it from environmental light, the probe was tightly taped to the skin. To measure oxygen consumption, a blood pressure cuff (Hokanson SC5 and SC12; D.E. Hokanson Inc., Bellevue, WA) was placed proximally of the probe above the knee joint and on the upper arm. The cuff was powered and controlled by a rapid cuff inflator system (Hokanson E20 and AG101 Air source; D.E. Hokanson Inc.) set to a pressure of 230-250 mm Hg. Post-exercise muscle oxygen consumption recovery was assessed similar to previously published protocols (19). In summary, the protocol consists of three 30-second rest measurements of resting oxygen consumption. To calibrate the signal between individuals, the minimal-oxygenation (0%) of the tissue underneath the probe was determined by 30-second maximal hand grip exercise for wrist flexors or by plantar flexion exercise using a rubber resistance band for *gastrocnemius*, followed by a 4-minute arterial occlusion. The hyperemic response after the cuff was released was considered maximal oxygenation (100%). Recovery of muscle oxygen consumption after exercise was measured after 30 seconds of intermittent (approximately 0.5 Hz) handgrip exercise at 40% of MVC for the wrist flexors or plantar flexion exercise using a rubber resistance band until 50% of maximal oxygenation for *gastrocnemius*. Right after exercise, a series of transient occlusions (5 \* 5 seconds on / 5 seconds off, 5 \* 7 seconds on / 7 seconds off, 10 \* 10 seconds on / 10 seconds off) was used to measure the recovery of muscle

oxygen consumption after exercise. Recovery measurements were performed in duplicate with 2 minutes rest in between tests.

### Analysis of muscle oxygen consumption data

NIRS data were analyzed using Matlab-based (The Mathworks, MA, USA) analysis software (NIRS\_UGA, GA, USA). Optode distance of 45 mm or 55 mm was used, based on inspection of data of raw light counts during measurements. Data were analyzed as % of maximal oxygenation.  $\dot{m}\dot{V}O_2$  was calculated during every arterial occlusion using the slope of the change in HHb and  $O_2Hb$  (Hb difference) for 3 seconds for the 5-second occlusions, for 5 seconds for the 7-second occlusions, 7 seconds for the 10-second occlusions and 15 seconds for the basal measurements. A blood volume correction factor was used for each data point (20) to correct for redistribution of blood distally from the cuff. In short; changes in HHb and  $O_2Hb$  should be proportional during arterial occlusions. A blood volume correction factor ( $\beta$ ) was calculated to account for possible changes and was used to correct each data point.  $\dot{m}\dot{V}O_2$  recovery measurements post-exercise were fitted to a mono-exponential curve:

$$y(t) = End - \Delta * e^{-k \cdot t}$$

with  $y$  representing the  $\dot{m}\dot{V}O_2$  during the arterial occlusions;  $End$  being the  $\dot{m}\dot{V}O_2$  immediately after the cessation of exercise;  $\Delta$  being the difference between  $\dot{m}\dot{V}O_2$  after exercise and  $\dot{m}\dot{V}O_2$  during rest;  $k$  being the rate constant expressed in time units;  $t$  being time. Recovery of muscle oxygen consumption follows mono-exponential curve (21), therefore data points outside curve were considered artifacts and omitted from curve fitting. Data were analyzed blinded by two researchers. In case of discrepancy between analyses, third researcher analyzed data set (blinded) and consensus was reached. Rate constants calculated from curve fitting with  $R^2 < 0.95$  were excluded from analysis as a measure of poor data quality. Rate constants of duplicates were averaged.

### Statistical analyses

Data are presented as mean  $\pm$  standard deviation (SD), unless indicated otherwise. Statistical analyses were performed using GraphPad Prism v.5 (GraphPad Software, CA, USA). Means between the two groups were compared using a Students unpaired t-test. Correlations between variables were compared using regression analysis. Significance was accepted at  $P < 0.05$ . Normality was tested using Shapiro-Wilk normality test. Not-normal data were compared using Mann-Whitney tests.

## Results

Physical characteristics are shown in [Table 1](#). All subjects completed all tests without any contraindications. All maximal exercise tests met at least two out of three preset criteria. Subjects were either on monophasic oral contraceptive containing synthetic estradiol and progesterone (N = 13), used a copper spiral (N = 1) or did not use any contraceptives (N = 18). The use of oral control contraceptives was N = 7 in high-fitness and N = 6 in low-fitness group. No significant difference in 17 $\beta$ -estradiol levels was observed between the high-fitness and low-fitness group in subjects that did not use hormonal birth control contraceptives ([Table 1](#)).

**Table 1** Subjects characteristics

	Low-fitness (N = 16)	High-fitness (N = 16)
Age (years)	24.0 [21.3 - 25.5]	21.8 [21.5 - 23.6]
Ethnicity	Caucasian (11), Asian (1), Indo-pacific (4)	All Caucasian
Weight (kg)	59.2 $\pm$ 7.2	60.8 $\pm$ 6.9
Height (m)	1.63 $\pm$ 0.07	1.68 $\pm$ 0.04 *
Fat mass (% of weight)	28.9 $\pm$ 3.9	24.6 $\pm$ 4.7 **
$\dot{V}O_2$ peak (mL $\cdot$ kg <sup>-1</sup> $\cdot$ min <sup>-1</sup> )	35.1 [32.2 - 35.7]	51.0 [49.2 - 55.4] ***
MVC dominant arm	30.0 [25.3 - 33.5]	36.5 [32.0 - 39.50] *
MVC non-dominant arm	27.5 [24.0 - 33.5]	33.5 [30.3 - 37.0] *
Hemoglobin (mM)	8.4 $\pm$ 0.6	8.5 $\pm$ 0.6
Usage of birth control pill	6/16	7/16
If not; 17 $\beta$ -estradiol (pM)	470.9 [337 - 590]	153.8 [84 - 806]
ATT wrist flexors (mm)	5.3 [4.3 - 6.9]	4.0 [2.3 - 5.0] *
ATT GAS (mm)	8.6 [6.9 - 10.6]	6.9 [6.0 - 7.9] *

$\dot{V}O_2$ peak = Maximal oxygen consumption, MVC = maximal voluntary contraction handgrip strength, ATT = adipose tissue thickness, GAS = *gastrocnemius*. Values are mean  $\pm$  SD for normally distributed data, and median [interquartile range (IQR)] for not normally distributed data. \*P < 0.05, \*\*P < 0.01, \*\*\*P < 0.001.

### Recovery of $m\dot{V}O_2$ in gastrocnemius and wrist flexors

The NIRS protocol, which was used both for the *gastrocnemius* and wrist flexors, included 3 measurements of basal  $m\dot{V}O_2$ , assessment of minimal and maximal oxygenation level and the repeated occlusions to assess recovery of oxygen consumption after a short exercise protocol ([Figure 1A](#)). For *gastrocnemius*, two data sets were excluded due to  $R^2 < 0.95$ , two were excluded due to failed calibration measurement, i.e. no plateau for minimal oxygenation was reached, and one data

set was excluded due to technical issues (only had 15 mm channel). For all other measurements, plateau for minimal oxygenation was reached. Recovery rate constants were significantly different between the high and low-fitness group for *gastrocnemius* ( $2.06 \pm 0.57$  vs.  $1.48 \pm 0.47$ ,  $P = 0.009$ , **Figure 1B, C**), but not for the wrist flexors ( $1.24 \pm 0.23$  vs.  $1.10 \pm 0.15$ ,  $P = 0.0528$ , **Figure 1D, E**).

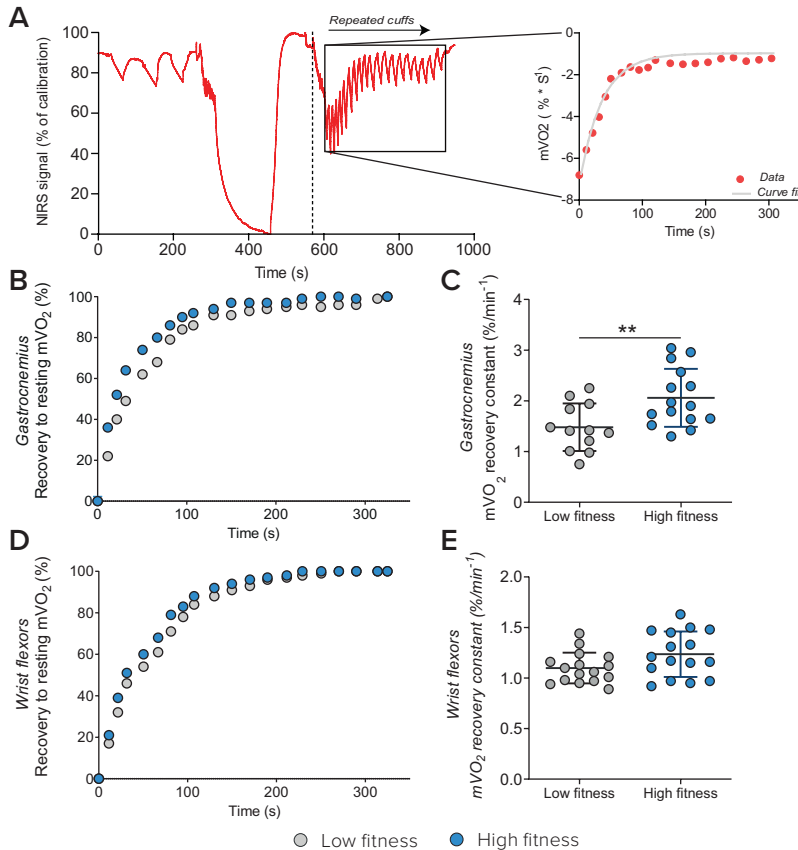


**Figure 1: Representative plot of NIRS protocol and recovery constants in high-fitness and low-fitness females.** (A) Red line represents NIRS signal of the Hb difference during protocol as percentage of maximal oxygenation. Repeated measurement  $m\dot{V}O_2$  (red dots) are fitted to a monoexponential curve fit (grey line) from which a recovery constant is derived. (B, D) Average curve fits for the low-fitness (grey) and high-fitness (blue) group for  $m\dot{V}O_2$  recovery presented as percentage of basal  $m\dot{V}O_2$  after 30s of plantar flexion exercise in *gastrocnemius* (B) and after a handgrip exercise in wrist flexors (D). (C, E) Recovery constants derived from monoexponentially curve fits for *gastrocnemius* (C) and wrist flexors (E). For *gastrocnemius* muscle  $N = 12$  vs.  $N = 15$ . Values are represented as mean  $\pm$  SD. \*\* $P < 0.01$ .

### Relationship between $\dot{V}O_2$ recovery and whole-body oxygen uptake

In order to test the relationship between endurance capacity, measured as  $\dot{V}O_{2peak}$ , and  $\dot{V}O_2$  recovery, measured using NIRS, a correlation analysis was performed. The  $\dot{V}O_2$  recovery constant of the *gastrocnemius* was significantly correlated to  $\dot{V}O_{2peak}$  ( $R^2 = 0.27$ ,  $P = 0.0051$ , **Figure 2A**). Furthermore, in the wrist flexors a significant correlation was observed between  $\dot{V}O_2$  recovery constant and  $\dot{V}O_{2peak}$  ( $R^2 = 0.13$ ,  $P = 0.0393$ , **Figure 2B**).

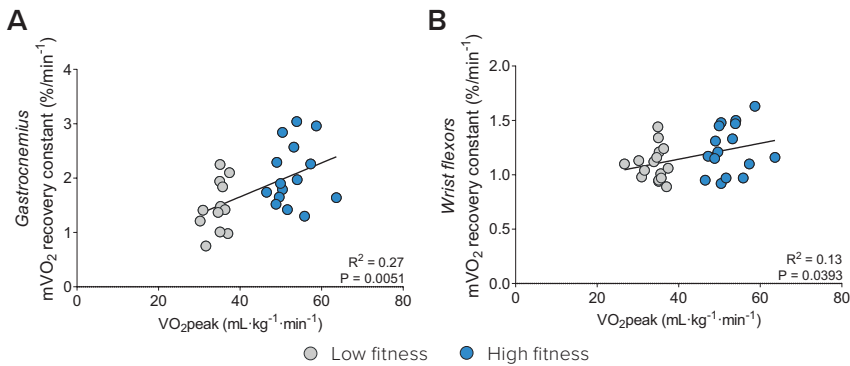


**Figure 2: Correlation between aerobic fitness level and recovery constants.** Correlation between maximal oxygen consumption ( $\dot{V}O_{2peak}$ ) measured during an incremental exercise test and recovery constants for muscle oxygen consumption recovery ( $\dot{V}O_2$ ) measured using NIRS in *gastrocnemius* (A) calculated after 30s of plantar flexion and wrist flexors (B) calculated after 30 seconds of handgrip exercise at 50% of MVC in the high-fitness (blue) and low-fitness (grey) group.

## Discussion

The aim of this study was to measure skeletal muscle mitochondrial capacity using NIRS in healthy females in the *gastrocnemius* and wrist flexors muscles to test whether NIRS can measure relevant differences in mitochondrial capacity and to further support NIRS assessment of mitochondrial capacity in this population. We are the first to show that recovery of  $\dot{V}O_2$  after a short bout of exercise as measure for mitochondrial capacity is significantly faster in the *gastrocnemius* muscle of high-fitness compared to low-fitness individuals in an exclusively female population. Recovery of  $\dot{V}O_2$  in the wrist flexors muscle was not statistically different in between two groups. Furthermore, when taking both groups together, we found a significant correlation between  $\dot{V}O_{2peak}$  and recovery of  $\dot{V}O_2$  in the *gastrocnemius* and wrist flexors.

### **$\dot{m}\dot{V}O_2$ recovery in gastrocnemius between high and low-fitness females**

This study shows that NIRS is able to detect physiological relevant differences in mitochondrial capacity in a healthy, recreationally active female population. The differences in mitochondrial capacity likely reflect a higher mitochondrial capacity in high-fitness individuals, i.e., more or more efficient mitochondria were able to reinstate muscle homeostasis faster. In a previous, but unique, study we showed a 40% faster  $\dot{m}\dot{V}O_2$  recovery in the *gastrocnemius* muscle of high-fitness compared to low-fitness males (10). The difference in magnitude of  $\dot{V}O_{2\text{peak}}$  was comparable with the current study, in which we likewise observed a 40% faster  $\dot{m}\dot{V}O_2$  recovery in high-fitness compared to low-fitness females. Brizendine et al. showed an approximate doubling of mitochondrial capacity in the *vastus lateralis* muscle in endurance athletes compared to inactive individuals (15). Although this study included both males and females, the vast majority of the endurance athletes were males and with an absolute difference in  $\dot{V}O_{2\text{peak}}$  of 40 mL/kg/min between the groups, the distinction between the groups was twice as large compared to the current study. Therefore, the present study highlights the sensitivity of NIRS measurements of  $\dot{m}\dot{V}O_2$  recovery to detect smaller differences in mitochondrial capacity and further extends the applicability of the technique, also in an exclusively female population.

The highly comparable results between in  $\dot{m}\dot{V}O_2$  recovery in the *gastrocnemius* muscle between the two sexes indicates the applicability of this NIRS-based technique to detect physiological relevant differences also in an exclusively female population. This is an important finding, as sex differences that could affect the light scattering, and thus the  $\dot{m}\dot{V}O_2$  recovery measurement, have been identified, such as a lower total hemoglobin and myoglobin in the *gastrocnemius* (9) and generally higher ATT in females compared to males. Higher levels of ATT can greatly affect the NIR-signal and consequently the signal to noise ratio of the measurement (7,9). Even though in the current experimental protocol the difference in ATT was accounted for by normalization of the signal within each person using a physiological calibration (22). Still, interrogation depth of the muscle is decreased with increasing ATT and this can result in a substantial attenuation of the signal from muscle tissue, such that a doubling of ATT from 4 to 8 mm reduces the contribution of total-[Hb+Mb] to the signal by 50% using a 20 mm source-detector distance (9). In the current population, average ATT on the *gastrocnemius* muscle was 8.1 mm, which was expectedly higher than previously observed in males (5.9 mm) (10). Not many studies have measured in these ranges of ATT in females (7,12,15,23,24). Yet, studies that did measure close to our range in ATT either reported difficulties (23), adapted the penetration depth according to the ATT per individual (14,19) or used a frequency-domain NIRS device that can better quantify the degree of light scattering (13).

To overcome the relatively high ATT, we used a greater source-detector distance of 45mm or 55mm in females, compared to 35mm in males. A greater source-detector distance allows for deeper tissue penetration and consequently increased attribution of muscle to the NIR-signal. Nevertheless, increasing source-detector distance will also cause less light to reach the detector, as more signal is lost due to scattering in the tissue. Still, our results showed that with a distance of 45 mm and 55 mm, tissue penetration and signal to noise ratios were sufficiently high to obtain reliable, i.e.  $R^2 > 0.95$ ,  $\dot{m}\dot{V}O_2$  recovery curves and to be able to identify differences in  $\dot{m}\dot{V}O_2$  recovery between two fitness groups in the *gastrocnemius* muscle of a healthy, recreationally active female population. Nevertheless, two data sets were excluded from analysis due to low curve fitting, or  $R^2$ . The data sets excluded for low  $R^2$  were among the highest in ATT thickness (10.95 mm and 11.05 mm). Therefore, although other measurements with higher ATT (e.g., 11.05 and 11.35 mm) were successful, and the NIR signal is also affected by other factors such as optode placement, exercise execution and movement artifacts, it could be that the larger contribution of adipose tissue to the NIR signal negatively affected the reliability of the  $\dot{m}\dot{V}O_2$  recovery curves. Therefore, our results suggest that increasing the source-detector distance is an effective, yet limited, approach for the application of NIRS to assess mitochondrial capacity in muscles with a substantial ATT.

All test days were planned within the end of the follicular phase until menstruation, i.e. luteal phase, based on self-reported occurrence of last menstruation. Due to variation of estradiol levels in luteal phase and the effect of 17 $\beta$ -estradiol on mitochondrial capacity (25), differences in 17 $\beta$ -estradiol levels could have affected the  $\dot{m}\dot{V}O_2$  recovery measurements. Yet, we observed no difference in 17 $\beta$ -estradiol between the two groups and we did not observe a correlation between 17 $\beta$ -estradiol and  $\dot{m}\dot{V}O_2$  recovery (data not shown). For these reasons, it is unlikely that differences in circulating levels 17 $\beta$ -estradiol could explain the significant difference in  $\dot{m}\dot{V}O_2$  recovery between the two groups. Nevertheless, we cannot rule out effects of the menstrual cyclical patterns, as, for example, neuromuscular function and fatigability showed modulations based on the phase of menstrual cycle in knee extensor muscles (26). Yet, because the current study also included monophasic oral contraceptive users, effects of menstrual cycle on the outcome measures were expected to be limited.

### The relationship between aerobic fitness and $\dot{m}\dot{V}O_2$ recovery

Although our primary aim was to find differences in  $\dot{m}\dot{V}O_2$  recovery in high and low-fitness females, when taking both groups together, we found a significant correlation between  $\dot{V}O_{2peak}$  and recovery of  $\dot{m}\dot{V}O_2$  in the *gastrocnemius*.

A correlation between mitochondrial capacity of skeletal muscle tissue and  $\dot{V}O_{2\text{peak}}$  has been established before. For instance, several NIRS studies describe a correlation between  $m\dot{V}O_{2\text{recovery}}$  and  $\dot{V}O_{2\text{peak}}$ , in particular in the *gastrocnemius* muscle of males (10), and in the *vastus lateralis* of mixed populations (12,15). Such a correlation has also been observed in a female population, using  $^{31}\text{P}$ -MRS, showing the rate of PCr resynthesis in the *gastrocnemius* muscle was correlated to  $\dot{V}O_{2\text{peak}}$  (27). Comparable to NIRS,  $^{31}\text{P}$ -MRS uses the recovery of muscle homeostasis after exercise, assessed by measuring the regeneration of PCr as a proxy for mitochondrial capacity (4,21) and the two techniques show a good agreement (16,19). Even though the correlations in the current study should be treated with caution because of the discontinuous distribution of the  $\dot{V}O_{2\text{peak}}$  values, our data are in agreement with the established correlation between skeletal muscle mitochondrial capacity and  $\dot{V}O_{2\text{peak}}$ , further supporting the applicability and physiological relevance of this technique in females.

### **$m\dot{V}O_2$ recovery in wrist flexors between high and low-fitness females**

Although a significant difference was found in  $m\dot{V}O_2$  recovery in the *gastrocnemius* muscle, a significant difference in  $m\dot{V}O_2$  recovery was not observed in wrist flexors between high-fitness and low-fitness females. This result is similar to data obtained in males with similar differences in  $\dot{V}O_{2\text{peak}}$  (10). However, with a P-value near significance and the weak correlation between  $m\dot{V}O_2$  recovery and  $\dot{V}O_{2\text{peak}}$ , one might argue that a slight increase in sample size would have resulted in a statistically significant difference. Nevertheless, not considering statistical significance, the difference  $m\dot{V}O_2$  recovery kinetics is rather small and could be less biologically relevant. This discrepancy between the wrist flexor and *gastrocnemius* muscle might be attributed to less frequent activation of the wrist flexors during endurance exercise and consequently less mitochondrial adaptations, such as increased amount and the efficiency of the mitochondria (28). Therefore, although the wrist flexors are a convenient muscle group to measure due to low ATT levels and exercise standardization, it is likely a poorer reflection of aerobic fitness. Therefore,  $m\dot{V}O_2$  recovery kinetics in this muscle should therefore not be used as a predictor for aerobic capacity or exercise performance.

### **Conclusion and further perspectives**

This study provides evidence for sensitive measurements of mitochondrial capacity using NIRS in a female population. In a population of healthy, recreationally active females, mitochondrial capacity was significantly higher in the *gastrocnemius* of high-fitness compared to low-fitness females. Furthermore, mitochondrial capacity was significantly correlated to  $\dot{V}O_{2\text{peak}}$ . These results further substantiate the use of  $m\dot{V}O_2$  recovery as a measure for mitochondrial capacity measured non-

invasively using NIRS as a relevant physiological parameter. Furthermore, these results support the applicability of this technique to detect relevant physiological differences in a female population with higher ATT by using a physiological calibration and greater source-detector distances. However, increasing source-detector distance comes with limitations, such as decreased signal intensity at the detector due to the scattering of light in the tissue. Furthermore, one has to consider portability, as commercially available portable NIRS often have a smaller maximal source-detector distance compared to wired NIRS optodes (29). Portability, besides relative faster testing and lower costs, is a promising feature of the NIRS assessment of mitochondrial capacity, allowing measurements in an onsite, field-based setting. Therefore, testing different populations should be considered good practice to further increase applicability of the technique.

Additionally, in a recent study looking at predictors of exercise performance on a time-to-completion cycling trial, it was shown that  $\dot{m}\dot{V}O_2$  recovery measured using NIRS best predicted performance on the trial (30). This supports the physiological relevance of NIRS assessment of  $\dot{m}\dot{V}O_2$  recovery assessment as a relevant marker in sports and exercise science. Additionally, NIRS has advantages over established techniques, such as less invasive than a muscle biopsy and more portable and lower cost compared to  $^{31}P$ -MRS. Moreover, recently it has been shown that using a 6-occlusion protocol is a valid and reproducible alternative to protocols using more occlusions, such as the current one (31). Using a shorter protocol reduces testing time or could, if desired, increase replicates to increase precision of the measurement. The strong prediction for exercise performance, relative fast testing and the portability, appoint  $\dot{m}\dot{V}O_2$  recovery measurements using NIRS as a promising approach to monitor aerobic performance in both laboratory and field-based settings, also in females.

## Acknowledgements

The authors greatly acknowledge the commitment of the volunteers who participated in the study. We acknowledge Laura Kessels for assistance with data collection during the study. We acknowledge professor McCully from the University of Georgia USA for providing the software for data analysis. We would like to thank Jenny Visser for her help with the analysis of estradiol levels.

## Funding

This project was financed by the TIFN research program Mitochondrial Health and the Netherlands Organization for Scientific Research (NWO) (ALWTF.2015.5).

### Conflict of interest

No conflicts of interest, financial or otherwise, are declared by the authors. The Companies FrieslandCampina and Danone Nutricia Research are sponsors of the TIFN program and partly financed the project. They had no role in data collection and analysis, decision to publish, or preparation of the manuscript, but commented the study design.

### Statement of contribution

BL, JJEJ, IC performed all experiments. BL, IC performed principal data analysis; BL, JJEJ, AGN, VCJB, JK performed conception and design of research; data analysis and interpretation. BL drafted the manuscript. All authors edited, revised, and approved final version of manuscript.

## References

1. Lanza IR, Nair KS. Muscle mitochondrial changes with aging and exercise. *Am J Clin Nutr.* 2009 Jan 1;89(1):467S-471S.
2. Weibel ER, Taylor CR, Hoppeler H. The concept of symmorphosis: a testable hypothesis of structure-function relationship. *Proc Natl Acad Sci.* 1991 Nov;88(22):10357–61.
3. Holloszy JO, Coyle EF. Adaptations of skeletal muscle to endurance exercise and their metabolic consequences. *J Appl Physiol.* 1984 Apr;56(4):831–8.
4. Nagasawa T, Hamaoka T, Sako T, Murakami M, Kime R, Homma T, et al. A practical indicator of muscle oxidative capacity determined by recovery of muscle O<sub>2</sub> consumption using NIR spectroscopy. *Eur J Sport Sci.* 2003 Apr;3(2):1–10.
5. Motobe M, Murase N, Osada T, Homma T, Ueda C, Nagasawa T, et al. Noninvasive monitoring of deterioration in skeletal muscle function with forearm cast immobilization and the prevention of deterioration. *Dyn Med.* 2004 Feb 6;3(1):2.
6. McMahon S, Jenkins D. Factors Affecting the Rate of Phosphocreatine Resynthesis Following Intense Exercise. *Sport Med.* 2002;32(12):761–84.
7. van Beekvelt MC, Borghuis MS, van Engelen BG, Wevers RA, Colier WN. Adipose tissue thickness affects in vivo quantitative near-IR spectroscopy in human skeletal muscle. *Clin Sci (London, England).* 2001 Jul;101(1):21–8.
8. Wassenaar EB, Van den Brand JGH. Reliability of Near-Infrared Spectroscopy in People With Dark Skin Pigmentation. *J Clin Monit Comput.* 2005;19(3):195–9.
9. Craig JC, Broxterman RM, Wilcox SL, Chen C, Barstow TJ. Effect of adipose tissue thickness, muscle site, and sex on near-infrared spectroscopy derived total-[hemoglobin + myoglobin]. *J Appl Physiol.* 2017 Sep 21;123(6):1571–8.
10. Lagerwaard B, Keijer J, McCully KK, de Boer VCJ, Nieuwenhuizen AG. In vivo assessment of muscle mitochondrial function in healthy, young males in relation to parameters of aerobic fitness. *Eur J Appl Physiol.* 2019;
11. Scalzo RL, Peltonen GL, Binns SE, Shankaran M, Giordano GR, Hartley DA, et al. Greater muscle protein synthesis and mitochondrial biogenesis in males compared with females during sprint interval training. *FASEB J.* 2014 Jun;28(6):2705–14.
12. Beever AT, Tripp TR, Zhang J, MacInnis MJ. NIRS-derived skeletal muscle oxidative capacity is correlated with aerobic fitness and independent of sex. *J Appl Physiol.* 2020 Sep;129(3):558–68.
13. Ryan TE, Brophy P, Lin C-T, Hickner RC, Neufer PD. Assessment of in vivo skeletal muscle mitochondrial respiratory capacity in humans by near-infrared spectroscopy: a comparison with in situ measurements. *J Physiol.* 2014 Aug;592(15):3231–41.
14. Ryan TE, Brizendine JT, McCully KK, Belardinelli R, Barstow T, Nguyen P, et al. A comparison of exercise type and intensity on the noninvasive assessment of skeletal muscle mitochondrial function using near-infrared spectroscopy. *J Appl Physiol.* 2013 Jan;114(2):230–7.
15. Brizendine JT, Ryan TE, Larson RD, McCully KK. Skeletal Muscle Metabolism in Endurance Athletes with Near-Infrared Spectroscopy. *Med Sci Sport Exerc.* 2013 May;45(5):869–75.
16. Sako T, Hamaoka T, Higuchi H, Kurosawa Y, Katsumura T. Validity of NIR spectroscopy for quantitatively measuring muscle oxidative metabolic rate in exercise. *J Appl Physiol.* 2001 Jan;90(1):338–44.
17. Hamaoka T, McCully KK, Niwayama M, Chance B. The use of muscle near-infrared spectroscopy in sport, health and medical sciences: recent developments. *Philos Trans R Soc A Math Phys Eng Sci.* 2011 Nov;369(1955):4591–604.
18. Costello JT, Bieuzen F, Bleakley CM. Where are all the female participants in Sports and Exercise Medicine research? *Eur J Sport Sci.* 2014;14(8):847–51.
19. Ryan TE, Southern WM, Reynolds MA, McCully KK. A cross-validation of near-infrared spectroscopy measurements of skeletal muscle oxidative capacity with phosphorus magnetic resonance spectroscopy. *J Appl Physiol.* 2013;115(12):1757–66.

20. Ryan TE, Erickson ML, Brizendine JT, Young H-J, McCully KK. Noninvasive evaluation of skeletal muscle mitochondrial capacity with near-infrared spectroscopy: correcting for blood volume changes. *J Appl Physiol*. 2012 Jul;113(2):175–83.
21. Meyer RA. A linear model of muscle respiration explains monoexponential phosphocreatine changes. *Am J Physiol Physiol*. 1988 Apr;254(4):C548–53.
22. Hamaoka T, Iwane H, Shimomitsu T, Katsumura T, Murase N, Nishio S, et al. Noninvasive measures of oxidative metabolism on working human muscles by near-infrared spectroscopy. *J Appl Physiol*. 1996 Sep;81(3):1410–7.
23. Adami A, Cao R, Porszasz J, Casaburi R, Rossiter HB. Reproducibility of NIRS assessment of muscle oxidative capacity in smokers with and without COPD. *Respir Physiol Neurobiol*. 2017 Jan;235:18–26.
24. Southern WM, Ryan TE, Reynolds MA, McCully K. Reproducibility of near-infrared spectroscopy measurements of oxidative function and postexercise recovery kinetics in the medial gastrocnemius muscle. *Appl Physiol Nutr Metab*. 2014 May;39(5):521–9.
25. Torres MJ, Kew KA, Ryan TE, Pennington ER, Lin C Te, Buddo KA, et al. 17 $\beta$ -Estradiol Directly Lowers Mitochondrial Membrane Microviscosity and Improves Bioenergetic Function in Skeletal Muscle. *Cell Metab*. 2018;27(1):167-179.e7.
26. Ansdell P, Brownstein CG, Škarabot J, Hicks KM, Simoes DCM, Thomas K, et al. Menstrual cycle-associated modulations in neuromuscular function and fatigability of the knee extensors in eumenorrheic women. *J Appl Physiol*. 2019 Jun;126(6):1701–12.
27. Larson-Meyer DE, Newcomer BR, Hunter GR, Hetherington HP, Weinsier RL. 31P MRS measurement of mitochondrial function in skeletal muscle: reliability, force-level sensitivity and relation to whole body maximal oxygen uptake. *NMR Biomed*. 2000 Feb;13(1):14–27.
28. Hamner SR, Seth A, Delp SL. Muscle contributions to propulsion and support during running. *J Biomech*. 2010 Oct;43(14):2709–16.
29. Perrey S, Ferrari M. Muscle Oximetry in Sports Science: A Systematic Review. *Sport Med*. 2018 Mar;48(3):597–616.
30. Batterson PM, Norton MR, Hetz SE, Rohilla S, Lindsay KG, Subudhi AW, et al. Improving biologic predictors of cycling endurance performance with near-infrared spectroscopy derived measures of skeletal muscle respiration: E pluribus unum. *Physiol Rep*. 2020 Jan;8(2):e14342.
31. Sumner MD, Beard S, Pryor EK, Das I, McCully KK. Near Infrared Spectroscopy Measurements of Mitochondrial Capacity Using Partial Recovery Curves. *Front Physiol*. 2020 Feb;11:111.



# 3

## Novel standardized method for extracellular flux analysis of oxidative and glycolytic metabolism in peripheral blood mononuclear cells

Joëlle J.E. Janssen<sup>1,2</sup>, Bart Lagerwaard<sup>1,3</sup>, Annelies Bunschoten<sup>1</sup>, Huub F.J. Savelkoul<sup>2</sup>, R.J. Joost van Neerven<sup>2</sup>, Jaap Keijer<sup>1</sup>, Vincent C.J. de Boer<sup>1</sup>

<sup>1</sup> *Human and Animal Physiology, Wageningen University and Research, P.O. Box 338, 6700 AH, Wageningen, the Netherlands*

<sup>2</sup> *Cell Biology and Immunology, Wageningen University and Research, P.O. Box 338, 6700 AH, Wageningen, the Netherlands*

<sup>3</sup> *TI Food and Nutrition, P.O. Box 557, 6700 AN, Wageningen, the Netherlands*

**Sci Rep. 2021;** Jan 18;11(1):1662  
doi: 10.1038/s41598-021-81217-4

## Abstract

Analyzing metabolism of peripheral blood mononuclear cells (PBMCs) provides key opportunities to study the pathophysiology of several diseases, such as type 2 diabetes, obesity, and cancer. Extracellular flux (XF) assays provide dynamic metabolic analysis of living cells that can capture *ex vivo* cellular metabolic responses to biological stressors. To obtain reliable data from PBMCs from individuals, novel methods are needed that allow for standardization and take into account the non-adherent and highly dynamic nature of PBMCs. We developed a novel method for extracellular flux analysis of PBMCs, where we combined brightfield imaging with metabolic flux analysis and data integration in R. Multiple buffy coat donors were used to demonstrate assay linearity with low levels of variation. Our method allowed for accurate and precise estimation of XF assay parameters by reducing the standard score and standard score interquartile range of PBMC basal oxygen consumption rate and glycolytic rate. We applied our method to freshly isolated PBMCs from sixteen healthy subjects and demonstrated that our method reduced the coefficient of variation in group mean basal oxygen consumption rate and basal glycolytic rate, thereby decreasing the variation between PBMC donors. Our novel brightfield image procedure is a robust, sensitive and practical normalization method to reliably measure, compare and extrapolate XF assay data using PBMCs, thereby increasing the relevance for PBMCs as marker tissue in future clinical and biological studies and enabling the use of primary blood cells instead of immortalized cell lines for immunometabolic experiments.

## Introduction

Immune cells have a critical role in host defense and tissue homeostasis. They dynamically respond to environmental signals such as infectious stimuli and physiological stresses, which initiate immune cell activation, proliferation, differentiation, and migration. Recent evidence has linked these functional immunological parameters to alterations in cellular metabolism. Metabolic pathways do not only provide energy substrates and metabolic building blocks for immune cell proliferation, but also dictate differentiation and effector functions of immune cells (1,2). This dynamic and intimate crosstalk between cellular metabolism and immune cells has resulted in the emergence of the research field that is called immunometabolism (1,2). Dysregulation of immunometabolic pathways was shown to play a critical role in the development and progression of chronic metabolic diseases such as type 2 diabetes and obesity (3) and autoimmune disorders such as rheumatoid arthritis (4,5). Furthermore, immunomodulation of tumor cell survival can be targeted using enhancers or inhibitors of metabolic pathways resulting in lowering tumor burden in pre-clinical models.

Peripheral blood mononuclear cells (PBMCs) are a readily accessible source of cells from individuals and are commonly used in immunometabolic research. PBMCs have a single round nucleus and mainly include T- and B-lymphocytes, monocytes, dendritic cells and natural killer cells. To study how metabolic pathways serve immune cell function, PBMCs are often artificially stimulated with mitogenic compounds or vaccines (6–12). PBMCs are also used as a surrogate tissue to monitor nutritional responses (13,14) and provide predictive disease risk markers (15), because they can be sampled relatively easy and with little invasiveness. Studies in model animals have shown that certain metabolic responses of PBMCs can reflect responses in tissues that cannot or can hardly be sampled in humans, such as liver (16,17) and brain (18). As marker tissue or liquid biopsy, bioenergetic profiles of PBMCs are increasingly studied in the context of multiple physiological and pathological conditions (19–25).

To correctly interpret results from immunometabolic studies, good understanding of cellular metabolism is essential. Metabolic pathways are a complex set of controlled biochemical reactions that convert energy substrates in metabolic building blocks and ATP (26). ATP is mostly generated via oxidative phosphorylation in the mitochondria and glycolysis in the cytosol. Mitochondrial and glycolytic ATP production rates are fueled by metabolic reactions. Oxygen consumption in the oxidative phosphorylation pathway is needed for the oxidation of reducing equivalents that are generated from pyruvate and other energy substrates, which drives the

generation of mitochondrial ATP. Extracellular acidification results from lactate production in the glycolysis pathway that allows for NAD regeneration and ATP production, as well as from CO<sub>2</sub> production in the mitochondria. Therefore, measurement of extracellular oxygen fluxes (27–29) and proton fluxes (30,31) can reflect the rate and source of cellular ATP production. In extracellular flux assays, cellular oxygen consumption rates (OCR) and extracellular acidification rates (ECAR) are simultaneously measured in real-time in culture well-plates using fluorescent sensors in a Seahorse extracellular flux (XF) analyzer (32), and provides a powerful tool to study immune cell bioenergetics.

Normalization of XF assay results is critical for accurate and consistent data interpretation and comparison. Multiple parameters for XF assay data normalization in PBMCs have been used, of which normalization to the number of plated cells via pre-XF assay cell counting has been mostly applied (20,21,24,33–35). However, cell number and cell layer distribution are affected by daily and operator variation in counting, plating and handling, which can lead to inaccurate normalization. Alternative strategies such as determination of post-XF assay cellular protein content (19,22,25) or genomic DNA levels has been largely applied when using adherent cells but can introduce variation when using non-adherent cells such as PBMCs. Recent advances in XF assay normalization methods now also enable normalization to post-XF assay cell number via fluorescent imaging of Hoechst 33342 stained nuclei (36,37) or post-XF assay mitochondrial content via fluorescent imaging of MitoTracker (37). These are strategies that limit post-XF assay sample handling but requires compatibility of the XF assay chemicals with the fluorescent dyes in order to monitor the XF assay wells and might not be applicable to all cell types. Brightfield imaging of PBMCs prior to the XF assay would be a rapid and sensitive normalization strategy that limits post-assay handling of cells, performs independently of XF assay chemicals and minimizes variation introduced by counting, plating and handling. Therefore, we aim to optimize and validate brightfield image analysis of PBMCs and standardize the Seahorse XF assay workflow for human PBMCs.

## Materials and Methods

### Chemicals

Carbonyl cyanide-p-trifluoromethoxyphenylhydrazone (FCCP, C2920), antimycin A (A8674), rotenone (R8875), monensin sodium salt (monensin, M5273), 2-deoxy-glucose (2-DG, D6134), Hoechst 33342 (Hoechst, B2261), Concanavalin A (Con A, C2010), lipopolysaccharides (LPS) from *Escherichia coli* (L2637), bovine serum

albumin (BSA, A6003), Triton-X 100 (T8787), sodium chloride (S9888) and Roswell Park Memorial Institute (RPMI) 1640 medium powder without phenol red and HEPES (R8755) were purchased from Sigma-Aldrich (St. Louis, Missouri, USA). RPMI 1640 medium without phenol red and HEPES (11835030), Dulbecco's phosphate-buffered saline (DPBS, 14190094), Hanks' Balanced Salt Solution (HBSS, 14175095), and penicillin-streptomycin (15140122) were purchased from Thermo Fisher Scientific (Pittsburgh, Pennsylvania, USA). XF RPMI assay medium pH 7.4 (103576-100), XF 1.0 M glucose (103576-100), XF 100 mM pyruvate (103578-100) and XF 200 mM glutamine (103579-100) were purchased from Seahorse Biosciences, Agilent Technologies (Santa Clara, California, USA). Interleukin 4 (IL4, 214-14) and interferon-gamma (IFN $\gamma$ , 315-05) were purchased from Peprotech (London, UK).

### PBMC donors

Buffy coats (50 mL) obtained from three individual healthy blood donors (donor A, B and C) were independently received from Sanquin Blood Bank (Nijmegen, the Netherlands) and used for development, optimization and validation of the method on independent days. The optimized and validated method was applied to PBMC analysis of freshly drawn blood samples from sixteen healthy young female individuals (18 – 28 years of age, BMI 18.5 – 25 kg/m<sup>2</sup>) from the local university and community population. None of the participants had a history of cardiovascular, respiratory, hematological or metabolic disease including any medication. None of the participants had anemia (hemoglobin concentration < 12 g/dL), which was verified by using a HemoCue Hb 201 microcuvette (HemoCue AB, Sweden). None of the subjects were regular smokers (having more than 5 cigarettes per week) or used recreational drugs during the study. Subjects were not pregnant or lactating and did not use any hormonal contraceptives with exception of the birth control pill. All subjects were measured within the end of the follicular phase until menstruation. Written informed consent was obtained from every participant included in the study. The protocol for collection and handling of human samples was ethically approved by the medical ethical committee of Wageningen University & Research with reference number NL70136.081.19 and registered in the Dutch trial register (NL7891). All procedures performed were in accordance with the ethical standards of the institutional and/or national research committee and with the 1964 Helsinki declaration. Blood samples (5 x 10 mL) were collected from these participants by venipuncture in vacutainers containing dipotassium (K<sub>2</sub>-) ethylenediaminetetraacetic acid (EDTA) (K<sub>2</sub>-EDTA, BD Biosciences, Vianen, the Netherlands, 367525) as anticoagulant and processed within 30 minutes after blood collection.

### PBMC isolation

Buffy coats and EDTA-collected blood were diluted with DPBS (1X) without magnesium and calcium supplemented with sodium citrate buffer (1% v/v) as anticoagulant in a ratio of 1:4 and 1:1, respectively. Diluted blood was carefully poured into Leucosep tubes (Thermo Fisher Scientific, Pittsburgh, Pennsylvania, USA, 227289) that were filled with Ficoll Paque Plus (15 mL, GE Healthcare, Marlborough, Massachusetts, USA, 17144003) followed by density gradient centrifugation for 10 minutes at 1000g at room temperature (RT) with acceleration five and zero braking. The PBMC fraction was collected using sterile Pasteur pipettes and centrifugated for 10 minutes at 600g at RT with brake to concentrate the PBMC layer and facilitate removal of residual Ficoll and plasma. Supernatant was discarded and cells were three times washed using DPBS (1X, 20 mL) without magnesium and calcium supplemented with sodium citrate buffer (1% v/v) and fetal bovine serum (FBS, 2% v/v) and centrifugated for 7 minutes at 250g at RT. Supernatant was discarded and cells were resuspended in RPMI 1640 medium without phenol red and HEPES (30 mL, Thermo Fisher Scientific, 11835030) supplemented with FBS (10% v/v). Total PBMC number and PBMC viability was determined for each donor in a 1:10 dilution using acridine orange and propidium iodide staining (ViaStain, Nexcelom Bioscience, Lawrence, Massachusetts, USA, CS2-0106) in a Nexcelcom Cell Counter (Nexcelcom Bioscience) in fluorescent mode (n = 8). Cell viability was evaluated as absolute numbers of viable and non-viable cells and the percentage of viable over non-viable cells. All cell viabilities were > 97% as assessed using acridine orange and propidium iodide staining.

### Monocyte isolation

PBMCs were diluted to  $50 \times 10^6$  cells/mL in RPMI 1640 medium with phenol red and without HEPES (Thermo Fisher Scientific, 11875085).  $120 - 150 \times 10^6$  PBMCs (3 mL) were loaded over hyperosmotic Percoll Plus solution (10 mL) containing 48.5% Percoll Plus (17544502 Cytiva, Marlborough, Massachusetts, USA), 41.5% sterile Milli-Q, and 10% 1.6M NaCl, followed by density gradient centrifugation for 15 minutes at 580g at RT with acceleration five and zero braking. The monocyte fraction was collected using sterile Pasteur pipettes and cells were washed three times with DPBS (1X, 50 mL) without magnesium and calcium supplemented with sodium citrate buffer (1% v/v) and fetal bovine serum (FBS, 2% v/v) and centrifugated for 7 minutes at 400g at RT. Supernatant was discarded and cells were resuspended in RPMI 1640 medium with phenol red and without HEPES (10 mL, Thermo Fisher Scientific, 11875085) supplemented with 10% FBS. Total monocyte number and monocyte viability was determined for each donor using ViaStain in a Nexcelcom Cell Counter in fluorescent mode (n = 8). Cell viability was evaluated as absolute

numbers of viable and non-viable cells and the percentage of viable over non-viable cells. All cell viabilities were > 97% as assessed using acridine orange and propidium iodide staining. XF assay measurements and total protein analysis were performed as described below.

### RAW 264.7 cell culture

RAW 264.7 mouse macrophage-like cells (ATCC, Rockville, USA) were cultured at  $50 \times 10^3$  cells / well ( $n = 8$ ) in Seahorse XF96 cell plates (Seahorse Bioscience, Agilent Technologies, Santa Clara, USA) in prepared RPMI 1640 without phenol red and HEPES (Sigma-Aldrich, R8755) supplemented with FBS (10% v/v), penicillin-streptomycin (5% v/v) and sodium bicarbonate (2 g/L) and were left unstimulated (M0 macrophages) or were incubated with LPS (1  $\mu$ g/mL) plus IFN $\gamma$  (20 ng/mL, M1 macrophages) or IL4 (20 ng/mL, M2 macrophages) for 24 hours in a humidified atmosphere at 37°C and 5% CO<sub>2</sub> level. On the next day, XF assay measurements were performed as described below. Afterwards, medium was discarded by gentle pipetting and cells were washed with HBSS (1X) without magnesium and calcium followed by cell lysis in NaOH (0.1M, Merck Millipore, Burlington, Massachusetts, United States, 106462). Samples were stored at -20°C for later protein level determination.

### XF analysis with Seahorse XFe96 analyzer

OCR and ECAR measurements were performed in a Seahorse XFe96 Analyzer (Seahorse Biosciences). For PBMCs isolated from donor A, B and C, 50 – 300,000 PBMCs per well ( $n = 14 - 16$ ) were plated onto Cell-Tak (Corning, New York, USA, 354240) coated XF96 cell plates in XF RPMI assay medium pH 7.4 (50  $\mu$ L, XF assay medium) supplemented with XF glucose (11 mM), XF pyruvate (1 mM) and XF glutamine (2 mM) and left for 10 minutes at RT. For PBMCs isolated from the sixteen healthy young female adults, 75 – 300,000 PBMCs per well ( $n = 3 - 4$ ) were plated for the calibration curve used for normalization and 225,000 PBMCs per well ( $n = 8$ ) were plated for reliable determination of basal OCR and GR responses. For monocytes used for total protein analysis, monocytes from donor X, Y and Z were plated at 150 – 300,000 cells per well ( $n = 8$ ) and for monocytes used for PIXI analysis, monocytes from donor D, E and F were plated at 75 – 225,000 cells per well ( $n = 8$ ). After seeding, cell plate was centrifugated for 1.5 minutes at 200g at RT with acceleration one and zero braking. Afterwards, an additional volume of XF assay medium (130  $\mu$ L) was added to the cells and cells were incubated for 30 minutes at 37°C without CO<sub>2</sub>. XF measurements included serial injections of FCCP (1.25  $\mu$ M), antimycin A (2.5  $\mu$ M) plus rotenone (1.25  $\mu$ M), and monensin (20  $\mu$ M) plus Hoechst (4  $\mu$ M) or XF assay medium plus Hoechst (4  $\mu$ M). The XF assay protocol consisted of twelve measurement cycles in total of which each cycle included 5

minutes of which 2 minutes mixing, 0 minutes waiting, 3 minutes measuring. In real-time activation XF assays, an additional injection of Con A (25 µg/mL, for real-time activated PBMCs) or XF assay medium (for quiescent PBMCs) followed by six measurement cycles (30 minutes activation) prior to the injection of FCCP and the final injection consisting of XF assay medium plus Hoechst (4 µM) was substituted by 2-DG (50 mM) plus Hoechst (4 µM). After the XF assay, medium was discarded via gentle pipetting and cells were washed with HBSS (1X) without magnesium and calcium followed by cell lysis in Triton X-100 (0.1%) in Tris-HCl pH 7.5 (50 mM). Samples were stored at -20°C for later protein level determination.

### High contrast brightfield imaging

High contrast brightfield images of the inner-probe area from each well of the XF96 cell plate were obtained prior to the XF assay run using the Cytation 1 Cell Imaging Multi-Mode Reader (BioTek, Winooski, Vermont, USA) set at 37°C using a 4x objective. For one experiment (Figure 1C), post-XF assay brightfield images were also obtained. LED intensity (5) and integration time (70 ms) were kept constant between donors and study subjects; focal height was adjusted per plate to obtain the suitable focus for proper image analysis (as represented at the top of Figure 2B). Image quality was checked based on visual inspection of the pictures.

### Brightfield image analysis in R

Original brightfield images were processed and quantified using an in-house generated R script that used the EBImage package available in Bioconductor (38) and included four steps. First a Gaussian blur low-pass filter was applied to generate a background image, followed by subtraction of the background image from the original image. Thereafter the background corrected image was inverted and as a final step 5% of the inverted image was cropped to remove potential boundary noise from the XF assay plate nodges. This in-house generated R script is available from the corresponding author upon request. The final processed images were used to calculate the total pixel intensity.

### Cellular protein level determination

Protein content in each well was determined using the DC Protein Assay kit (5000111, Bio-Rad, Hercules, California, USA) according to the manufacturer's protocol for M0, M1 and M2 RAW 264.7 macrophages (n = 8) and PBMCs from three independent donors (A, B and C, n = 14 – 16). Absorbance was measured using a BioTek Synergy HT plate reader and a standard curve of BSA (0.2%) in Triton X-100 (0.1%) in Tris-HCl pH 7.5 (50 mM) or NaOH (0.1M, Merck Millipore, Burlington, Massachusetts, United States, 106462).

### Hoechst staining and high-content fluorescent imaging

Hoechst (4  $\mu$ M final concentration) was added as a final 10x injection in the XF assay to stain PBMC nuclei. Fluorescent images of the inner-probe area from each well of the XF96 cell plate were obtained immediately after the XF assay run using the Cytation 1 imaging reader (BioTek, Winooski, Vermont, USA) set at 37°C, using a 4x objective and a 365 nm LED in combination with an EX337 EM447 filter cube

### Statistical analysis

Data are presented as mean  $\pm$  standard deviation (SD), unless indicated otherwise. Statistical analyses were performed using GraphPad Prism v.8 (GraphPad Software, CA, USA). Regression analyses using polynomial fits were used to transform total pixel intensity values into cell numbers and to compare correlations between variables. Normality was tested using Shapiro-Wilk normality tests, and Brown-Forsythe tests were used to test for equal variances. Mean OCR and GR levels between donors were compared one-way ANOVA analysis with Tukey post-hoc testing for multiple comparisons. Raw and normalized means were compared using a two-sided paired Student's t-test. All statistical tests assumed normality and equal variances. P-values < 0.05 were considered as statistically significant. \*P < 0.05, \*\*P < 0.01, \*\*\*P < 0.001, \*\*\*\*P < 0.0001.

## Results

### PBMC post-XF assay normalization using total protein analysis or fluorescent nuclear staining introduces high well to well variation

Since variation in plating efficiency could introduce bias in analyzing XF assay results, we tested whether total protein analysis would be suitable for normalizing PBMC XF assay results. For this, we plated human-derived PBMCs on Cell-Tak coated assay plates, to have the PBMC stick to the bottom of the well. For comparison, we used adherent RAW 264.7 macrophages (M0) and stimulated them towards LPS/IFN $\gamma$ -induced (M1) and IL4-induced (M2) states, and we used human-derived monocytes that were plated on Cell-Tak coated assay plates, but have the intrinsic property of attaching to wells better than PBMCs (39). The mean coefficient of variation (CV) of total protein concentration for RAW264.7 cells was  $10.3 \pm 3.2\%$ ,  $7.8 \pm 2.9\%$  and  $9.5 \pm 3.1\%$  for M0, M1 and M2 RAW 264.7 macrophages, respectively (Figure 1A). For monocytes, mean CV of post-XF assay total protein concentration were  $5.18 \pm 1.96\%$ ,  $4.88 \pm 2.27\%$  and  $3.22 \pm 1.16\%$  for donor X, Y and Z, respectively (Figure 1B). On the other hand, mean CV total protein concentration in wells for PBMC analysis was  $46.8 \pm 18.0\%$ ,  $35.4 \pm 19.5\%$  and  $46.1 \pm 29.3\%$  for PBMCs independently obtained from three different donors, A, B and C,

respectively (**Figure 1C**). The relatively high CV for PBMCs as compared to RAW 264.7 macrophages and monocytes indicated that determination of total protein levels introduced higher variation between wells for PBMC XF assays than for XF assays with adherent RAW264.7 macrophages and monocytes, likely due to a higher loss of PBMCs compared to RAW 264.7 macrophages and monocytes after removal of XF assay medium and washing of the cells.

To determine cell number in XF assay plates for PBMC XF analysis, we next used a method in which cells are quantified using Hoechst stained nuclei (36,37). Although clear nuclear staining signals were observed, overlay of fluorescence images with brightfield images showed that not all PBMCs were stained with (inset **Figure 1D**). Especially, when XF assays were performed with injections of the  $\text{Na}^+/\text{K}^+$ -ATPase activator monensin, which maximizes glycolytic rate, we only observed partial staining of wells (**Figure 1D**) and nuclei were clearly less stained than without monensin injection (inset **Figure 1D** and **Supplementary Figure S1**), possibly indicating that monensin limits the accumulation of Hoechst in PBMCs.

Seahorse XF assay experimental set-ups allow additions of multiple acute immunological or chemical stimuli sequentially or in parallel. The use of immunological stimuli that alter metabolic and immunological cell states can also lead to changes in morphological characteristics of PBMCs, which could hamper post-XF assay image analysis of Hoechst-stained cells. Therefore, we compared the response of naïve PBMCs that remain in their quiescent, steady state during the time course of the XF assay with the response of PBMCs that were *in situ* activated with 25  $\mu\text{g/mL}$  Con A, a mitogenic lectin that induces T-lymphocyte activation and proliferation (12,40) in the presence of monocytes (41). Whereas cell morphology and localization of quiescent PBMCs remain unaffected during the time course of the XF assay (inset **Figure 1E** and **Supplementary Figure S1**), real-time activation of T-lymphocyte subsets within the PBMC pool resulted in blast transformation of T-lymphocytes and migration of the cells within the monolayer on the XF cell plate (inset **Figure 1E** and **Supplementary Figure S1**), which impeded counting of separate Hoechst stained nuclei (**Supplementary Figure S1**) compared to quiescent PBMCs (**Supplementary Figure S1**). This effect was even more pronounced after monensin injection (**Supplementary Figure S1**) which was similar to our observations with quiescent PBMCs (**Figure 1D** and **Supplementary Figure S1**). Thus, in our hands, Hoechst staining to normalize XF assay data to cell number was not applicable, especially in assays where we stimulated PBMCs with immunological, metabolic or chemical stimuli.

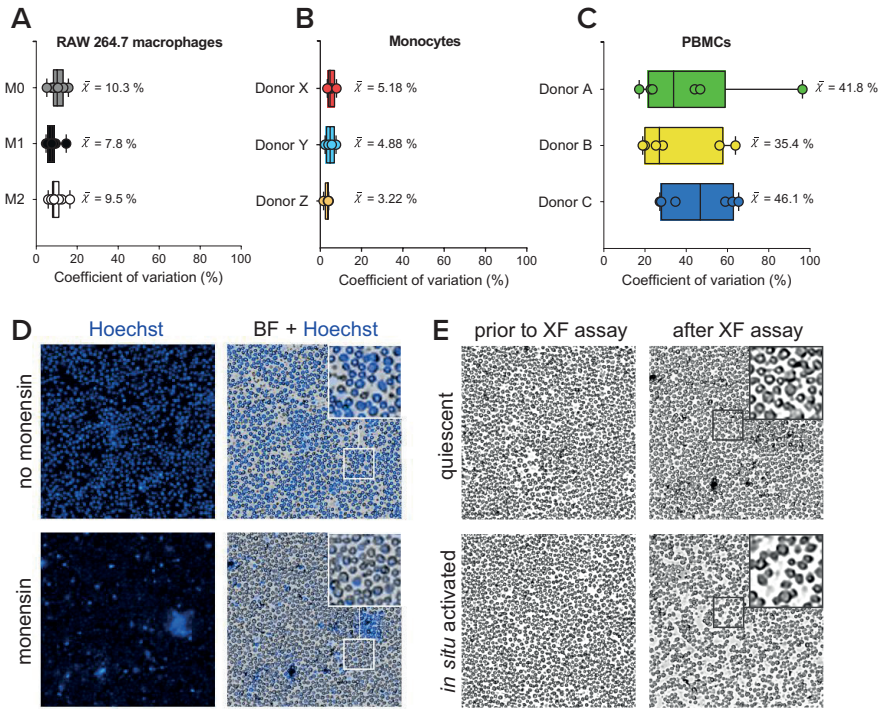


**Figure 1: Normalization strategies that rely on post-XF assay measurements introduce high variation when using PBMCs. (A)** Coefficients of variation (CV in %) in post-XF assay total protein levels of adherent RAW 264.7 macrophages in an unpolarized (M0), LPS/IFN $\gamma$  induced (M1 polarized) and IL4 induced (M2 polarized) state ( $50 \times 10^3$  cells / well /  $n = 8$ ), determined for each XF assay condition ( $\odot$ ) and represented as median + range ( $\blacksquare$ ); means are represented as  $\bar{x}$ -bar. **(B)** CV's in post-XF assay protein levels of adherent monocytes ( $150 - 300 \times 10^3$  cells / well,  $n = 8$ ) from three donors, calculated for each seeding density ( $\odot$ ) and represented as median + range ( $\blacksquare$ ); means are represented as  $\bar{x}$ -bar. **(C)** CV's in post-XF assay protein levels of non-adherent PBMCs ( $50 - 300 \times 10^3$  cells / well,  $n = 14 - 16$ ) from three independent donors, calculated for each seeding density ( $\odot$ ) and represented as median + range ( $\blacksquare$ ); means are represented as  $\bar{x}$ -bar. **(D)** The effect of XF assay injection strategies on post-XF assay fluorescent imaging. Brightfield images were obtained after the XF assay in naive PBMCs injected with Hoechst ( $4 \mu\text{M}$ ) plus 2-deoxyglucose ( $50 \text{ mM}$ , top, no monensin) or Hoechst ( $4 \mu\text{M}$ ) plus monensin ( $20 \mu\text{M}$ , bottom) ( $225 \times 10^3$  cells / well,  $n = 16$ ). Representative images of the middle of the wells is shown (4x objective). **(E)** The effect of *in situ* PBMC activation during the XF assay run on post-XF assay cell morphology. Brightfield images were taken prior to the XF assay (left) and after the XF assay (right) in naive, unstimulated PBMCs (top) and in PBMCs that were *in situ* stimulated with Con A for 90 minutes during the XF assay run (bottom) ( $225 \times 10^3$  cells / well,  $n = 16$ ). Representative images of the middle of the wells are shown (4x objective).

### Development of a pre-XF assay brightfield imaging tool

Since post-XF assay total protein analysis and nuclear Hoechst staining was found unsuitable for PBMC XF assay normalization, we set-out to validate a new method for normalizing PBMC XF assay data based on brightfield image analysis prior to the XF assay (Figure 2A). To build this brightfield image analysis tool, PBMCs were plated onto coated XF cell plates in seeding densities ranging from 50,000 to 300,000 cells per well (Figure 2B, top). This range was chosen to achieve a stepwise increase in plated cell number until the cell monolayer covered the entire well. Brightfield images of the inner-probe area from each well were taken using the Cytation 1 imaging reader and processed and quantified using an in-house generated R script (Figure 2B, bottom). The combined brightfield imaging procedure and image analysis was called ‘R-integrated pixel intensity (PIXI) analysis’, with total pixel intensity as normalization parameter. To examine if the size of the original brightfield image had an effect on the relationship between the number of plated cells and total pixel intensity, each border of the processed image was cropped with percentages ranging from 5 to 25% (Figure 2C). Total pixel intensity was significantly correlated to the number of plated cells for all cropping percentages (Pearson  $R^2 = 0.97 - 0.98$ ,  $P < 0.001$ , Figure 2D), showing a strong linear relationship and indicating that cropping did not alter the relative differences in total pixel intensity between the seeding densities. To rule out possible imaging artefacts that could be introduced with imprecise positioning of the wells under the microscope (Supplementary Figure S2), we used 5% border cropping of all images in further experiments. Next, we assessed cell subset contributions to the overall brightfield image in each well, based on the analysis of cell diameter using automated analysis in the Cytation 1 Cell Analysis software. Different cell populations were clearly distinguishable and were accurately quantified. The distribution of cell subsets in images of different cell densities were not uniform and appeared not to be linear with plated cell density (Supplementary Figure S3). At higher cell plating densities, the contribution of the smallest cell types, like the platelets, becomes much smaller than at lower cell plating densities, indicating that XF analysis at high cell densities might not be representative for the whole PBMC population and thus plating density should be carefully considered when performing PBMC XF assay experiments.

### PIXI analysis from brightfield images as a reproducible image analysis tool

To investigate whether the linear relationship between total pixel intensity, and the number of plated PBMCs isolated from buffy coats was reproducible across multiple, independently measured PBMC donors, brightfield images from three different donors were analyzed. Significant correlations between total pixel intensity

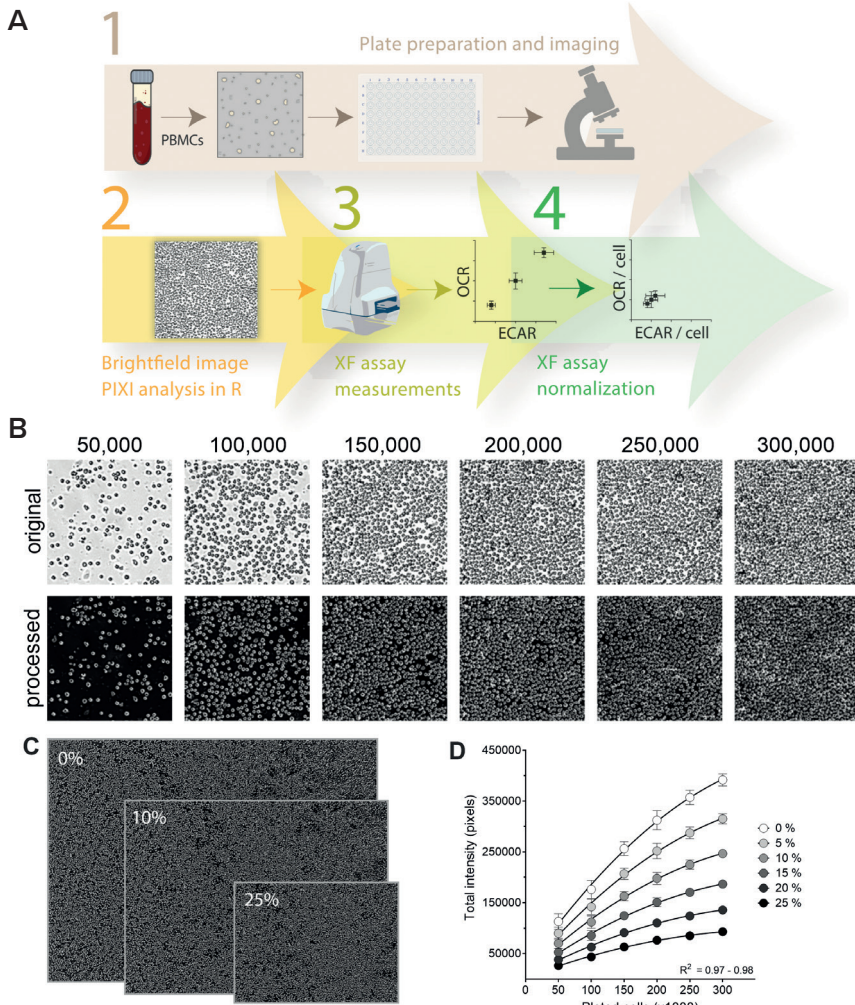


**Figure 2: R-integrated pixel intensity (PIXI) analysis from brightfield images integrated in the PBMC XF assay workflow.** (A) Method workflow for PBMC XF assay data normalization using brightfield image analysis. (B) Original pre-XF assay brightfield images (top, 4x objective) were processed using an in-house generated R script, generating images in which the total pixel intensity was quantified (bottom). A magnification from the middle of the brightfield image is shown for each seeding density ( $n = 14 - 16$ ), for one donor. (C) Effect of 0%, 10% and 25% image border cropping on the size of the processed image at a seeding density of 200,000 cells/well. Images have the same scale bar. (D) Effect of border cropping percentage (0 - 25%) on the curve fit of plated cells vs. total pixel intensity values.

and the number of plated cells were found for donor A, B and C, respectively (Pearson  $R^2 = 0.98, 0.99$  and  $0.98$ ,  $P < 0.001$ , **Figure 3A**). Although many studies use PBMCs for their immunometabolic assays, individual PBMC subpopulations, such as monocytes (42,43) or T-lymphocytes (44,45), are often separated from the total PBMC pool for specific downstream immunological or metabolic assays. Therefore, monocytes were isolated from the total PBMC pools of three buffy coat donors and plated onto Cell-Tak coated assay plates in seeding densities ranging from 75,000 to 225,000 cells per well, followed by brightfield imaging and PIXI analysis (**Supplementary Figure S4A**). Significant correlations between total pixel intensity and the number of plated monocytes were found for donor D, E and F, respectively (Pearson  $R^2 = 0.99$  ( $P < 0.01$ ),  $0.97$  ( $P < 0.05$ ) and  $0.98$  ( $p < 0.01$ ), **Supplementary Figure S4B**), showing the potency of PIXI analysis in more specific fields of PBMC research.

The calibration curve between PBMC cell number and total pixel intensity was used to transform total pixel intensity to the corresponding cell number for each individual well using second-order polynomial regression analyses, referred to as 'PIXI analyzed cells'. Next, we compared the mean CVs of replicate wells of identical conditions, with the mean CVs of the cell counting results of the different donors. To determine the technical variation of the PIXI analysis tool, mean CVs were calculated and compared to the mean CVs obtained with cell counts of the total PBMC pool as an alternative and widely used pre-XF assay normalization parameter. Mean CVs in total pixel intensity between wells were  $7.1 \pm 4.1\%$ ,  $7.1 \pm 4.5\%$  and  $8.3 \pm 5.2\%$  for donor A, B and C, respectively, whereas the CV in cell counts were 13.0%, 10.2% and 12.4% for (**Figure 3B**). Since the cell plating and processing steps subsequently to cell counting also introduce variation, and brightfield images are obtained without additional steps before the XF assay, PIXI analysis outperforms cell counts, even though mean CV differences between PIXI analysis and cell counts were small. From these experiments we concluded that PIXI analysis from brightfield images can be used as a reproducible image analysis tool to quantify PBMCs with low levels of technical variation.

### Response of XF assay parameters to increasing cell density is preserved after PIXI analysis

To determine the effect of brightfield image normalization on XF assay parameters, initial OCR, basal OCR, FCCP-uncoupled OCR, basal glycolytic rate (GR) and monensin-induced GR were plotted against the number of plated cells or the number of PIXI analyzed cells. We used GR instead of ECAR, because GR estimates glycolysis more accurately compared to ECAR due to correction for the contribution of mitochondrial-derived  $\text{CO}_2$  production to acidification of the XF assay medium

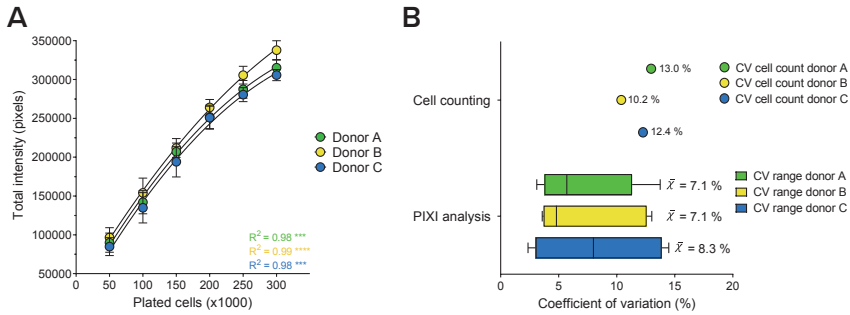


**Figure 3: R-integrated pixel intensity (PIXI) analysis from brightfield images as a reproducible image analysis tool. (A)** Curve fit of the number of plated cells ( $50 - 300 \times 10^3$  cells / well,  $n = 14 - 16$ ) vs. total brightfield pixel intensity values, indicated by Pearson correlation coefficients ( $R^2$ ). Data is represented as mean  $\pm$  SD. Calibration curves were used to transform total pixel intensity values back into cell numbers using second-order polynomial regression analyses. **(B)** Coefficients of variation (CV in %) within each donor for the cell counts of the total PBMC pool before seeding ( $n = 8$ , represented as mean) and the brightfield image PIXI analysis (represented as median  $\pm$  range; means are visualized by  $\bar{x}$ -bar).

(46). Initial OCR (Pearson  $R^2 = 0.96, 0.97$  and  $0.98$ ,  $P < 0.0001$ ), basal OCR (Pearson  $R^2 = 0.92, 0.92$  and  $0.97$ ,  $P < 0.0001$ ), FCCP-uncoupled OCR (Pearson  $R^2 = 0.95, 0.95$  and  $0.98$ ,  $P < 0.0001$ ), basal GR (Pearson  $R^2 = 0.51, 0.79$  and  $0.67$ ,  $P < 0.0001$ ) and monensin-induced GR (Pearson  $R^2 = 0.77, 0.87$  and  $0.86$ ,  $P < 0.0001$ ) all showed significant positive correlations with the number of plated cells for donor A, B and C, respectively (Figure 4A – E). Transforming the number of plated cells into the number of PIXI analyzed cells resulted in similar, significant positive correlations for initial OCR (Pearson  $R^2 = 0.96, 0.96$  and  $0.97$ ,  $P < 0.0001$ ), basal OCR (Pearson  $R^2 = 0.94, 0.93$  and  $0.96$ ,  $P < 0.0001$ ), FCCP-uncoupled OCR (Pearson  $R^2 = 0.96$  for all donors,  $P < 0.0001$ ), basal GR (Pearson  $R^2 = 0.52, 0.79$  and  $0.64$ ,  $P < 0.0001$ ) and monensin-induced GR (Pearson  $R^2 = 0.72, 0.87$  and  $0.85$ ,  $P < 0.0001$  for donor A, B and C, respectively (Figure 4F – J). To study if transformation to the number of PIXI analyzed cells altered the mean differences in XF assay parameters between donors, mean OCR and GR levels at 200,000 plated cells per well (plated cell values) were compared to mean OCR and GR levels at 200,000 PIXI analyzed cells per well (PIXI analyzed cell values). PIXI analysis resulted in the same or similar levels of significance between donor A, B and C for all measured XF assay parameters, without or with small changes in the corresponding p-values (Figure 4K – O). Based on these findings, we concluded that PIXI analysis did not interfere with biological XF assay responses, since transforming the number of plated cells into the number of PIXI analyzed cells preserved similar correlations with XF assay parameters.

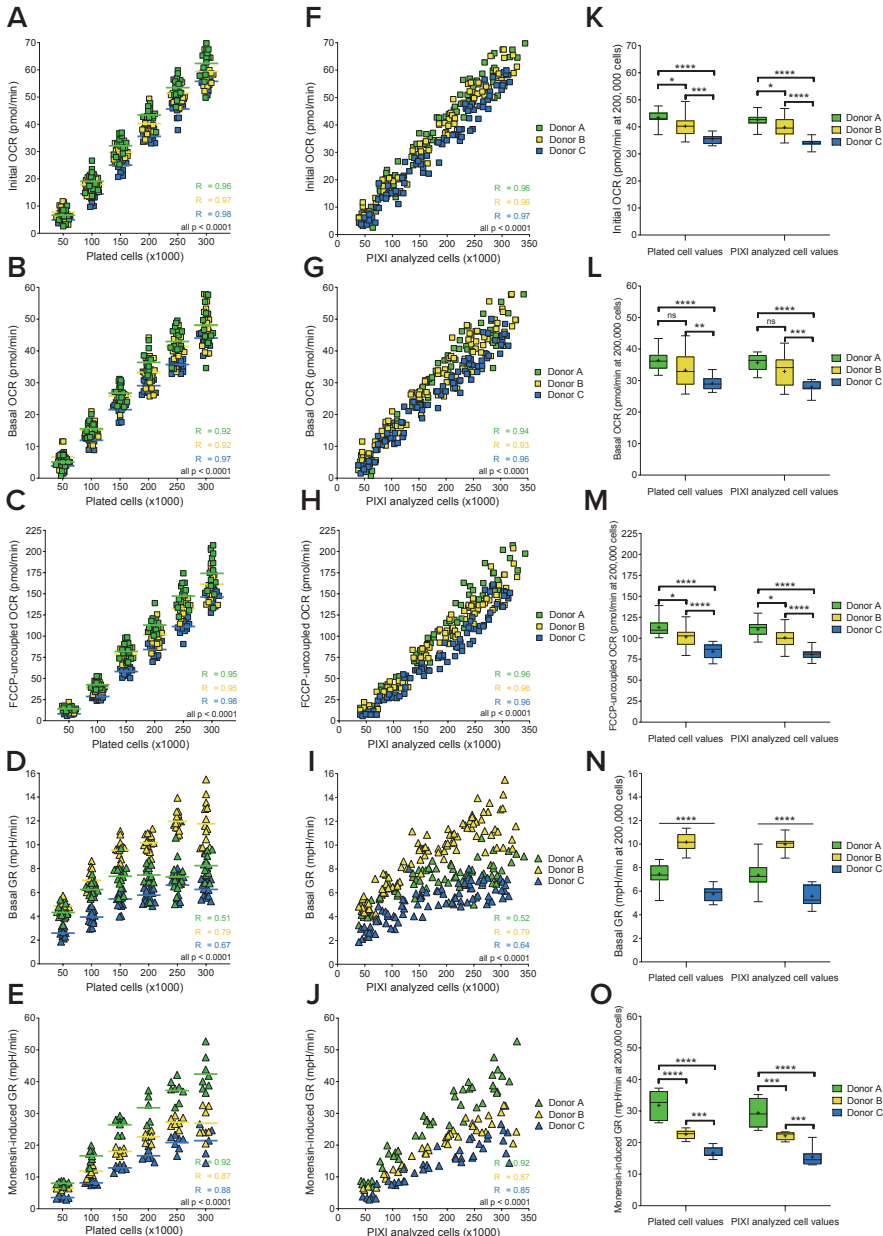


**Figure 4: PIXi analysis preserves the correlations between the number of plated cells and XF assay parameters. (A – J)** Comparison of the linear relationship between initial OCR, basal OCR, FCCP-uncoupled OCR, basal GR or monensin-induced GR and number of plated cells (A – E) or number of PIXi analyzed cells (F – J) (50 - 300 x 10<sup>3</sup> cells / well, n = 14

- 16). Means at each seeding density (**A - D**) are represented by a dash (–). (**K – O**) Comparison of mean OCR and GR levels between donor A, B and C at 200,000 plated cells (left) or at 200,000 PIXI analyzed cells (right) per well (n = 16). Data is represented as mean ± range. Means are represented by a plus sign (+). \*P < 0.05, \*\*P < 0.01, \*\*\*P < 0.001, \*\*\*\*P < 0.0001, ns = not significant.

### Brightfield image analysis is a robust normalization technique for PBMCs

To validate if brightfield image analysis is a robust method for XF assay data normalization, we studied the effect of PIXI analysis normalization on the accuracy and precision of XF assay parameter determination. The accuracy of brightfield image analysis was tested by assessing if individual observations, i.e. technical replicate values, were closer to the overall group mean after transforming the number of plated cells to the number of PIXI analyzed cells, using standard scores. Standard scores that come closer to zero indicate that individual observations are better predictors of the overall mean and therefore correspond to a higher level of accuracy. Normalization to the number of PIXI analyzed cells decreased the average standard score of initial OCR (from 0.694 to 0.663), basal OCR (from 0.684 to 0.654) and basal GR (from 0.675 to 0.668) (**Figure 5A** and **Table 1**), indicating that PIXI analysis improved the accuracy of mean XF assay parameter estimation between technical replicates. To test the precision of brightfield image analysis, the effect of PIXI analysis on the distribution of standard scores was calculated via calculation of standard score interquartile ranges (IQR). If IQRs are smaller, individual standard scores deviate less from the mean standard scores, and therefore correspond to a higher level of precision. Normalization to the number of PIXI analyzed cells lowered the average IQR of initial OCR (from 1.520 to 1.332), basal OCR (from 1.435 to 1.297) and basal GR (from 1.499 to 1.382) (**Figure 5B** and **Table 1**) which indicated that PIXI analysis resulted in higher levels of precision when estimating mean XF assay parameters between technical replicates. Overall, these results indicated that PIXI analysis resulted in accurate and precise estimation of XF assay parameters, and can therefore be considered as a robust normalization technique.

### Integration of brightfield image analysis in the Seahorse XF assay workflow in clinical studies reduced the between donor variation

Clinical studies that investigate PBMC metabolism in individuals usually perform multiple Seahorse XF assays across several weeks or months, since the necessary sample size is often larger than the amount of PBMC donors that can reliably be measured within one XF assay. To assess if brightfield image analysis can reduce

the variation between distinct PBMC donors analyzed on different days, we integrated PIXI analysis in the XF analysis of freshly isolated PBMCs from sixteen healthy lean individuals (females, 18 – 25 years of age, BMI 18.5 – 25 kg/m<sup>2</sup>). Importantly, for each donor we used a calibration curve on the same plate and was assayed for XF analysis as well as image analysis. Since the outcome for each donor is biased by both biological and technical variation, we aimed to reduce technical variation with our PIXI analysis, which can be reflected by a reduction in the coefficient of variation of the group mean. The CV of basal OCR and basal GR

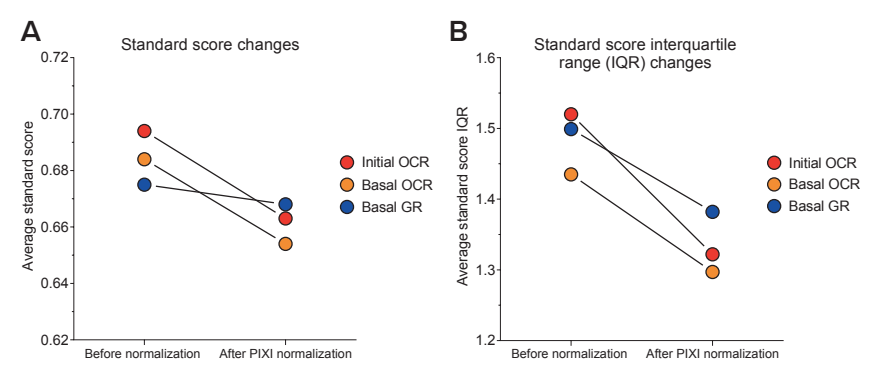


**Figure 5: The effects of PIXI analysis normalization on the standard scores and standard score interquartile ranges.** Mean standard scores and standard score interquartile ranges (IQR) of all technical replicates within each cell density (50 - 300 x 10<sup>3</sup> cells / well, n = 14 - 16) were averaged and used to create an overall average standard score and standard score IQR for each XF assay parameter (N = 18) as a measure of accuracy (standard score) and precision (IQR). **(A, B)** Effects of brightfield image PIXI analysis normalization on the average standard score **(A)** or standard score IQR **(B)** in initial OCR, basal OCR and basal GR (not significant).

**Table 1** Summary of the changes in average standard score and average IQR (represented as  $\bar{x}$ ) after brightfield image PIXI analysis normalization.

	Initial OCR		Basal OCR		Basal GR	
	Standard score ( $\bar{x}$ )	IQR ( $\bar{x}$ )	Standard score ( $\bar{x}$ )	IQR ( $\bar{x}$ )	Standard score ( $\bar{x}$ )	IQR ( $\bar{x}$ )
Before normalization	0.694	1.520	0.684	1.435	0.675	1.499
After PIXI normalization	0.663	1.322	0.654	1.297	0.668	1.382
Effect of normalization	-0.030	-0.199	-0.030	-0.138	-0.007	-0.116

decreased from 17.7% to 14.0% and 18.8 to 18.7%, respectively, when PIXI analysis was applied instead of standard analysis, i.e. normalization to the counted number of plated PBMCs (Table 2), indicating that PIXI analysis contributed to a reduction of the between donor variation in basal OCR. Basal GR variation between donors reduced only to a limited extent. To provide insight in the effect of PIXI analysis normalization on individual PBMC donors, it was assessed how PIXI analysis contributed to the relative improvement in the estimation of group mean basal OCR and basal GR. Individual basal OCR values moved closer to the group mean by PIXI analysis, compared to cell counting, in 9 out of 16 individuals with more than 5%, with an average improvement of 10.9% (Figure 6A). Individual basal OCR values from the remaining 7 individuals did not move closer to the group mean, although the average decrease was only 4.1%, with only 2 individuals showing a worsening of more than 5% (Figure 6A). This demonstrated that PIXI analysis overall contributed to a more precise estimation of the group basal OCR. Estimation of basal GR improved similarly, as 10 out of 16 individuals moved closer to the group mean, with an average improvement of 8.2% and 8 out of 10 individuals improving more than 5%, while the average percentage by which basal GR moved away from the group mean again was smaller (6.1%) and seen in a smaller number of individuals (6 out of 16, with 4 worsening more than 5%) (Figure 6B). This showed that PIXI analysis estimated the group mean basal GR more precisely. Based on these results, we concluded that integration of PIXI analysis in the Seahorse XF assay workflow decreased the variation between donors, and overall contributed to a more precise estimation of the group mean XF assay that is calculated from multiple XF assays with distinct PBMC donors.

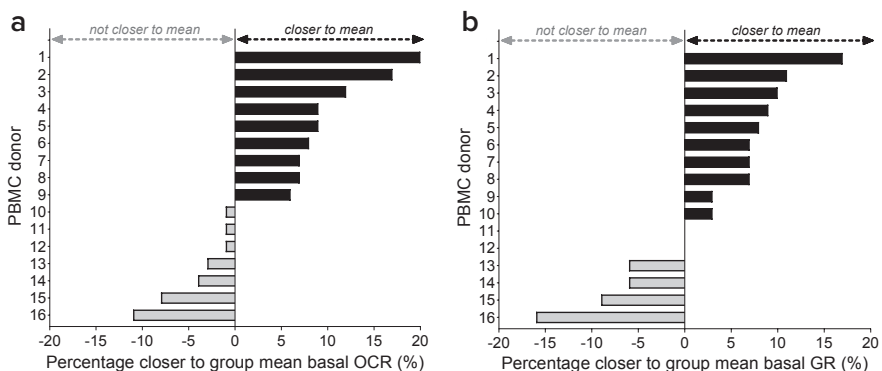


**Figure 6: Effects of PIXI analysis on the variation between PBMC donors. (A, B)** The percentage by which individual donor basal OCR (A) and basal GR (B) levels moved closer to the group mean after PIXI analysis.

**Table 2** Effects of PIXI analysis on the variation between PBMC donors.

	Basal OCR		Basal GR	
	mean $\pm$ SD (pmol/min)	CV (%)	mean $\pm$ SD (mpH/min)	CV (%)
Standard analysis	28.96 $\pm$ 5.11	17.7	6.38 $\pm$ 1.20	18.8
PIXI analysis	26.69 $\pm$ 3.74	14.0	5.94 $\pm$ 1.11	18.7
Effect of PIXI analysis	-2.27 $\pm$ -1.37	-3.7	-0.44 $\pm$ -0.09	-0.1

PBMCs were isolated from sixteen healthy lean individuals (18 – 25 years of age, BMI 18.5 – 25 kg/m<sup>2</sup>) and plated at 75 - 300 x 10<sup>3</sup> cells / well (n = 3 - 4) to generate a calibration curve that was used to transform total pixel intensity values into PIXI analyzed cell numbers. XF assay measurements were performed at 225 x 10<sup>3</sup> cells / well (n = 8) and basal OCR and basal GR levels were normalized against the number of plated cells (standard analysis) or PIXI analyzed cells (PIXI analysis). Here a summary of the changes in group mean, SD and CV for basal OCR and basal GR after standard analysis or PIXI analysis is represented.

## Discussion

The aim of this study was to optimize and validate a Seahorse XF assay workflow for human PBMCs based on brightfield imaging. This is the first study that describes the application of brightfield image analysis to obtain a normalization parameter that ensures more accurate, precise and consistent XF assay data interpretation. We developed a combined brightfield imaging and image analysis procedure called PIXI analysis that was integrated in the Seahorse XF assay workflow. The inclusion of a unique calibration curve for each donor creates a solid link between the normalization parameter and number of PBMCs per well. Brightfield image analysis showed relatively low technical variation compared to commonly used normalization methods and reduced the between donor variation when measuring different PBMC donors, highlighting the relevance of this novel normalization strategy.

Applying the PIXI method for analyzing PBMC metabolism in a young healthy human population, lowered the technical variation in OCR, allowing for better estimation of differences in PBMC OCR responses between populations. Another advantage of our brightfield image analysis method is that our procedure does not involve additional plate and cell handling steps after the XF assay, which can damage or influence the attached cell monolayer. Moreover, in-line injection of typical XF assay chemicals, like FCCP and monensin, can induce morphological changes or even cell detachment in some cell types or metabolic conditions, which will hamper normalization techniques based on post-XF assay protein, DNA or nuclei analysis. Another advantage is that pre-XF assay brightfield image

analysis allows for proper quality control and inspection of plated cells, because all 96 wells are captured and stored in a database. Since brightfield images were obtained during the necessary 30 – 60 minutes degassing step with XF assay medium at 37°C before start of the XF assay, this procedure is directly incorporated within the existing XF assay workflow. Since brightfield image PIXI analysis in isolated monocytes generated similar results as obtained in PBMCs, the PIXI method can be integrated in XF assays with isolated PBMC subsets, increasing the relevance and applicability of PIXI analysis in studies using other immune cell types than PBMCs.

We observed that brightfield image analysis to quantify PBMC number showed lower technical variation than post-XF assay total protein analysis or Hoechst nuclear staining. Brightfield image analysis did not involve any additional post-XF assay sample preparation, which is necessary for total protein content normalization (19,22,25) and demonstrated high levels of variation in our assays with non-adherent PBMCs compared to adherent RAW 264.7 cells or monocytes. Furthermore, brightfield image analysis does not require the nuclear stain Hoechst 33342 (36,37), which is especially advantageous when XF assay injections limit effective nuclear staining by Hoechst, as was observed for monensin. This ionophore increases cellular ATP demand by activating  $\text{Na}^+/\text{K}^+$ -ATPases (47) and boosts glycolytic ATP production when mitochondrial respiration is fully inhibited (48). Limited nuclear staining in the presence of monensin can potentially be attributed to monensin-induced upregulation of P-glycoprotein expression and function (49), which in turn could promote cellular exclusion of Hoechst (50–52). Brightfield image analysis is therefore especially suitable in XF assays that affect substrates for multidrug transport proteins acting on fluorescent dyes. In addition, brightfield imaging analysis could be relevant for studies aiming at metabolic characterization of multi-drug resistant cells using XF assays, as these cell types have often high expression of multidrug transport proteins such as P-glycoprotein (53,54).

Brightfield image analysis contributed to better standardization of the Seahorse XF assay workflow for human PBMCs, which is of crucial importance due to the highly dynamic nature of metabolic PBMC responses. A standardized XF assay protocol ensures reliable and comparable results across different PBMC donors, which increases the applicability of human PBMCs in experimental studies. Over the past decade, several clinical studies tested the applicability of metabolic PBMC responses as a marker in the context of multiple disease pathologies such as diabetes (19,20,34,55,56), cardiovascular disease (35,57), obesity (21), inherited metabolic diseases (22,58), neurodegenerative diseases (23,59), autoimmune disease (24) and schizophrenia (60), as well as in the context of altered physiological

conditions such as pregnancy (25) or responses to changed micronutrient status (33). Future use of brightfield image analysis in such studies will standardize the XF assay workflow and improve data interpretation and comparison across studies. This further advances the use of PBMCs as a marker tissue or liquid biopsy, which is especially relevant because PBMCs can be sampled with relative ease and is less invasive as compared to taking biopsies from other tissues. Next to the application of PBMCs in cross-sectional study designs, a standardized and validated XF assay protocol for PBMCs will likely motivate future studies to consider the use of PBMCs to investigate the effect of drug therapies, nutritional interventions, or physiological diversities.

Whereas OCR from all three donors were linearly correlated with cell number, GR correlated to a lesser extent with cell number, especially at higher cell densities. Since OCR, GR and cell number are analyzed in the same well, it seems that cellular GR is relatively inhibited at higher cell densities. Possibly this can be explained by a reduced glucose absorption or increased reabsorption of extracellular lactate when the XF assay medium is increasingly being acidified at higher cell densities. Indeed, adding excessive lactate to monocyte cultures repressed glycolysis (43,61), indicating that accumulation of lactate because of high cell density might lower GR which could explain why we did not observe a linear relationship between GR and cell number. Furthermore, although mean OCR levels were similar between donor A, B and C, mean GR levels were markedly different. A similar difference in GR between donors was observed in a study with PBMC subsets that found that PBMC derived monocytes and lymphocytes showed similar OCR but distinct extracellular acidification levels (62). Furthermore, XF analyses with freshly isolated lymphocytes has shown that *in vivo* activation of T- and B-lymphocytes also upregulates their glycolytic machinery (63,64), which suggests that glycolytic metabolism is sensitive to *in vivo* physiological alterations. Therefore, our observed OCR and GR responses might be a consequence of distinct lymphocyte to monocyte ratios within the total PBMC pool, or differences in physiological conditions between donors.

Previous studies have also focused on optimization of the XF assay workflow for human PBMCs (25,55,62,65) and have identified multiple factors that influence XF assay measurements and data interpretation. For example, in an attempt to minimize technical variation and donor heterogeneity in larger cohort studies, the effect of PBMC cryopreservation on XF assay results has been studied (25,55,65). Although mixed results have been reported, cryopreserved and resuscitated PBMCs demonstrated generally lower mitochondrial function (25,65), and higher (65) or similar (25) glycolysis compared to freshly isolated PBMCs, indicating that

analysis of freshly isolated PBMCs is preferred. To commit to analyzing PBMCs freshly, available sample volume can become a limiting factor, especially when PBMC subsets are isolated. We showed that using our method, we were able to get accurate readings above a limit of 20 pmol/min OCR using 150,000 PBMCs per well, which is 2 to 4-fold lower than the frequently used seeding densities that range from 300,00 to 700,000 PBMCs per well (19–21,33,55). Furthermore, basal OCR and GR were still linear with cell number at this seeding density. Therefore, the use of brightfield image analysis allows researchers to obtain reliable XF assay measurements with smaller sampled blood volumes, which contributes to the refinement of human studies. Another aspect that we optimized in XF assays with PBMCs is the correction for the between donor variation and day-to-day variation. In order to account for these variations, we now performed PBMC calibration curves on all assay plates that we ran, making internal calibration possible for imaging and XF assays. Although some studies used baselining as standardization method to lower the between donor variation for Seahorse analysis (55), this is likely not a preferred method, because valuable data will be lost and only relative comparisons can be performed essentially within one experiment, making data sharing and reproducibility more difficult to achieve. Of note, our study population was a relatively homogenous population consisting of healthy young females. Thus, we analyzed PBMC metabolism in a condition where we expected relatively low level of variation to ensure validity of our findings.

Nevertheless, our study also entails some limitations. Firstly, PIXI analysis does not account for the heterogeneity of PBMCs, which can possibly influence the interpretation of XF assay results. PBMC subset frequencies can vary across individuals, but PBMCs typically consist of 70 – 85% T-lymphocytes, 5 – 10% B-lymphocytes, 5 – 20% natural killer cells, 10 – 20% monocytes and 1 – 2% dendritic cells (66,67), which are not only immunologically, but also metabolically distinct (62,68), especially upon immune cell activation (2,68–71). Therefore, pathological conditions that drive an increase in pro- or anti-inflammatory PBMC subsets will likely cause a shift in the overall bioenergetic PBMC response as well. For example, increased numbers of T-helper 17 (Th17) lymphocytes and decreased numbers of regulatory T (Treg) lymphocytes were found in type 2 diabetic patients, who showed insulin resistance and chronic low-grade inflammation (72). Whereas the anti-inflammatory properties of Treg lymphocytes drive fatty acid oxidation and thus oxidative metabolism (69), Th17 lymphocytes strongly upregulate their glycolytic machinery upon activation to boost their pro-inflammatory response (73). Together with an increased expression of pro-inflammatory markers in monocytes (74) and enhancement of the pro-inflammatory function of Th17 cells by B-lymphocytes (75), the overall PBMC profile of type 2 diabetic patients has a

pro-inflammatory phenotype compared to healthy controls, which should be taken into account in the biological interpretation of XF assay results from patient cohorts. Importantly, PBMC subset variation does not affect pre-XF assay brightfield image acquisition and PIXI analysis, and thus our proposed method is suitable for XF assay normalization in samples from patients with metabolic disease. To get additional insight into the biological interpretation of XF assay data in PBMCs, especially in pathophysiological conditions, it is needed to combine PIXI analysis with additional flow cytometry experiments for characterization of the PBMC pool. A second limitation of our study was that we did not evaluate possible (dietary) confounding factors that could influence metabolic profiles of individuals. For example, vitamin D status has been shown to influence PBMC metabolism (33,76) and vitamin D status could have thus acted as a potential confounding factor in our study population. Calton et al. showed that PBMCs from adults with low vitamin D status displayed higher oxidative and glycolytic metabolism as well as increased systemic inflammation markers, which both decreased when vitamin D status improved (33,76). Since all our study subjects have been measured in late autumn and winter season, at least seasonal variation in vitamin D status, as indicated by Calton et al. (33), is likely not contributing to the observed heterogeneity in our study population. It would be interesting to assess vitamin D status and the influence of other (marginal) vitamin deficiencies on PBMC metabolism in follow up studies. Since effects of (marginal) vitamin deficiencies on PBMC metabolism are likely small, using PIXI analysis will likely improve the data quality and will allow for lower sample sizes.

In conclusion, we optimized, validated and standardized the Seahorse XF assay workflow for human PBMCs by using a combined brightfield imaging and analysis approach called 'R-integrated pixel intensity (PIXI) analysis'. We demonstrated that brightfield image analysis is a robust, sensitive and practical normalization method to reliably measure, compare and extrapolate XF assay data using PBMCs, thereby increasing the relevance for PBMCs as marker tissue in future clinical studies and enabling the use of primary blood cells instead of immortalized cell lines for immunometabolic experiments.

### Acknowledgements

The authors greatly acknowledge the commitment of the volunteers who participated in the study. We acknowledge Anna Bekebrede and Taolin Yuan for assistance with conceptualization of the method.

### Authors' contributions

Conceptualization, J.J.E.J., B.L., V.C.J.d.B.; Methodology, J.J.E.J., V.C.J.d.B.; Software, V.C.J.d.B.; Validation, J.J.E.J., B.L., V.C.J.d.B.; Formal analysis, J.J.E.J., V.C.J.d.B.; Investigation, J.J.E.J., B.L.; Resources, A.B.; Data curation, V.C.J.d.B.; Writing – Original draft preparation, J.J.E.J., Writing – Review and Editing, J.J.E.J., B.L., H.F.J.S., R.J.J.v.N., J.K., V.C.J.d.B.; Visualization, J.J.E.J., V.C.J.d.B.; Supervision, J.K., V.C.J.d.B.; Funding acquisition, J.J.E.J., J.K., V.C.J.d.B.

### Competing interests

The authors declare that they have no competing interests.

### Availability of data and materials

All data supporting the findings of this study included in this published article and its supplementary information files. The in-house generated R script is available from the corresponding author upon request.

## References

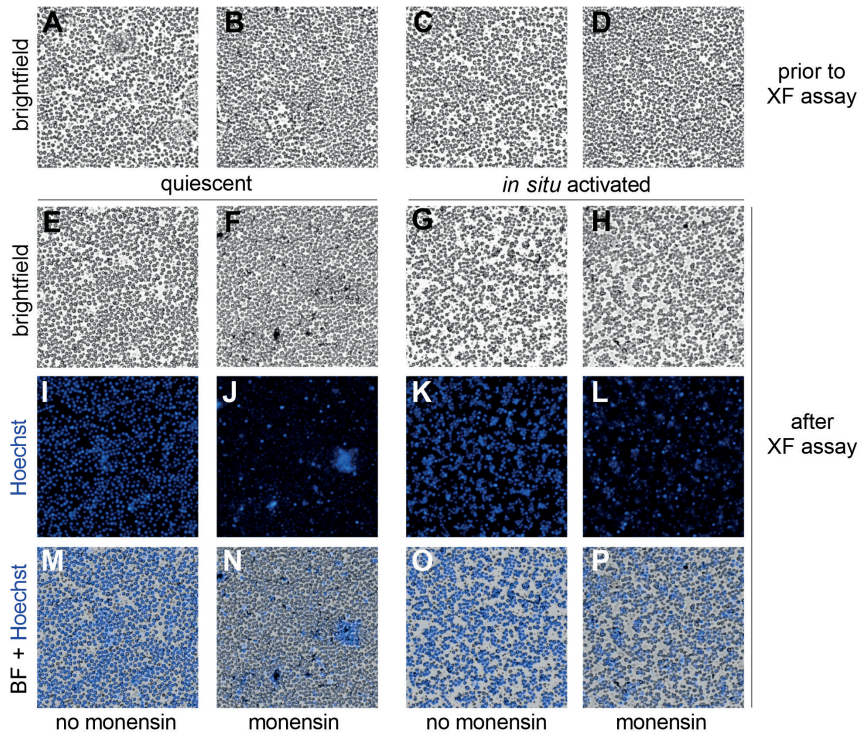
1. Buck MD, Sowell RT, Kaech SM, Pearce EL. Metabolic Instruction of Immunity. *Cell*. 2017;169(4):570–86.
2. O'Neill LAJ, Kishton RJ, Rathmell J. A guide to immunometabolism for immunologists. *Nat Rev Immunol*. 2016;16(9):553–65.
3. Hotamisligil GS. Foundations of Immunometabolism and Implications for Metabolic Health and Disease. *Immunity*. 2017 Sep;47(3):406–20.
4. Rhoads JP, Major AS, Rathmell JC. Fine tuning of immunometabolism for the treatment of rheumatic diseases. *Nat Rev Rheumatol*. 2017;13(5):313–20.
5. Pålsson-McDermott EM, O'Neill LAJ. Targeting immunometabolism as an anti-inflammatory strategy. *Cell Res*. 2020;30(4):300–14.
6. Izquierdo E, Cuevas VD, Fernández-Arroyo S, Riera-Borrull M, Orta-Zavalza E, Joven J, et al. Reshaping of Human Macrophage Polarization through Modulation of Glucose Catabolic Pathways. *J Immunol*. 2015;195(5):2442–51.
7. Van den Bossche J, Baardman J, Otto NAA, van der Velden S, Neele AEE, van den Berg SM, et al. Mitochondrial Dysfunction Prevents Repolarization of Inflammatory Macrophages. *Cell Rep*. 2016 Oct 11;17(3):684–96.
8. Cichocki F, Wu C-Y, Zhang B, Felices M, Tesi B, Tuininga K, et al. ARID5B regulates metabolic programming in human adaptive NK cells. *J Exp Med*. 2018 Sep;215(9):2379–95.
9. De Rosa V, Galgani M, Porcellini A, Colamatteo A, Santopaolo M, Zuchegna C, et al. Glycolysis controls the induction of human regulatory T cells by modulating the expression of FOXP3 exon 2 splicing variants. *Nat Immunol*. 2015;16(11):1174–84.
10. Frauwirth KA, Riley JL, Harris MH, Parry R V, Rathmell JC, Plas DR, et al. The CD28 Signaling Pathway Regulates Glucose Metabolism. *Immunity*. 2002 Jun 1;16(6):769–77.
11. Jones N, Cronin JG, Dolton G, Panetti S, Schauenburg AJ, Galloway SAE, et al. Metabolic Adaptation of Human CD4+ and CD8+ T-Cells to T-Cell Receptor-Mediated Stimulation. Vol. 8, *Frontiers in Immunology*. 2017. p. 1516.
12. Schmid D, Burmester GR, Tripmacher R, Kuhnke A, Buttgerit F. Bioenergetics of Human Peripheral Blood Mononuclear Cell Metabolism in Quiescent, Activated, and Glucocorticoid-Treated States. *Biosci Rep*. 2000;20(4):289–302.
13. Sánchez J, Bonet ML, Keijer J, Van Schothorst EM, Möller I, Chetrit C, et al. Blood cells transcriptomics as source of potential biomarkers of articular health improvement: Effects of oral intake of a rooster combs extract rich in hyaluronic acid. *Genes Nutr*. 2014;9(5).
14. Picó C, Serra F, Rodríguez AM, Keijer J, Palou A. Biomarkers of nutrition and health: New tools for new approaches. *Nutrients*. 2019;11(5):1–30.
15. Szostaczuk N, van Schothorst EM, Sánchez J, Priego T, Palou M, Bekkenkamp-Grovenstein M, et al. Identification of blood cell transcriptome-based biomarkers in adulthood predictive of increased risk to develop metabolic disorders using early life intervention rat models. *FASEB J*. 2020 Jul 1;34(7):9003–17.
16. Díaz-Rúa R, Keijer J, Caimari A, van Schothorst EM, Palou A, Oliver P. Peripheral blood mononuclear cells as a source to detect markers of homeostatic alterations caused by the intake of diets with an unbalanced macronutrient composition. *J Nutr Biochem*. 2015 Apr;26(4):398–407.
17. Caimari A, Oliver P, Rodenburg W, Keijer J, Palou A. Feeding conditions control the expression of genes involved in sterol metabolism in peripheral blood mononuclear cells of normoweight and diet-induced (cafeteria) obese rats. *J Nutr Biochem*. 2010;21(11):1127–33.
18. Reynés B, Hazebroek MK, García-Ruiz E, Keijer J, Oliver P, Palou A. Specific features of the hypothalamic leptin signaling response to cold exposure are reflected in peripheral blood mononuclear cells in rats and ferrets. *Front Physiol*. 2017;8(581):1–11.
19. Czajka A, Ajaz S, Gnudi L, Parsade CK, Jones P, Reid F, et al. Altered Mitochondrial Function, Mitochondrial DNA and Reduced Metabolic Flexibility in Patients With Diabetic Nephropathy. *EBioMedicine*. 2015;2(6):499–512.

20. Hartman M-L, Shirihaï OS, Holbrook M, Xu G, Kocherla M, Shah A, et al. Relation of mitochondrial oxygen consumption in peripheral blood mononuclear cells to vascular function in type 2 diabetes mellitus. *Vasc Med*. 2014 Feb;19(1):67–74.
21. Tyrrell DJ, Bharadwaj MS, Van Horn CG, Marsh AP, Nicklas BJ, Molina AJA. Blood-cell bioenergetics are associated with physical function and inflammation in overweight/obese older adults. *Exp Gerontol*. 2015 Oct;70:84–91.
22. Audano M, Pedretti S, Cermenati G, Brioschi E, Diaferia GR, Ghisletti S, et al. Zc3h10 is a novel mitochondrial regulator. *EMBO Rep*. 2018 Apr 1;19(4):e45531.
23. Maynard S, Hejl AM, Dinh TST, Keijzers G, Hansen ÅM, Desler C, et al. Defective mitochondrial respiration, altered dNTP pools and reduced AP endonuclease 1 activity in peripheral blood mononuclear cells of Alzheimer's disease patients. *Aging (Albany NY)*. 2015;7(10):793–815.
24. Lee H-T, Lin C-S, Pan S-C, Wu T-H, Lee C-S, Chang D-M, et al. Alterations of oxygen consumption and extracellular acidification rates by glutamine in PBMCs of SLE patients. *Mitochondrion*. 2019;44:65–74.
25. Jones N, Piasecka J, Bryant AH, Jones RH, Skibinski DOF, Francis NJ, et al. Bioenergetic analysis of human peripheral blood mononuclear cells. *Clin Exp Immunol*. 2015/07/24. 2015 Oct;182(1):69–80.
26. Erecińska M, Wilson DF. Homeostatic regulation of cellular energy metabolism. *Trends Biochem Sci*. 1978;3(4):219–23.
27. Clark LCJ. Monitor and control of blood and tissue oxygen tensions. *ASAIO J*. 1956;2(1).
28. Clark Jr. LC, Lyons C. Electrode systems for continuous monitoring in cardiovascular surgery. *Ann N Y Acad Sci*. 1962;102(1):29–45.
29. Gnaiger E, Steinlechner-Maran R, Méndez G, Eberl T, Margreiter R. Control of mitochondrial and cellular respiration by oxygen. *J Bioenerg Biomembr*. 1995;27(6):583–96.
30. Owicki JC, Parce JW. Biosensors based on the energy metabolism of living cells: the physical chemistry and cell biology of extracellular acidification. *Biosens Bioelectron*. 1992;7(4):255–72.
31. Parce JW, Owicki JC, Kercso KM, Sigal GB, Wada HG, Muir VC, et al. Detection of cell-affecting agents with a silicon biosensor. *Science (80- )*. 1989 Oct;246(4927):243–7.
32. Ferrick DA, Neilson A, Beeson C. Advances in measuring cellular bioenergetics using extracellular flux. *Drug Discov Today*. 2008;13(5):268–74.
33. Calton EK, Keane KN, Raizel R, Rowlands J, Soares MJ, Newsholme P. Winter to summer change in vitamin D status reduces systemic inflammation and bioenergetic activity of human peripheral blood mononuclear cells. *Redox Biol*. 2017;12:814–20.
34. Mahapatra G, Smith SC, Hughes TM, Wagner B, Maldjian JA, Freedman BI, et al. Blood-based bioenergetic profiling is related to differences in brain morphology in African Americans with Type 2 diabetes. *Clin Sci*. 2018 Dec 5;132(23):2509–18.
35. DeConne TM, Muñoz ER, Sanjana F, Hobson JC, Martens CR. Cardiometabolic risk factors are associated with immune cell mitochondrial respiration in humans. *Am J Physiol Circ Physiol*. 2020 Jul 17;319:H481–487.
36. Kovalenko I, Glasauer A, Schöckel L, Sauter DRP, Ehrmann A, Sohler F, et al. Identification of KCa 3.1 channel as a novel regulator of oxidative phosphorylation in a subset of pancreatic carcinoma cell lines. *PLoS One*. 2016;11(8):1–20.
37. Little AC, Kovalenko I, Goo LE, Hong HS, Kerk SA, Yates JA, et al. High-content fluorescence imaging with the metabolic flux assay reveals insights into mitochondrial properties and functions. *Commun Biol*. 2020;3(1):271.
38. Pau G, Fuchs F, Sklyar O, Boutros M HW. EBIImage—an R package for image processing with applications to cellular phenotypes. *Bioinformatics*. 2010;26(7):979–981.
39. Bennett S, Breit SN. Variables in the isolation and culture of human monocytes that are of particular relevance to studies of HIV. *J Leukoc Biol*. 1994 Sep;56(3):236–40.
40. Krauss S, Buttgerit F, Brand MD. Effects of the mitogen concanavalin A on pathways of thymocyte energy metabolism. *Biochim Biophys Acta - Bioenerg*. 1999;1412(2):129–38.
41. Hedfors E, Holm G, Pettersson D. Activation of human peripheral blood lymphocytes by concanavalin A dependence of monocytes. *Clin Exp Immunol*. 1975;22(2):223–9.

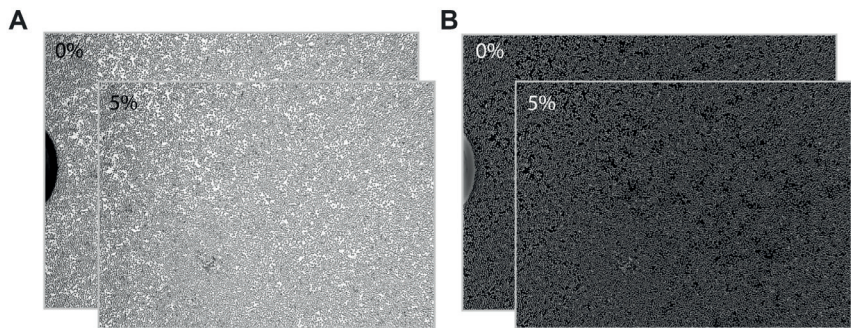
42. Lachmandas E, Boutens L, Ratter JM, Hijmans A, Hooiveld GJ, Joosten LAB, et al. Microbial stimulation of different Toll-like receptor signalling pathways induces diverse metabolic programmes in human monocytes. *Nat Microbiol.* 2016;2(3):16246.
43. Dietl K, Renner K, Dettmer K, Timischl B, Eberhart K, Dorn C, et al. Lactic Acid and Acidification Inhibit TNF Secretion and Glycolysis of Human Monocytes. *J Immunol.* 2010;184(3):1200–9.
44. Menk A V, Scharping NE, Moreci RS, Zeng X, Guy C, Salvatore S, et al. Early TCR Signaling Induces Rapid Aerobic Glycolysis Enabling Distinct Acute T Cell Effector Functions. *Cell Rep.* 2018 Feb;22(6):1509–21.
45. Jones N, Vincent EE, Cronin JG, Panetti S, Chambers M, Holm SR, et al. Akt and STAT5 mediate naive human CD4+ T-cell early metabolic response to TCR stimulation. *Nat Commun.* 2019;10(1):2042.
46. Mookerjee SA, Goncalves RLS, Gerencser AA, Nicholls DG, Brand MD. The contributions of respiration and glycolysis to extracellular acid production. *Biochim Biophys Acta.* 2015 Feb;1847(2):171–81.
47. Pressman BC, Fahim M. Pharmacology and toxicology of the monovalent carboxylic ionophores. *Annu Rev Pharmacol Toxicol.* 1982;22:465–90.
48. Mookerjee SA, Nicholls DG, Brand MD. Determining Maximum Glycolytic Capacity Using Extracellular Flux Measurements. *PLoS One.* 2016;11(3):e0152016.
49. Park SW, Lomri N, Simeoni LA, Fruehauf JP, Mechetner E. Analysis of P-glycoprotein-mediated membrane transport in human peripheral blood lymphocytes using the UIC2 shift assay. *Cytom A J Int Soc Anal Cytol.* 2003 Jun;53(2):67–78.
50. Shapiro AB, Ling V. Extraction of Hoechst 33342 from the cytoplasmic leaflet of the plasma membrane by P-glycoprotein. *Eur J Biochem.* 1997;250(1):122–9.
51. Chaudhary PM, Roninson IB. Expression and activity of P-glycoprotein, a multidrug efflux pump, in human hematopoietic stem cells. *Cell.* 1991 Jul;66(1):85–94.
52. Neyfakh AA. Use of fluorescent dyes as molecular probes for the study of multidrug resistance. *Exp Cell Res.* 1988 Jan;174(1):168–76.
53. Ho G-T, Aird RE, Liu B, Boyapati RK, Kennedy NA, Dorward DA, et al. MDR1 deficiency impairs mitochondrial homeostasis and promotes intestinal inflammation. *Mucosal Immunol.* 2018 Jan;11(1):120–30.
54. Lopes-Rodrigues V, Di Luca A, Mieczko J, Meleady P, Henry M, Pesic M, et al. Identification of the metabolic alterations associated with the multidrug resistant phenotype in cancer and their intercellular transfer mediated by extracellular vesicles. *Sci Rep.* 2017;7(1):44541.
55. Nicholas D, Proctor EA, Raval FM, Ip BC, Habib C, Ritou E, et al. Advances in the quantification of mitochondrial function in primary human immune cells through extracellular flux analysis. *PLoS One.* 2017;12(2):1–19.
56. Widlansky ME, Wang J, Shenouda SM, Hagen TM, Smith AR, Kizhakekuttu TJ, et al. Altered mitochondrial membrane potential, mass, and morphology in the mononuclear cells of humans with type 2 diabetes. *Transl Res.* 2010;156(1):15–25.
57. Li P, Wang B, Sun F, Li Y, Li Q, Lang H, et al. Mitochondrial respiratory dysfunctions of blood mononuclear cells link with cardiac disturbance in patients with early-stage heart failure. *Sci Rep.* 2015;5(1):10229.
58. Dixon N, Li T, Marion B, Faust D, Dozier S, Molina A, et al. Pilot study of mitochondrial bioenergetics in subjects with acute porphyrias. *Mol Genet Metab.* 2019;128(3):228–35.
59. Smith AM, Depp C, Ryan BJ, Johnston GI, Alegre-Abarregui J, Evetts S, et al. Mitochondrial dysfunction and increased glycolysis in prodromal and early Parkinson's blood cells. *Mov Disord.* 2018 Oct 1;33(10):1580–90.
60. Herberth M, Koethe D, Cheng TMK, Krzyszton ND, Schoeffmann S, Guest PC, et al. Impaired glycolytic response in peripheral blood mononuclear cells of first-onset antipsychotic-naïve schizophrenia patients. *Mol Psychiatry.* 2011;16(8):848–59.
61. Brooks GA. The Science and Translation of Lactate Shuttle Theory. *Cell Metab.* 2018;27(4):757–85.
62. Chacko BK, Kramer PA, Ravi S, Johnson MS, Hardy RW, Ballinger SW, et al. Methods for defining distinct bioenergetic profiles in platelets, lymphocytes, monocytes, and neutrophils, and the oxidative burst from human blood. *Lab Invest.* 2013;93(6):690–700.

63. Deng J, Lü S, Liu H, Liu B, Jiang C, Xu Q, et al. Homocysteine Activates B Cells via Regulating PKM2-Dependent Metabolic Reprogramming. *J Immunol.* 2017;198(1):170–83.
64. Ma EH, Verway MJ, Johnson RM, Roy DG, Steadman M, Hayes S, et al. Metabolic Profiling Using Stable Isotope Tracing Reveals Distinct Patterns of Glucose Utilization by Physiologically Activated CD8+ T Cells. *Immunity.* 2019;51(5):856–870.e5.
65. Keane KN, Calton EK, Cruzat VF, Soares MJ, Newsholme P. The impact of cryopreservation on human peripheral blood leucocyte bioenergetics. *Clin Sci.* 2015;128(10):723–33.
66. Kleiveland CR. Peripheral Blood Mononuclear Cells. In: Verhoeckx K, Cotter P, López-Expósito I, Kleiveland C, Lea T, Mackie A, et al., editors. *The Impact of Food Bioactives on Health: in vitro and ex vivo models.* Cham: Springer International Publishing; 2015. p. 161–7.
67. Autissier P, Soulas C, Burdo TH, Williams KC. Evaluation of a 12-color flow cytometry panel to study lymphocyte, monocyte, and dendritic cell subsets in humans. *Cytometry A.* 2010 May;77(5):410–9.
68. Krawczyk CM, Holowka T, Sun J, Blagih J, Amiel E, DeBerardinis RJ, et al. Toll-like receptor-induced changes in glycolytic metabolism regulate dendritic cell activation. *Blood.* 2010;115(23):4742–9.
69. Michalek RD, Gerriets VA, Jacobs SR, Macintyre AN, MacIver NJ, Mason EF, et al. Cutting Edge: Distinct Glycolytic and Lipid Oxidative Metabolic Programs Are Essential for Effector and Regulatory CD4+ T Cell Subsets. *J Immunol.* 2011;186(6):3299–303.
70. Waters LR, Ahsan FM, Wolf DM, Shiriha O, Teitell MA. Initial B Cell Activation Induces Metabolic Reprogramming and Mitochondrial Remodeling. *iScience.* 2018;5:99–109.
71. Rodriguez-Prados J-C, Traves PG, Cuenca J, Rico D, Aragones J, Martin-Sanz P, et al. Substrate Fate in Activated Macrophages: A Comparison between Innate, Classic, and Alternative Activation. *J Immunol.* 2010;185(1):605–14.
72. Jagannathan-Bogdan M, McDonnell ME, Shin H, Rehman Q, Hasturk H, Apovian CM, et al. Elevated Proinflammatory Cytokine Production by a Skewed T Cell Compartment Requires Monocytes and Promotes Inflammation in Type 2 Diabetes. *J Immunol.* 2011;186(2):1162–72.
73. Shi LZ, Wang R, Huang G, Vogel P, Neale G, Green DR, et al. HIF1 $\alpha$ -dependent glycolytic pathway orchestrates a metabolic checkpoint for the differentiation of TH17 and Treg cells. *J Exp Med.* 2011 Jul;208(7):1367–76.
74. Giuliatti A, van Etten E, Overbergh L, Stoffels K, Bouillon R, Mathieu C. Monocytes from type 2 diabetic patients have a pro-inflammatory profile. 1,25-Dihydroxyvitamin D3 works as anti-inflammatory. *Diabetes Res Clin Pract.* 2007;77(1):47–57.
75. DeFuria J, Belkina AC, Jagannathan-Bogdan M, Snyder-Cappione J, Carr JD, Nersesova YR, et al. B cells promote inflammation in obesity and type 2 diabetes through regulation of T-cell function and an inflammatory cytokine profile. *Proc Natl Acad Sci U S A.* 2013;110(13):5133–8.
76. Calton EK, Keane KN, Soares MJ, Rowlands J, Newsholme P. Prevailing vitamin D status influences mitochondrial and glycolytic bioenergetics in peripheral blood mononuclear cells obtained from adults. *Redox Biol.* 2016;10:243–50.

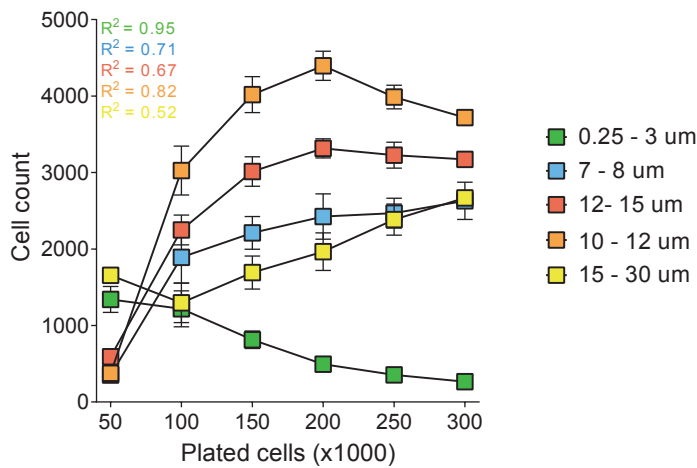
# Supplementary materials



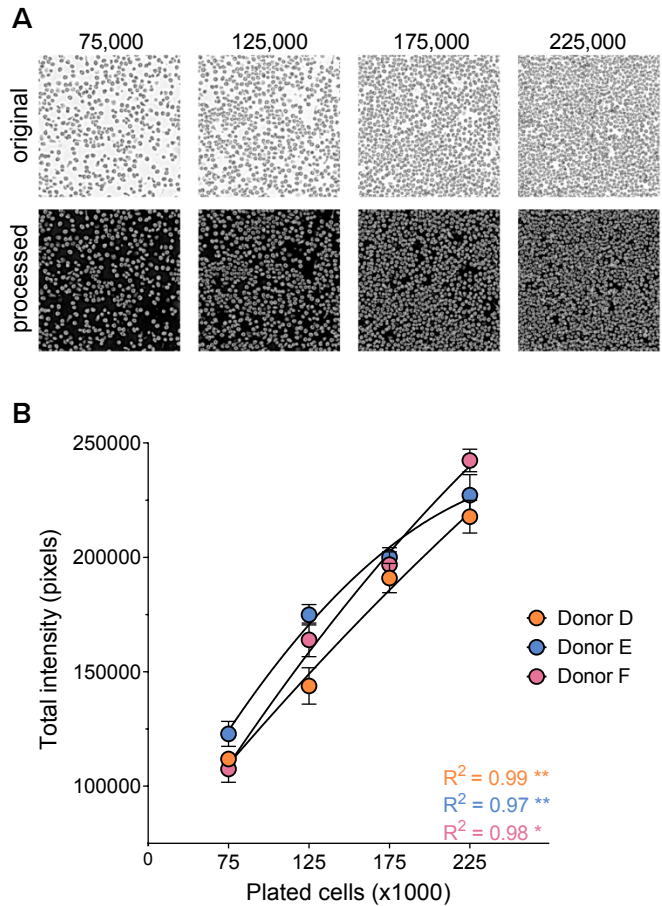
**Supplementary Figure S1: XF assay measurement conditions affect nuclear staining by Hoechst in PBMCs.** (A – D) Brightfield images were taken prior to the XF assay run ( $225 \times 10^3$  cells / well, 4x objective). XF measurements were performed in quiescent, unstimulated PBMCs (left panel) and in PBMCs that were in situ stimulated with Con A for 90 minutes during the XF assay run (right panel). (E – H) The effects of *in situ* PBMC activation and monensin injection on post-XF assay imaging. For all images a representation of the middle of the well is shown.



**Supplementary Figure S2: A 5% border cropping percentage prevents imaging artefacts due to XF assay plate positioning.** Presence of the XF assay plate nodule within the original brightfield image (A) contributed to the total pixel intensity in the processed image (B), resulting in an overestimation of the total pixel intensity of an image when using a 0% cropping percentage. The application of a 5% cropping percentage prevents overestimation and excludes XF assay plate positioning artefacts.



**Supplementary Figure S3: Contribution of cell subset counts to the overall brightfield image.** Brightfield images of PBMCs were obtained at 50 – 300 x 10<sup>3</sup> cells/well (n = 14 - 16) using Cytation 1 (LED intensity 7, integration time 50 ms). PBMC cell subsets were counted based on the analysis of cell diameter using automated analysis in the Cytation Cell Analysis software.



**Supplementary Figure S4: Implementation of R-integrated pixel intensity (PIXI) analysis in experiments with isolated primary monocytes.** (A) Monocytes were isolated from PBMCs of using density gradient separation and plated at 75 - 225 x 10<sup>3</sup> cells / well (n = 6 - 8). Original brightfield images were taken prior to the XF assay run (top, 4x objective) and processed using the in-house generated R-script that was validated for PBMCs (bottom). A magnification from the middle of the brightfield image is shown for each seeding density, for one donor. (B) Curve fit of the number of plated cells vs. total brightfield pixel intensity values, indicated by Pearson correlation coefficients ( $R^2$ ). Data is represented as mean  $\pm$  SD.





# 4

## Extracellular flux analyses reveal differences in mitochondrial PBMC metabolism between high-fit and low-fit females

Joëlle J.E. Janssen<sup>1,2</sup>, Bart Lagerwaard<sup>1,3</sup>, Mojtaba Porbahaie<sup>2</sup>, Arie G. Nieuwenhuizen<sup>1</sup>, Huub F.J. Savelkoul<sup>2</sup>, R.J. Joost van Neerven<sup>2</sup>, Jaap Keijer<sup>1</sup>, Vincent C.J. de Boer<sup>1</sup>

<sup>1</sup> *Human and Animal Physiology, Wageningen University and Research, P.O. Box 338, 6700 AH, Wageningen, the Netherlands*

<sup>2</sup> *Cell Biology and Immunology, Wageningen University and Research, P.O. Box 338, 6700 AH, Wageningen, the Netherlands*

<sup>3</sup> *TI Food and Nutrition, P.O. Box 557, 6700 AN, Wageningen, the Netherlands*

**Am J Physiol Endocrinol Metab.** 2022; Feb 1;322(2):E141-E153  
doi:10.1152/ajpendo.00365.2021

## Abstract

Analyzing metabolism of peripheral blood mononuclear cells (PBMCs) can possibly serve as a cellular metabolic read-out for lifestyle factors and lifestyle interventions. However, the impact of PBMC composition on PBMC metabolism is not yet clear, neither is the differential impact of a longer-term lifestyle factor vs. a short-term lifestyle intervention. We investigated the effect of aerobic fitness level and a recent exercise bout on PBMC metabolism in females. PBMCs from 31 young female adults divided into a high-fit ( $\dot{V}O_{2\text{peak}} \geq 47$  mL/kg/min, N = 15) and low-fit ( $\dot{V}O_{2\text{peak}} \leq 37$  mL/kg/min, N = 16) group were isolated at baseline and overnight after a single bout of exercise (60 minutes, 70%  $\dot{V}O_{2\text{peak}}$ ). Oxygen consumption rate (OCR) and glycolytic rate (GR) were measured using extracellular flux (XF) assays and PBMC subsets were characterized using fluorescence-activated cell sorting (FACS). Basal OCR, FCCP-induced OCR, spare respiratory capacity, ATP-linked OCR, and proton leak were significantly higher in high-fit compared to low-fit females (all  $P < 0.01$ ), while no significant differences in glycolytic rate (GR) were found (all  $P > 0.05$ ). A recent exercise bout did not significantly affect GR or OCR parameters (all  $P > 0.05$ ). The overall PBMC composition was similar between high-fit and low-fit females. Mitochondrial PBMC function was significantly higher in PBMCs from high-fit compared to low-fit females, which was unrelated to PBMC composition and not impacted by a recent bout of exercise. Our study reveals a link between PBMC metabolism and levels of aerobic fitness, increasing the relevance of PBMC metabolism as a marker to study the impact of lifestyle factors on human health.

## Introduction

Lifestyle factors play a dominant role in health maintenance and the prevention of chronic diseases, such as type 2 diabetes (1), cardiovascular disease (2), and cancer (3). Adopting a healthy lifestyle that includes regular physical activity, a balanced diet, a healthy body mass index (BMI), and avoidance of smoking and alcohol intake, is associated with a lower chronic disease risk (4). Many biomarkers are available to assess the impact of lifestyle factors on chronic disease risk or disease progression (5), yet biomarkers that assess how lifestyle factors can contribute to optimizing human health have been less investigated. To this end, accurate, reproducible, clinically relevant and sensitive biomarkers are needed, especially because metabolic differences between healthy individuals are smaller as compared to differences observed during disease pathology.

Immune cells are highly dynamic and reactive to acute environmental signals, such as infectious stimuli, but they can also respond to chronic lifestyle factors, such as physical activity (6), diet (7), and smoking (8). Peripheral blood mononuclear cells (PBMCs) are a readily accessible source of live immune cells from individuals and have been found to provide predictive disease markers for metabolic disorders, including obesity (9,10). Additionally, PBMCs have been used as surrogate tissue to monitor nutritional and metabolic responses (10,11). Using animal models, it was shown that PBMCs can display specific metabolic alterations in response to e.g., unbalanced diets (12) and fasting and refeeding (13). Since PBMCs could thus memorize or reflect metabolic alterations and can be readily obtained from individuals and, they are of particularly interest for studying the effect of lifestyle and lifestyle interventions on health outcomes in humans.

PBMCs are white blood cells with a single round nucleus that comprise several immune cell classes, including T- and B-lymphocytes, natural killer (NK) cells, monocytes, and dendritic cells (14,15). Typically, 70 – 90% of the PBMCs are lymphocytes, 10 – 20% monocytes and 1 – 2% dendritic cells. Cell type frequencies within the lymphocyte population include 70 – 85% cluster of differentiation (CD)3<sup>+</sup> T cells, 5 – 10% B cells and 5 – 20% NK cells. The CD3<sup>+</sup> T cells are composed of CD4<sup>+</sup> and CD8<sup>+</sup> T cells, roughly in a 2:1 ratio. Different PBMC subsets do not only provoke different immune responses; they can also display distinct metabolic states (16–18). Importantly, apart from providing energy substrates and metabolic building blocks for immune cell proliferation and synthesis of macromolecules (e.g., cytokines), metabolic pathways have recently been shown to not only act as a consequence but also as driver of immune cell differentiation (16), which further increases the relevance of monitoring cellular metabolism as a biomarker for

health. PBMCs are sampled with relative ease, low invasiveness and high viability (19) and are thus highly suitable for metabolic profiling of immune cells *ex vivo*. A further advantage of PBMCs is their immediate metabolic response that is seen upon activation (20), which enables the assessment of metabolic flexibility on top of steady-state metabolic analysis and determination of metabolic capacity.

PBMC metabolism was found to be altered in several disease conditions, including type 2 diabetes (21), cardiovascular diseases (22), and obesity (23), and could possibly also be used as a cellular metabolic read-out of lifestyle factors and targeted lifestyle interventions for optimizing human health. To evaluate this potential in healthy individuals, we should better understand how longer-term lifestyle factors impact PBMC metabolism, and whether this is affected by a short-term lifestyle intervention. For example, previous studies have shown that PBMC metabolism responds to longer-term exercise training (24) but also to an acute exercise challenge (25). Since a single exercise bout often elicits a transient pro-inflammatory response whereas regular bouts of exercise induce an anti-inflammatory state (6,26), the impact of regular physical activity (long-term effect) and a single exercise session (short-term effect) on PBMC metabolism could differ, yet this has not been studied in detail. Furthermore, it is not yet clear whether the metabolic responses in PBMCs upon these exercise interventions are primarily related to alterations in cellular energy metabolism *per se*, or that these responses reflect changes in PBMC composition, since changes in PBMC subset frequencies have been demonstrated in response to exercise (27–29), and PBMC subsets are not only immunologically but also metabolically distinct (17,18). Better understanding of the variation in PBMC subsets and overall PBMC composition between healthy donors and their contribution to the overall metabolic outcomes in PBMCs is therefore also needed.

We investigated in females how PBMC metabolism and PBMC composition are affected by high and low levels of aerobic fitness, i.e., a difference in longer-term physical activity, by comparing endurance-trained (high-fit) and untrained (low-fit) females at baseline and after a recent bout of exercise (21 hours before blood sampling). This study will improve our understanding of the use of PBMC metabolism as a biomarker to study the impact of lifestyle factors and lifestyle interventions on human health.

## Materials and Methods

### Ethical approval and study registration

The protocol for collection and handling of human samples was ethically approved by the medical ethical committee of Wageningen University and Research with reference number NL70136.081.19 and registered in the Dutch trial register (NL7891) on 2019-07-23. All procedures performed were in accordance with the ethical standards of the institutional and/or national research committee and with the 1964 Helsinki declaration. Written informed consent was obtained from all individual subjects included in the study.

### Study subjects

Healthy young females (18 – 28 years of age, BMI 18.5 – 25 kg/m<sup>2</sup>) were recruited from the local university and community population. Exclusion criteria were: history of cardiovascular, respiratory, hematological, or metabolic disease; use of prescribed chronic medication; anemia (hemoglobin concentration < 12 g/dL); blood donation within two months before the start of the study; smoking (> 5 cigarettes per week); recreational drug use or over the counter drug use during the study; use of performance-enhancing supplements; pregnancy or lactating. The use of oral contraceptives was not excluded; only the use of monophasic oral contraceptives containing low synthetic estradiol and progesterone was allowed and was controlled for (N = 7 in the high-fit and N = 6 in the low-fit group). Subjects were selected if they had a  $\dot{V}O_{2peak} \geq 47$  mL/kg/min (high-fit group) or  $\leq 37$  mL/kg/min (low-fit group) determined using a maximal exercise test, measured using the validated screening protocol of Lagerwaard et al. (30,31), which minimized the risk for selective bias. The  $\dot{V}O_{2peak}$  cut-offs were based on previous findings from our lab in high-fit (trained) and low-fit (untrained) males (31) and previous studies in high-fit (trained) and low-fit (untrained) females (32–34). Sixteen high-fit and sixteen low-fit subjects were included. A total of 111 exercise tests were performed to end up with the desired sample size. One subject was excluded due to medication intake. For sufficient power, we focused on one sex, because PBMC metabolism was found to differ between males and females (35) and previous exercise studies have been mainly performed in males (36–38). The  $\dot{V}O_{2peak}$  data and results of skeletal muscle mitochondrial capacity of these included subjects has been published previously by our group (30).

### Study design

Subjects refrained from heavy physical exercise 48 hours prior to the first study day and from any physical exercise and alcohol consumption 24 hours prior to the first study day. Subjects adhered to dietary guidelines 24 hours prior to each study

day, which included the consumption of a standardized evening meal (73% carbohydrates/16% protein/11% fat, 1818 kJ) before 8:00PM and dietary guidelines for the consumption of breakfast, lunch, drinks, and snacks. After an overnight fast, blood was collected in the morning of the first study day (= baseline timepoint) and on the morning of the second study day, i.e., 21 hours after a single bout of exercise (= post-exercise timepoint). Blood samples (5 x 10 mL) were collected by venipuncture in vacutainers containing dipotassium (K<sub>2</sub>-) ethylenediamine-tetraacetic acid (EDTA) (K<sub>2</sub>-EDTA, BD Biosciences, Vianen, the Netherlands, 367525) as anticoagulant and processed within 30 minutes after blood collection. Body fat percentage was measured according to the four-site method by Durnin-Womersley using the skinfold measurements of the triceps, biceps, sub scapula and supra iliac, measured using a skinfold calliper (Harpenden, UK). Subjects received breakfast and after two hours, subjects completed an individualized exercise protocol consisting of 60 minutes cycling on an electrically braked bicycle ergometer (Corival CPET, Lode, the Netherlands) at a workload aiming to equal 70% of their  $\dot{V}O_{2\text{peak}}$ . Oxygen consumption, carbon dioxide production, and air flow were measured using MAX-II metabolic cart (AEI technologies, Landivisiau, France). Exhaled air was continuously sampled from a mixing chamber and averaged over 15-second time windows. Oxygen consumption was measured in the first and last 15 minutes of the exercise test and used to confirm the relative oxygen consumption. If needed, small adjustments in workload were made to reach 70%. After the exercise protocol subjects went home and refrained from moderate to heavy physical activity, kept low levels of light physical activity, and refrained alcohol consumption until blood collection on the second study day. The habitual dietary intake of the study subjects was determined via a validated food frequency questionnaire (FFQ) that assessed dietary intake in the past four weeks (39). The self-reported diets of the high-fit and low-fit subjects were similar with no significant differences in total daily energy intake, carbohydrate intake, protein intake or fat intake ([Supplementary Figure S1 \(40\)](#)).

## Chemicals

Carbonyl cyanide-p-trifluoromethoxyphenylhydrazone (FCCP, C2920), oligomycin (OM, O4867, antimycin A (AA, A8674), rotenone (Rot, R8875), monensin sodium salt (MON, M5273), 2-deoxyglucose (2-DG, D6134), Concanavalin A (Con A, C2010), bovine serum albumin (BSA, A6003), sodium chloride (S9888) and Roswell Park Memorial Institute (RPMI) 1640 medium without phenol red and HEPES (11835030) were purchased from Sigma-Aldrich (St. Louis, MO, USA). Dulbecco's phosphate-buffered saline (DPBS, 14190094) and Hanks' Balanced Salt Solution (HBSS, 14175095) were purchased from Thermo Fisher Scientific (Pittsburgh, Pennsylvania, USA). XF RPMI assay medium pH 7.4 (103576-100), XF 1.0 M glucose

(103576-100), XF 100 mM pyruvate (103578-100) and XF 200 mM glutamine (103579-100) were purchased from Seahorse Biosciences, Agilent Technologies (Santa Clara, California, USA).

### PBMC isolation

EDTA-collected blood (50 mL  $\pm$  1 mL, except for two samplings where we took 48 and 45 mL blood) was diluted with DPBS (1X) without magnesium and calcium supplemented with sodium citrate buffer (1% v/v) as anticoagulant in a 1:1 ratio. Diluted blood was carefully poured into Leucosep tubes (Thermo Fisher Scientific, 227289) that were filled with Ficoll Paque Plus (15 mL, GE Healthcare, Marlborough, Massachusetts, USA, 17144003), followed by density gradient centrifugation for 10 minutes at 1000g at room temperature (RT) with acceleration five and zero braking. The PBMC fraction was collected using sterile Pasteur pipettes and centrifugated for 10 minutes at 600g at RT with brake to concentrate the PBMC layer and facilitate removal of residual Ficoll and plasma. Supernatant was discarded, and cells were three times washed using DPBS (1X, 20 mL) without magnesium and calcium, supplemented with sodium citrate buffer (1% v/v) and fetal bovine serum (FBS, 2% v/v, DPBS-1% citrate-2% FBS) and centrifugated for 7 minutes at 250g at RT. Supernatant was discarded, and cells were resuspended in RPMI 1640 medium without phenol red and HEPES (30 mL, Thermo Fisher Scientific, 11835030), supplemented with FBS (10% v/v). Total PBMC number and PBMC viability was determined for each donor in a 1:10 dilution using acridine orange and propidium iodide staining (ViaStain, Nexcelom Bioscience, Lawrence, Massachusetts, USA, CS2-0106) in a Nexcelcom Cell Counter (Nexcelcom Bioscience) in fluorescent mode (n = 8). PBMCs were directly used for XF assay measurements or cryopreserved and stored in liquid nitrogen for later FACS staining and analysis. For cryopreservation,  $6 \times 10^6$  PBMCs were washed with DPBS-1% citrate-2% FBS and centrifugated for 5 minutes at 400g at RT. Supernatant was discarded and cells were resuspended with ice-cold FBS (1 mL), followed by gentle droplet wise addition of ice-cold FBS-DMSO (80% / 20% v/v, 1 mL) to achieve a final FBS-DMSO concentration of 90% / 10% v/v, and transferred to cold cryovials ( $3 \times 10^6$  PBMCs per vial). Cryovials were inserted in a cold (4°C) isopropanol chamber, stored overnight at -80°C, and transferred to liquid nitrogen the next day.

### High contrast brightfield imaging and image analysis

High contrast brightfield images were obtained prior to the XF assay run using the Cytation 1 Cell Imaging Multi-Mode Reader (BioTek, Winooski, Vermont, USA) followed by image analysis according to our previously published 'R-integrated pixel intensity (PIXI) analysis' protocol for normalization of XF assay data (41).

### XF analysis with Seahorse XFe96 analyzer

Oxygen consumption rate (OCR) and proton efflux rate (PER) measurements were performed in a Seahorse extracellular flux (XF)e96 Analyzer (Seahorse Biosciences).  $225 \times 10^3$  PBMCs per well ( $n = 8$ ) were plated onto Cell-Tak (Corning, New York, USA, 354240) coated XF96 cell plates in XF RPMI assay medium pH 7.4 (50  $\mu$ L, XF assay medium) supplemented with XF glucose (11 mM), XF pyruvate (1 mM) and XF glutamine (2 mM) and left for 10 minutes at RT. Additionally,  $75 - 300 \times 10^3$  PBMCs per well ( $n = 3 - 4$ ) were plated for the internal calibration curve that was used for normalization. Cell plate was centrifugated for 1.5 minutes at 200g at RT with acceleration one and zero braking. Afterwards, an additional volume of XF assay medium (130  $\mu$ L) was added to the cells and cells were incubated for 30 minutes at 37°C without CO<sub>2</sub>. XF measurements included two injection strategies (A and B) that were used in parallel. Injection strategy A included serial injections of FCCP (1.25  $\mu$ M), AA plus Rot (AA/Rot, 2.5  $\mu$ M/1.25  $\mu$ M) and 2-DG (50 mM), injection strategy B included serial injections of OM (1.5  $\mu$ M), AA/Rot (2.5  $\mu$ M/1.25  $\mu$ M) and MON (20  $\mu$ M). These injection strategies were preceded by injection with XF assay medium (for non-activated, control PBMCs) or Con A (25  $\mu$ g/mL, for real-time activated PBMCs). The total XF assay protocol consisted of eighteen measurement cycles of which each cycle included 5 minutes of which 2 minutes mixing, 0 minutes waiting, 3 minutes measuring. The first injection (XF assay medium or Con A) was inserted after three measurement cycles and was followed by six measurement cycles without injection to allow PBMC activation. Each injection strategy (A with XF assay medium, A with Con A, B with XF assay medium, B with Con A) included 2 to 8 technical replicates per subject. The time window (from isolated PBMCs until the start of the Seahorse assay) was on average  $180 \pm 26$  min. Glycolytic PER (glycoPER) values were calculated by subtracting mitochondrial PER ( $= \text{OCR} * 0.61$ ) values from total PER values in order to correct for the contribution of mitochondrial-derived CO<sub>2</sub> production to acidification of the XF assay medium (42) and reported as glycolytic rate (GR). OCR and GR values were normalized against the number of PIXI analyzed cells (41).

### Flow cytometry staining and analysis

PBMCs were stained with fluorochrome-conjugated antibodies against extra-cellular markers for cell phenotyping (Table 1). Every antibody was titrated individually within the recommended range (4, 2, 1, 0.5, 0  $\mu$ L/sample). The staining index (SI) was calculated, and the highest value was selected as the optimal concentration for FACS staining. The optimal antibody concentrations are presented in Supplementary Table S1. For FACS staining,  $3.0 \times 10^6$  PBMCs were quickly thawed in a 37°C water bath under continuous agitation and transferred to a pre-filled 50 mL tube containing RPMI-1640 medium supplemented with FBS

**Table 1** Fluorochrome-conjugated antibodies used for FACS staining

Antibody	Fluorochrome	Reactivity	Light chain	Clone	Company#	Catalog number	RRID
anti-CD3	AF700	Human	κ	UCHT1	Biolegend	300424	AB_493741
anti-CD4	BV510	Human	κ	OKT4	Biolegend	317444	AB_2561866
anti-CD8a	BV650	Human	κ	RPA-T8	Biolegend	301042	AB_2563505
anti-CD25	BV421	Human	κ	BC96	Biolegend	302630	AB_11126749
anti-CD127	APC	Human	κ	A019D5	Biolegend	351342	AB_2564137
anti-CD14	BV605	Human	κ	63D3	Biolegend	367126	AB_2716231
anti-HLA-DR <sup>*</sup>	FITC	Human	κ	L243	Biolegend	307632	AB_1089142
anti-CD56	PE	Human	κ	5.1H11	Biolegend	362524	AB_2564161
anti-CD19	PE/Cy7	Human	κ	HIB19	Biolegend	302216	AB_314246
anti-CD20	PE/Daz594	Human	κ	2H7	Biolegend	302348	AB_2564387
anti-CD45	PerCp	Human	κ	2D1	Biolegend	368506	AB_2566358

<sup>\*</sup>Human Leukocyte Antigen – DR isotype

<sup>#</sup>All antibodies were developed, produced, and distributed by Biolegend.

(20% v/v, 10 mL). Cell suspension was centrifugated for 10 minutes at 300g at RT and the supernatant was discarded. Cells were washed twice with RPMI-1640 with FBS (20% v/v, 10 mL) and centrifugated for 10 minutes at 300g at RT. Supernatant was discarded, and cells were resuspended in RPMI-1640 with FBS (20% v/v, 500 µL).  $1.5 \times 10^6$  PBMCs per well (250 µL) was added to a 96 well NUNC plate (Thermo Fisher Scientific, 267245) and cells were washed by adding DPBS (1x, 100 µL) followed by plate centrifugation for 4 minutes at 400g at RT. Supernatant was discarded and cells were washed again with DPBS (1x, 200 µL) and the plate was centrifugated for 4 minutes at 400g at RT. For live/dead staining, Zombie near-infrared (NIR) viability solution (Biolegend, San Diego, CA, USA, 423105) was 500x diluted in DPBS and added (100 µL) followed by incubated for 25 minutes at RT, in the dark. Supernatant was discarded and cells were washed with FACS buffer (200 µL) containing DPBS (1X) supplemented with BSA (0.5% v/v), EDTA, 2.5 mM, and sodium azide ( $\text{NaN}_3$ , 10% v/v) (final pH 7.4). The plate was centrifugated for 3 minutes at 400g at RT and fluid was discarded. The mixture of antibodies ([Table 1](#)) diluted in FACS buffer was added to the cells and the plate was incubated for 30 minutes at 4°C in the dark. Cells were washed three times by adding cold FACS buffer (200 µL) and plate centrifugation for 3 minutes at 400g at 4°C.

Supernatant was discarded, and the cell pellet was resuspended in FACS buffer (300  $\mu$ L) and measured on CytoFLEX LX (Beckman Coulter's, Indianapolis, IN, USA). The generated flow cytometry data were analyzed using FlowJo v10 (FlowJo LLC, Ashland, OR, USA, RRID:SCR\_008520). Cell frequencies are depicted as the percentage CD45<sup>+</sup>NIR<sup>-</sup> leukocytes (% viable leukocytes) determined by live/dead staining.

### Statistical analyses

Statistical analyses were performed using IBM SPSS Statistics for Windows (Version 25.0, IBM Corp, Armonk, NY, USA, RRID:SCR\_002865). Graphs were created using GraphPad Prism (Version 8.0, Graphpad Software, CA, USA, RRID:SCR\_002798). Normality was checked using Shapiro-Wilk normality tests. Data is presented as mean  $\pm$  standard deviation (SD) for normally distributed data and as median [interquartile range (IQR)] for not normally distributed data. Not normally distributed data was log-transformed for statistical analysis. Repeated-measures ANOVA (RM-ANOVA) was used to study the effect of fitness level (between-subjects factor) and the effect of a recent bout of exercise or *ex vivo* Con A stimulation (within-subjects factors) on the response of XF assay parameters and the interaction between them. All assumptions for RM-ANOVA were met. Two-sided unpaired Student's t-tests were used to compare the normally distributed subject characteristics and the relative Con A-induced differences between high-fit and low-fit females. Mann-Whitney U tests were used to compare not normally distributed subject characteristics. P-values < 0.05 were considered as statistically significant.

## Results

### Total PBMC number is not affected by fitness level, but lower upon a recent bout of exercise

PBMC were isolated from females with high ( $\dot{V}O_{2\text{peak}} \geq 47$  mL/kg/min, N = 15) and low ( $\dot{V}O_{2\text{peak}} \leq 37$  mL/kg/min, N = 16) levels of aerobic fitness representing trained, physically active females and untrained, low physically active females, respectively. Subject characteristics are shown in **Table 2**. The total number of isolated PBMCs per total blood volume was not significantly different between high-fit ( $102.5 \pm 29.6 \times 10^6$  cells) and low-fit ( $104.3 \pm 27.1 \times 10^6$  cells) females ( $P_{\text{group}} = 0.829$ ) and significantly lower after the recent bout of exercise in both groups ( $95.2 \pm 22.2 \times 10^6$  cells and  $97.04 \pm 18.1 \times 10^6$  cells respectively,  $P_{\text{exercise}} = 0.036$ ), but again not different between the two groups ( $P = 0.981$ ). All cell viabilities were > 97% and not significantly different between high-fit ( $97.6 \pm 0.5\%$ ) and low-fit ( $97.8$

**Table 2** Subject characteristics

	Low-fit (N = 16)	High-fit (N = 15)
Age (years)	24.0 [21.3 - 25.5]	21.8 [21.6 - 23.7]
Ethnicity	Caucasian (11), Asian (1), Indo-pacific (4)	All Caucasian
Weight (kg)	59.2 ± 7.2	61.2 ± 7.0
Height (m)	1.63 ± 0.08 *	1.68 ± 0.05 *
Fat mass (% of weight)	28.9 ± 3.9 *	25.1 ± 4.4 *
$\dot{V}O_{2peak}$ (mL · kg <sup>-1</sup> · min <sup>-1</sup> )	35.1 [32.2 - 35.7] ****	50.4 [49.0 - 54.0] ****
Baecke total score	7.3 ± 1.0 ****	9.5 ± 0.8 ****
Hemoglobin (mM)	8.4 ± 0.6	8.5 ± 0.6

$\dot{V}O_{2peak}$  = maximal oxygen consumption values. Values are mean ± SD for normally distributed data, and median [IQR] for not normally distributed data. \*P < 0.05, \*\*\*\* P < 0.0001.

± 0.4%) females ( $P_{group} = 0.182$ ) and not significantly impacted by the recent bout of exercise ( $P_{exercise} = 0.580$ ).

### The overall PBMC composition is not significantly affected by fitness level and a recent bout of exercise

To investigate how physical fitness level is related to metabolic PBMC activity, we first characterized various cell subsets in PBMCs from high- and low-fit females and studied whether these subsets are affected by a recent bout of exercise. We used lineage-specific antibodies against T cells, B cells, NK cells, and monocytes (**Supplementary Figure S2** (43)) and found that the overall PBMC composition was similar between high-fit and low-fit females at baseline as well as after a recent bout of exercise (**Figure 1A**). The number of viable leukocytes (CD45<sup>+</sup>NIR<sup>-</sup> leukocytes) was >90% after thawing. In line with overall similar PBMC composition, subset analysis at baseline showed that frequencies of CD56<sup>+</sup> NK cells, CD19<sup>+</sup>CD20<sup>+</sup> B cells, and CD3<sup>+</sup> total T cells, including CD3<sup>+</sup>CD4<sup>+</sup> T helper (Th) cells and CD3<sup>+</sup>CD8<sup>+</sup> cytotoxic T cells, were not significantly different between PBMCs from high-fit and low-fit females ( $P_{group} = 0.137, 0.291, 0.528, 0.478, 0.660$ , respectively). We did observe that PBMCs from high-fit and low-fit females significantly differed in frequencies of CD14<sup>+</sup> monocytes ( $7.52 \pm 2.35\%$  in high-fit compared to  $5.69 \pm 2.15\%$  in low-fit females,  $P_{group} = 0.047$ ) and of CD3<sup>+</sup>CD4<sup>+</sup>CD25<sup>+</sup> activated T cells ( $3.10\% [2.30 - 4.20\%]$  in PBMCs from high-fit compared to  $2.35\% [1.70 - 2.90\%]$  in PBMCs from low-fit females,  $P_{group} = 0.014$ , **Figure 1B – H**). When co-expression of CD127 and CD25 was analyzed, PBMCs from high-fit and low-fit females did not significantly differ in the frequencies CD3<sup>+</sup>CD4<sup>+</sup>CD25<sup>+</sup>CD127<sup>-</sup> Treg cells ( $1.77 \pm 0.48\%$  in high-fit compared to  $1.52 \pm 0.50\%$  in low-fit females,  $P_{group} =$

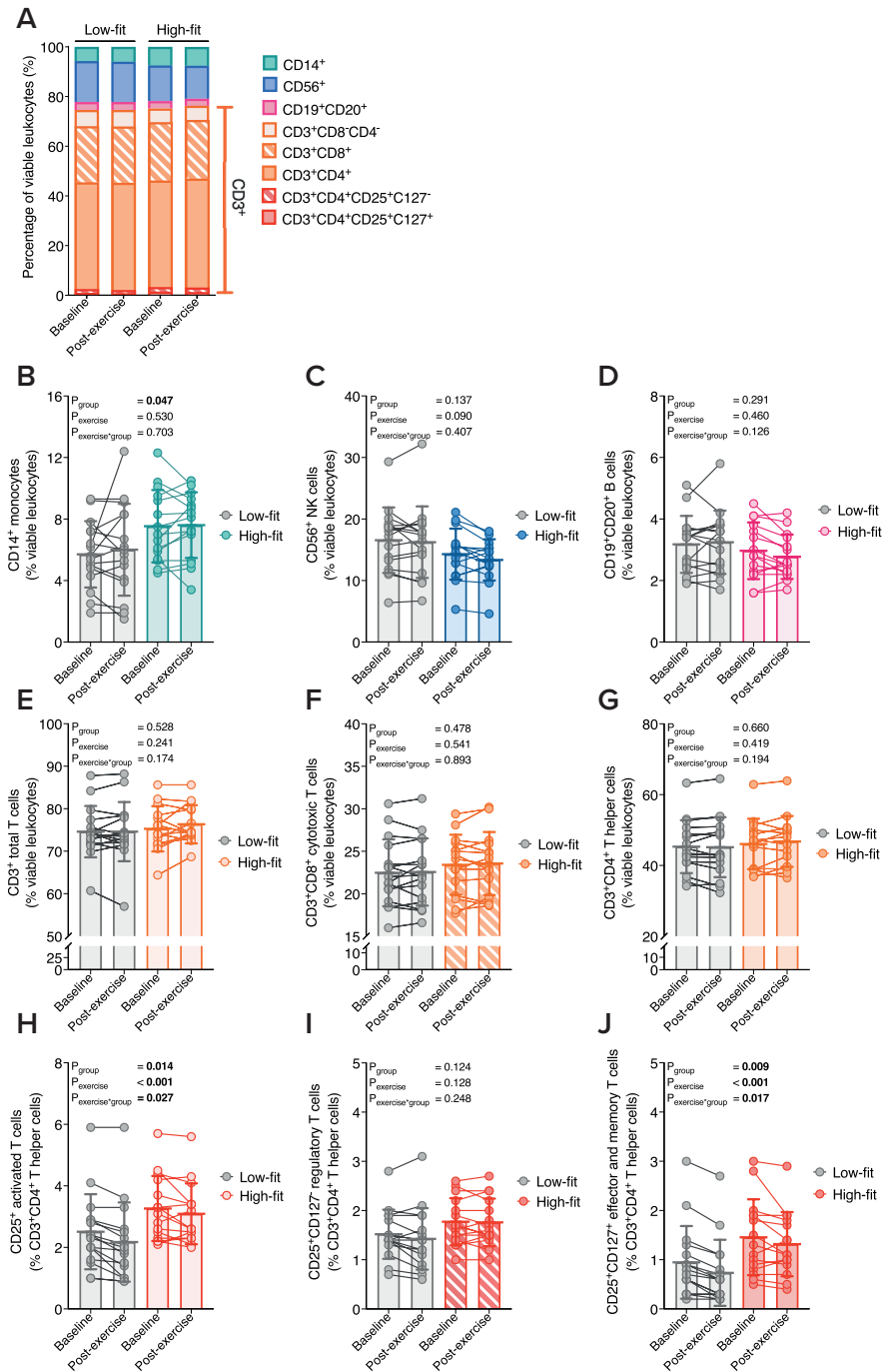


**Figure 1: Characterization of PBMC cell types in high-fit and low-fit females at baseline and after a recent bout of exercise.** (A – J) Stacked (A) and single (B – J) percentages of CD14<sup>+</sup> (B), CD56<sup>+</sup> (C), CD19<sup>+</sup>CD20<sup>+</sup> (D), CD3<sup>+</sup>CD8<sup>+</sup>CD4<sup>+</sup> (E), CD3<sup>+</sup>CD8<sup>+</sup> (F), CD3<sup>+</sup>CD4<sup>+</sup> (G), CD3<sup>+</sup>CD4<sup>+</sup>CD25<sup>+</sup> (H), CD3<sup>+</sup>CD4<sup>+</sup>CD25<sup>+</sup>CD127<sup>+</sup> (I) and CD3<sup>+</sup>CD4<sup>+</sup>CD25<sup>+</sup>CD127<sup>+</sup> (J) subsets relative to the total number of viable PBMCs (%) at baseline and post-exercise in low-fit (N = 16, left in stacked plot, grey in single plots) and high-fit (N = 15, right in stacked plot, colored in single plots) females. Main effects (fitness level and recent exercise) and interaction effects were analyzed using RM-ANOVA. Significant P-values (< 0.05) are indicated in bold.

0.124, **Figure 1I**), yet frequencies CD3<sup>+</sup>CD4<sup>+</sup>CD25<sup>+</sup>CD127<sup>+</sup> non-Treg cells, i.e., effector and memory T cells, were significantly different between PBMCs from high-fit (1.30% [0.80 – 1.90%]) compared to PBMCs from low-fit 0.75% [0.38 – 1.25%] females,  $P_{\text{group}} = 0.009$ , **Figure 1J**). Although there is a 24% difference in CD14<sup>+</sup> monocyte frequency between the two groups, just like the CD3<sup>+</sup>CD4<sup>+</sup>CD25<sup>+</sup> activated T cells, they constitute a relative minor part of the total PBMC fraction (< 10%), and thus changes are likely not substantially affecting the overall PBMC composition. PBMC cell type frequencies were also not significantly altered after a recent exercise bout ( $P_{\text{exercise}} > 0.05$  for all, **Figure 1B – G and I**), except for the small subset of CD3<sup>+</sup>CD4<sup>+</sup>CD25<sup>+</sup> activated T cells ( $P_{\text{exercise}} < 0.001$ , **Figure 1H**) and CD3<sup>+</sup>CD4<sup>+</sup>CD25<sup>+</sup>CD127<sup>+</sup> T cells ( $P_{\text{exercise}} < 0.001$ , **Figure 1J**).

### Baseline and post-exercise mitochondrial function is significantly higher in PBMCs from high-fit compared to low-fit females

Next, we aimed to study whether PBMCs from high-fit and low-fit females are metabolically different by analyzing oxidative and glycolytic metabolism using XF analysis. We used a standardized experimental set-up that was validated for low technical variation and sampling of many individuals on multiple days (41). Using two different injection strategies (injection strategy A (**Figure 2A, 3A**) and injection strategy B (**Figure 2B, 3B**), we were able to probe a complete set of parameters of mitochondrial and glycolytic function and capacity, in a relatively short run time. PBMCs from high-fit females had significantly higher basal OCR ( $14.23 \pm 1.44$  pmol O<sub>2</sub>/min/10<sup>5</sup> cells) compared to PBMCs from low-fit females ( $11.65 \pm 1.65$  pmol O<sub>2</sub>/min/10<sup>5</sup> cells,  $P_{\text{group}} < 0.001$ , **Figure 2C**). Similarly, FCCP-induced OCR was significantly higher in PBMCs from high-fit ( $52.01 \pm 6.79$  pmol O<sub>2</sub>/min/10<sup>5</sup> cells) compared to PBMCs from low-fit ( $40.36 \pm 7.64$  pmol O<sub>2</sub>/min/10<sup>5</sup> cells) females ( $P_{\text{group}} < 0.001$ , **Figure 2D**). Since spare respiratory capacity (SRC) was also significantly higher in PBMCs from high-fit ( $300 \pm 26\%$ ) compared to PBMCs from low-fit ( $264 \pm 33\%$ ) females ( $P_{\text{group}} < 0.001$ , **Figure 2E**), mitochondrial respiratory capacity was significantly higher in PBMCs from high-fit females. Adenosine

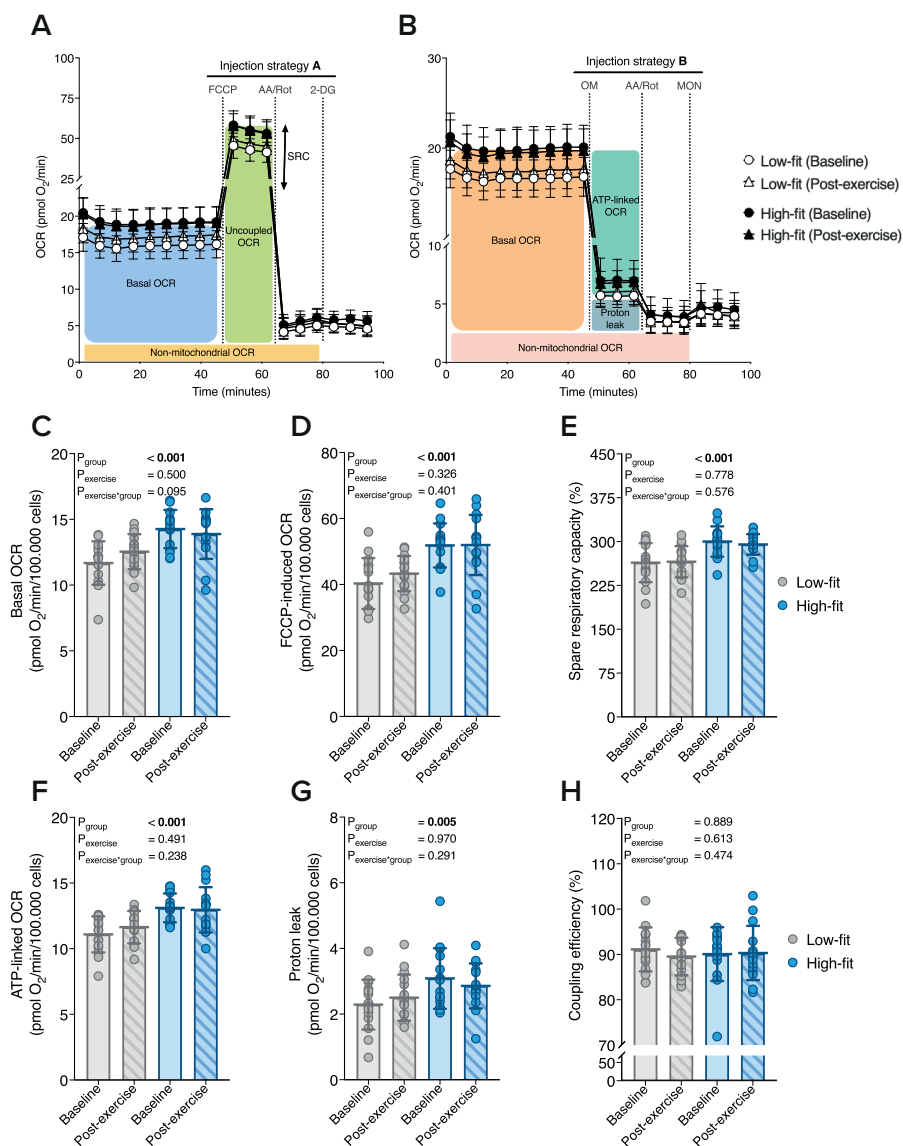


**Figure 2: Mitochondrial PBMC function in high-fit and low-fit females at baseline and after a recent bout of exercise.** (A, B) Representation of mitochondrial parameters derived from the XF assay using injection strategy A (A) or B (B) and traces for low-fit (N = 16, white) and high-fit (N = 15, black) at baseline (dots) and post-exercise (triangles). (C - E) Basal OCR (C), FCCP-induced OCR (D) and corresponding spare respiratory capacity (E). (F - H) ATP-linked OCR (F), proton leak (G) and corresponding coupling efficiency (H). Parameters are

calculated for low-fit (N = 16, grey) and high-fit (N = 15, blue) females at baseline (clear bars) or post-exercise (striped bars). Values are depicted per  $10^5$  PIXI analyzed cells for absolute rates or as a percentage (%) for ratios of corresponding values. Main effects (fitness level and recent exercise) and interaction effects were analyzed using RM-ANOVA. Significant P-values (< 0.05) are indicated in bold.

triphosphate (ATP)-linked OCR and mitochondrial proton leak were significantly higher in PBMCs from high-fit females ( $13.10 \pm 1.10$  pmol  $O_2$ /min/ $10^5$  cells and  $3.09 \pm 0.92$  pmol  $O_2$ /min/ $10^5$  cells, respectively) compared to PBMCs from low-fit females ( $11.09 \pm 1.37$  pmol  $O_2$ /min/ $10^5$  cells and  $2.29 \pm 0.76$  pmol  $O_2$ /min/ $10^5$  cells) ( $P_{\text{group}} < 0.001$  and  $P = 0.005$ , respectively) (Figure 2F, G). However, the percentage of mitochondrial respiration that is linked to ATP production, also defined as mitochondrial coupling efficiency, was not significantly different between high-fit (91.7% [88.7 – 93.8%]) and low-fit (91.1% [87.2 – 94.3%]) females ( $P_{\text{group}} = 0.889$ , Figure 2H). The recent exercise bout allows us to analyze the effect of a single, short-term exercise intervention on PBMC metabolism, while simultaneously minimizing the impact of a temporary shift in PBMC subsets upon acute exercise, which has returned to baseline within 24 hours after exercise completion (27–29). PBMC mitochondrial respiration and respiratory capacity were not significantly affected by the recent bout of exercise ( $P_{\text{exercise}} > 0.05$  for all OCR parameters), and the exercise response did not significantly differ between high-fit and low-fit females ( $P_{\text{exercise} \times \text{group}} > 0.05$  for all OCR parameters (Figure 2C – H). Thus, mitochondrial function was significantly higher in PBMCs from high-fit as compared to low-fit females, at baseline as well as after a recent exercise intervention.

### Glycolytic function does not significantly differ between PBMCs from high-fit and low-fit females

In a similar way, we studied whether parameters of glycolytic function were affected by fitness level and a recent bout of exercise. Basal GR was not significantly different between PBMCs from high-fit ( $14.58$  [12.13 – 19.04] pmol  $H^+$ /min/ $10^5$  cells) and low-fit ( $13.55$  [11.19 – 16.31] pmol  $H^+$ /min/ $10^5$  cells) females ( $P_{\text{group}} = 0.739$ , Figure 3C). To assess PBMC glycolytic capacity, we first blocked mitochondrial respiration using AA and Rot injection, which forces the cells to upregulate their glycolytic machinery to compensate for the respiratory loss of ATP, which is therefore defined as compensatory glycolysis. Next, we injected the ionophore monensin (MON), which promotes cellular  $Na^+$  import and stimulates ATP hydrolysis by  $Na^+/K^+$ -ATPase (44), thereby further increasing cellular ATP demands and maximizing the glycolytic rate when mitochondrial respiration is fully blocked (45). We did not find a significant difference in compensatory GR,

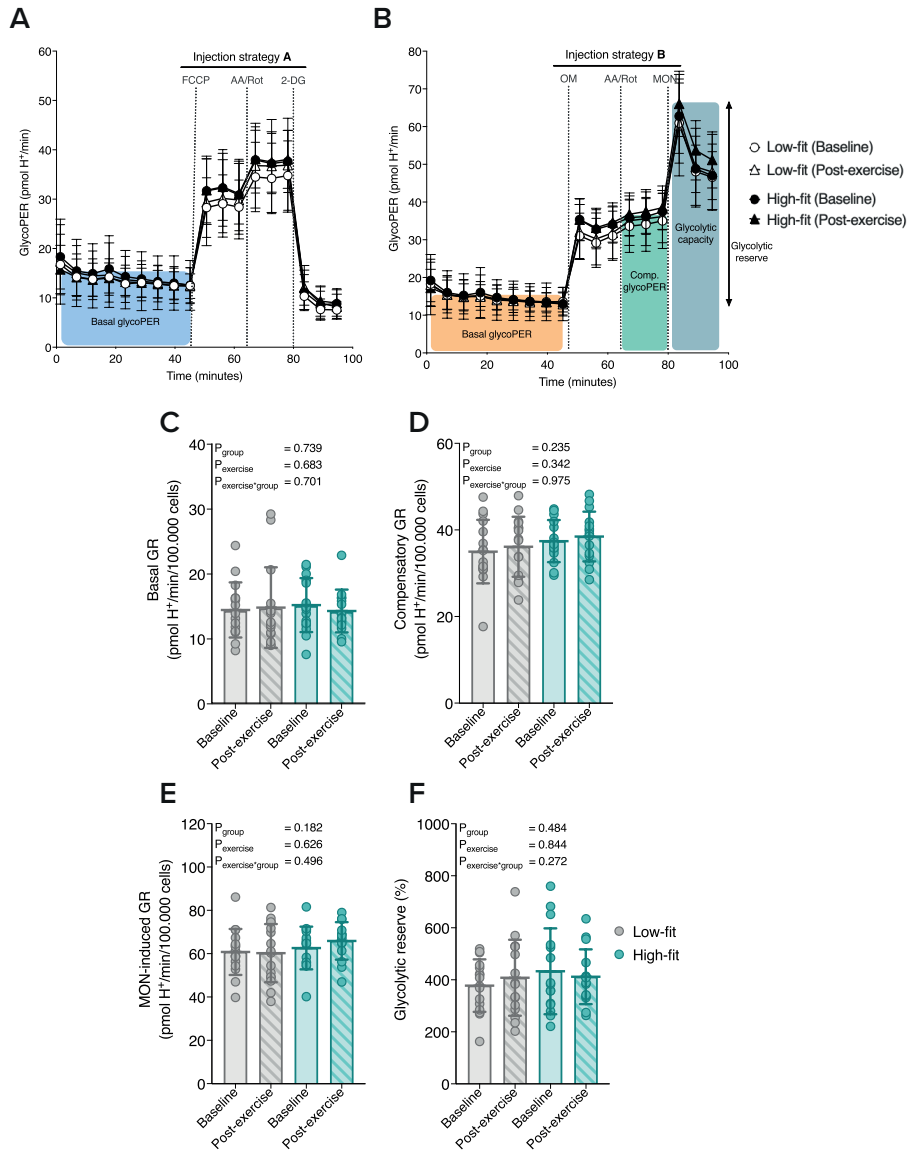


Figure 3: Glycolytic PBMC function in high-fit and low-fit females at baseline and after a recent bout of exercise. (A, B) Representation of glycolytic parameters derived from the XF assay using injection strategy A (A) or B (B) and traces for low-fit (N = 16, white) and high-fit (N = 15, black) females at baseline (dots) and post-exercise (triangles). (C – F) Basal GR (C), compensatory GR (D), MON-induced GR (E) and the glycolytic reserve calculated as the ratio between MON-induced GR and basal GR (F). Parameters are calculated for low-fit

(N = 16, grey) and high-fit (N = 15, **turquoise**) females at baseline (clear bars) or post-exercise (striped bars). Values are depicted per  $10^5$  PIXI analyzed cells for absolute rates or as a percentage (%) for ratios of corresponding values. Main effects (fitness level and recent exercise) and interaction effects were analyzed using RM-ANOVA. Significant P-values ( $< 0.05$ ) are indicated in bold.

MON-induced GR or glycolytic reserve between PBMCs from high-fit ( $37.45 \pm 4.86$  pmol  $H^+$ /min/ $10^5$  cells,  $62.76 \pm 9.86$  pmol  $H^+$ /min/ $10^5$  cells and  $433 \pm 165\%$ , respectively) and PBMCs from low-fit females ( $35.02 \pm 7.33$  pmol  $H^+$ /min/ $10^5$  cells,  $60.94 \pm 10.62$  pmol  $H^+$ /min/ $10^5$  cells and  $378 \pm 101\%$ , respectively,  $P_{\text{group}} = 0.235$ , 0.182, 0.484, **Figure 3D – F**). Furthermore, PBMC glycolytic function and capacity were not significantly affected by a recent bout of exercise ( $P_{\text{exercise}} > 0.05$  for all GR parameters) and high-fit and low-fit females did not respond differently to exercise ( $P_{\text{exercise*group}} > 0.05$  for all GR parameters (**Figure 3C – F**)). Thus, glycolytic function parameters did not significantly differ between PBMCs from high-fit and low-fit females, and were not significantly affected by a recent bout of exercise.

### Acute immunometabolic stimulation of PBMCs with Con A does not impact the relative differences in PBMC metabolism between high-fit and low-fit females

To study alterations in metabolic pathways in response to immune cell activation, PBMCs are often *ex vivo* stimulated with mitogenic compounds (20,46–49). To investigate whether fitness level influences the acute metabolic switch that is seen upon mitogenic stimulation, we measured oxidative and glycolytic metabolism in *in situ* activated PBMCs and compared this to naïve, quiescent PBMCs. Concanavalin A (Con A) was used as a mitogenic lectin, which upregulates the respiratory and glycolytic machinery to provide the increased energy requirements that is necessary to support Con A-induced T cell activation and proliferation (20,50), which includes for example enhanced ion signaling and increased cytokine synthesis (51,52). Indeed, we demonstrated that acute PBMC stimulation with Con A upregulated mitochondrial respiration and glycolytic rate in PBMCs (**Figure 4A, B**). This resulted in a significant elevation of basal OCR (acutely activated OCR) and FCCP-induced OCR, in PBMCs from both high-fit and low-fit females (both  $P_{\text{activation}} < 0.001$ , **Figure 4C, D**). The absolute Con A-induced increase in basal OCR and FCCP-induced OCR was significantly higher in high-fit compared to low-fit females ( $P_{\text{activation*group}} = 0.010$  and 0.006, respectively, **Figure 4C, D**). When plotted relatively to non-activated PBMCs, the Con A-induced increase in basal OCR and FCCP-induced OCR did not significantly differ between the two groups ( $P = 0.558$  and  $P = 0.725$ , respectively, **Figure 4E, F**). Similarly, Con A

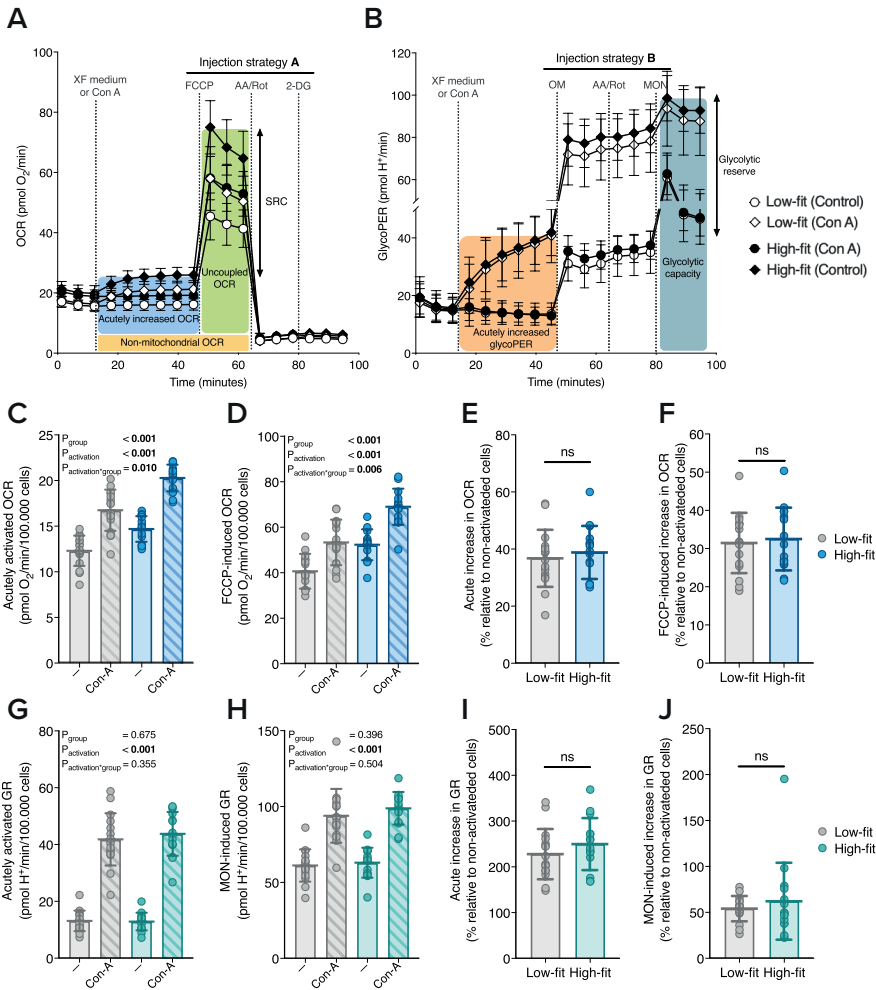


**Figure 4: The effect of acute PBMC stimulation on mitochondrial and glycolytic PBMC function in high-fit and low-fit females. (A, B)** Representation of the mitochondrial (A) and glycolytic (B) parameters derived from the induced XF assay using a first injection with XF assay medium for quiescent, control PBMCs (dots) or the mitogen Con A for activated PBMCs (diamonds) followed by injection strategy A (A) or B (B) for low-fit (N = 16, white) and high-fit (N = 15, black) females. (C, D) Acutely activated (C) and FCCP-induced (D) OCR per 10<sup>5</sup> PIXI analyzed cells in control PBMCs (clear bars) or Con A stimulated PBMCs (striped bars) from low-fit (N = 16, grey) and high-fit (N = 15, blue) females. (E – F) The acute increase in OCR (E) and FCCP-induced OCR (F) in Con A stimulated PBMCs compared to control PBMCs (%) in low-fit (N = 16, grey) and high-fit (N = 15, blue) females. (G, H) Acutely activated (G) and MON-induced (H) GR per 10<sup>5</sup> PIXI analyzed cells in control PBMCs (clear bars) or

Con A stimulated PBMCs (striped bars) from low-fit (N = 16, grey) and high-fit (N = 15, **turquoise**) females. (I, J) The acute increase in GR (I) and MON-induced GR (J) in Con A stimulated PBMCs compared to control PBMCs (%) in low-fit (N = 16, grey) and high-fit (N = 15, **turquoise**) females. Main effects (fitness level and Con A) and interaction effects were analyzed using RM-ANOVA (**Figure 4C, D, G, H**) and the relative Con A induced differences were analyzed using unpaired Student's t-tests (**Figure 4E, F, I, J**). Significant P-values (< 0.05) are indicated in bold, ns = not significant.

stimulation resulted in a significant increase in basal GR (acutely activated GR) and MON-induced GR, in PBMCs from both high-fit and low-fit females (both  $P_{\text{activation}} < 0.001$ , **Figure 4G, H**). Here, the absolute Con A-induced increase in basal and MON-induced GR was not significantly different between high- and low-fit females ( $P_{\text{activation} \times \text{group}} = 0.355$  and  $0.504$ , respectively, **Figure 4G, H**), neither were the relative increases ( $P = 0.285$  and  $0.473$ , respectively, **Figure 4I, J**). Thus, PBMCs from high-fit females showed higher mitochondrial respiration and capacity in response to Con A stimulation compared to low-fit females, but the relative metabolic response was not different between the two groups.

## Discussion

This study demonstrates that high-fit females had significantly higher PBMC mitochondrial function parameters than low-fit females, whereas glycolytic parameters were not different. Furthermore, either a recent exercise challenge, or an ex vivo immunological challenge did not significantly alter metabolic function in isolated PBMCs. This indicated that especially long-term lifestyle differences can be imprinted in PBMC metabolism, whereas a short-term, recent exercise intervention is not reflected in PBMC metabolic functions. We also showed that the overall PBMC composition was similar between high-fit and low-fit females, i.e., the major contributing PBMC subsets were not significantly affected by fitness level or a recent bout of exercise.

We are the first study that revealed a link between levels of aerobic fitness and mitochondrial function in PBMCs, by showing that mitochondrial respiration and capacity was significantly higher in high-fit (trained) than low-fit (untrained or sedentary) young female adults, which was unrelated to immune cell composition. We also demonstrated that a recent bout of exercise did not alter PBMC mitochondrial function neither high-fit and low-fit female individuals, indicating that a longer period of aerobic exercise training exposure might be required before the effects are reflected in metabolic PBMC profiles. This is in line with

previous studies, which showed that six or twelve weeks of aerobic exercise training increased mitochondrial function in respectively lymphocytes (36) and PBMCs (24) and found that protein and gene expression levels of mitochondrial markers in PBMCs were enhanced with eight weeks of aerobic exercise training (38), while a two-week aerobic exercise protocol did not alter mitochondrial function in PBMCs (37), indeed suggesting that longer-, but not shorter-term training status impacts PBMC mitochondrial function.

The bodily adaptations that occur upon regular exercise could possibly underly our observation that PBMC metabolism is different between high-fit and low-fit females (53). Exercise triggers the release of biologically active proteins and metabolites by multiple tissues that are secreted into the systemic circulation and impact other organs and physiological systems (26,54). For example, interleukin (IL) 6 (IL6) is a cytokine that is acutely secreted from contracting skeletal muscle, which promotes the release of the anti-inflammatory cytokines IL10 and IL1 receptor antagonist (IL-1RA) and increases the mobilization of nutrients from liver and adipose tissue (55). Regular exercise has been suggested to lower the magnitude of the IL6 response to exercise as well as resting IL6 levels (55), and IL6 levels were shown to negatively correlate with mitochondrial PBMC function (22,23). Furthermore, serum lipid metabolite levels, such as triglycerides, fatty acids, and glycoproteins, were found to differ between high-fit and low-fit individuals (56). Since circulating lipid metabolites have been found to alter gene and protein expression levels of mitochondrial markers in isolated PBMCs (57) as well as *ex vivo* cytokine production in isolated PBMCs (58,59), the altered metabolic make-up of the plasma upon regular aerobic exercise could imprint a long-lasting adaptation of PBMC mitochondrial function. Given that a single, recent exercise bout or an *ex vivo* immunological stimulus did not alter mitochondrial function in our study, it is likely that prolonged alteration of the plasma metabolome and/or cytokine levels is needed to observe changes in PBMC mitochondrial function. Previously, metabolic markers in PBMCs have been shown to respond to alterations in dietary intake (60,61) and body weight (62). Our study demonstrates that PBMCs can also reflect differences in aerobic fitness level in healthy adult females, which further increases the potential of PBMCs as a biomarker to study the impact of lifestyle factors on human health.

Our study also demonstrated that a single, recent bout of exercise did not affect mitochondrial nor glycolytic metabolism in PBMCs from high-fit or low-fit females. However, a single bout of exercise was shown to increase mitochondrial PBMC metabolism in a previous study (25). Differences in sampling time might underlie these different observations, as Liepinsh et al. sampled directly after exercise (25)

while we sampled 21 hours after exercise. Since PBMC subsets are metabolically different (17,18) and substantial shifts in PBMC subsets have been described after acute exercise (27–29), the increased mitochondrial PBMC function as observed by Liepinsh et al. could possibly be related to large differences in analyzed PBMC subsets between the two timepoints, while in our study PBMC composition was similar at baseline and after the recent bout of exercise. Secondly, differences in the metabolic substrates provided to the PBMCs during metabolic analysis might play a role. Fatty acid-dependent mitochondrial respiration was increased in permeabilized PBMCs after acute exercise (25), yet our study did not focus on substrate-dependent PBMC metabolism. Interestingly, in skeletal muscle, an acute, single bout of aerobic exercise is associated with alterations in metabolic fuel utilization, whereas regular bouts of aerobic exercise are associated with skeletal muscle adaptations, such as an increased number and function of mitochondria (63). This indicates that the impact of short- and longer-term exercise on cellular energy metabolism could be substantially different, and that differences between baseline and post-exercise PBMC metabolism in our study could possibly have been detected when using different levels or combinations of metabolic substrates.

For comprehensive analysis of PBMC metabolism, we analysed PBMC composition using flow cytometry in addition to our XF assays and showed that the major contributing PBMC cell types (~90%) were not significantly different between high-fit and low-fit female individuals. This is in line with findings from previous studies (28,64–67), although some studies also have shown that some lymphocyte subsets (e.g. CD3<sup>+</sup>, CD56<sup>+</sup>) were lower (68,69) or higher (69) in high-fit compared to low-fit individuals. We also demonstrated that high-fit females had significantly higher monocyte (CD14<sup>+</sup>) and activated T cell (CD3<sup>+</sup>CD4<sup>+</sup>CD25<sup>+</sup>) frequencies as compared to low-fit females. However, we consider it unlikely that these differences impact our metabolic findings, because glycolytic PBMC function was not significantly different between the two groups, while monocytes and activated T cells were shown to rely more on glycolysis than the other PBMC subsets that we analysed (17,70). Furthermore, the contribution of the monocyte and activated T cell subset to the total PBMC pool is only ~10% and the difference between the high-fit and low-fit group was only ~2.4% of total, while respiration differences for the total population were around the magnitude of 20%. The overall stability in PBMC composition does not only temper the concerns for the influence of PBMC subset variability on PBMC biomarker responses, it also enforces the notion of PBMCs as a relevant biomarker tissue to examine lifestyle interventions. Importantly, studies that deal with major shifts in PBMC cell types, such as studies that include acute exercise interventions or disease pathology, might experience

confounding by PBMC heterogeneity. Our study also included some limitations, such as the fact that we did not evaluate the effect of nutritional status on PBMC metabolism. For example, vitamin D status has been linked to mitochondrial PBMC function (61,71). As we measured all our subjects in late autumn and winter, vitamin D intake from food becomes more important compared to summer. However, dietary vitamin D intake and status was not controlled for and could thus have acted as a potential confounder in our study.

In conclusion, using XF analysis of PBMC metabolism we showed that PBMCs from high-fit female individuals had increased mitochondrial function, which was not explained by changes in PBMC subsets, but instead implies an inherent higher oxygen consumption. Our study reveals a link between PBMC metabolism and levels of aerobic fitness, increasing the relevance of PBMC metabolism as a marker to study the impact of lifestyle factors on human health in future clinical and biological studies.

### Acknowledgements

The authors greatly acknowledge the commitment of the volunteers who participated in the study. We acknowledge Camiel Oe and Maud Pijnenburg for data collection and Henriette Fick-Brinkhof and Diana Emmen-Benink for blood sampling.

### Authors' contributions

Study: J.J.E.J., B.L.; Analysis: J.J.E.J., M.P.; Data interpretation: J.J.E.J., M.P., H.F.J.S., R.J.J.v.N., J.K., V.C.J.d.B.; Writing: original draft preparation: J.J.E.J.; review and editing: J.J.E.J., B.L., M.P., A.G.N., H.F.J.S., R.J.J.v.N., J.K., V.C.J.d.B.; Funding: J.J.E.J., J.K., V.C.J.d.B.

### Funding

This work was supported by NWO-WIAS Graduate Program grant 2016 and the H2020-EU 3.2.2.1/2 PREVENTOMICS GA 818318 grant.

### Declaration of interest

All authors declare no conflict of interest.

## References

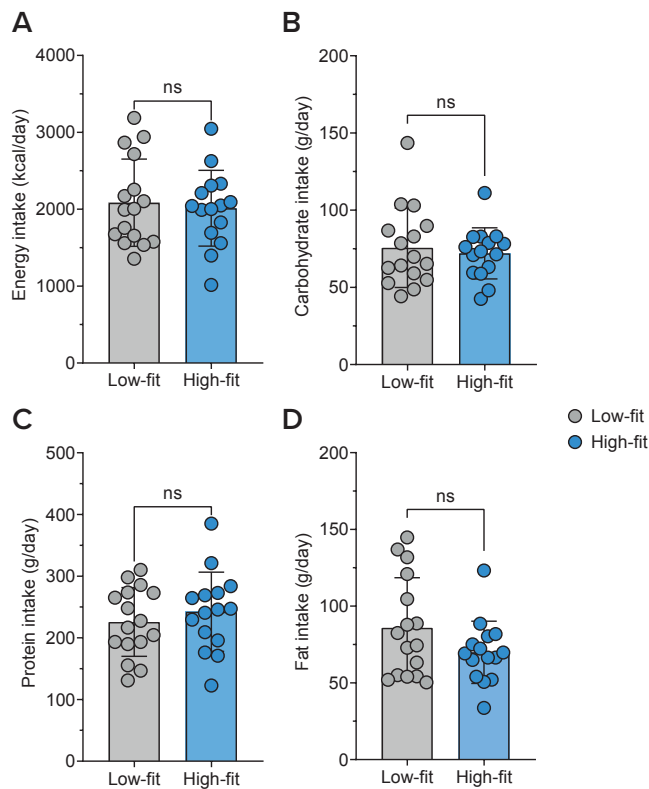
1. Zhang Y, Pan XF, Chen J, Xia L, Cao A, Zhang Y, et al. Combined lifestyle factors and risk of incident type 2 diabetes and prognosis among individuals with type 2 diabetes: a systematic review and meta-analysis of prospective cohort studies. *Diabetologia*. 2020;63(1):21–33.
2. Colpani V, Baena CP, Jaspers L, van Dijk GM, Farajzadegan Z, Dhana K, et al. Lifestyle factors, cardiovascular disease and all-cause mortality in middle-aged and elderly women: a systematic review and meta-analysis. *Eur J Epidemiol*. 2018;33(9):831–45.
3. Zhang YB, Pan XF, Chen J, Cao A, Zhang YG, Xia L, et al. Combined lifestyle factors, incident cancer, and cancer mortality: a systematic review and meta-analysis of prospective cohort studies. *Br J Cancer*. 2020;122(7):1085–93.
4. Lopez AD, Mathers CD, Ezzati M, Jamison DT, Murray CJ. Global and regional burden of disease and risk factors, 2001: systematic analysis of population health data. *Lancet*. 2006;367(9524):1747–57.
5. Califf RM. Biomarker definitions and their applications. *Exp Biol Med*. 2018;243(3):213–21.
6. Nieman DC, Wentz LM. The compelling link between physical activity and the body's defense system. *J Sport Heal Sci*. 2019;8(3):201–17.
7. Radzikowska U, Rinaldi AO, Çelebi Sözen Z, Karaguzel D, Wojcik M, Cypryk K, et al. The Influence of Dietary Fatty Acids on Immune Responses. Vol. 11, *Nutrients*. 2019.
8. Qiu F, Liang C-L, Liu H, Zeng Y-Q, Hou S, Huang S, et al. Impacts of cigarette smoking on immune responsiveness: Up and down or upside down? *Oncotarget*. 2016;8(1).
9. Szostaczuk N, van Schothorst EM, Sánchez J, Priego T, Palou M, Bekkenkamp-Grovenstein M, et al. Identification of blood cell transcriptome-based biomarkers in adulthood predictive of increased risk to develop metabolic disorders using early life intervention rat models. *FASEB J*. 2020 Jul 1;34(7):9003–17.
10. Reynés B, Priego T, Cifre M, Oliver P, Palou A. Peripheral Blood Cells, a Transcriptomic Tool in Nutrigenomic and Obesity Studies: Current State of the Art. *Compr Rev Food Sci Food Saf*. 2018 Jul;17(4):1006–20.
11. Picó C, Serra F, Rodríguez AM, Keijer J, Palou A. Biomarkers of nutrition and health: New tools for new approaches. *Nutrients*. 2019;11(5):1–30.
12. Díaz-Rúa R, Keijer J, Caimari A, van Schothorst EM, Palou A, Oliver P. Peripheral blood mononuclear cells as a source to detect markers of homeostatic alterations caused by the intake of diets with an unbalanced macronutrient composition. *J Nutr Biochem*. 2015 Apr;26(4):398–407.
13. Caimari A, Oliver P, Rodenburg W, Keijer J, Palou A. Feeding conditions control the expression of genes involved in sterol metabolism in peripheral blood mononuclear cells of normoweight and diet-induced (cafeteria) obese rats. *J Nutr Biochem*. 2010;21(11):1127–33.
14. Kleiveland CR. Peripheral Blood Mononuclear Cells. In: Verhoeckx K, Cotter P, López-Expósito I, Kleiveland C, Lea T, Mackie A, et al., editors. *The Impact of Food Bioactives on Health: in vitro and ex vivo models*. Cham: Springer International Publishing; 2015. p. 161–7.
15. Autissier P, Soulas C, Burdo TH, Williams KC. Evaluation of a 12-color flow cytometry panel to study lymphocyte, monocyte, and dendritic cell subsets in humans. *Cytometry A*. 2010 May;77(5):410–9.
16. Buck MD, Sowell RT, Kaech SM, Pearce EL. Metabolic Instruction of Immunity. *Cell*. 2017;169(4):570–86.
17. Chacko BK, Kramer PA, Ravi S, Johnson MS, Hardy RW, Ballinger SW, et al. Methods for defining distinct bioenergetic profiles in platelets, lymphocytes, monocytes, and neutrophils, and the oxidative burst from human blood. *Lab Invest*. 2013;93(6):690–700.
18. Rausser S, Trumpff C, McGill MA, Junker A, Wang W, Ho S-H, et al. Mitochondrial phenotypes in purified human immune cell subtypes and cell mixtures. Johnson SC, Akhmanova A, editors. *Elife*. 2021;10:e70899.
19. Chen H, Schürch CM, Noble K, Kim K, Krutzik PO, O'Donnell E, et al. Functional comparison of PBMCs isolated by Cell Preparation Tubes (CPT) vs. Lymphoprep Tubes. *BMC Immunol*. 2020 Mar;21(1):15.
20. Schmid D, Burmester GR, Tripmacher R, Kuhnke A, Buttgeriet F. Bioenergetics of Human Peripheral Blood Mononuclear Cell Metabolism in Quiescent, Activated, and Glucocorticoid-Treated States. *Biosci Rep*. 2000;20(4):289–302.

21. Hartman M-L, Shirihaï OS, Holbrook M, Xu G, Kocherla M, Shah A, et al. Relation of mitochondrial oxygen consumption in peripheral blood mononuclear cells to vascular function in type 2 diabetes mellitus. *Vasc Med.* 2014 Feb;19(1):67–74.
22. Li P, Wang B, Sun F, Li Y, Li Q, Lang H, et al. Mitochondrial respiratory dysfunctions of blood mononuclear cells link with cardiac disturbance in patients with early-stage heart failure. *Sci Rep.* 2015;5(1):10229.
23. Tyrrell DJ, Bharadwaj MS, Van Horn CG, Marsh AP, Nicklas BJ, Molina AJA. Blood-cell bioenergetics are associated with physical function and inflammation in overweight/obese older adults. *Exp Gerontol.* 2015 Oct;70:84–91.
24. Kocher M, McDermott M, Lindsey R, Shikuma CM, Gerschenson M, Chow DC, et al. Short Communication: HIV Patient Systemic Mitochondrial Respiration Improves with Exercise. *AIDS Res Hum Retroviruses.* 2017 Oct;33(10):1035–7.
25. Liepinsh E, Makarova E, Plakane L, Konrade I, Liepins K, Videja M, et al. Low-intensity exercise stimulates bioenergetics and increases fat oxidation in mitochondria of blood mononuclear cells from sedentary adults. *Physiol Rep.* 2020 Jun;8(12):e14489.
26. Pedersen BK, Hoffman-Goetz L. Exercise and the immune system: Regulation, integration, and adaptation. *Physiol Rev.* 2000;80(3):1055–81.
27. Sellami M, Gasmi M, Denham J, Hayes LD, Stratton D, Padulo J, et al. Effects of Acute and Chronic Exercise on Immunological Parameters in the Elderly Aged: Can Physical Activity Counteract the Effects of Aging? Vol. 9, *Frontiers in Immunology.* 2018. p. 2187.
28. Oshida Y, Yamanouchi K, Hayamizu S, Sato Y. Effect of acute physical exercise on lymphocyte subpopulations in trained and untrained subjects. *Int J Sports Med.* 1988 Apr;9(2):137–40.
29. Shinkai S, Shore S, Shek PN, Shephard RJ. Acute exercise and immune function. Relationship between lymphocyte activity and changes in subset counts. *Int J Sports Med.* 1992 Aug;13(6):452–61.
30. Lagerwaard B, Janssen JJE, Cuijpers I, Keijer J, de Boer VCJ, Nieuwenhuizen AG. Muscle mitochondrial capacity in high- and low-fitness females using near-infrared spectroscopy. *Physiol Rep.* 2021;9(9):1–10.
31. Lagerwaard B, Keijer J, McCully KK, de Boer VCJ, Nieuwenhuizen AG. In vivo assessment of muscle mitochondrial function in healthy, young males in relation to parameters of aerobic fitness. *Eur J Appl Physiol.* 2019;
32. Malek MH, Berger DE, Housh TJ, Coburn JW, Beck TW. Validity of  $\dot{V}O_{2\max}$  equations for aerobically trained males and females. *Med Sci Sports Exerc.* 2004;36(8):1427–32.
33. Decroix L, De Pauw K, Foster C, Meeusen R. Guidelines to classify female subject groups in sport-science research. *Int J Sports Physiol Perform.* 2016;11(2):204–13.
34. Enea C, Boisseau N, Ottavy M, Mulliez J, Millet C, Ingrand I, et al. Effects of menstrual cycle, oral contraception, and training on exercise-induced changes in circulating DHEA-sulphate and testosterone in young women. *Eur J Appl Physiol.* 2009;106(3):365–73.
35. Silaidos C, Pilatus U, Grewal R, Matura S, Lienerth B, Pantel J, et al. Sex-associated differences in mitochondrial function in human peripheral blood mononuclear cells (PBMCs) and brain. *Biol Sex Differ.* 2018;9(1):1–10.
36. Tsai H-H, Chang S-C, Chou C-H, Weng T-P, Hsu C-C, Wang J-S. Exercise Training Alleviates Hypoxia-induced Mitochondrial Dysfunction in the Lymphocytes of Sedentary Males. *Sci Rep.* 2016; 6(1):35170.
37. Hedges CP, Woodhead JST, Wang HW, Mitchell CJ, Cameron-Smith D, Hickey AJR, et al. Peripheral blood mononuclear cells do not reflect skeletal muscle mitochondrial function or adaptation to high-intensity interval training in healthy young men. *J Appl Physiol.* 2019;126(2):454–61.
38. Busquets-Cortés C, Capó X, Martorell M, Tur JA, Sureda A, Pons A. Training and acute exercise modulates mitochondrial dynamics in football players' blood mononuclear cells. *Eur J Appl Physiol.* 2017 Oct;117(10):1977–87.
39. Streppel MT, de Vries JHM, Meijboom S, Beekman M, de Craen AJM, Slagboom PE, et al. Relative validity of the food frequency questionnaire used to assess dietary intake in the Leiden Longevity Study. *Nutr J.* 2013;12(1):75.

40. Janssen JJE, Lagerwaard B, Porbahaie M, Nieuwenhuizen AG, Savelkoul HFJ, Van Neerven JR, et al. Supplementary Figure 1: Habitual dietary intake of the study subjects. Figshare. 2021.
41. Janssen JJE, Lagerwaard B, Bunschoten A, Savelkoul HFJ, van Neerven RJJ, Keijer J, et al. Novel standardized method for extracellular flux analysis of oxidative and glycolytic metabolism in peripheral blood mononuclear cells. *Sci Rep*. 2021;11(1).
42. Mookerjee SA, Goncalves RLS, Gerencser AA, Nicholls DG, Brand MD. The contributions of respiration and glycolysis to extracellular acid production. *Biochim Biophys Acta*. 2015 Feb;1847(2):171–81.
43. Janssen JJE, Lagerwaard B, Porbahaie M, Nieuwenhuizen AG, Savelkoul HFJ, Van Neerven JR, et al. Supplementary Figure 2: Fluorescence-activated cell sorting (FACS) gating strategy. Figshare. 2021.
44. Pressman BC, Fahim M. Pharmacology and toxicology of the monovalent carboxylic ionophores. *Annu Rev Pharmacol Toxicol*. 1982;22:465–90.
45. Mookerjee SA, Nicholls DG, Brand MD. Determining Maximum Glycolytic Capacity Using Extracellular Flux Measurements. *PLoS One*. 2016;11(3):e0152016.
46. Izquierdo E, Cuevas VD, Fernández-Arroyo S, Riera-Borrull M, Orta-Zavalza E, Joven J, et al. Reshaping of Human Macrophage Polarization through Modulation of Glucose Catabolic Pathways. *J Immunol*. 2015;195(5):2442–51.
47. Cichocki F, Wu C-Y, Zhang B, Felices M, Tesi B, Tuininga K, et al. ARID5B regulates metabolic programming in human adaptive NK cells. *J Exp Med*. 2018 Sep;215(9):2379–95.
48. Frauwirth KA, Riley JL, Harris MH, Parry R V, Rathmell JC, Plas DR, et al. The CD28 Signaling Pathway Regulates Glucose Metabolism. *Immunity*. 2002 Jun 1;16(6):769–77.
49. Jones N, Cronin JG, Dolton G, Panetti S, Schauenburg AJ, Galloway SAE, et al. Metabolic Adaptation of Human CD4+ and CD8+ T-Cells to T-Cell Receptor-Mediated Stimulation. Vol. 8, *Frontiers in Immunology*. 2017. p. 1516.
50. Krauss S, Buttgeriet F, Brand MD. Effects of the mitogen concanavalin A on pathways of thymocyte energy metabolism. *Biochim Biophys Acta - Bioenerg*. 1999;1412(2):129–38.
51. Crabtree G. Signal Transmission between the Plasma Membrane and Nucleus of T Lymphocytes. *Annu Rev Biochem*. 1994;63(1):1045–83.
52. Cahalan MD, Chandy KG. Ion channels in the immune system as targets for immunosuppression. *Curr Opin Biotechnol*. 1997;8(6):749–56.
53. McGee SL, Hargreaves M. Exercise adaptations: molecular mechanisms and potential targets for therapeutic benefit. *Nat Rev Endocrinol*. 2020;16(9):495–505.
54. Pedersen BK, Febbraio MA. Muscles, exercise and obesity: skeletal muscle as a secretory organ. *Nat Rev Endocrinol*. 2012;8(8):457–65.
55. Fischer CP. Interleukin-6 in acute exercise and training: what is the biological relevance? *Exerc Immunol Rev*. 2006;12:6–33.
56. Kujala UM, Vaara JP, Kainulainen H, Vasankari T, Vaara E, Kyröläinen H. Associations of Aerobic Fitness and Maximal Muscular Strength With Metabolites in Young Men. *JAMA Netw Open*. 2019 Aug 23;2(8):e198265–e198265.
57. Busquets-Cortés C, Capó X, Martorell M, Tur JA, Sureda A, Pons A. Training Enhances Immune Cells Mitochondrial Biosynthesis, Fission, Fusion, and Their Antioxidant Capabilities Synergistically with Dietary Docosahexaenoic Supplementation. *Oxid Med Cell Longev*. 2016;2016.
58. Zhao G, Etherton TD, Martin KR, Gillies PJ, West SG, Kris-Etherton PM. Dietary  $\alpha$ -linolenic acid inhibits proinflammatory cytokine production by peripheral blood mononuclear cells in hypercholesterolemic subjects. *Am J Clin Nutr*. 2007;85(2):385–91.
59. Endres S, Ghorbani R, Kelley VE, Georgilis K, Lonnemann G, van der Meer JW, et al. The effect of dietary supplementation with n-3 polyunsaturated fatty acids on the synthesis of interleukin-1 and tumor necrosis factor by mononuclear cells. *N Engl J Med*. 1989 Feb;320(5):265–71.
60. Caimari A, Oliver P, Keijer J, Palou A. Peripheral Blood Mononuclear Cells as a Model to Study the Response of Energy Homeostasis-Related Genes to Acute Changes in Feeding Conditions. *Omi A J Integr Biol*. 2010 Mar 17;14(2):129–41.

61. Calton EK, Keane KN, Soares MJ, Rowlands J, Newsholme P. Prevailing vitamin D status influences mitochondrial and glycolytic bioenergetics in peripheral blood mononuclear cells obtained from adults. *Redox Biol.* 2016;10:243–50.
62. Sánchez J, Picó C, Ahrens W, Foraita R, Fraterman A, Moreno LA, et al. Transcriptome analysis in blood cells from children reveals potential early biomarkers of metabolic alterations. *Int J Obes.* 2017 Oct;41(10):1481–8.
63. Egan B, Zierath JR. Exercise Metabolism and the Molecular Regulation of Skeletal Muscle Adaptation. *Cell Metab.* 2013;17(2):162–84.
64. Nieman DC, Brendle D, Henson DA, Suttles J, Cook VD, Warren BJ, et al. Immune function in athletes versus nonathletes. *Int J Sports Med.* 1995;16(5):329–33.
65. Nieman DC, Buckley KS, Henson DRUA, Warren BJ, Suttles J, Ahle JC, et al. Immune function in marathon runners versus sedentary controls. *Med Sci Sport Exerc.* 1995;27(7).
66. Mitchell JB, Paquet AJ, Pizza FX, Starling RD, Holtz RW, Grandjean PW. The effect of moderate aerobic training on lymphocyte proliferation. *Int J Sports Med.* 1996 Jul;17(5):384–9.
67. Pedersen BK, Tvede N, Christensen LD, Klarlund K, Kragbak S, Halkjær-Kristensen J. Natural killer cell activity in peripheral blood of highly trained and untrained persons. *Int J Sport Med Med.* 1989 Apr;10(2):129–31.
68. Baj Z, Kantorski J, Majewska E, Zeman K, Pokoca L, Fornalczy E, et al. Immunological status of competitive cyclists before and after the training season. *Int J Sports Med.* 1994;15(6):319–24.
69. Rhind SG, Shek PN, Shinkai S, Shephard RJ. Differential expression of interleukin-2 receptor alpha and beta chains in relation to natural killer cell subsets and aerobic fitness. *Int J Sports Med.* 1994 Aug;15(6):311–8.
70. Ahl PJ, Hopkins RA, Xiang WW, Au B, Kaliaperumal N, Fairhurst A-M, et al. Met-Flow, a strategy for single-cell metabolic analysis highlights dynamic changes in immune subpopulations. *Commun Biol.* 2020;3(1):305.
71. Calton EK, Keane KN, Raizel R, Rowlands J, Soares MJ, Newsholme P. Winter to summer change in vitamin D status reduces systemic inflammation and bioenergetic activity of human peripheral blood mononuclear cells. *Redox Biol.* 2017;12:814–20.

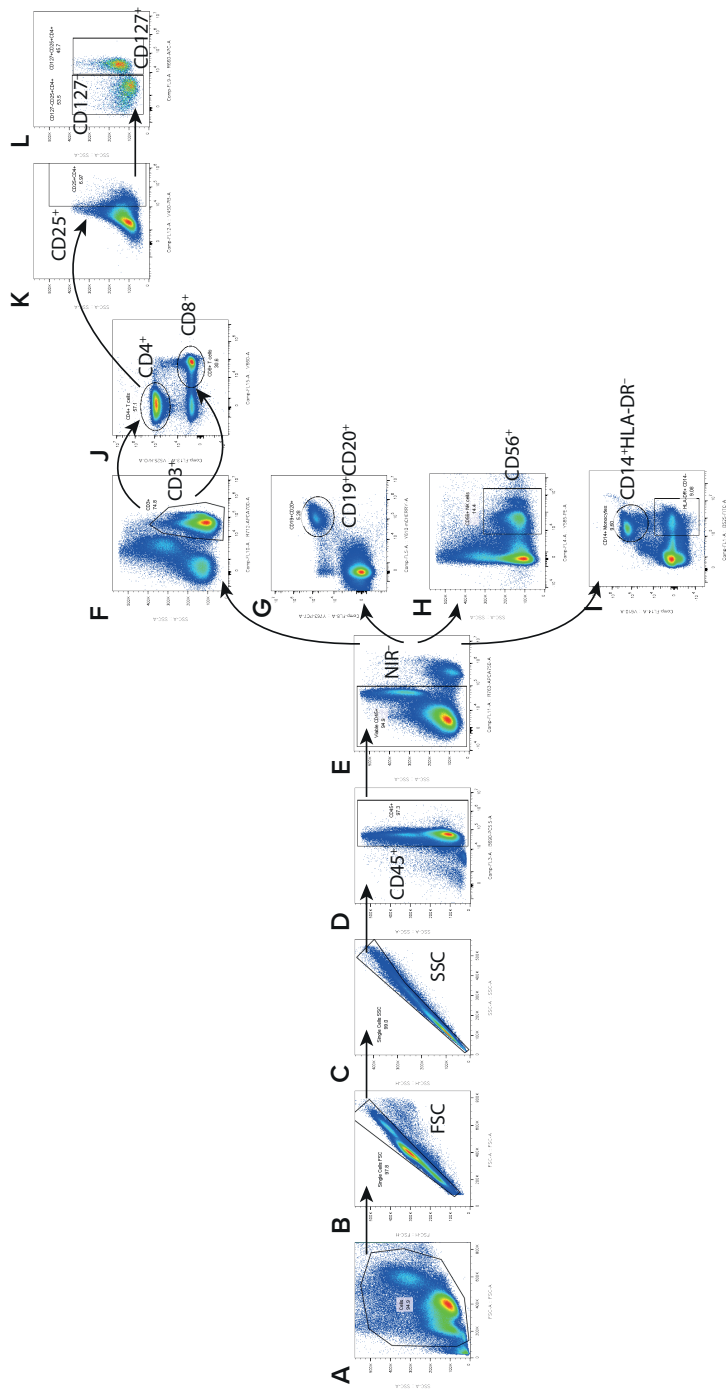
Supplementary materials



**Supplementary Figure S1: Habitual dietary intake of the study subjects.** Dietary intake of the subjects was assessed with a validated food frequency questionnaire (FFQ) and total daily energy intake (A) and intake of carbohydrates (B), proteins (C), and fats (D) were calculated for high-fit (blue) and low-fit (grey) females.

**Supplementary Table S1** Dilutions for fluorochrome-conjugated antibodies and optimal concentrations

Antibody	Company	Catalog number	Range tested ( $\mu\text{L}$ / 50 $\mu\text{L}$ )	Optimal conc. ( $\mu\text{L}$ / 50 $\mu\text{L}$ )
anti-CD3	Biolegend	300424	4, 2, 1, 0.5, 0	1
anti-CD4	Biolegend	317444	4, 2, 1, 0.5, 0	2
anti-CD8a	Biolegend	301042	4, 2, 1, 0.5, 0	1
anti-CD25	Biolegend	302630	4, 2, 1, 0.5, 0	1
anti-CD127	Biolegend	351342	4, 2, 1, 0.5, 0	1
anti-CD14	Biolegend	367126	4, 2, 1, 0.5, 0	1
anti-HLA-DR	Biolegend	307632	4, 2, 1, 0.5, 0	1
anti-CD56	Biolegend	362524	4, 2, 1, 0.5, 0	1
anti-CD19	Biolegend	302216	4, 2, 1, 0.5, 0	1
anti-CD20	Biolegend	302348	4, 2, 1, 0.5, 0	1
anti-CD45	Biolegend	368506	4, 2, 1, 0.5, 0	1



**Supplementary Figure S2: Fluorescence-activated cell sorting (FACS) gating strategy.** Lineage-specific antibodies against T cells, B cells, NK cells and monocytes were used to identify different PBMC cell types. **(A)** Selection of all cells. **(B)** Identification of single cells by plotting forward scatter-area (FSC-A) against forward scatter-height (FSC-H). **(C)** Separation of single cells from cellular debris by plotting side scatter-area (SSC-A) against side scatter-height (SSC-H). **(D)** Selection of CD45<sup>+</sup> leukocytes by gating on CD45<sup>+</sup> events. **(E)** Selection of viable cells by gating on Zombie-NIR<sup>-</sup> events. **(F, G)** Selection of CD3<sup>+</sup> T cells by gating on CD3<sup>+</sup> events **(F)** and discrimination between CD3<sup>+</sup>CD4<sup>+</sup> Th and CD3<sup>+</sup>CD8<sup>+</sup> cytotoxic T cells by gating on CD4<sup>+</sup> and CD8<sup>+</sup> events. **(H, I)** Selection of CD4<sup>+</sup>CD25<sup>+</sup> cells by gating on CD25<sup>+</sup> events **(H)** and discrimination between CD25<sup>+</sup>CD127<sup>+</sup> and CD127<sup>+</sup> events **(I)**. **(J)** Selection of CD19<sup>+</sup>CD20<sup>+</sup> B cells by gating on CD19<sup>+</sup>CD20<sup>+</sup> events. **(K)** Selection of CD56<sup>+</sup> NK cells by gating on CD56<sup>+</sup> events. **(L)** Selection of CD14<sup>+</sup> monocytes by discriminating between CD14<sup>+</sup>HLA-DR<sup>+</sup> and CD14<sup>+</sup>HLA-DR<sup>-</sup> events.



# 5

## Single and joined behaviour of circulating biomarkers in high-fit and low-fit healthy females

Joëlle J.E. Janssen<sup>1,2</sup>, Bart Lagerwaard<sup>1,3</sup>, Arie G Nieuwenhuizen<sup>1</sup>,  
Xavier Escoté<sup>4</sup>, Núria Canela<sup>5</sup>, Josep M. del Bas<sup>4</sup>,  
Vincent C.J. de Boer<sup>1</sup>, Jaap Keijer<sup>1</sup>

<sup>1</sup> Human and Animal Physiology, Wageningen University and Research,  
P.O. Box 338, 6700 AH, Wageningen, the Netherlands

<sup>2</sup> Cell Biology and Immunology, Wageningen University and Research,  
P.O. Box 338, 6700 AH, Wageningen, the Netherlands

<sup>3</sup> TI Food and Nutrition, P.O. Box 557, 6700 AN, Wageningen, the Netherlands

<sup>4</sup> Nutrition and Health Unit, EURECAT, Technology Centre of Catalunya, 43204 Reus, Spain

<sup>5</sup> Centre for Omic Sciences (COS), Universitat Rovira i Virgili-EURECAT,  
Technology Centre of Catalunya, 43204 Reus, Spain

**Submitted**

## Abstract

Biomarkers are important in the assessment of health and disease but are poorly studied in healthy individuals. Especially responses of biomarkers in the systemic circulation to longer-term and short-term lifestyle interventions are incompletely understood, neither is their relative response to each other. This study investigated how single biomarkers, functional biomarker categories and total biomarker profiles respond to a difference in longer-term physical activity and to recent exercise in healthy individuals. A total of 102 biomarkers were analysed in serum or plasma samples from 30 young, healthy, female adults divided into a high-fit ( $\dot{V}O_{2\text{peak}} \geq 47$  mL/kg/min,  $N = 15$ ) and low-fit ( $\dot{V}O_{2\text{peak}} \leq 37$  mL/kg/min,  $N = 15$ ) group, at baseline and overnight after a single bout of exercise (60 min, 70%  $\dot{V}O_{2\text{peak}}$ ). Total biomarker profiles were similar between high-fit and low-fit females, with only significantly lower leptin levels in high-fit females (adj. $P_{\text{group}} = 0.076$ ). Recent exercise significantly affected several single biomarkers related to inflammation and lipid metabolism, and adiponectin (all adj. $P_{\text{exercise}} < 0.01$ ). Furthermore, functional biomarker categories corresponded to biomarker clusters generated via hierarchical clustering models. This study provides insight in the single and joined behaviour of circulating biomarkers in healthy females, and identified functional biomarker categories that may be used for characterization of human health physiology.

## Introduction

Lifestyle factors play a dominant role in health maintenance and the prevention of chronic diseases, such as type 2 diabetes (1), cardiovascular disease (2), and cancer (3). Adopting a healthy lifestyle, including regular physical activity performance, is associated with a lower chronic disease risk (4). Biomarkers are important in the assessment of the impact of lifestyles on health status (5). For monitoring disease risk and the progression from a healthy to an unhealthier state, the use of biomarkers that reflect key physiological processes, such as metabolism, inflammation, and oxidative stress, has been proposed (6). The dynamics of biomarkers has often been studied in disease conditions, but it is hardly understood how these biomarkers behave in healthy individuals adhering to different lifestyles and how they respond to a short-term lifestyle interventions. Moreover, many of these biomarkers have not been studied relatively to each other, especially not in healthy individuals.

Physical activity is one of the lifestyle factors that has been associated with systemic changes that are linked to a reduced chronic disease risk (7). High levels of physical activity has been shown to reduce insulin resistance (8), improve lipoprotein profiles (9), and lower interleukin (IL)6 levels on the long-term (10), which contributes to a lower chronic disease risk (11–14). However, short-term exercise, e.g., a single bout of exercise, also provokes acute systemic changes, which can last for up to 24 hours (15–17). These short-term exercise responses can differ between individuals with high and low levels of physical activity, due to the metabolic and physiological adaptations of the body to regular exercise (18,19). Hence, not only the basal levels of circulating biomarkers could differ between high- and low physically active individuals, but the biomarker response to a single exercise session might also be affected. This, however, has been studied only to a limited extent, with most studies focusing on male individuals (15), while physiological responses between males and females can be strikingly different (20).

This study investigated how serum and plasma biomarkers are affected by different longer-term physical activity levels and by recent exercise. Routine physiological biomarkers such as insulin, LDL cholesterol, and c-reactive protein (CRP) were included as well as markers that represent other metabolic, immunological, and oxidative stress-related processes. All biomarkers were allocated to three functional biomarker categories: 1) peptide hormones, 2) inflammation and oxidative stress-related markers, and 3) metabolism markers, the latter comprising protein, carbohydrate, and lipid metabolism. Biomarker analysis was performed in high aerobically fit (high-fit) and low aerobically fit (low-fit) females with a validated

difference in  $\dot{V}O_{2\text{peak}}$  to reflect a difference in training status. Previously, we found a significant difference in skeletal muscle mitochondrial capacity (21) and mitochondrial function in peripheral blood mononuclear cells (PBMCs) (22) in our healthy study population. Biomarker analysis in this study will now show whether single biomarkers, functional biomarker categories and total biomarker profiles differ between these high-fit and low-fit females, and how these biomarkers respond to a recent bout of exercise. This information will improve our understanding on the effect of longer-term lifestyle differences and recent lifestyle interventions on biomarkers of health and disease and contribute to the application of preventative and health improvement interventions.

## Materials and Methods

### Ethical approval and study registration

The protocol for collection and handling of human samples was ethically approved by the medical ethical committee (METC) of Wageningen University (since January 2021 replaced by METC Oost-Nederland) with reference number NL70136.081.19 and registered in the Dutch trial register (NL7891) on 2019-07-23. All procedures performed were in accordance with institutional ethical standards, national law (WMO, The Hague, 1998) and with the 1964 Helsinki declaration and its amendments. Written informed consent was obtained from all individual subjects included in the study.

### Study subjects

Healthy young females (18 – 28 years of age, BMI 18.5 – 25 kg/m<sup>2</sup>) were recruited from the local university and community population. Exclusion criteria were as follows: history of cardiovascular, respiratory, hematological, or metabolic disease; use of prescribed chronic medication; anemia (hemoglobin concentration < 12 g/dL); blood donation within two months before the start of the study; smoking (> 5 cigarettes per week); recreational drug use or over the counter drug use during the study; use of performance-enhancing supplements; pregnancy or lactating. Subjects were selected if they had a  $\dot{V}O_{2\text{peak}} \geq 47$  mL/kg/min (high-fit group) or  $\leq 37$  mL/kg/min (low-fit group) determined using a maximal exercise test, measured using the validated screening protocol of Lagerwaard et al. (21,23), which minimized the risk for selective bias. Sixteen high-fit and sixteen low-fit subjects were included. The  $\dot{V}O_{2\text{peak}}$  data and results of skeletal muscle mitochondrial capacity of these subjects has been published previously by our group (21). A total of 111 maximal exercise tests were performed to end up with the desired sample size. One subject was excluded due to medication intake and one

subject was excluded due to symptoms of illness directly after completion of the study protocol. The use of oral contraceptives (OC) was not excluded; only the use of monophasic OC containing low synthetic estradiol and progesterone was allowed and was controlled for (N = 7 in the high-fit and N = 6 in the low-fit group). The 17 $\beta$ -estradiol levels were measured using a chemiluminescent immunoassay on a Lumipulse G1200 analyzer (Fujirebio IncI) at the Erasmus Medical Centre (Rotterdam, the Netherlands) and were not significantly different between those high-fit (527.7 [353.1 – 610.0]) and low-fit females (217.4 [109.1 – 895.2]) that did not use oral OC (P = 0.321).

### Study design

Subjects refrained from heavy physical exercise 48 hours prior to the first study day and from any physical exercise and alcohol consumption 24 hours prior to the first study day. Subjects adhered to dietary guidelines 24 hours prior to each study day, which included the consumption of a standardized evening meal (73% carbohydrates/16% protein/11% fat, 1818 kJ) before 8:00PM and dietary guidelines for the consumption of breakfast, lunch, drinks, and snacks. After an overnight fast, blood was collected in the morning of the first study day (= baseline timepoint) and on the morning of the second study day, i.e., 21 hours after a single bout of exercise (= post-exercise timepoint). Blood samples (3 x 6 mL) were collected by venipuncture in vacutainers containing dipotassium dipotassium (K2-) ethylenediaminetetraacetic acid (EDTA) (K2-EDTA) as anticoagulant for plasma collection (2 x 6 mL, BD Biosciences, Vianen, the Netherlands, 367525) and a vacutainer containing silica as a clot activator for serum collection (1 x 6 mL, BD Biosciences, Vianen, the Netherlands, 367837). Blood tubes for plasma collection were kept on ice-water and processed within 30 minutes after blood collection. Blood tubes for serum collection were kept at room temperature (RT) for 60 minutes to allow clotting and immediately processed afterwards. Body fat percentage was measured according to the four-site method by Durnin-Womersley using the skinfold measurements of the triceps, biceps, sub scapula and supra iliac, measured using a skinfold calliper (Harpender, UK). Subjects received breakfast and after two hours, subjects completed an individualized exercise protocol consisting of 60 minutes cycling on an electrically braked bicycle ergometer (Corival CPET, Lode, the Netherlands) at a workload aiming to equal 70% of their  $\dot{V}O_{2\text{peak}}$ . Oxygen consumption, carbon dioxide production, and air flow were measured using MAX-II metabolic cart (AEI technologies, Landivisiau, France). Exhaled air was continuously sampled from a mixing chamber and averaged over 15-second time windows. Oxygen consumption was measured in the first and last 15 minutes of the exercise test and used to confirm the relative oxygen consumption. If needed, small adjustments in workload were made to reach 70% of the  $\dot{V}O_2$

peak of the individual. After the exercise protocol subjects went home, refrained from moderate to heavy physical activity, were instructed to keep low levels of light physical activity, and refrained alcohol consumption until blood collection on the second study day. The habitual dietary intake of the study subjects was determined via a validated food frequency questionnaire (FFQ) that assessed dietary intake in the past four weeks (24). The self-reported diets of the high-fit and low-fit subjects were similar with no significant differences in total daily energy intake, carbohydrate intake, protein intake or fat intake ([Supplementary Figure S1](#)).

### Plasma and serum isolation

Plasma tubes were centrifuged for 10 minutes at 1200g at 4°C, and the supernatant (plasma) was collected, transferred to a new tube, and mixed. In case of turbid plasma, samples were centrifuged again for 10 minutes at 1200g at 4°C to remove any insoluble matter. Plasma samples were snap-frozen in liquid nitrogen and afterwards cryopreserved at -80°C. Serum tubes were centrifuged for 10 minutes at 1300g at RT, and the supernatant (serum) was collected, transferred to a new tube, and mixed. In case of turbid serum, samples were centrifuged again for 10 minutes at 1300g at RT to remove any insoluble matter. Serum samples were snap-frozen in liquid nitrogen and afterwards cryopreserved at -80°C. For biomarker analysis, plasma and serum samples were thawed on ice and individually mixed until a clear solution was reached.

### ELISAs in serum and plasma

Commercially available enzyme-linked immunoassay (ELISA) kits were used to analyse serum levels of the peptide hormones leptin, insulin, and adiponectin and the plasma levels of inflammatory and oxidative stress-related markers (tumour necrosis factor (TNF), IL6, IL10, CRP, the soluble monocyte differentiation antigen cluster of differentiation 14 (CD14), monocyte chemoattractant protein 1 (CCL2, better known as MCP1), soluble intercellular adhesion molecule 1 (ICAM1), lipopolysaccharide binding protein (LBP), and oxidized low density lipoprotein (oxidized LDL) according to the manufacturers' instructions ([Table 1](#)).

### Proton NMR (<sup>1</sup>H NMR) in plasma

EDTA-plasma samples were measured using the standardized, targeted high-throughput proton NMR (<sup>1</sup>H NMR) metabolomics from Nightingale Health (Nightingale Health Ltd., Helsinki, Finland, [nightingalehealth.com/biomarkers](https://nightingalehealth.com/biomarkers)). This platform provides simultaneous quantification of 162 individual metabolites and 87 metabolite ratios or sizes. For analysis of this study, all individual metabolites were selected, except for metabolite concentrations within lipoproteins or lipoprotein subclasses (e.g., 'total lipids in VLDL'), and concentrations of clinical LDL cholesterol,

**Table 1** ELISA kits used for serum and plasma biomarker analysis

Biomarker	Matrix	Company	Catalogue number
Leptin	Serum	R&D Systems <sup>a</sup>	DLP00
Insulin	Serum	Mercodia <sup>b</sup>	10-1113-01
Adiponectin	Serum	R&D Systems	DRP300
TNF	Plasma	R&D Systems	HSTA00E
IL6	Plasma	R&D Systems	HS600C
IL10	Plasma	Invitrogen <sup>c</sup>	BMS215HS
CRP	Plasma	R&D Systems	DCRP00
CD14	Plasma	R&D Systems	DC140
MCP1	Plasma	R&D Systems	DCP00
Soluble ICAM 1	Plasma	R&D Systems	BBE1B
LBP	Plasma	Hycult Biotech <sup>d</sup>	HK315-01
Oxidized LDL	Plasma	Mercodia	10-1143-01

<sup>a</sup>R&D systems Inc., Minneapolis, MN, Canada

<sup>b</sup>Mercodia, Uppsala, Sweden

<sup>c</sup>Invitrogen, Thermo Fisher Scientific, Inc., Waltham, MA, USA

<sup>d</sup>Hycult Biotech, Uden, the Netherlands

remnant cholesterol, total cholesterol minus HDL cholesterol and total branched-chain amino acids (BCAAs). All metabolite ratios or sizes were also excluded from analysis. A complete list of the selected metabolites included in the analysis can be found in [Supplementary Table S1](#).

### Proton NMR (<sup>1</sup>H NMR) in serum

Serum samples were measured using targeted high throughput <sup>1</sup>H NMR metabolomics at the EURECAT Technology Centre (Barcelona, Spain). For metabolite extraction, samples were placed in 2 mL 96 deep well plates using 200 µL methanol:water (8:1, for aqueous extraction) or 100 µL methyl-tert-butylether (MTBE):methanol:water (3:10:2, for lipidic extraction) in an automated fashion in the Bravo liquid handler (Agilent Technologies Santa Clara, California, USA). Methanol and MTBE were purchased at Merck (Darmstadt, Germany). After extraction, solvents from the samples were removed using a speed vacuum concentrator and samples were stored at -80°C until analysis. Some samples were lyophilized before <sup>1</sup>H NMR analysis. For <sup>1</sup>H NMR measurements, the hydrophilic extracts were reconstituted in 600 µL deuterium oxide (D<sub>2</sub>O, Deutero, Kastellaun, Germany) PBS (Sigma-Aldrich, St. Louis, MO, USA), 0.05 mM, pH 7.4, 99.5% D<sub>2</sub>O) containing 0.73 mM 3-(Trimethylsilyl) propionic-2,2,3,3-d<sub>4</sub> acid sodium salt (TSP,

Sigma-Aldrich), and the dried lipophilic extracts were reconstituted with a solution of deuterated chloroform ( $\text{CDCl}_3$ )/deuterated methanol ( $\text{CD}_3\text{OD}$ ) (2:1, chloroform d-1 and methanol d-4 from Deutero) containing 1.18 mM tetramethylsilane (TMS, Sigma-Aldrich) and then vortexed. Both extracts were transferred into 5 mm NMR glass tube for  $^1\text{H}$  NMR analysis.  $^1\text{H}$  NMR spectra were recorded at 300 K on an Avance III 600 spectrometer (Bruker, Billerica, Massachusetts, MA, USA) operating at a proton frequency of 600.20 MHz using a 5 mm PABBO gradient probe. Aqueous extracted samples were measured and recorded in processing number (procno) 11. For aqueous extracts one-dimensional  $^1\text{H}$  pulse experiments were carried out using the nuclear Overhauser effect spectroscopy (NOESY) presaturation sequence ( $\text{RD}-90^\circ-\text{t1}-90^\circ-\text{tm}-90^\circ$  ACQ) to suppress the residual water peak, and the mixing time was set at 100 milliseconds. Solvent presaturation with irradiation power of 160 mW was applied during recycling delay ( $\text{RD} = 5$  seconds) and mixing time. The  $90^\circ$  pulse length was calibrated for each sample and varied from 9.72 to 10.06  $\mu\text{s}$ . The spectral width was 12 kHz (20 ppm), and a total of 256 transients were collected into 64 k data points for each  $^1\text{H}$  spectrum. Lipidic extracted samples were measured and recorded in procno 22. In the case of lipophilic extracts, a  $90^\circ$  pulse with presaturation sequence (zgpr) was used to suppress water residual signal of methanol. A RD of 5.0 seconds with acquisition time of 2.94 seconds were used. The  $90^\circ$  pulse length was calibrated for each sample and varied from 9.92 to 10.04  $\mu\text{s}$ . After 4 dummy scans, a total of 128 scans were collected into 64K data points with a spectral width of 18.6 ppm. The exponential line broadening applied before Fourier transformation was of 0.3 Hz. The frequency domain spectra were phased, baseline-corrected and referenced to TSP or TMS signal ( $\text{d} = 0$  ppm) using TopSpin software (version 3.6, Bruker). All acquired  $^1\text{H}$  NMR were compared to standards of the pure selected compounds from AMIX spectra database (Bruker®), HMDB, and ChemoX databases for metabolite identification. In addition, we assigned metabolites by  $^1\text{H}$ - $^1\text{H}$  homonuclear correlation (COSY and TOCSY) and  $^1\text{H}$ - $^{13}\text{C}$  heteronuclear (HSQC) 2D NMR experiments and by correlation with pure compounds run in-house when were needed. After pre-processing, specific  $^1\text{H}$  NMR regions identified in the spectra were integrated using the AMIX 3.9 software package. Curated identified regions across the spectra that were integrated using the same AMIX 3.9 software package were exported to Excel to evaluate the robustness of the different  $^1\text{H}$  NMR signals and to calculate the concentrations.

### LC-MS/MS in plasma

Plasma acylcarnitines were quantified or semi-quantitated in plasma by liquid chromatography with tandem mass spectrometry (LC-MS/MS). Plasma samples were thawed at  $4^\circ\text{C}$  and 30  $\mu\text{L}$  sample were mixed with 270  $\mu\text{L}$  100% methanol

containing the set of labelled internal standards (see [Supplementary Table S2](#)). The mixture was vortexed for 15 seconds and centrifuged for 10 minutes at 3800g at 4°C. The supernatant was transferred into a new plate and injected onto a Kinetex 2.6 µm Polar C18 column, 100 Å, 150 x 2.1 mm (Phenomenex, Torrance, CA, USA) using a UHPLC 1290 Infinity II Series system coupled to a QqQ/MS 6470 Series system (Agilent Technologies, Santa Clara, CA, USA). Metabolite extraction was carried out with a semi-automated process using Agilent Bravo Automated Liquid Handling Platform (Agilent Technologies, Santa Clara, CA, USA).

### Statistical analyses

Statistical analyses were performed using IBM SPSS Statistics for Windows (Version 25.0, IBM Corp, Armonk, NY, USA), and R (Version 4.1.2, R Core Team, Vienna, Austria). Graphs were created using GraphPad Prism (Version 9.0, Graphpad Software, CA, USA) and R. In total 102 variables were included in the main analyses (RM-ANOVA, main effect analysis, PCA, heatmaps, correlation matrices). In the comparative analysis between identical metabolites in serum and plasma, 16 variables per platform (Nightingale or EURECAT) were included.

### Data representation and transformation

Normality was checked using Shapiro-Wilk normality tests and tests for skewness and kurtosis. Normally distributed data is presented as mean ± standard deviation (SD) and not normally distributed data is presented as median [interquartile range (IQR)]. For univariate analyses (repeated-measures analysis of variance (RM-ANOVA) and main effect analysis), not normally distributed data was transformed (log, inverse, square, inverse square root). For multivariate analyses (principal component analysis (PCA), hierarchical clustering and heatmap plotting and correlation matrix analyses) all data was range scaled using the formula  $(x - \min(x)) / (\max(x) - \min(x))$  (25) because all biomarkers were measured in different units. Scaling resulted in a value ranging from 0 – 1 for every variable but preserved the dynamic range within each biomarker. One sample on the EURECAT platform did not pass the quality assurance tests during <sup>1</sup>H NMR analysis and was excluded from the analysis, resulting in N = 14 samples for the low-fit and N = 15 samples for the high-fit group for some analyses.

### Bivariate tests, RM-ANOVA and main effects analysis

Subject characteristics were compared using a Student's unpaired t-test or Mann-Whitney U test. RM-ANOVA was used to study the effect of fitness level (between-subjects factor) and the effect of a recent bout of exercise (within-subjects factor) on single biomarker levels and the interaction between these two factors. All assumptions for RM-ANOVA were met. Partial eta square ( $\eta^2$ ) is given

per effect as measure for effect size. Since our study includes two repeated measures and the non-parametric alternative for a RM-ANOVA (Friedman ANOVA) requires three repeated measures, the six variables that did not achieve normality after data transformation were analysed using non-parametric bivariate analyses. Mann-Whitney U tests on the ranked baseline values were used to study the fitness level effect and on the ranked difference between baseline and post-exercise values to study the interaction effect. Wilcoxon-Signed rank tests on the ranked baseline and post-exercise values were used to study the exercise effect. No partial effect size measure could be calculated for these non-parametric tests. Raw P-values were corrected for multiple testing using Benjamini-Hochberg correction in the R package 'FSA' (26) and a false discovery rate (FDR) set at 10%. FDR-corrected P-values  $< 0.10$  (adjusted P ( $P_{adj.}$ )) were considered statistically significant. None of the interactions between fitness level and the recent bout of exercise ( $P_{group \times exercise}$ ) were  $< 0.10$  and the main effects of fitness level and the recent bout of exercise were therefore also analysed in a model without the interaction term ([Supplementary Tables S6, S7, S8](#)).

### PCA, hierarchical clustering and heatmap plotting

For PCA, the covariance matrix was computed, eigenvector decomposition was performed for principal component identification, and the first and second largest principal components were plotted in a projection matrix, using the R packages 'ggplot2' (27), 'tidyverse' (28), 'factoextra' (29) and 'FactoMineR' (30). Hierarchical clustering was performed using Euclidean distance as the dissimilarity measure and complete linkage as the similarity measure between the clusters using the *hclust* function from R (31). Heatmaps were generated using the R package 'ComplexHeatmap' (32).

### Correlation analyses

Levels of identical metabolites measured in serum (EURECAT) and plasma (Nightingale) were compared using Spearman rank (for not normally distributed data) or Pearson (for normally distributed data) correlations on the raw data (16 variables per platform) to compare relative as well as absolute values. Spearman rho ( $\rho$ ) or Pearson r ( $r$ ) are given as effect size measures and P-values  $< 0.05$  were considered statistically significant. The correlation matrix was generated by performing Spearman rank correlation analyses for all biomarker pairs. All scaled biomarker data (102 variables) of high-fit and low-fit subjects at baseline as well as at post-exercise ([Figure 5](#)) or at baseline only ([Supplementary Figure S4](#)) was included. The correlation analysis used all scaled biomarker values without considering the fitness level or recent exercise effect. The correlation matrix was generated using the *hclust* function from R (31) and the R packages 'corrplot' (33)

and 'Hmisc' (34), returning a correlation plot based on hierarchically clustered biomarkers. Significant correlations ( $P < 0.05$ ) are depicted by coloured wells and non-significant correlations ( $P > 0.05$ ) are left blank.

## Results

All 102 biomarkers were analysed in samples from a well characterized study (21,22,35) of healthy females. This study population represents trained, physically active (high-fit;  $\dot{V}O_{2\text{peak}} \geq 47$  mL/kg/min,  $N = 15$ ) and untrained, low physically active (low-fit;  $\dot{V}O_{2\text{peak}} \leq 37$  mL/kg/min,  $N = 15$ ) females (Table 2), which was supported by a significantly higher skeletal muscle mitochondrial capacity (21) and a better mitochondrial function in PBMCs (22) in the high-fit compared to the low-fit females. Both groups were assessed at baseline and 21 hours after a single bout of exercise. To establish the reproducibility of the biomarker determination, a random subset of 16 biomarkers involved in protein and lipid metabolism, was also determined using a similar  $^1\text{H}$  NMR technology, but with different matrices and laboratories. Significant correlations were observed for all 16 markers, with correlation coefficients between 0.59 – 0.90 for the amino acids (all eight  $P < 0.0001$ ), 0.42 – 0.65 for the six fatty acids (one  $P < 0.01$ , three  $P < 0.001$ , two  $P < 0.0001$ ) and 0.63 and 0.86 for the two ketone bodies (both  $P < 0.0001$ , Supplementary Figure S2). This supports the validity of these biomarker measurements and demonstrates the robustness of our approach.

### Single biomarker analysis demonstrates a similar biomarker profile between high-fit and low-fit females

To better evaluate which functional processes are affected upon alterations in biomarker levels, we first linked each biomarker to one of the following physiological processes: hormone signaling, inflammation and oxidative stress responses, and metabolism. This resulted in three overarching, functional biomarker categories: 1) peptide hormones (Supplementary Table S3), 2) inflammation and oxidative stress responses (Supplementary Table S4), and 3) metabolism (which was further divided in protein, carbohydrate, and lipid metabolites, Supplementary Table S5). Since many biomarkers were related to lipid metabolism, this subcategory was further subdivided into fatty acids, cholines, ketone bodies, acylcarnitines, cholesterol metabolites and lipoproteins. All mean or median biomarker values and ranges for high-fit and low-fit females at baseline and after recent exercise are in Supplementary Table S3. To assess the effect of fitness level and the recent bout of exercise on the individual biomarker responses, RM-ANOVA on the raw data (for normally distributed biomarkers) or transformed

**Table 2** Subject characteristics

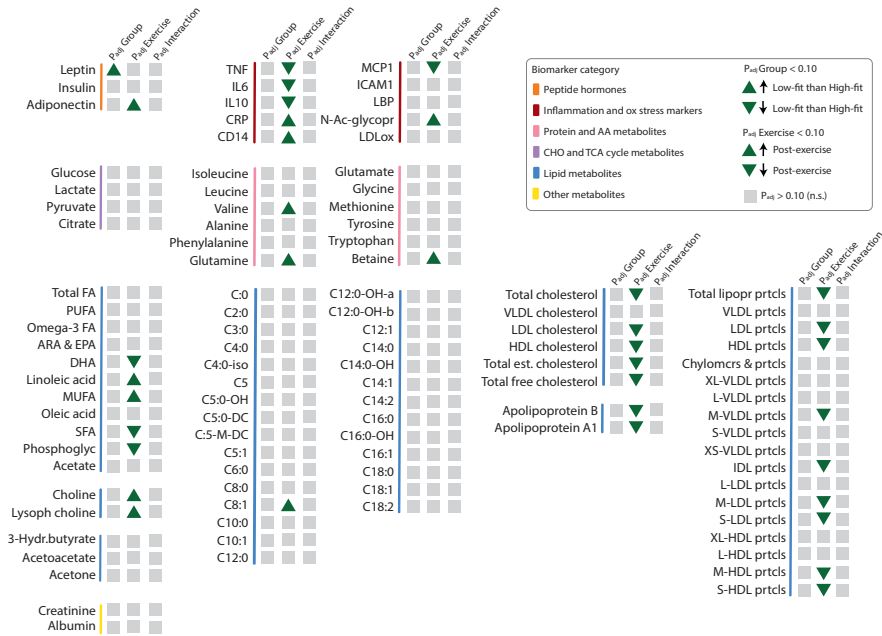
	Low-fit (N = 15)	High-fit (N = 15)
Age (years)	24.5 [22.9 – 25.6]	21.8 [21.6 - 23.7]
Ethnicity	Caucasian (11), Asian (1), Indo-pacific (4)	All Caucasian
Weight (kg)	59.7 ± 7.1	61.2 ± 7.0
Height (m)	1.63 ± 0.08	1.68 ± 0.05
BMI (kg/m <sup>2</sup> )	22.4 ± 1.4	21.7 ± 1.9
Fat mass (% of weight)	28.7 ± 3.9	25.1 ± 4.4 *
Hemoglobin (mM)	8.4 ± 0.6	8.5 ± 0.6
Use of birth control pill	6 / 15	7 / 15
$\dot{V}O_{2peak}$ (mL · kg <sup>-1</sup> · min <sup>-1</sup> )	35.0 [31.6 - 35.6]	50.4 [49.0 – 54.0] ****
Baecke total score	7.3 ± 1.0	9.5 ± 0.8 ****
$m\dot{V}O_2$ recovery constant (% · min <sup>-1</sup> )	1.53 ± 0.46 <sup>#</sup>	2.06 ± 0.57 *

BMI = body mass index,  $\dot{V}O_{2peak}$  = maximal oxygen consumption values,  $m\dot{V}O_2$  = maximal oxygenation recovery constant in the *gastrocnemius* as proxy for skeletal muscle mitochondrial capacity. <sup>#</sup>N = 11. Values are mean ± SD for normally distributed data, and median [IQR] for not normally distributed data. \*P < 0.05, \*\*\* P < 0.001, \*\*\*\* P < 0.0001.

data (for not normally distributed biomarkers) was performed. This resulted in a fitness level effect ( $rawP_{group}$ ), a recent exercise effect ( $rawP_{exercise}$ ), and an interaction effect ( $rawP_{group \times exercise}$ ) for each biomarker, and these raw P-values were corrected for multiple testing, with a significance cut-off of < 0.10 for  $adj. P_{group}$ ,  $adj. P_{exercise}$  and  $adj. P_{group \times exercise}$ . The detailed results of these analyses and the measure of effect size ( $\eta^2$ ) are in [Supplementary Tables S3 – S5](#). None of the individual biomarkers was significantly impacted by fitness level, except for the ‘peptide hormone’ leptin ([Figure 1](#)), which was significantly higher in low-fit females compared to high-fit females ( $adj. P_{group} = 0.076$ , [Figure 2A](#)). Thus, none of the markers related to inflammation, oxidative stress, or metabolism was significantly impacted by fitness level in our healthy females, indicating that high-fit and low-fit females have similar biomarker profiles.

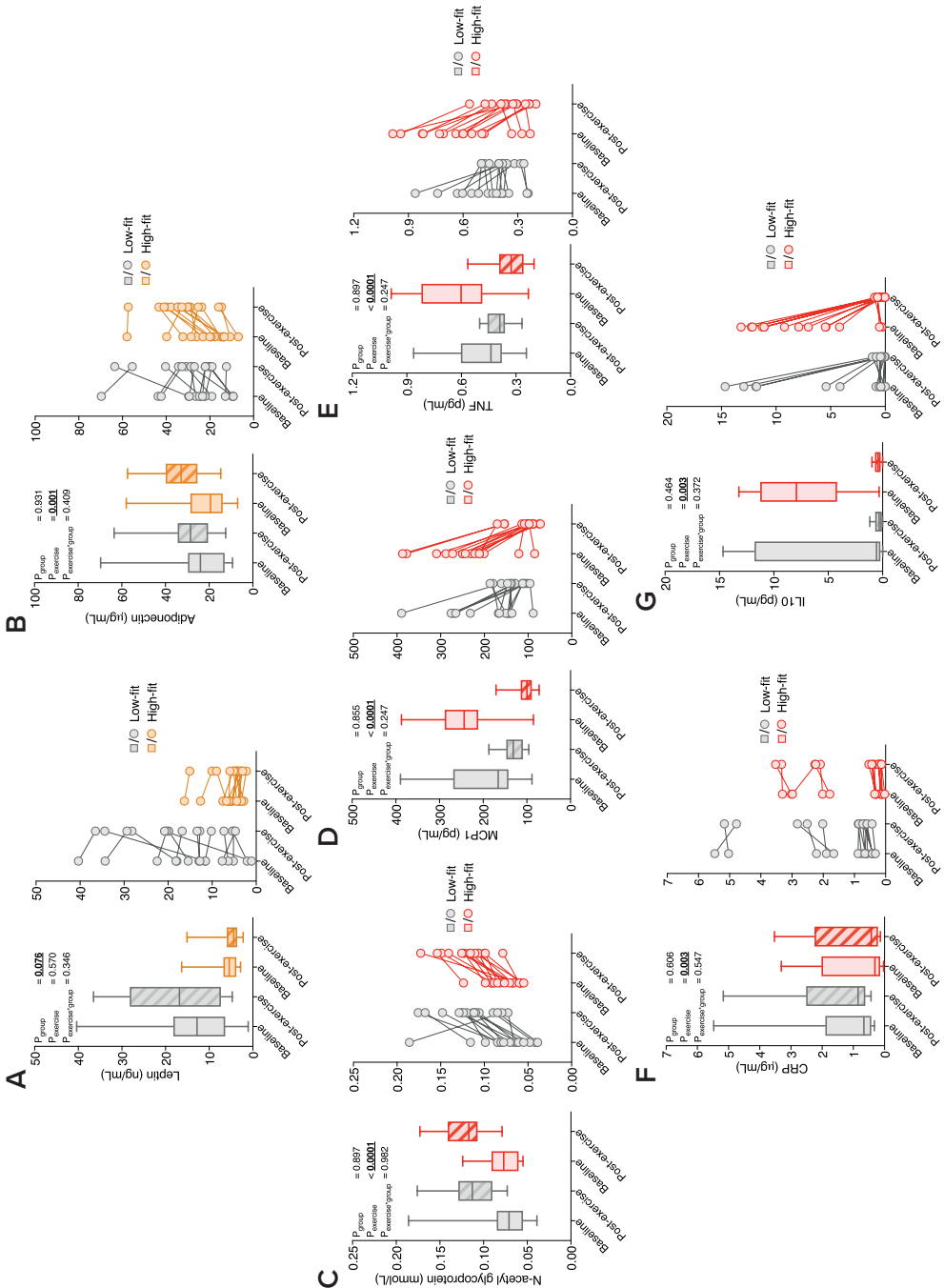
### Recent exercise regulates single biomarkers related to inflammation, lipid metabolism and hormone signaling

Next, we assessed whether recent exercise altered individual biomarker levels and examined whether high-fit and low-fit females responded differently to recent exercise. Recent exercise significantly regulated 35 of the 102 biomarkers, related to hormone signaling, inflammation and oxidative stress, lipid metabolism, and



**Figure 1: The effect of fitness level and a recent exercise bout on individual biomarker levels.** Graphical summary representing the fitness level effect ( $P_{adj} \text{ Group}$ ), recent exercise effect ( $P_{adj} \text{ Exercise}$ ) and interaction effect ( $P_{adj} \text{ Group} \times \text{Exercise}$ , shown as  $P_{adj} \text{ Interaction}$ ) on individual biomarker levels within each functional biomarker category (indicated by colour). Significant fitness level effects ( $\text{adj.}P_{\text{group}} < 0.10$ ) or recent exercise effects ( $\text{adj.}P_{\text{exercise}} < 0.10$ ) are depicted by upward and downward green triangles that indicate the direction of the effect. Non-significant effects ( $\text{adj.}P_{\text{group}}$ ,  $\text{adj.}P_{\text{exercise}}$  or  $\text{adj.}P_{\text{group} \times \text{exercise}} > 0.10$ ) are depicted in grey squares (all interaction effects were not significant). Main effects (fitness level and recent exercise) and interaction effects were analyzed using RM-ANOVA.

increased after exercise in both groups ( $\text{adj.}P_{\text{exercise}} = 0.001$ , **Figure 2B**). Of the 10 biomarkers that are related to inflammation and oxidative stress, 7 were significantly regulated by exercise, the top-5 being N-acetylglycoproteins (up;  $\text{adj.}P_{\text{exercise}} = 4.16 \times 10^{-6}$ ), MCP1 (down,  $\text{adj.}P_{\text{exercise}} = 4.16 \times 10^{-6}$ ), TNF (down,  $\text{adj.}P_{\text{exercise}} = 3.09 \times 10^{-4}$ ), CRP (up,  $\text{adj.}P_{\text{exercise}} = 0.003$ ), and IL10 (down,  $\text{adj.}P_{\text{exercise}} = 0.003$ , **Figure 2C – G**). In total 27 metabolic markers were significantly regulated by exercise, with the top-5 all linked to lipid metabolism, with increased levels of lysophosphatidylcholine ( $\text{adj.}P_{\text{exercise}} = 3.51 \times 10^{-6}$ , **Figure 2H**) and increased levels of apolipoprotein A1, total esterified cholesterol, total cholesterol, and HDL cholesterol (**Figure 2I – L**, all  $\text{adj.}P_{\text{exercise}} = 0.001$ ). Importantly, for none of the



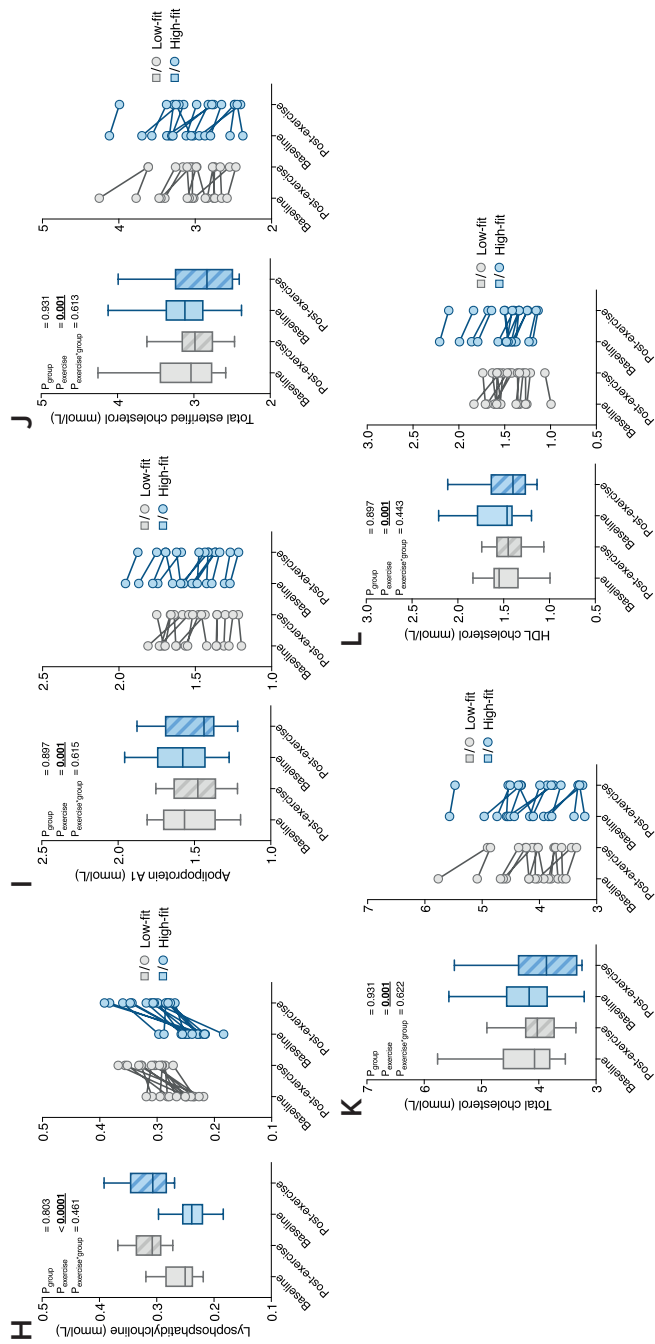


**Figure 2: The response of the top-5 significantly regulated biomarkers within each biomarker category by fitness level or a recent bout of exercise. (A, B)** Median group levels (box plots, left) and individual levels (scatter plots, right) of leptin (A) and adiponectin (B) in low-fit (N = 15, grey) and high-fit (N = 15, orange) females at baseline (transparent bars and dots) and after recent exercise (post-exercise; dashed bars and transparent dots). (C – G) Median group levels (box plots, left) and individual levels (scatter plots, right) of N-acetylglycoproteins (C), MCP1 (D), TNF (E), CRP (F), and IL10 (G) in low-fit (N = 15, grey) and high-fit (N = 15, red) females at baseline (transparent bars and dots) and post-exercise (dashed bars and transparent dots). (H – L) Median group levels (box plots, left) and individual levels (scatter plots, right) of lysophosphatidylcholine (H), apolipoprotein A1 (I), total esterified cholesterol (J), total cholesterol (K) and HDL cholesterol (L) in low-fit (N = 15, grey) (N = 14 for lysophosphatidylcholine) and high-fit (N = 15, blue) females at baseline (transparent bars and dots) and post-exercise (dashed bars and transparent dots). Main effects (fitness level and recent exercise) and interaction effects were analyzed using RM-ANOVA. Significant adj.P-values (< 0.10) are indicated in underlined bold.

102 biomarkers, the exercise response significantly differed between high-fit and low-fit females (all  $\text{adj.}P_{\text{group} \times \text{exercise}} > 0.10$ ). We therefore performed an additional main effect analysis without the interaction term, which resulted in the same significantly regulated biomarkers as compared to the full interaction model, except for MUFA ( $\text{adj.}P_{\text{exercise}} = 0.101$ , [Supplementary Tables S4, S5, S6](#)).

In summary, this single biomarker analysis demonstrated that various biomarkers linked to inflammation, lipid and protein metabolism, and adiponectin were significantly regulated by recent exercise, while only leptin was affected by fitness level in these healthy females ([Figure 3](#)).

### Data-driven biomarker clusters link with functional biomarker categories

Next, we studied the joined dynamics of these biomarkers. Hierarchical clustering was applied on the scaled biomarker levels and visualized in a heatmap ([Figure 4](#)). The heatmap generated multiple biomarker clusters that corresponded to our predefined functional biomarker categories, indicated by clustering of inflammation and oxidative stress related markers, amino acids, fatty acids, ketone bodies, acylcarnitines, lipoproteins and cholesterol metabolites along the y-axis ([Figure 4](#)). Although some of these functional biomarker categories also displayed x-axis clustering (e.g., the lipoproteins and fatty acids), the overall heatmap pattern was only slightly related to fitness level and not related to recent exercise. Instead, the intra-individual biomarker response, i.e., baseline and post-exercise values within one subject, accounted for most of the x-axis clustering. The notion that biomarker levels were primarily affected by interindividual differences, rather than fitness level or the recent bout of exercise, was confirmed by PCA, where no clear separation was observed between our experimental conditions ([Supplementary Figure S3](#)). To obtain a more detailed understanding on data-driven relationships between biomarkers, a hierarchically clustered ( $P < 0.05$ ) correlation matrix was generated, with significant Spearman  $\rho > 0.6$  or  $< -0.6$  correlations indicated as potential physiological relevant links ([Figure 5](#)). As above, these data-driven correlations corresponded to functional categories, such as amino acids (especially the branched-chain amino acids (BCAAs)), fatty acids, ketone bodies, acylcarnitines, cholesterol metabolites and lipoproteins ([Figure 5](#)). However, some data-driven correlated biomarkers were not in line with our predefined functional biomarker categories, such as CRP and glycine ( $r = -0.72$ ), glutamine and hydroxyisovaleryl-carnitine (C5:0-OH,  $r = 0.60$ ), tyrosine and hydroxyisovalerylcarnitine (C5:0-OH,  $r = 0.64$ ), tyrosine and methylcrotonylcarnitine (C5:1,  $r = 0.66$ ), betaine and octadecadienylcarnitine (C18:2,  $r = 0.65$ ), and N-acetylglycoproteins and lyso-phosphatidylcholine ( $r = 0.65$ ), all having a  $P < 1.0 \times 10^{-7}$ . Of note, similar patterns were observed when only the baseline levels from high-fit and low-fit females

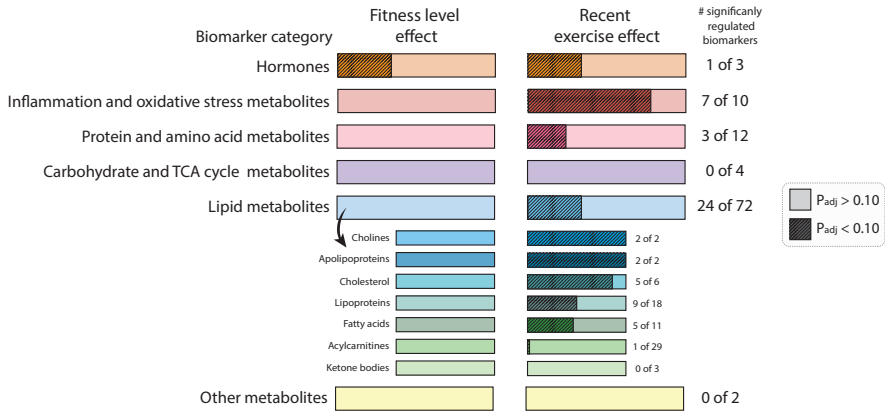


**Figure 3: The effect of fitness level and a recent exercise bout on biomarker category responses.** Graphical summary representing the number of significantly regulated biomarkers between high-fit and low-fit females (fitness level effect, left bars) and the number of significantly regulated biomarkers between baseline and post-exercise (recent exercise effect, right bars). Non-significant effects ( $\text{adj.}P_{\text{group}}$  or  $\text{adj.}P_{\text{exercise}} > 0.10$ ) are depicted in light coloured bars and significant effects ( $\text{adj.}P_{\text{group}}$  or  $\text{adj.}P_{\text{exercise}} < 0.10$ ) are depicted in dark coloured, dashed bars. The filled area is calculated relatively to the number of biomarkers within the corresponding functional category.

were included ([Supplementary Figure S4](#)). Overall, this integrated biomarker analysis demonstrated that data-driven biomarker clusters include biomarkers that are also functionally linked, and that various of these clusters correspond with our predefined functional biomarker categories.

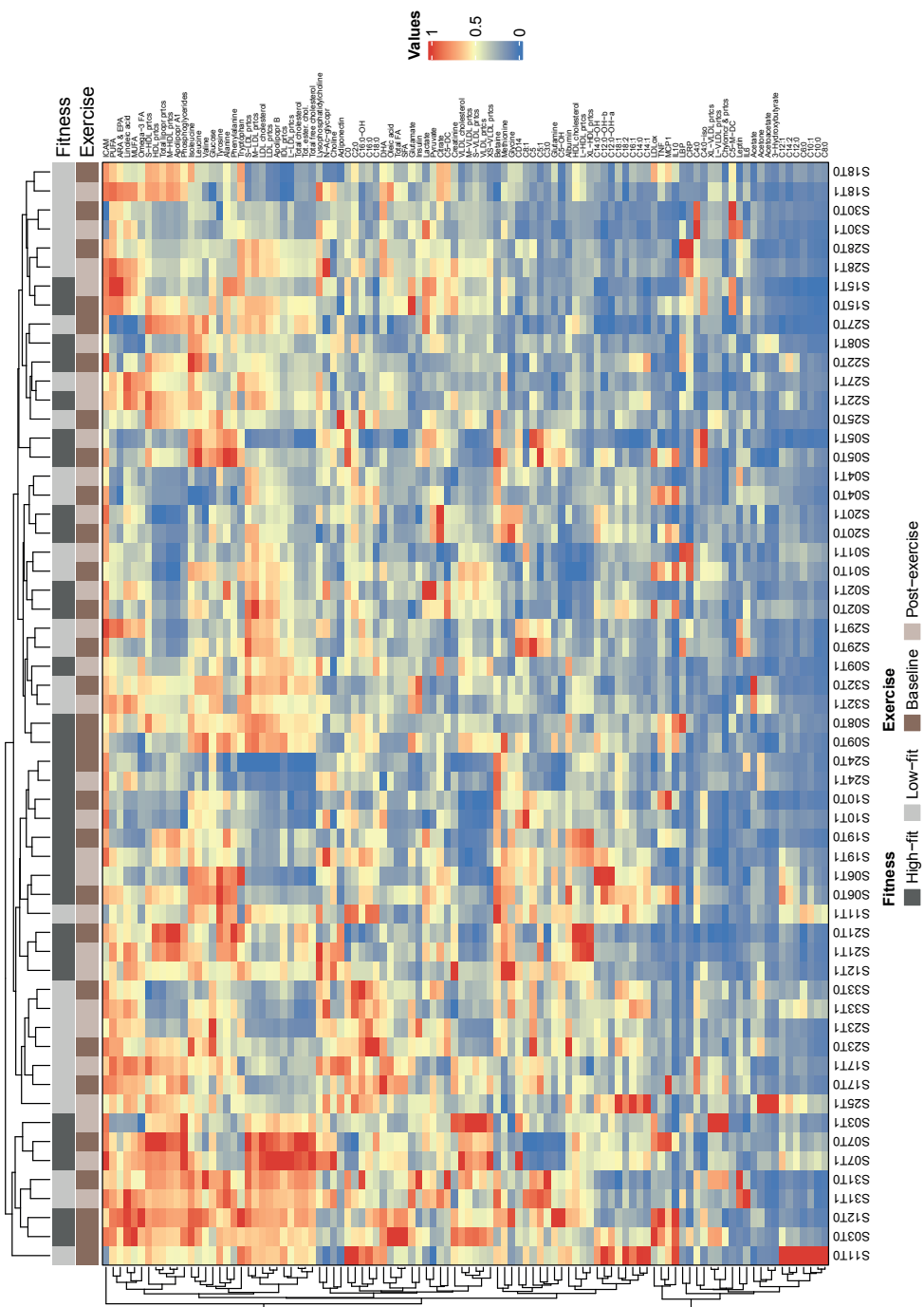


**Figure 4: Heatmap of hierarchical clustered biomarkers and the association with fitness level and recent exercise.** Heatmap based on hierarchical clustering of all 102 biomarkers based on Euclidean distance and complete linkage clustering. Biomarkers are clustered along the y-axis and individual subjects are clustered along the x-axis. Subject ID (S0x) and timepoint (T0 for baseline, T1 for post-exercise) are given for each subject. Subject IDs are coupled to fitness level (dark grey for high-fit and light grey for low-fit subjects) and timepoint (dark brown for baseline and beige for post-exercise). The colour scale represents low (dark orange) to medium (dark blue) biomarker values.

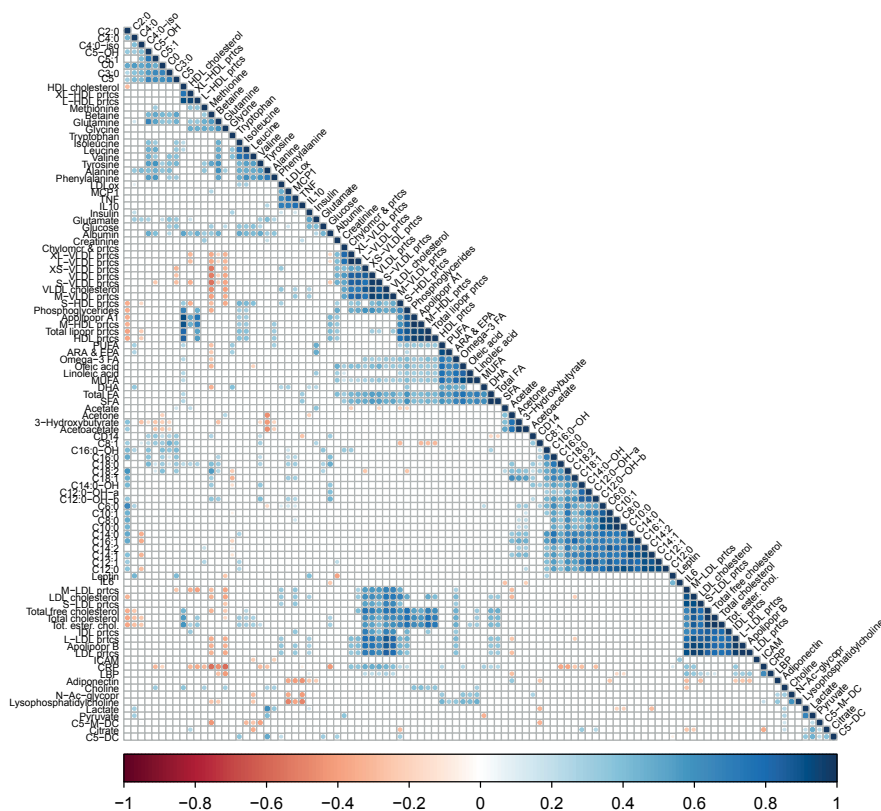


**Figure 5: Correlation matrix showing the relationships between biomarker pairs.** The correlation matrix based on Spearman correlation coefficients between biomarker pairs. Spearman rank correlation analysis was performed on the scaled biomarker values for all biomarker pairs using the combined data of high-fit and low-fit females at baseline and post-exercise. Relationships were considered statistically significant when  $P < 0.05$ . Significant relationships are indicated in **red** (negative correlation) or **blue** (positive correlation). Non-significant relationships ( $P > 0.05$ ) are left blank.

## Discussion

We performed an elaborate analysis of 102 circulating biomarkers, previously studied in disease conditions such as type 2 diabetes, obesity, and cardiovascular disease (36–39), but hardly in healthy individuals with different lifestyles. Analysis of a selection of these biomarkers across two platforms showed similar results, underpinning their reliability, and indicating the robustness of these platforms. Except for leptin, individual biomarker levels were not significantly different between high and low aerobically fit females. Since leptin levels have been positively correlated to body fat percentage (40,41), the difference in leptin presumably results from a significant difference in body fat percentage between high-fit and low-fit females, further underpinning the validity of our data. Our observation that all other biomarkers were similar between the two groups, while previous studies in high and low aerobically fit individuals found significant differences in e.g., lipid and protein metabolites (42–47), is likely related to our standardized experimental set-up, as compared to other studies. We studied healthy, young-adult females of similar age and body mass index (BMI) in a highly controlled setting, while previous studies were performed with metabolically impaired individuals (38) and individuals with different BMI (42–44,47) or wider age ranges (42,47), in experimental conditions that were less standardized (42–45,47), and especially these factors impact circulating metabolite levels (38,42,43). Given that the levels of the analysed biomarkers were similar among the healthy females in our study, and multiple of these biomarkers showed dysregulation during disease, our findings imply that this biomarker set could be used to monitor progress from a healthy to an unhealthier state and may be use in health improvement interventions.

Studies that focus on recent exercise effects, i.e., effects on the day after exercise completion, are scarce compared to studies on acute or chronic exercise (15,18). Yet, recent exercise is especially relevant for biomarkers, as they can indicate whether physical activity of study subjects should be controlled prior to sampling. Here, we demonstrated that adiponectin, lipid metabolites, and inflammatory markers were most responsive to recent exercise, which is line with data from other studies (48–51). These findings suggest that future biomarker studies should consider standardization of study subjects' physical activity 24 hours prior to blood sampling, especially when they include hormones, and markers related to lipid metabolism and inflammation.

Multiple separate clusters that were obtained in the heatmap and correlation matrix included biomarkers that corresponded to biomarkers embedded in our predefined, functional biomarker categories. Examples are the BCAAs, fatty acids, ketone bodies, short-chain acylcarnitines, long-chain acylcarnitines, cholesterol metabolites, and lipoproteins, which suggests that the response of biomarkers within these (sub)categories are interdependent. This has two important implications. First, one biomarker within a cluster could be considered as representative of the total cluster (e.g., isoleucine for the BCAAs), which could be of relevance for studies that measure only one or a limited number of biomarkers from one correlated cluster. Second, it provides opportunities for future studies to compute one total, standardized score for all biomarkers within a cluster that are strongly correlated (e.g., a total BCAA score). From a disease risk assessment point of view, such an integrated score will likely have a larger power and stronger predictive value as compared to individual biomarker levels. Previously, Wang et al. have found that BCAA levels could predict type 2 diabetes risk (36). Integrated BCAA analysis is therefore promising as health-status biomarker. Not all biomarkers from functional categories can be integrated because of differences in the individual responses (e.g., peptide hormones, inflammation markers, and short- vs. longer-chain acylcarnitines). Clustering outside the functional category was also observed. The inverse association between CRP and the amino acid glycine has also been demonstrated previously (52,53) and likely results from the inflammation modulating capacity of glycine (54,55). The positive association between N-acetylglycoprotein and lysophosphatidylcholine is also likely mediated via inflammation, since N-acetylglycoproteins plasma levels correlate with lipoprotein-associated phospholipase A2 levels (56), which generates lysophosphatidylcholine to promote inflammation (57,58). Direct positive links between glutamine, tyrosine, C5:0-OH and C5:1 acylcarnitines have not yet been described, but could be mediated by BCAA breakdown (59,60). The positive link between betaine and C18:2 acylcarnitine has not yet been demonstrated in humans, but may be related to fatty acid incorporation, as previously demonstrated in pigs (61). The observed correlations imply some revision of our a-priory functional categorization and, importantly, provide leads for biomarker integration and functional interpretation of changes in biomarker levels.

Next to the functional links between biomarker pairs, the hierarchical clustering models also showed that the degree of clustering for the intraindividual biomarker response i.e., the baseline and post-exercise biomarker values of one subject, was higher than the degree of clustering of the group (high-fit vs. low-fit) and the timepoint (baseline vs. post-exercise) biomarker responses. This finding suggests a considerable level of interindividual variation in our study population, which

might also explain our observation that ~35% of the biomarkers was significantly impacted by recent exercise, but that clustering did not separate total baseline and post-exercise biomarker profiles. Since Krug et al., also showed that the inter-individual variability was increased by using challenge tests (62), one could speculate that the challenged biomarker responses within one individual over time might act as a better predictor of health status, as compared to a singular analysis of the average biomarker levels of a larger group during basal homeostasis.

Our study included some strengths and limitations. One of the strengths is the integrated approach to analyze single as well as joined biomarker behavior in a healthy, homogenous study population at basal as well as challenged conditions, which provides us better insight in the behavior of biomarkers relatively to each other. An understanding of biomarkers in the healthy individuals is a prerequisite for their use in preventive health, for example biomarker guided dietary advice for health improvement. Another strength of our study is the focus on female individuals, since sex can affect metabolic responses (20,42), and females are often underrepresented in biomarker studies (15). One of the limitations of our study is that we could not determine the contribution of intraindividual variation, i.e., the day-to-day variation within an individual, as we sampled only twice in a relatively short time span. Although previous studies have demonstrated that the intraindividual variation for circulating adipokines (63), inflammatory markers (63,64), and metabolites (65,66) is smaller than the interindividual variation, we cannot exclude this source of error in our study. Second, we did not include additional post-exercise sampling timepoints, e.g., immediately post-exercise or a few hours post-exercise. Since the levels of most inflammatory markers, oxidative stress related markers and metabolites change acutely or in the first few hours after exercise, with each marker having its own kinetic profile (15,18) and the fact that biomarker kinetics can also differ between individuals as a result of interindividual variation (62), sampling at multiple timepoints after the exercise bout would have given insight in the exercise-induced biomarker behavior over time. Third, our study focused on a total of 102 biomarkers related to hormone signaling, inflammation and oxidative stress, and metabolism, while fitness level and single exercise stimulation have been associated with alterations in markers that were not included in our study, such as vitamins (44,45), ceramides (38), and individual lysophosphatidylcholines (38,42), which could possibly have provided additional insights in these biomarkers in view of the homogeneity of our study subjects characteristics and high level of study standardization.

In conclusion, we showed that the overall circulating biomarker profiles were similar between high-fit and low-fit young, healthy, adult females. Although recent exercise had a limited impact on the overall biomarker profiles, it significantly affected a selected number of individual biomarkers. This study provides insight in the single and joined behaviour of circulating biomarkers in healthy females, and identified functional biomarker categories that may be used for characterization of human health physiology.

### Acknowledgements

The authors greatly acknowledge the commitment of the volunteers who participated in the study and Klaas Frankena for assistance with statistical analysis. We acknowledge Rosanne Hendriksen, Sophie Bagchus, Camiel Oe, Maud Pijnenburg, Henriette Fick-Brinkhof, and Diana Emmen-Benink for human data acquisition, and Miguel Ángel Rodríguez, Héctor Palacios, María Guirro, Antoni del Pino, Juan María Alcaide, Yaiza Tobajas, Anna Antolin, Gertruda Chomiciute, Cristina Egea, and Iris Triguero for technical support in biomarker analysis.

### Authors' contributions

Study: J.J.E.J., B.L.; Analysis: J.J.E.J., X.E., N.C.; Data interpretation: J.J.E.J., X.E., V.C.J.d.B., J.K.; Writing: original draft preparation: J.J.E.J.; review and editing: J.J.E.J., B.L., A.G.N., X.E., V.C.J.d.B., J.K.; Funding: J.J.E.J., V.C.J.d.B., J.K.

### Funding

This work was supported by NWO-WIAS Graduate Program grant 2016 and the H2020-EU 3.2.2.1/2 PREVENTOMICS GA 818318 grant.

### Declaration of interest

All authors declare no conflict of interest.

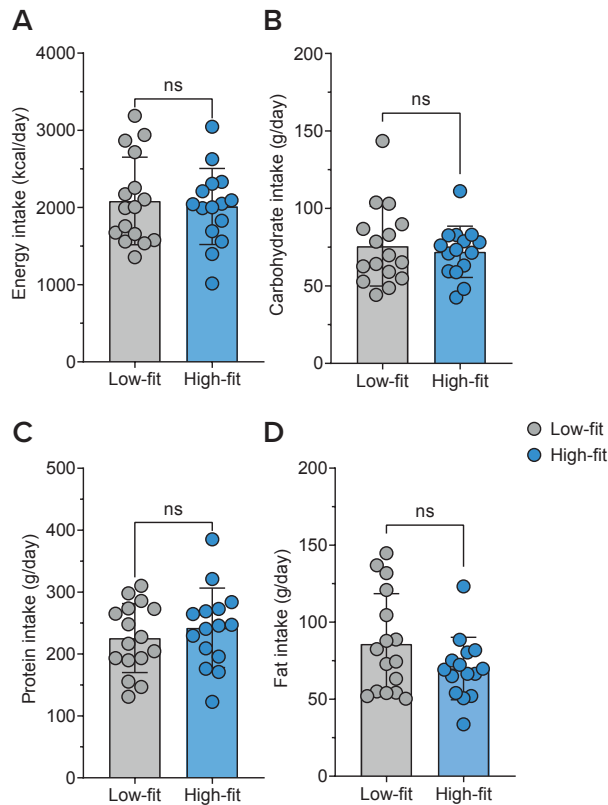
## References

1. Zhang Y, Pan XF, Chen J, Xia L, Cao A, Zhang Y, et al. Combined lifestyle factors and risk of incident type 2 diabetes and prognosis among individuals with type 2 diabetes: a systematic review and meta-analysis of prospective cohort studies. *Diabetologia*. 2020;63(1):21–33.
2. Colpani V, Baena CP, Jaspers L, van Dijk GM, Farajzadegan Z, Dhana K, et al. Lifestyle factors, cardiovascular disease and all-cause mortality in middle-aged and elderly women: a systematic review and meta-analysis. *Eur J Epidemiol*. 2018;33(9):831–45.
3. Zhang YB, Pan XF, Chen J, Cao A, Zhang YG, Xia L, et al. Combined lifestyle factors, incident cancer, and cancer mortality: a systematic review and meta-analysis of prospective cohort studies. *Br J Cancer*. 2020;122(7):1085–93.
4. Lopez AD, Mathers CD, Ezzati M, Jamison DT, Murray CJ. Global and regional burden of disease and risk factors, 2001: systematic analysis of population health data. *Lancet*. 2006;367(9524):1747–57.
5. Califf RM. Biomarker definitions and their applications. *Exp Biol Med*. 2018;243(3):213–21.
6. van Ommen B, Keijer J, Heil SG, Kaput J. Challenging homeostasis to define biomarkers for nutrition related health. *Mol Nutr Food Res*. 2009;53(7):795–804.
7. Blair SN, Kohl HW 3rd, Paffenbarger RSJ, Clark DG, Cooper KH, Gibbons LW, et al. Physical Fitness and All-Cause Mortality: A Prospective Study of Healthy Men and Women. *JAMA*. 1989 Nov 3;262(17):2395–401.
8. Bird SR, Hawley JA. Update on the effects of physical activity on insulin sensitivity in humans. *BMJ Open Sport Exerc Med*. 2017 Mar 1;2(1):e000143.
9. Mann S, Beedie C, Jimenez A. Differential effects of aerobic exercise, resistance training and combined exercise modalities on cholesterol and the lipid profile: review, synthesis and recommendations. *Sport Med*. 2014 Feb;44(2):211–21.
10. Fischer CP. Interleukin-6 in acute exercise and training: what is the biological relevance? *Exerc Immunol Rev*. 2006;12:6–33.
11. Ridker PM, Rifai N, Stampfer MJ, Hennekens CH. Plasma Concentration of Interleukin-6 and the Risk of Future Myocardial Infarction Among Apparently Healthy Men. *Circulation*. 2000 Apr 18;101(15):1767–72.
12. Hawley JA. Exercise as a therapeutic intervention for the prevention and treatment of insulin resistance. *Diabetes Metab Res Rev*. 2004;20(5):383–93.
13. Lee DC, Pate RR, Lavie CJ, Sui X, Church TS, Blair SN. Leisure-time running reduces all-cause and cardiovascular mortality risk. *J Am Coll Cardiol*. 2014;64(5):472–81.
14. Gordon T, Castelli WP, Hjortland MC, Kannel WB, Dawber TR. High density lipoprotein as a protective factor against coronary heart disease. The Framingham Study. *Am J Med*. 1977 May;62(5):707–14.
15. Schraner D, Kastenmüller G, Schönfelder M, Römisch-Margl W, Wackerhage H. Metabolite Concentration Changes in Humans After a Bout of Exercise: a Systematic Review of Exercise Metabolomics Studies. *Sport Med - Open*. 2020;6(1):11.
16. Muhsen Ali A, Burleigh M, Daskalaki E, Zhang T, Easton C, Watson DG. Metabolomic Profiling of Submaximal Exercise at a Standardised Relative Intensity in Healthy Adults. Vol. 6, *Metabolites*. 2016.
17. Nieman DC, Gillitt ND, Sha W, Meaney MP, John C, Pappan KL, et al. Metabolomics-Based Analysis of Banana and Pear Ingestion on Exercise Performance and Recovery. *J Proteome Res*. 2015 Dec;14(12):5367–77.
18. Pedersen BK, Hoffman-Goetz L. Exercise and the immune system: Regulation, integration, and adaptation. *Physiol Rev*. 2000;80(3):1055–81.
19. McGee SL, Hargreaves M. Exercise adaptations: molecular mechanisms and potential targets for therapeutic benefit. *Nat Rev Endocrinol*. 2020;16(9):495–505.
20. Krumsiek J, Mittelstrass K, Do KT, Stücker F, Ried J, Adamski J, et al. Gender-specific pathway differences in the human serum metabolome. *Metabolomics*. 2015;11(6):1815–33.
21. Lagerwaard B, Janssen JJE, Cuijpers I, Keijer J, de Boer VCJ, Nieuwenhuizen AG. Muscle mitochondrial capacity in high- and low-fitness females using near-infrared spectroscopy. *Physiol Rep*. 2021;9(9):1–10.

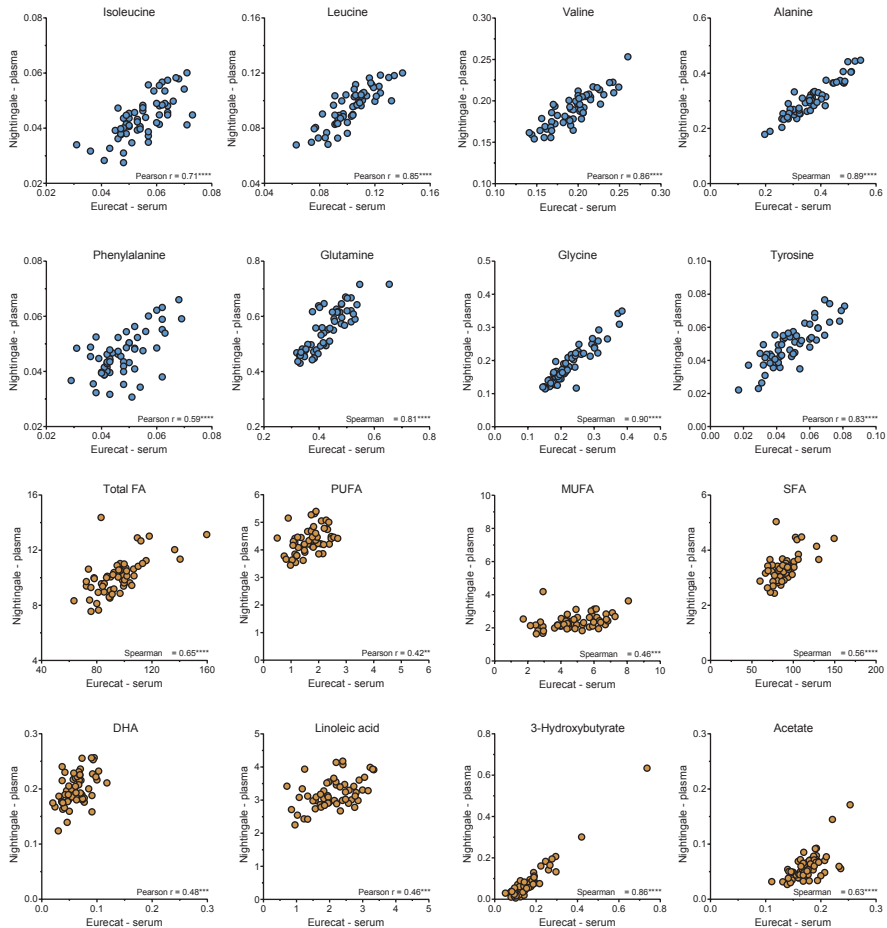
22. Janssen JJE, Lagerwaard B, Porbahaie M, Nieuwenhuizen AG, Savelkoul HFJ, van Neerven RJJ, et al. Extracellular flux analyses reveal differences in mitochondrial PBMC metabolism between high-fit and low-fit females. *Am J Physiol Metab.* 2022 Jan 10;
23. Lagerwaard B, Keijer J, McCully KK, de Boer VCJ, Nieuwenhuizen AG. In vivo assessment of muscle mitochondrial function in healthy, young males in relation to parameters of aerobic fitness. *Eur J Appl Physiol.* 2019;
24. Streppel MT, de Vries JHM, Meijboom S, Beekman M, de Craen AJM, Slagboom PE, et al. Relative validity of the food frequency questionnaire used to assess dietary intake in the Leiden Longevity Study. *Nutr J.* 2013;12(1):75.
25. van den Berg RA, Hoefsloot HCJ, Westerhuis JA, Smilde AK, van der Werf MJ, Ialongo C. Centering, scaling, and transformations: Improving the biological information content of metabolomics data. *BMC Genomics.* 2006;7(2):1–15.
26. Ogle D, Doll J, Wheeler P, Dinno A. FSA: Fisheries Stock Analysis. R package version 0.9.1 [Internet]. 2021. Available from: <https://github.com/droglenc/FSA>
27. Wickham H. *Elegant Graphics for Data Analysis.* ggplot2. New York: Springer-Verlag; 2016.
28. Wickham H. Welcome to the Tidyverse. *J Open Source Softw.* 2019;4(43):1686.
29. Kassambara A, Mundt F. *factoextra: Extract and Visualize the Results of Multivariate Data Analyses.* R package version 1.0.7. 2020.
30. Lê S, Josse J, Huisson F. FactoMineR: An R Package for Multivariate Analysis. *J Stat Softw.* 2008 Mar 18;25(1 SE-Articles):1–18.
31. R Core Team. *R: A language and environment for statistical computing.* R Foundation for Statistical Computing. Vienna, Austria; 2021.
32. Gu Z, Eils R, Schlesner M. Complex heatmaps reveal patterns and correlations in multidimensional genomic data. *Bioinformatics.* 2016 Sep;32(18):2847–9.
33. Wei T, Simko V. R package “corrplot”: Visualization of a Correlation Matrix (Version 0.92) [Internet]. 2021. Available from: <https://github.com/taiyun/corrplot>
34. Harrell FE. *Hmisc: Harrell Miscellaneous.* R package version 4.6-0. 2021;
35. Janssen JJE, Lagerwaard B, Nieuwenhuizen AG, Timmers S, de Boer VCJ, Keijer J. The Effect of a Single Bout of Exercise on Vitamin B2 Status Is Not Different between High- and Low-Fit Females. *Nutrients.* 2021 Nov 16;13(11):4097.
36. Wang TJ, Larson MG, Vasani RS, Cheng S, Rhee EP, McCabe E, et al. Metabolite profiles and the risk of developing diabetes. *Nat Med.* 2011;17(4):448–53.
37. Hayashino Y, Jackson JL, Hirata T, Fukumori N, Nakamura F, Fukuhara S, et al. Effects of exercise on C-reactive protein, inflammatory cytokine and adipokine in patients with type 2 diabetes: A meta-analysis of randomized controlled trials. *Metabolism.* 2014;63(3):431–40.
38. Carrard J, Guerini C, Appenzeller-Herzog C, Infanger D, Königstein K, Streesse L, et al. The Metabolic Signature of Cardiorespiratory Fitness: A Systematic Review. *Sports Medicine.* New Zealand; 2021.
39. Aleksandrova K, Mozaffarian D, Pischon T. Addressing the Perfect Storm: Biomarkers in Obesity and Pathophysiology of Cardiometabolic Risk. *Clin Chem.* 2018 Jan 1;64(1):142–53.
40. Considine R V, Sinha MK, Heiman ML, Kriauciunas A, Stephens TW, Nyce MR, et al. Serum Immuno-reactive-Leptin Concentrations in Normal-Weight and Obese Humans. *N Engl J Med.* 1996 Feb 1;334(5):292–5.
41. Pérusse L, Collier G, Gagnon J, Leon AS, Rao DC, Skinner JS, et al. Acute and chronic effects of exercise on leptin levels in humans. *J Appl Physiol.* 1997 Jul 1;83(1):5–10.
42. Kistner S, Döring M, Krüger R, Rist MJ, Weinert CH, Bunzel D, et al. Sex-Specific Relationship between the Cardiorespiratory Fitness and Plasma Metabolite Patterns in Healthy Humans—Results of the KarMeN Study. Vol. 11, *Metabolites.* 2021.
43. Kujala UM, Vaara JP, Kainulainen H, Vasankari T, Vaara E, Kyröläinen H. Associations of Aerobic Fitness and Maximal Muscular Strength With Metabolites in Young Men. *JAMA Netw Open.* 2019 Aug 23;2(8):e198265–e198265.
44. Choresell E, Svensson MB, Moritz T, Antti H. Physical fitness level is reflected by alterations in the human plasma metabolome. *Mol Biosyst.* 2012;8(4):1187–96.

45. Lustgarten MS, Price LL, Logvinenko T, Hatzis C, Padukone N, Reo N V, et al. Identification of serum analytes and metabolites associated with aerobic capacity. *Eur J Appl Physiol.* 2013 May;113(5):1311–20.
46. Yan B, A J, Wang G, Lu H, Huang X, Liu Y, et al. Metabolomic investigation into variation of endogenous metabolites in professional athletes subject to strength-endurance training. *J Appl Physiol.* 2009 Feb;106(2):531–8.
47. Morris C, Grada CO, Ryan M, Roche HM, De Vito G, Gibney MJ, et al. The relationship between aerobic fitness level and metabolic profiles in healthy adults. *Mol Nutr Food Res.* 2013 Jul;57(7):1246–54.
48. Sakaguchi CA, Nieman DC, Signini EF, Abreu RM, Catai AM. Metabolomics-Based Studies Assessing Exercise-Induced Alterations of the Human Metabolome: A Systematic Review. Vol. 9, *Metabolites*. 2019.
49. Stander Z, Luies L, Mienie LJ, Van Reenen M, Howatson G, Keane KM, et al. The unaided recovery of marathon-induced serum metabolome alterations. *Sci Rep.* 2020;10(1):11060.
50. Wooten JS, Biggerstaff KD, Anderson C. Response of lipid, lipoprotein-cholesterol, and electrophoretic characteristics of lipoproteins following a single bout of aerobic exercise in women. *Eur J Appl Physiol.* 2008;104(1):19.
51. Nieman DC, Scherr J, Luo B, Meaney MP, Dréau D, Sha W, et al. Influence of Pistachios on Performance and Exercise-Induced Inflammation, Oxidative Stress, Immune Dysfunction, and Metabolite Shifts in Cyclists: A Randomized, Crossover Trial. *PLoS One.* 2014 Nov 19;9(11):e113725.
52. Ding Y, Svingen GFT, Pedersen ER, Gregory JF, Ueland PM, Tell GS, et al. Plasma Glycine and Risk of Acute Myocardial Infarction in Patients With Suspected Stable Angina Pectoris. *J Am Heart Assoc.* 2022 Feb 16;5(1):e002621.
53. Tabung FK, Liang L, Huang T, Balasubramanian R, Zhao Y, Chandler PD, et al. Identifying metabolomic profiles of inflammatory diets in postmenopausal women. *Clin Nutr.* 2020 May;39(5):1478–90.
54. Wheeler MD, Ikejima K, Enomoto N, Stacklewitz RF, Seabra V, Zhong Z, et al. Glycine: a new anti-inflammatory immunonutrient. *Cell Mol Life Sci C.* 1999;56(9):843–56.
55. Cheng Z, Guo C, Chen Z, Yang T, Zhang J, Wang J, et al. Glycine, serine and threonine metabolism confounds efficacy of complement-mediated killing. *Nat Commun.* 2019;10(1):3325.
56. Gruppen EG, Connelly MA, Dullaart RPF. Higher circulating GlycA, a pro-inflammatory glycoprotein biomarker, relates to lipoprotein-associated phospholipase A2 mass in nondiabetic subjects but not in diabetic or metabolic syndrome subjects. *J Clin Lipidology.* 2016;10(3):512–8.
57. Sotirios T, T. WJ, M. RP. C-Reactive Protein and Other Emerging Blood Biomarkers to Optimize Risk Stratification of Vulnerable Patients. *J Am Coll Cardiol.* 2006 Apr 18;47(8\_Supplement):C19–31.
58. Grzelczyk A, Gendaszewska-Darmach E. Novel bioactive glycerol-based lysophospholipids: New data – New insight into their function. *Biochimie.* 2013;95(4):667–79.
59. Brosnan JT, Brosnan ME. Branched-chain amino acids: enzyme and substrate regulation. *J Nutr.* 2006 Jan;136(1 Suppl):207S–11S.
60. Schooneman MG, Vaz FM, Houten SM, Soeters MR. Acylcarnitines: reflecting or inflicting insulin resistance? *Diabetes.* 2013 Jan;62(1):1–8.
61. Wang LS, Shi Z, Gao R, Su BC, Wang H, Shi BM, et al. Effects of conjugated linoleic acid or betaine on the growth performance and fatty acid composition in backfat and belly fat of finishing pigs fed dried distillers grains with solubles. *Animal.* 2015;9(4):569–75.
62. Krug S, Kastenmüller G, Stücker F, Rist MJ, Skurk T, Sailer M, et al. The dynamic range of the human metabolome revealed by challenges. *FASEB J.* 2012;26(6):2607–19.
63. Lee S-A, Kallianpur A, Xiang Y-B, Wen W, Cai Q, Liu D, et al. Intra-individual Variation of Plasma Adipokine Levels and Utility of Single Measurement of These Biomarkers in Population-Based Studies. *Cancer Epidemiol Biomarkers Prev.* 2007 Nov 15;16(11):2464–70.
64. Biancotto A, Wank A, Perl S, Cook W, Olnes MJ, Dagur PK, et al. Baseline Levels and Temporal Stability of 27 Multiplexed Serum Cytokine Concentrations in Healthy Subjects. *PLoS One.* 2013 Dec 12;8(12):e76091.
65. Agueusop I, Musholt PB, Klaus B, Hightower K, Kannt A. Short-term variability of the human serum metabolome depending on nutritional and metabolic health status. *Sci Rep.* 2020;10(1):16310.
66. Li-Gao R, Hughes DA, le Cessie S, de Mutsert R, den Heijer M, Rosendaal FR, et al. Assessment of reproducibility and biological variability of fasting and postprandial plasma metabolite concentrations using 1H NMR spectroscopy. *PLoS One.* 2019 Jun 20;14(6):e0218549.

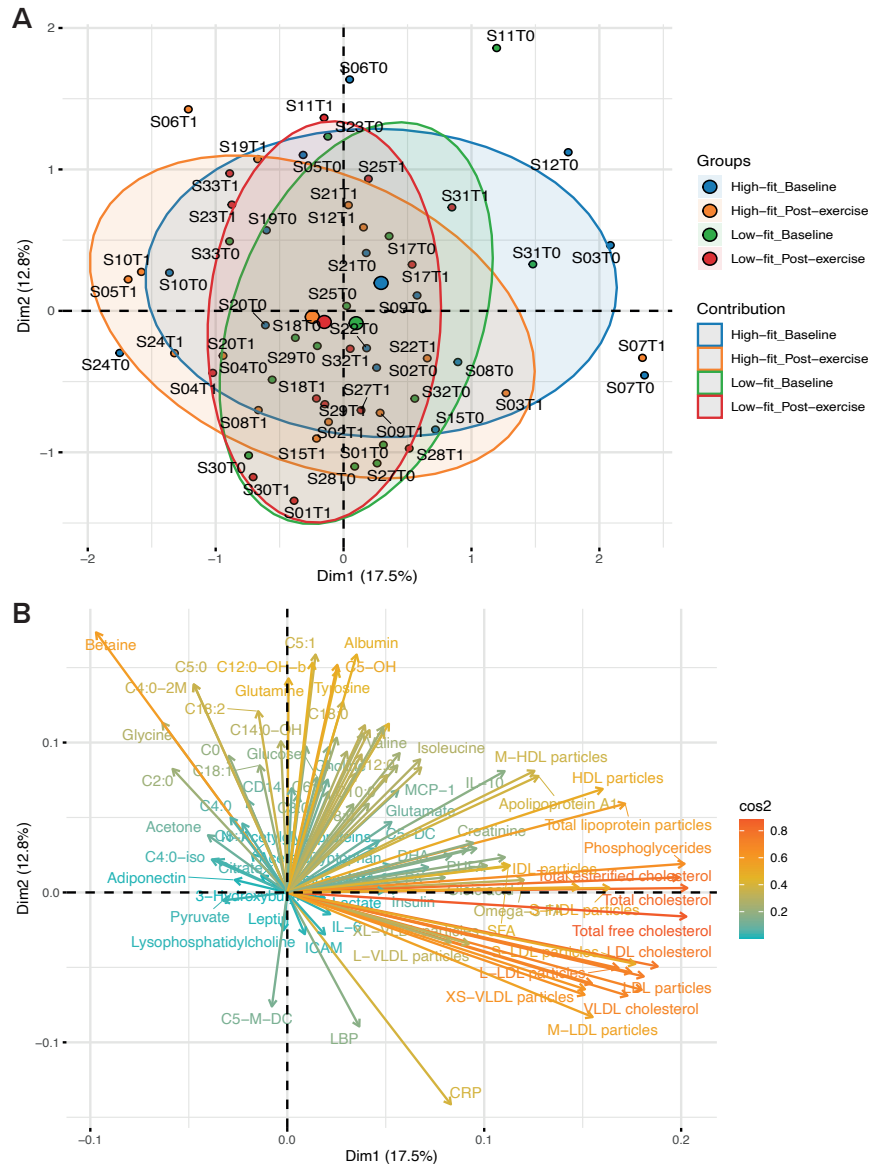
# Supplementary materials



**Supplementary Figure S1: Habitual dietary intake of the study subjects.** Dietary intake of the subjects was assessed with a validated food frequency questionnaire (FFQ) and total daily energy intake (A) and intake of carbohydrates (B), proteins (C), and fats (D) were calculated for high-fit (blue) and low-fit (grey) females.

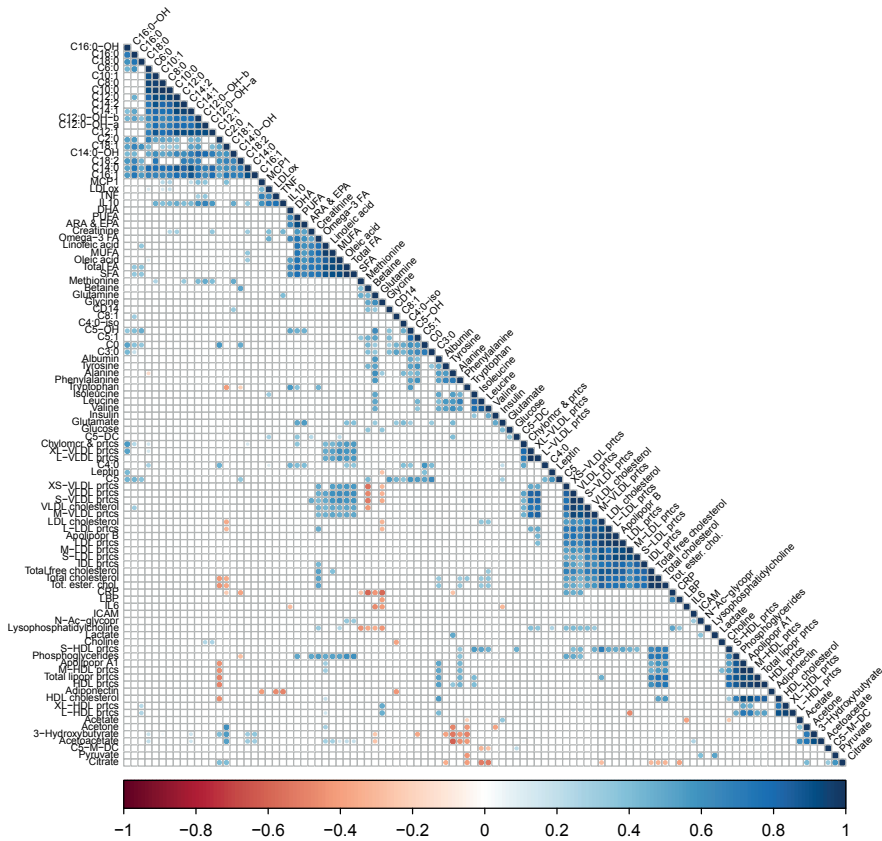


**Supplementary Figure S2: Correlations between biomarkers in serum and plasma with two platforms. (A - P)** Correlations of amino acid derivatives (A - H, blue) or fatty acids (I - P, beige) analyzed in serum at Eurecat (x-axis) or in plasma at Nightingale (y-axis). All concentrations are in mM. Pearson correlation coefficients ( $r$ ) were calculated normally distributed variables and Spearman rank correlation coefficients ( $\rho$ ) were calculated for not-normally distributed variables. \*\*\*\* $P < 0.0001$ , \*\*\* $P < 0.001$ , \*\* $P < 0.01$ .



Supplementary Figure S3: Principal component analysis (PCA) of the biomarker profiles.

(A) PCA scores plot showing the separation of high-fit females at baseline (blue) and post-exercise (orange), and low-fit females at baseline (green) and post-exercise (red) on PC1 and PC2. (B) PCA loadings plot showing the biomarker contribution (indicating by cos2) to PC1 and PC2. Small contributions are indicated in turquoise and large contributions are indicated in dark orange.



**Supplementary Figure S4: Correlation matrix showing the relationships between biomarker pairs.** The correlation matrix based on Spearman correlation coefficients between biomarker pairs. Spearman rank correlation analysis was performed on the scaled biomarker values for all biomarker pairs using the combined data of high-fit and low-fit females at baseline. Relationships were considered statistically significant when  $P < 0.05$ . Significant relationships are indicated in **red** (negative correlation) or **blue** (positive correlation). Non-significant relationships ( $P > 0.05$ ) are left blank.

**Supplementary Table S1** Standards and internal standards used for LC-MS/MS analyses

Standards	Company <sup>#</sup>	Catalogue number #
L-carnitine (C0)	CIL	NSK-B-US-1
O-acetyl-L-carnitine (C2:0)	CIL	NSK-B-US-1
O-propionyl-L-carnitine (C3:0)	CIL	NSK-B-US-1
O-butyryl-L-carnitine (C4:0)	CIL	NSK-B-US-1
O-isovaleryl-L-carnitine (C5:0)	CIL	NSK-B-US-1
O-glutaryl-L-carnitine (C5:0-DC)	CIL	NSK-B-G1-US-1
O-3-hydroxyisovaleryl-L-carnitine (C5:0-OH)	CIL	NSK-B-G1-US-1
O-octanoyl-L-carnitine (C8:0)	CIL	NSK-B-US-1
O-dodecanoyl-L-carnitine (C12:0)	CIL	NSK-B-G1-US-1
O-myristoyl-L-carnitine (C14:0)	CIL	NSK-B-US-1
O-palmitoyl-L-carnitine (C16:0)	CIL	NSK-B-US-1
O-2-DL-hydroxypalmitoyl-L-carnitine (C16:0-OH)	CIL	NSK-B-G1-US-1
O-octadecanoyl-L-carnitine (C18:0)	CIL	NSK-B-G1-US-1

Internal standards	Company <sup>#</sup>	Catalogue number #
L-carnitine (C0)	CIL	NSK-B-1
O-acetyl-L-carnitine (C2:0)	CIL	NSK-B-1
O-propionyl-L-carnitine (C3:0)	CIL	NSK-B-1
O-butyryl-L-carnitine (C4:0)	CIL	NSK-B-1
O-isovaleryl-L-carnitine (C5:0)	CIL	NSK-B-1
O-octanoyl-L-carnitine (C8:0)	CIL	NSK-B-1
O-myristoyl-L-carnitine (C14:0)	CIL	NSK-B-1
O-palmitoyl-L-carnitine (C16:0)	CIL	NSK-B-1

<sup>#</sup>CIL = Cambridge Isotope Laboratories

**Supplementary Table S2** Selected metabolites from Nightingale platform

Metabolite	Performed analyses*
Isoleucine	B
Leucine	B
Valine	B
Alanine	B
Glutamine	B
Glycine	B
Phenylalanine	B
Tyrosine	B
Glucose	A
Lactate	A
Pyruvate	A
Citrate	A
Total fatty acids (FAs)	B
Polyunsaturated fatty acids (PUFA)	B
Monounsaturated fatty acids (MUFA)	B
Saturated fatty acids (SFA)	B
Linoleic acid	B
Docosahexaenoic acid (DHA)	B
Phosphoglycerides	A
3-Hydroxybutyrate	A, B
Acetate	A, B
Acetoacetate	A
Acetone	A
Total cholesterol	A
VLDL cholesterol	A
LDL cholesterol	A
HDL cholesterol	A
Total esterified cholesterol	A
Total free cholesterol	A
Apolipoprotein B	A
Apolipoprotein A1	A
Total concentration of lipoprotein particles	A
Concentration of VLDL particles	A
Concentration of LDL particles	A
Concentration of HDL particles	A

Supplementary Table S2 Continued

Metabolite	Performed analyses*
Concentration of chylomicrons and extremely large VLDL particles	A
Concentration of very large VLDL particles	A
Concentration of large VLDL particles	A
Concentration of medium VLDL particles	A
Concentration of small VLDL particles	A
Concentration of very small VLDL particles	A
Concentration of IDL particles	A
Concentration of large LDL particles	A
Concentration of medium LDL particles	A
Concentration of small LDL particles	A
Concentration of very large HDL particles	A
Concentration of large HDL particles	A
Concentration of medium HDL particles	A
Concentration of small HDL particles	A
Creatinine	A
Albumin	A

\*A = used for main analyses (RM-ANOVA, main effects, PCA, heatmaps, correlation matrices), B = used for correlation analysis (comparison with serum levels in Eurecat platform)



Supplementary Table S3 Peptide hormone markers

Biomarker <sup>a</sup>	Matrix	Method	Concentration	Low-fit (Baseline)	Low-fit (Post-exercise)	High-fit (Baseline)	High-fit (Post-exercise)
Leptin	Serum	ELISA	ng/mL	12.8 [7.1 – 18.1]	16.8 [8.8 – 24.5]	5.6 [3.9 – 6.6]	4.4 [3.7 – 5.6]
Insulin	Serum	ELISA	mU/L	4.1 [3.4 – 5.0]	3.9 [2.8 – 4.8]	3.3 [2.6 – 4.3]	2.5 [2.2 – 3.7]
Adiponectin	Serum	ELISA	μg/mL	24.0 [16.0 – 29.6]	28.6 [21.3 – 33.6]	19.4 [13.9 – 27.4]	32.9 [27.2 – 38.9]

Data is represented as median [IQR]. Raw P-values were adjusted using an FDR of 10%.

Significant raw P-values are indicated in **bold**.

Significant FDR-adjusted P-values (Padj < 0.10) are indicated in **underlined bold**.

#Log-transformation was applied on not normally distributed variables.

<sup>a</sup>Analyzed using the EURECAT platform.

Supplementary Table S4 Inflammation and oxidative stress related markers

Biomarker <sup>a</sup>	Matrix	Method	Concentration	Low-fit (Baseline)	Low-fit (Post-exercise)	High-fit (Baseline)	High-fit (Post-exercise)
TNF	Plasma	ELISA	pg/mL	0.44 [0.38 – 0.58]	0.39 [0.36 – 0.43]	0.60 [0.49 – 0.78]	0.34 [0.28 – 0.39]
IL6	Plasma	ELISA	pg/mL	1.02 [0.64 – 1.29]	0.66 [0.41 – 1.16]	0.76 [0.55 – 1.41]	0.43 [0.26 – 0.58]
IL10	Plasma	ELISA	pg/mL	0.57 [0.31 – 8.61]	0.33 [0.09 – 0.60]	7.93 [4.82 – 11.2]	0.43 [0.21 – 0.70]
CRP	Serum	ELISA	μg/mL	0.66 [0.51 – 1.78]	0.85 [0.63 – 2.27]	0.31 [0.14 – 1.91]	0.43 [0.22 – 2.17]
Soluble CD14	Plasma	ELISA	μg/mL	1.26 [1.15 – 1.43]	1.38 [1.23 – 1.46]	1.33 [1.15 – 1.43]	1.56 [1.26 – 1.68]
MCP1	Plasma	ELISA	pg/mL	166 [144 – 267]	131 [111 – 144]	244 [212 – 280]	100 [89.1 – 111]
Soluble ICAM1	Plasma	ELISA	ng/mL	161 [117 – 184]	151 [129 – 189]	169 [165 – 182]	189 [129 – 197]
LBP	Plasma	ELISA	μg/μL	6.84 [5.82 – 8.89]	6.62 [5.66 – 10.3]	6.35 [5.49 – 8.37]	6.21 [5.84 – 7.72]
N-acetyl glycoproteins	Serum	NMR	mmol/L	0.07 [0.06 – 0.08]	0.11 [0.10 – 0.13]	0.08 [0.06 – 0.09]	0.12 [0.11 – 0.13]
Oxidized LDL	Plasma	ELISA	U/L	103 [86 – 151]	85 [66 – 120]	190 [27 – 389]	82 [65 – 123]

Normally distributed data is represented as mean (SD) and non-normally distributed data is represented as median [IQR]. Raw P-values were adjusted using an FDR of 10%. Significant raw P-values are indicated in **bold**.

Significant FDR-adjusted P-values (Padj < 0.10) are indicated in **underlined bold**.

#Transformations (log, inverse, square) were applied on not normally distributed variables.

<sup>a</sup>Analyzed using the EURECAT platform.

Transformation#	Fitness level effect			Recent exercise effect			Interaction effect		
	P <sub>group raw</sub>	P <sub>group adj</sub>	Partial $\eta^2$	P <sub>exercise raw</sub>	P <sub>exercise adj</sub>	Partial $\eta^2$	P <sub>group* exercise raw</sub>	P <sub>group* exercise adj</sub>	Partial $\eta^2$
Log	<b>0.001</b>	<u>0.076</u>	0.339	0.391	0.570	0.026	0.067	0.346	0.114
Log	<b>0.039</b>	0.464	0.144	<b>0.037</b>	0.105	0.148	0.439	0.656	0.022
Log	0.914	0.931	4.29E-04	<b>1.55E-04</b>	<u>0.001</u>	0.405	0.143	0.409	0.075

Transformation#	Fitness level effect			Recent exercise effect			Interaction effect		
	P <sub>group raw</sub>	P <sub>group adj</sub>	Partial $\eta^2$	P <sub>exercise raw</sub>	P <sub>exercise adj</sub>	Partial $\eta^2$	P <sub>group* exercise raw</sub>	P <sub>group* exercise adj</sub>	Partial $\eta^2$
Log	0.693	0.897	0.006	<b>1.20E-05</b>	<u>3.09E-04</u>	0.502	<b>0.009</b>	0.247	0.220
Log	0.154	0.640	0.071	<b>0.004</b>	<u>0.017</u>	0.256	<b>0.036</b>	0.325	0.147
Log	<b>0.025</b>	0.464	0.167	<b>3.46E-04</b>	<u>0.003</u>	0.372	0.116	0.372	0.086
Log	0.065	0.606	0.117	<b>3.31E-04</b>	<u>0.003</u>	0.374	0.250	0.547	0.047
Log	0.546	0.897	0.013	<b>0.004</b>	<u>0.015</u>	0.265	0.082	0.352	0.104
Inverse	0.379	0.855	0.028	<b>1.21E-07</b>	<u>4.16E-06</u>	0.638	<b>0.005</b>	0.247	0.247
Square	0.160	0.640	0.069	0.939	0.972	2.14x10 <sup>-4</sup>	0.709	0.815	0.005
Log	0.604	0.897	0.010	0.620	0.718	0.009	0.967	0.989	6.20E-05
Log	0.513	0.897	0.015	<b>1.02E-07</b>	<u>4.16E-06</u>	0.642	0.938	0.982	2.24E-04
Log	0.679	0.897	0.006	0.315	0.508	0.036	0.581	0.739	0.011

Supplementary Table S5 Metabolism markers

Metabolism class	Biomarker <sup>a</sup>	Matrix	Method	Concentration	Low-fit (Baseline)	Low-fit (Post-exercise)	High-fit (Baseline)
Protein and amino acid related metabolites <sup>a</sup>	Isoleucine	Serum	NMR	mmol/L	0.05 (0.01)	0.054 (0.010)	0.054 (0.006)
	Leucine	Serum	NMR	mmol/L	0.10 (0.01)	0.099 (0.014)	0.097 (0.011)
	Valine	Serum	NMR	mmol/L	0.20 (0.03)	0.204 (0.028)	0.185 (0.017)
	Alanine	Serum	NMR	mmol/L	0.36 (0.06)	0.355 (0.057)	0.341 (0.073)
	Phenylalanine	Serum	NMR	mmol/L	0.04 (0.01)	0.044 (0.005)	0.047 (0.007)
	Glutamine	Serum	NMR	mmol/L	0.42 [0.40 – 0.45]	0.422 [0.398 – 0.454]	0.389 [0.348 – 0.473]
	Glutamate	Serum	NMR	mmol/L	0.07 [0.06 – 0.08]	0.071 [0.064 – 0.082]	0.080 [0.065 – 0.095]
	Glycine	Serum	NMR	mmol/L	0.20 [0.18 – 0.24]	0.204 [0.182 – 0.238]	0.218 [0.186 – 0.229]
	Methionine	Serum	NMR	mmol/L	0.017 (0.007)	0.017 (0.007)	0.021 (0.014)
	Tyrosine	Serum	NMR	mmol/L	0.047 (0.014)	0.047 (0.014)	0.048 (0.014)
	Tryptophan	Serum	NMR	mmol/L	0.057 (0.013)	0.057 (0.013)	0.051 (0.017)
Carbohydrate and TCA cycle metabolites <sup>b</sup>	Betaine	Serum	NMR	mmol/L	0.03 [0.02 – 0.04]	0.031 [0.022 – 0.036]	0.027 [0.019 – 0.033]
	Glucose	Plasma	NMR	mmol/L	4.80 (0.28)	4.78 (0.32)	4.85 (0.22)
	Lactate	Plasma	NMR	mmol/L	0.72 (0.16)	0.71 (0.192)	0.79 (0.17)
	Pyruvate	Plasma	NMR	mmol/L	0.054 (0.014)	0.056 (0.009)	0.054 (0.010)
	Citrate	Plasma	NMR	mmol/L	0.066 (0.009)	0.065 (0.013)	0.067 (0.010)
Lipid metabolites – Fatty acids <sup>a, \$</sup>	Total FA chains	Serum	NMR	mmol/L	99 [92 – 105]	94 [90 – 100]	91 [83 – 110]
	PUFA	Serum	NMR	mmol/L	1.63 (0.47)	2.00 (0.44)	1.58 (0.47)
	Omega-3 FA	Serum	NMR	mmol/L	0.167 (0.021)	0.179 (0.030)	0.161 (0.043)
	ARA & EPA	Serum	NMR	mmol/L	0.450 (0.085)	0.514 (0.086)	0.439 (0.101)
	DHA	Serum	NMR	mmol/L	0.074 (0.020)	0.065 (0.018)	0.060 (0.022)
	Linoleic acid	Serum	NMR	mmol/L	1.88 (0.44)	2.57 (0.47)	1.94 (0.63)
	MUFA	Serum	NMR	mmol/L	4.28 (0.95)	5.72 (1.03)	4.52 (1.50)
	Oleic acid	Serum	NMR	mmol/L	1.63 [1.41 – 1.75]	2.03 [1.89 – 2.32]	1.60 [1.27 – 1.90]
	SFA	Serum	NMR	mmol/L	93 [87 – 98]	86 [82 – 91]	86 [79 – 103]
	Phosphoglycerides <sup>b</sup>	Plasma	NMR	mmol/L	2.15 [1.92 – 2.32]	2.02 [1.84 – 2.26]	2.15 [1.99 – 2.40]
Lipid metabolites – Cholines <sup>b</sup>	Acetate <sup>b</sup>	Plasma	NMR	mmol/L	0.046 [0.039 – 0.074]	0.068 [0.052 – 0.072]	0.050 [0.045 – 0.057]
	Choline	Serum	NMR	mmol/L	0.047 (0.009)	0.055 (0.014)	0.054 (0.008)
Lipid metabolites – Ketone bodies <sup>b</sup>	Lysophosphatidylcholine	Serum	NMR	mmol/L	0.261 (0.030)	0.316 (0.028)	0.240 (0.028)
	3-Hydroxybutyrate	Plasma	NMR	mmol/L	0.064 [0.052 – 0.136]	0.078 [0.043 – 0.103]	0.056 [0.028 – 0.076]
	Acetoacetate	Plasma	NMR	mmol/L	0.032 [0.022 – 0.071]	0.036 [0.025 – 0.048]	0.027 [0.017 – 0.035]
Lipid metabolites – Acylcarnitines <sup>a</sup>	Acetone	Plasma	NMR	mmol/L	0.018 [0.015 – 0.022]	0.018 [0.015 – 0.023]	0.016 [0.016 – 0.020]
	Carnitine (C:0)	Plasma	LC/MS	μmol/L	20.7 (4.7)	19.9 (4.5)	18.7 (5.0)
	Acetylcarnitine (C2:0)	Plasma	LC/MS	μmol/L	11.4 (3.0)	11.9 (2.5)	9.6 (2.4)
	Propionylcarnitine (C3:0)	Plasma	LC/MS	μmol/L	0.319 [0.257 – 0.382]	0.299 [0.249 – 0.382]	0.302 [0.228 – 0.344]
	Butyrylcarnitine (C4:0)	Plasma	LC/MS	μmol/L	0.159 [0.137 – 0.222]	0.187 [0.139 – 0.219]	0.131 [0.114 – 0.166]
	Isobutyrylcarnitine (C4:0-iso)	Plasma	LC/MS	μmol/L	0.093 [0.069 – 0.121]	0.079 [0.070 – 0.120]	0.087 [0.060 – 0.171]

High-fit (Post-exercise)	Transformation#	Fitness level effect			Recent exercise effect			Interaction effect		
		P <sub>group</sub> raw	P <sub>group</sub> adj	Partial η <sup>2</sup>	P <sub>exercise</sub> raw	P <sub>exercise</sub> adj	Partial η <sup>2</sup>	P <sub>group* exercise</sub> raw	P <sub>group* exercise</sub> adj	Partial η <sup>2</sup>
0.058 (0.009)	-	0.287	0.806	0.042	0.447	0.622	0.022	0.447	0.657	0.022
0.109 (0.019)	-	0.081	0.640	0.108	0.298	0.508	0.040	0.812	0.889	0.002
0.202 (0.030)	-	0.991	0.931	0.000	<b>0.002</b>	<u>0.009</u>	0.316	0.764	0.855	0.003
0.402 (0.085)	-	0.187	0.664	0.064	0.060	0.146	0.125	0.385	0.615	0.028
0.051 (0.010)	-	0.129	0.640	0.083	0.927	0.972	3.18E-04	0.054	0.346	0.131
0.465 [0.397 – 0.516]	Log	0.406	0.855	0.026	<b>0.005</b>	<u>0.018</u>	0.257	0.720	0.815	0.005
0.065 [0.060 – 0.089]	Log	0.315	0.812	0.037	0.984	0.972	1.40E-05	0.170	0.443	0.069
0.233 [0.200 – 0.306]	Log	0.148	0.640	0.076	0.566	0.685	0.012	0.371	0.615	0.030
0.032 (0.014)	-	<b>0.010</b>	0.376	0.221	0.963	0.972	8.10E-05	0.188	0.450	0.063
0.051 (0.016)	-	0.676	0.897	0.007	0.549	0.673	0.013	0.320	0.615	0.037
0.053 (0.019)	-	0.592	0.897	0.011	0.270	0.472	0.045	0.685	0.812	0.006
0.032 [0.022 – 0.041]	Inverse Sqrt	0.740	0.897	0.004	<b>0.002</b>	<u>0.011</u>	0.293	0.477	0.680	0.019
4.81 (0.10)	-	0.620	0.897	0.009	0.363	0.559	0.030	0.710	0.815	0.005
0.75 (0.23)	-	0.382	0.855	0.027	0.589	0.698	0.011	0.809	0.889	0.002
0.061 (0.015)	-	0.531	0.897	0.014	0.123	0.257	0.083	0.343	0.615	0.032
0.073 (0.012)	-	0.204	0.677	0.057	0.238	0.435	0.049	0.143	0.409	0.075
84 [76 – 98]	Log	0.310	0.812	0.038	<b>0.040</b>	0.111	0.147	0.344	0.615	0.033
1.57 (0.48)	-	0.127	0.640	0.084	0.074	0.169	0.114	0.056	0.346	0.129
0.160 (0.037)	-	0.197	0.677	0.061	0.515	0.655	0.016	0.475	0.680	0.019
0.442 (0.086)	-	0.158	0.640	0.072	0.097	0.208	0.099	0.122	0.380	0.086
0.051 (0.019)	-	<b>0.041</b>	0.464	0.146	<b>0.032</b>	<u>0.095</u>	0.159	0.987	0.989	1.10x10 <sup>-5</sup>
2.00 (0.74)	-	0.165	0.640	0.070	<b>0.012</b>	<u>0.041</u>	0.213	<b>0.031</b>	0.325	0.162
4.62 (1.57)	-	0.276	0.806	0.044	<b>0.023</b>	<u>0.070</u>	0.177	<b>0.046</b>	0.336	0.140
1.74 [1.22 – 2.12]	Log	0.426	0.878	0.024	0.053	0.134	0.132	0.076	0.352	0.112
79 [71 – 91]	Log	0.351	0.855	0.032	<b>0.012</b>	<u>0.041</u>	0.213	0.434	0.656	0.023
2.11 [1.87 – 2.22]	Log	0.814	0.897	0.002	<b>2.24E-04</b>	<u>0.002</u>	0.390	0.614	0.772	0.009
0.051 [0.043 – 0.062]	Log	0.166	0.640	0.067	0.160	0.318	0.069	0.294	0.613	0.039
0.059 (0.016)	-	0.191	0.664	0.062	<b>0.015</b>	<u>0.049</u>	0.201	0.560	0.737	0.013
0.317 (0.038)	-	0.257	0.803	0.047	<b>3.41E-08</b>	<b>3.51E-06</b>	0.682	0.197	0.461	0.061
0.061 [0.038 – 0.079]	Log	0.142	0.640	0.075	0.159	0.318	0.070	0.388	0.615	0.027
0.030 [0.021 – 0.042]	Log	0.143	0.640	0.075	0.241	0.435	0.049	0.540	0.722	0.014
0.019 [0.015 – 0.023]	Log	0.610	0.897	0.009	0.310	0.508	0.037	0.348	0.615	0.032
19.3 (4.7)	-	0.466	0.897	0.019	0.878	0.946	0.001	<b>0.039</b>	0.325	0.144
9.9 (1.9)	-	<b>0.030</b>	0.464	0.157	0.374	0.566	0.028	0.881	0.946	0.001
0.295 [0.250 – 0.357]	Log	0.357	0.855	0.030	0.906	0.962	0.001	0.380	0.615	0.028
0.123 [0.109 – 0.168]	Log	<b>0.034</b>	0.464	0.151	0.882	0.946	0.001	0.574	0.739	0.011
0.099 [0.068 – 0.147]	Log	0.640	0.897	0.008	0.713	0.807	0.005	0.854	0.926	0.001

Supplementary Table S5 Continued

Metabolism class	Biomarker <sup>a</sup>	Matrix	Method	Concentration	Low-fit (Baseline)	Low-fit (Post-exercise)	High-fit (Baseline)
Lipid metabolites – Acylcarnitines <sup>a</sup>	Valerylcarnitine (C5:) <sup>†</sup>	Plasma	LC/MS	μmol/L	0.076 [0.066 – 0.100]	0.077 [0.068 – 0.098]	0.076 [0.059 – 0.088]
	Hydroxyisovalerylcarnitine (C5:0-OH)	Plasma	LC/MS	μmol/L	0.034 [0.030 – 0.049]	0.036 [0.030 – 0.047]	0.038 [0.032 – 0.043]
	Glutaryl carnitine (C5:0-DC)	Plasma	LC/MS	μmol/L	0.069 [0.063 – 0.082]	0.067 [0.061 – 0.080]	0.079 [0.071 – 0.087]
	Methylglutaryl carnitine (C5-M-DC)	Plasma	LC/MS	μmol/L	0.050 [0.037 – 0.057]	0.047 [0.038 – 0.056]	0.039 [0.035 – 0.055]
	Methylcrotonyl carnitine (C5:1)	Plasma	LC/MS	μmol/L	0.010 [0.009 – 0.014]	0.011 [0.010 – 0.012]	0.011 [0.010 – 0.014]
	Hexanoylcarnitine (C6:0)	Plasma	LC/MS	μmol/L	0.044 [0.038 – 0.049]	0.042 [0.039 – 0.065]	0.036 [0.034 – 0.044]
	Octanoylcarnitine (C8:0)	Plasma	LC/MS	μmol/L	0.145 [0.119 – 0.208]	0.156 [0.131 – 0.254]	0.159 [0.131 – 0.176]
	Octenoylcarnitine (C8:1)	Plasma	LC/MS	μmol/L	0.138 [0.101 – 0.159]	0.143 [0.125 – 0.170]	0.117 [0.085 – 0.138]
	Decanoylcarnitine (C10:0)	Plasma	LC/MS	μmol/L	0.284 [0.216 – 0.425]	0.320 [0.261 – 0.565]	0.347 [0.255 – 0.398]
	Decenoylcarnitine (C10:1)	Plasma	LC/MS	μmol/L	0.177 [0.162 – 0.193]	0.189 [0.178 – 0.281]	0.213 [0.178 – 0.262]
	Dodecanoylcarnitine (C12:0)	Plasma	LC/MS	μmol/L	0.093 [0.073 – 0.128]	0.116 [0.088 – 0.160]	0.123 [0.094 – 0.166]
	Hydroxydodecanoylcarnitine-a (C12:0-OH-a)	Plasma	LC/MS	μmol/L	0.012 [0.008 – 0.013]	0.015 [0.012 – 0.021]	0.019 [0.014 – 0.025]
	Hydroxydodecanoylcarnitine-a (C12:0-OH-b)	Plasma	LC/MS	μmol/L	0.024 [0.015 – 0.027]	0.023 [0.018 – 0.027]	0.030 [0.022 – 0.035]
	Dodecenyl carnitine (C12:1)	Plasma	LC/MS	μmol/L	0.127 [0.094 – 0.139]	0.135 [0.103 – 0.171]	0.154 [0.125 – 0.185]
	Tetradecanoylcarnitine (C14:0)	Plasma	LC/MS	μmol/L	0.045 [0.039 – 0.058]	0.051 [0.041 – 0.059]	0.045 [0.037 – 0.057]
	Hydroxytetradecanoylcarnitine (C14:0-OH)	Plasma	LC/MS	μmol/L	0.024 [0.020 – 0.029]	0.027 [0.024 – 0.029]	0.028 [0.025 – 0.036]
	Tetradecenoylcarnitine (C14:1)	Plasma	LC/MS	μmol/L	0.184 [0.130 – 0.200]	0.188 [0.155 – 0.248]	0.186 [0.158 – 0.251]
	Tetradecadienyl carnitine (C14:2)	Plasma	LC/MS	μmol/L	0.064 [0.057 – 0.074]	0.080 [0.066 – 0.096]	0.086 [0.064 – 0.102]
	Hexadecanoylcarnitine (C16:0)	Plasma	LC/MS	μmol/L	0.102 [0.087 – 0.111]	0.092 [0.088 – 0.107]	0.093 [0.087 – 0.099]
	Hydroxyhexadecanoylcarnitine (C16:0-OH)	Plasma	LC/MS	μmol/L	0.004 (0.002)	0.004 (0.001)	0.003 (0.001)
	Hexadecenyl carnitine (C16:1)	Plasma	LC/MS	μmol/L	0.036 [0.031 – 0.045]	0.036 [0.031 – 0.048]	0.038 [0.032 – 0.043]
	Octadecanoylcarnitine (C18:0)	Plasma	LC/MS	μmol/L	0.058 [0.051 – 0.075]	0.058 [0.050 – 0.067]	0.057 [0.052 – 0.062]
	Octadecenyl carnitine (C18:1)	Plasma	LC/MS	μmol/L	0.112 (0.028)	0.112 (0.028)	0.114 (0.020)
	Octadecadienyl carnitine (C18:2)	Plasma	LC/MS	μmol/L	0.037 [0.032 – 0.046]	0.042 [0.032 – 0.045]	0.039 [0.035 – 0.042]
Lipid metabolites – Cholesterol metabolites <sup>b</sup>	Total cholesterol	Plasma	NMR	mmol/L	4.07 [3.82 – 4.61]	4.03 [3.72 – 4.24]	4.17 [3.88 – 4.56]
	VLDL cholesterol	Plasma	NMR	mmol/L	0.48 (0.08)	0.44 (0.07)	0.44 (0.13)
	LDL cholesterol	Plasma	NMR	mmol/L	1.57 (0.31)	1.50 (0.23)	1.55 (0.30)
	HDL cholesterol	Plasma	NMR	mmol/L	1.55 [1.35 – 1.61]	1.45 [1.32 – 1.57]	1.47 [1.41 – 1.68]
	Total esterified cholesterol	Plasma	NMR	mmol/L	3.04 [2.80 – 3.42]	2.99 [2.76 – 3.14]	3.12 [2.91 – 3.36]
	Total free cholesterol	Plasma	NMR	mmol/L	1.05 [1.01 – 1.18]	1.04 [0.95 – 1.09]	1.10 [0.98 – 1.19]

High-fit (Post-exercise)	Transformation#	Fitness level effect			Recent exercise effect			Interaction effect		
		P <sub>group</sub> raw	P <sub>group</sub> adj	Partial $\eta^2$	P <sub>exercise</sub> raw	P <sub>exercise</sub> adj	Partial $\eta^2$	P <sub>group*exercise</sub> raw	P <sub>group*exercise</sub> adj	Partial $\eta^2$
0.073 [0.068 – 0.091]	Log	0.366	0.855	0.028	0.427	0.613	0.024	0.180	0.443	0.064
0.040 [0.032 – 0.042]	X	0.806*	0.897*	NA	0.187*	0.357*	NA	0.305*	0.615*	NA
0.081 [0.079 – 0.085]	Log	0.140	0.640	0.076	0.537	0.666	0.014	0.089	0.353	0.100
0.042 [0.036 – 0.063]	Inverse	0.922	0.931	0.000	0.066	0.155	0.115	<b>0.022</b>	0.325	0.173
0.013 [0.010 – 0.014]	X	0.174*	0.641*	NA	0.253*	0.449*	NA	0.775*	0.855*	NA
0.036 [0.031 – 0.039]	Inverse	<b>0.011</b>	0.376	0.210	0.861	0.943	0.001	0.086	0.353	0.101
0.147 [0.126 – 0.165]	Inverse	0.402	0.855	0.025	0.532	0.666	0.014	<b>0.026</b>	0.325	0.165
0.135 [0.101 – 0.155]	Log	0.241	0.775	0.049	<b>0.005</b>	<u>0.018</u>	0.251	0.941	0.982	0.000
0.306 [0.238 – 0.371]	Inverse	0.745	0.897	0.004	0.478	0.648	0.018	<b>0.038</b>	0.325	0.145
0.213 [0.160 – 0.228]	Inverse	0.822	0.897	0.002	0.748	0.829	0.004	0.065	0.346	0.117
0.097 [0.087 – 0.172]	Log	0.808	0.897	0.002	0.514	0.655	0.015	0.081	0.352	0.105
0.016 [0.014 – 0.024]	Log	<b>0.036</b>	0.464	0.148	0.052	0.133	0.129	0.061	0.346	0.120
0.024 [0.021 – 0.030]	Log	0.168	0.640	0.067	0.393	0.570	0.026	0.648	0.783	0.008
0.134 [0.116 – 0.172]	Log	0.298	0.806	0.040	0.736	0.824	0.004	0.112	0.372	0.088
0.042 [0.037 – 0.056]	Log	0.407	0.855	0.025	0.961	0.972	8.90E-05	0.340	0.615	0.032
0.029 [0.025 – 0.032]	Log	0.281	0.806	0.041	0.588	0.698	0.011	0.244	0.547	0.048
0.170 [0.152 – 0.267]	Log	0.828	0.897	0.002	0.435	0.613	0.022	0.137	0.409	0.077
0.075 [0.062 – 0.104]	Log	0.658	0.897	0.007	0.638	0.730	0.008	0.107	0.367	0.090
0.086 [0.088 – 0.091]	Log	0.088	0.640	0.101	0.084	0.183	0.103	0.944	0.982	1.7E-04
0.003 (0.001)	-	0.123	0.640	0.083	0.304	0.508	0.038	0.654	0.783	0.007
0.037 [0.033 – 0.039]	Log	0.685	0.897	0.006	0.607	0.711	0.010	0.101	0.367	0.093
0.061 [0.048 – 0.068]	Log	0.714	0.897	0.005	0.327	0.511	0.034	0.642	0.783	0.008
0.109 (0.019)	-	0.907	0.931	4.98E-04	0.468	0.643	0.019	0.515	0.708	0.015
0.038 [0.036 – 0.042]	Log	0.822	0.897	0.002	0.497	0.648	0.017	0.491	0.684	0.017
3.87 [3.48 – 4.35]	Log	0.899	0.931	0.001	<b>9.70E-05</b>	<b>0.001</b>	0.424	0.398	0.622	0.026
0.45 (0.15)	-	0.745	0.897	0.004	0.175	0.339	0.065	<b>0.010</b>	0.247	0.216
1.40 (0.28)	-	0.567	0.897	0.012	<b>0.002</b>	<u>0.010</u>	0.292	0.229	0.524	0.051
1.40 [1.30 – 1.58]	Log	0.626	0.897	0.009	<b>1.06E-04</b>	<b>0.001</b>	0.421	0.169	0.443	0.066
2.83 [2.57 – 3.23]	Log	0.908	0.931	4.80E-05	<b>9.50E-05</b>	<b>0.001</b>	0.425	0.298	0.613	0.039
1.01 [0.91 – 1.13]	Log	0.894	0.931	0.001	<b>1.49E-04</b>	<b>0.001</b>	0.407	0.980	0.989	0.000

Supplementary Table S5 Continued

Metabolism class	Biomarker <sup>a</sup>	Matrix	Method	Concentration	Low-fit (Baseline)	Low-fit (Post-exercise)	High-fit (Baseline)
Lipid metabolites – Apolipoproteins <sup>b</sup>	Apolipoprotein B	Plasma	NMR	mmol/L	0.706 (0.106)	0.676 (0.086)	0.694 (0.114)
	Apolipoprotein A1	Plasma	NMR	mmol/L	1.53 (0.19)	1.48 (0.16)	1.58 (0.19)
Lipid metabolites – Lipoproteins <sup>b, §</sup>	Total lipoprotein particles	Plasma	NMR	μmol/L	18.1 [15.5 – 18.9]	17.2 [15.4 – 18.6]	18.3 [16.3 – 18.7]
	VLDL particles	Plasma	NMR	μmol/L	0.108 [0.100 – 0.116]	0.098 [0.089 – 0.106]	0.102 [0.076 – 0.116]
	LDL particles	Plasma	NMR	μmol/L	1.02 (0.17)	0.99 (0.14)	1.01 (0.17)
	HDL particles	Plasma	NMR	μmol/L	16.8 [14.2 – 17.7]	15.9 [14.1 – 17.1]	16.9 [14.7 – 17.3]
	Chylomicrons & XXL-VLDL particles	Plasma	NMR	nmol/L	0.18 [0.03 – 0.60]	0.09 [0.03 – 0.43]	0.02 [0.02 – 0.23]
	XL-VLDL particles	Plasma	NMR	nmol/L	1.85 [1.56 – 2.39]	1.58 [1.26 – 2.04]	1.68 [1.19 – 1.85]
	L-VLDL particles	Plasma	NMR	nmol/L	6.79 [6.21 – 8.06]	6.03 [5.05 – 7.57]	6.32 [5.02 – 7.13]
	M-VLDL particles	Plasma	NMR	nmol/L	25.3 [23.4 – 29.7]	24.5 [21.2 – 27.2]	26.1 [17.8 – 28.4]
	S-VLDL particles	Plasma	NMR	nmol/L	30.5 [27.9 – 34.1]	28.9 [24.9 – 33.3]	32.1 [20.0 – 34.8]
	XS-VLDL particles	Plasma	NMR	nmol/L	40.0 [35.6 – 43.7]	37.0 [34.0 – 39.9]	38.2 [33.7 – 45.1]
	IDL particles	Plasma	NMR	nmol/L	246 (36)	231 (28)	247 (32)
	L-LDL particles	Plasma	NMR	nmol/L	617 (87)	598 (85)	601 (99)
	M-LDL particles	Plasma	NMR	nmol/L	254 (57)	244 (40)	255 (60)
	S-LDL particles	Plasma	NMR	nmol/L	152 (28)	145 (21)	149 (22)
	XL-HDL particles	Plasma	NMR	nmol/L	240 [205 – 261]	224 [193 – 270]	216 [183 – 283]
	L-HDL particles	Plasma	NMR	μmol/L	1.78 [1.53 – 1.98]	1.70 [1.35 – 1.83]	1.61 [1.32 – 2.18]
	M-HDL particles	Plasma	NMR	μmol/L	4.21 (0.73)	4.02 (0.62)	4.37 (0.71)
	S-HDL particles	Plasma	NMR	μmol/L	10.03 (1.29)	9.81 (0.99)	10.11 (1.19)
Other metabolites – Fluid balance <sup>b</sup>	Creatinine	Plasma	NMR	μmol/L	60.6 [59.1 – 66.1]	59.8 [55.4 – 66.9]	63.0 [61.1 – 69.6]
	Albumin	Plasma	NMR	g/L	38.2 (2.6)	38.3 (2.1)	39.1 (2.8)

Normally distributed data is represented as mean (SD) and non-normally distributed data is represented as median [IQR]. Raw P-values were adjusted using an FDR of 10%. Significant raw P-values are indicated in **bold**. Significant FDR-adjusted P-values (Padj < 0.10) are indicated in underlined bold.

<sup>#</sup>Transformations (log, inverse, inverse square root) were applied on not normally distributed variables. Variables that did not achieve a normal distribution after transformation are represented with an X. For these variables non-parametric tests were used: the fitness level effect ( $P_{\text{group}}$ ) was analyzed using a Mann-Whitney U test on the ranked baseline values; the exercise effect ( $P_{\text{exercise}}$ ) was analyzed using a Wilcoxon-Signed rank test on the ranked baseline and post-exercise values; the interaction effect ( $P_{\text{group} \times \text{exercise}}$ ) was analyzed using a Mann-Whitney U test on the ranked difference between baseline and post-exercise values. These p-values are marked with an asterisk (\*). NA = not applicable

<sup>§</sup>Abbreviations: FA = fatty acid, PUFA = polyunsaturated fatty acid, ARA & EPA = arachidonic acid & eicosapentaenoic acid, DHA = docosahexaenoic acid, MUFA = monounsaturated fatty acid, SFA = saturated fatty acid, XXL = extremely large, XL = very large, L = large, M = medium, I = intermediate, S = small, XS = very small.

<sup>\*</sup>Refer to the two isomers 2-methylbutyrylcarnitine (C4:0-2M) and isovalerylcarnitine (C5:0).

<sup>a</sup>Analyzed using the EURECAT platform.

<sup>b</sup>Analyzed using the Nightingale platform.

High-fit (Post-exercise)	Transformation#	Fitness level effect			Recent exercise effect			Interaction effect		
		P <sub>group</sub> raw	P <sub>group</sub> adj	Partial η <sup>2</sup>	P <sub>exercise</sub> raw	P <sub>exercise</sub> adj	Partial η <sup>2</sup>	P <sub>group* exercise</sub> raw	P <sub>group* exercise</sub> adj	Partial η <sup>2</sup>
0.664 (0.115)	-	0.763	0.897	0.003	<b>0.001</b>	<u>0.008</u>	0.317	0.989	0.989	7.00x10 <sup>-6</sup>
1.50 (0.19)	-	0.615	0.897	0.009	<b>1.33E-04</b>	<u>0.001</u>	0.412	0.384	0.615	0.027
16.1 [15.4 – 18.2]	X	0.595*	0.897*	NA	<b>0.002*</b>	<u>0.010*</u>	NA	0.187*	0.443*	NA
0.101 [0.077 – 0.114]	Log	0.610	0.897	0.009	<b>0.048</b>	0.126	0.133	0.065	0.346	0.116
0.95 (0.17)	-	0.825	0.897	0.002	<b>4.20E-04</b>	<u>0.003</u>	0.364	0.326	0.615	0.034
14.8 [14.3 – 16.8]	X	0.567*	0.897*	NA	<b>0.003*</b>	<u>0.013*</u>	NA	0.148*	0.412*	NA
0.35 [0.04 – 0.62]	X	<b>0.045*</b>	0.464*	NA	0.229*	0.429	NA	<b>0.007*</b>	0.247*	NA
1.64 [1.21 – 1.99]	X	0.174*	0.640*	NA	0.491*	0.648*	NA	<b>0.041*</b>	0.325*	NA
5.94 [4.60 – 6.98]	Log	0.312	0.812	0.037	0.083	0.183	0.104	0.103	0.367	0.092
23.0 [17.7 – 27.2]	Log	0.403	0.855	0.025	<b>0.016</b>	<u>0.051</u>	0.191	0.363	0.615	0.030
27.7 [20.3 – 32.7]	Log	0.516	0.897	0.015	0.125	0.257	0.082	0.347	0.615	0.032
39.7 [34.1 – 44.3]	Log	0.795	0.897	0.002	0.316	0.508	0.036	<b>0.014</b>	0.294	0.196
242 (36)	-	0.678	0.897	0.006	<b>0.002</b>	<u>0.010</u>	0.297	0.079	0.352	0.106
591 (105)	-	0.739	0.897	0.004	<b>0.042</b>	0.114	0.140	0.482	0.680	0.018
222 (48)	-	0.574	0.897	0.011	<b>0.004</b>	<u>0.015</u>	0.265	0.093	0.354	0.098
138 (20)	-	0.544	0.897	0.013	<b>0.001</b>	<u>0.008</u>	0.315	0.410	0.631	0.024
236 [191 – 279]	Log	0.560	0.897	0.012	0.497	0.648	0.017	0.267	0.574	0.044
1.63 [1.30 – 1.98]	Log	0.558	0.897	0.012	0.066	0.155	0.116	0.526	0.713	0.014
4.09 (0.67)	-	0.644	0.897	0.008	<b>1.41E-04</b>	<u>0.001</u>	0.409	0.380	0.615	0.028
9.38 (0.965)	-	0.644	0.897	0.008	<b>0.016</b>	<u>0.051</u>	0.189	0.181	0.443	0.063
67.9 [64.1 – 71.1]	Log	0.078	0.640	0.107	0.382	0.570	0.027	<b>0.035</b>	0.325	0.149
38.9 (1.9)	-	0.370	0.855	0.029	0.951	0.972	1.36E-04	0.623	0.773	0.009

Supplementary Table S6 Main effect analysis of peptide hormone markers

Biomarker	Fitness level effect				Recent exercise effect			
	RM-ANOVA		Main effect analysis		RM-ANOVA		Main effect analysis	
	P <sub>group</sub> raw	P <sub>group</sub> adj	P <sub>group</sub> raw	P <sub>group</sub> adj	P <sub>exercise</sub> raw	P <sub>exercise</sub> adj	P <sub>exercise</sub> raw	P <sub>exercise</sub> adj
Leptin	<b>0.001</b>	<u>0.076</u>	<b>0.001</b>	<u>0.076</u>	0.391	0.570	0.411	0.605
Insulin	<b>0.039</b>	0.464	<b>0.039</b>	0.464	<b>0.037</b>	0.105	<b>0.035</b>	0.101
Adiponectin	0.914	0.931	0.914	0.931	<b>1.55E-04</b>	<u><b>0.001</b></u>	1.88E-04	<u><b>0.002</b></u>

Raw P-values were adjusted using an FDR of 10%. Significant raw P-values are indicated in **bold**. Significant FDR-adjusted P-values (Padj < 0.10) are indicated in underlined bold.

Supplementary Table S7 Main effect analysis of inflammation and oxidative stress-related markers

Biomarker	Fitness level effect				Recent exercise effect			
	RM-ANOVA		Main effect analysis		RM-ANOVA		Main effect analysis	
	P <sub>group raw</sub>	P <sub>group adj</sub>	P <sub>group raw</sub>	P <sub>group adj</sub>	P <sub>exercise raw</sub>	P <sub>exercise adj</sub>	P <sub>exercise raw</sub>	P <sub>exercise adj</sub>
TNF	0.693	0.897	0.693	0.870	1.20E-05	<u>3.09E-04</u>	4.70E-05	<u>0.001</u>
IL6	0.154	0.640	0.154	0.640	0.004	<u>0.017</u>	0.007	<u>0.025</u>
IL10	<b>0.025</b>	0.464	<b>0.025</b>	0.464	3.46E-04	<u>0.003</u>	4.44E-04	<u>0.003</u>
CRP	0.065	0.606	0.065	0.606	3.31E-04	<u>0.003</u>	3.38E-04	<u>0.003</u>
Soluble CD14	0.546	0.897	0.546	0.870	0.004	<u>0.015</u>	0.005	<u>0.018</u>
MCPI	0.379	0.855	0.379	0.806	1.21E-07	<u>4.16E-06</u>	9.03E-06	<u>2.32E-04</u>
Soluble ICAM1	0.160	0.640	0.160	0.640	0.939	0.972	0.938	0.979
LBP	0.604	0.897	0.604	0.870	0.620	0.718	0.614	0.716
N-acetyl glycoproteins	0.513	0.897	0.513	0.870	1.02E-07	<u>4.16E-06</u>	6.03E-07	<u>3.11E-05</u>
Oxidized LDL	0.679	0.897	0.679	0.870	0.315	0.508	0.309	0.514

Raw P-values were adjusted using an FDR of 10%. Significant raw P-values are indicated in **bold**. Significant FDR-adjusted P-values (Padj < 0.10) are indicated in underlined bold.

Supplementary Table S8 Main effect analysis of metabolism markers

Metabolism class	Biomarker	Fitness level effect						Recent exercise effect					
		RM-ANOVA			Main effect analysis			RM-ANOVA			Main effect analysis		
		P <sub>group raw</sub>	P <sub>group adj</sub>	P <sub>group raw</sub>	P <sub>group adj</sub>	P <sub>group raw</sub>	P <sub>group adj</sub>	P <sub>exercise raw</sub>	P <sub>exercise adj</sub>	P <sub>exercise raw</sub>	P <sub>exercise adj</sub>	P <sub>exercise raw</sub>	P <sub>exercise adj</sub>
Protein and amino acid related metabolites	Isoleucine	0.287	0.806	0.287	0.784	0.447	0.622	0.428	0.614				
	Leucine	0.081	0.640	0.081	0.640	0.298	0.508	0.286	0.499				
	Valine	0.991	0.931	0.991	0.991	<b>0.002</b>	<b>0.009</b>	<b>0.001</b>	<b>0.008</b>				
	Alanine	0.187	0.664	0.187	0.655	0.060	0.146	0.055	0.144				
	Phenylalanine	0.129	0.640	0.129	0.640	0.927	0.972	0.983	0.992				
	Glutamine	0.406	0.855	0.406	0.806	<b>0.005</b>	<b>0.018</b>	<b>0.004</b>	<b>0.017</b>				
	Glutamate	0.315	0.812	0.315	0.792	0.984	0.972	0.947	0.979				
	Glycine	0.148	0.640	0.148	0.640	0.566	0.685	0.543	0.674				
	Methionine	<b>0.010</b>	0.376	<b>0.010</b>	0.376	0.963	0.972	0.999	0.999				
	Tyrosine	0.676	0.897	0.676	0.870	0.549	0.673	0.526	0.665				
Carbohydrate and TCA cycle metabolites	Tryptophan	0.592	0.897	0.592	0.870	0.270	0.472	0.268	0.477				
	Betaine	0.740	0.897	0.740	0.882	<b>0.002</b>	<b>0.011</b>	<b>0.002</b>	<b>0.010</b>				
	Glucose	0.620	0.897	0.620	0.870	0.363	0.559	0.356	0.560				
	Lactate	0.382	0.855	0.382	0.806	0.589	0.698	0.583	0.698				
	Pyruvate	0.531	0.897	0.531	0.870	0.123	0.257	0.122	0.255				
	Citrate	0.204	0.677	0.204	0.656	0.238	0.435	0.247	0.455				
	Total FA	0.310	0.812	0.310	0.792	<b>0.040</b>	0.111	0.036	0.101				
	PUFA	0.127	0.640	0.127	0.640	0.074	0.169	0.100	0.218				
	Omega-3 FA	0.197	0.677	0.197	0.655	0.515	0.655	0.527	0.665				
	ARA & EPA	0.158	0.640	0.158	0.640	0.097	0.208	0.116	0.250				
Lipid metabolites – Fatty acids	DHA	<b>0.041</b>	0.464	<b>0.041</b>	0.464	<b>0.032</b>	<b>0.095</b>	<b>0.029</b>	<b>0.088</b>				

Lipid metabolites – Cholines	Linoleic acid	0.165	0.640	0.165	0.640	<b>0.012</b>	<b>0.041</b>	<b>0.021</b>	<b>0.065</b>
	MUFA	0.276	0.806	0.276	0.784	<b>0.023</b>	<b>0.070</b>	<b>0.036</b>	0.101
	Oleic acid	0.426	0.878	0.426	0.828	0.053	0.134	0.070	0.169
	SFA	0.351	0.855	0.351	0.806	<b>0.012</b>	<b>0.041</b>	<b>0.010</b>	<b>0.037</b>
	Phosphoglycerides	0.814	0.897	0.814	0.888	<b>2.24E-04</b>	<b>0.002</b>	<b>1.87E-04</b>	<b>0.002</b>
Lipid metabolites – Cholines	Choline	0.191	0.897	0.191	0.655	<b>0.015</b>	<b>0.049</b>	<b>0.014</b>	<b>0.049</b>
	Lysophosphatidylcholine	0.257	0.803	0.257	0.780	<b>3.41E-08</b>	<b>3.51E-06</b>	<b>3.04E-07</b>	<b>3.11E-05</b>
Lipid metabolites – Ketone bodies	3-Hydroxybutyrate	0.142	0.640	0.142	0.640	0.159	0.318	0.157	0.316
	Acetate	0.166	0.640	0.166	0.640	0.160	0.318	0.161	0.319
	Acetoacetate	0.143	0.640	0.143	0.640	0.241	0.435	0.235	0.441
	Acetone	0.610	0.897	0.610	0.870	0.310	0.508	0.309	0.514
	Carnitine (C:0)	0.466	0.897	0.466	0.870	0.878	0.946	0.885	0.950
Lipid metabolites – Acylcarnitines	Acetyl/carnitine (C2:0)	<b>0.030</b>	0.464	<b>0.030</b>	0.464	0.374	0.566	0.366	0.562
	Propionyl/carnitine (C3:0)	0.357	0.855	0.357	0.806	0.906	0.962	0.906	0.962
	Butyryl/carnitine (C4:0)	<b>0.034</b>	0.464	<b>0.034</b>	0.464	0.882	0.946	0.881	0.950
	Isobutyryl/carnitine (C4:0-iso)	0.640	0.897	0.640	0.870	0.713	0.807	0.708	0.802
	2-Methylbutyryl/carnitine (C4:0-2M)	0.367	0.855	0.367	0.806	0.429	0.613	0.436	0.614
	Isovaleryl/carnitine (C5:0)	0.366	0.855	0.366	0.806	0.427	0.613	0.436	0.614
	Hydroxyisovaleryl/carnitine (C5:0-OH)	0.806*	0.897*	0.806*	0.888*	0.187*	0.357*	0.187*	0.376*
	Glutaryl/carnitine (C5:0-DC)	0.140	0.640	0.140	0.640	0.537	0.666	0.550	0.675
	Methylglutaryl/carnitine (C5-M-DC)	0.922	0.931	0.922	0.931	0.066	0.155	0.087	0.200
	Methylcrotonyl/carnitine (C5:1)	0.174*	0.641*	0.174*	0.640*	0.253*	0.449*	0.253*	0.457*
	Hexanoyl/carnitine (C6:0)	<b>0.011</b>	0.376	<b>0.011</b>	0.376	0.861	0.943	0.866	0.949
	Octanoyl/carnitine (C8:0)	0.402	0.855	0.402	0.806	0.532	0.666	0.561	0.680
	Octenoyl/carnitine (C8:1)	0.241	0.775	0.241	0.752	<b>0.005</b>	<b>0.018</b>	<b>0.004</b>	<b>0.017</b>
	Decanoyl/carnitine (C10:0)	0.745	0.897	0.745	0.882	0.478	0.648	0.504	0.657
	Decenoyl/carnitine (C10:1)	0.822	0.897	0.822	0.888	0.748	0.829	0.759	0.840

Supplementary Table S8 Continued

Metabolism class	Biomarker	Fitness level effect				Recent exercise effect			
		RM-ANOVA		Main effect analysis		RM-ANOVA		Main effect analysis	
		P <sub>group raw</sub>	P <sub>group adj</sub>	P <sub>group raw</sub>	P <sub>group adj</sub>	P <sub>exercise raw</sub>	P <sub>exercise adj</sub>	P <sub>exercise raw</sub>	P <sub>exercise adj</sub>
	Dodecanoylcarnitine (C12:0)	0.808	0.897	0.808	0.888	0.514	0.655	0.529	0.665
	Hydroxydodecanoylcarnitine-a (C12:0-OH-a)	<b>0.036</b>	0.464	<b>0.036</b>	0.464	0.052	0.133	0.062	0.155
	Hydroxydodecanoylcarnitine-a (C12:0-OH-b)	0.168	0.640	0.168	0.640	0.393	0.570	0.386	0.585
	Dodecenylcarnitine (C12:1)	0.298	0.806	0.289	0.784	0.736	0.824	0.743	0.832
	Tetradecanoylcarnitine (C14:0)	0.407	0.855	0.407	0.806	0.961	0.972	0.961	0.980
	Hydroxytetradecanoylcarnitine (C14:0-OH)	0.281	0.806	0.281	0.784	0.588	0.698	0.590	0.699
	Tetradecenylcarnitine (C14:1)	0.828	0.897	0.828	0.888	0.435	0.613	0.445	0.619
	Tetradecadienylcarnitine (C14:2)	0.658	0.897	0.658	0.870	0.638	0.730	0.648	0.741
	Hexadecanoylcarnitine (C16:0)	0.088	0.640	0.088	0.640	0.084	0.183	0.078	0.183
	Hydroxyhexadecanoylcarnitine (C16:0-OH)	0.123	0.640	0.123	0.640	0.304	0.508	0.297	0.509
	Hexadecenylcarnitine (C16:1)	0.685	0.897	0.685	0.870	0.607	0.711	0.618	0.716
	Octadecanoylcarnitine (C18:0)	0.714	0.897	0.714	0.882	0.327	0.511	0.321	0.517
	Octadecenylcarnitine (C18:1)	0.907	0.931	0.907	0.931	0.468	0.643	0.464	0.637
	Octadecadienylcarnitine (C18:2)	0.822	0.897	0.822	0.888	0.497	0.648	0.493	0.657
Lipid metabolites – Cholesterol metabolites	Total cholesterol	0.899	0.931	0.905	0.931	<b>9.70E-05</b>	<b>0.001</b>	<b>8.70E-05</b>	<b>0.001</b>
	VLDL cholesterol	0.745	0.897	0.745	0.882	0.175	0.339	0.220	0.427
	LDL cholesterol	0.567	0.897	0.567	0.870	<b>0.002</b>	<b>0.010</b>	<b>0.002</b>	<b>0.011</b>
	HDL cholesterol	0.626	0.897	0.627	0.870	<b>1.06E-04</b>	<b>0.001</b>	<b>1.19E-04</b>	<b>0.001</b>

Lipid metabolites – Apolipoproteins	Total esterified cholesterol	0.908	0.931	0.908	0.931	<b>9.50E-05</b>	<b>0.001</b>	<b>1.19E-04</b>	<b>0.001</b>
	Total free cholesterol	0.894	0.931	0.897	0.931	<b>1.49E-04</b>	<b>0.001</b>	<b>1.07E-04</b>	<b>0.001</b>
Lipid metabolites – Lipoproteins	Apolipoprotein B	0.763	0.897	0.763	0.888	<b>0.001</b>	<b>0.008</b>	<b>0.001</b>	<b>0.007</b>
	Apolipoprotein A1	0.615	0.897	0.616	0.870	<b>1.33E-04</b>	<b>0.001</b>	<b>1.19E-04</b>	<b>0.001</b>
Chylomicrons & XXL-VLDL particles	Total lipoprotein particles	0.595*	0.897*	0.595	0.870	<b>0.002*</b>	<b>0.010*</b>	<b>0.002</b>	<b>0.010</b>
	VLDL particles	0.610	0.897	0.609	0.870	<b>0.048</b>	0.126	0.057	0.146
	LDL particles	0.825	0.897	0.649	0.870	<b>4.20E-04</b>	<b>0.003</b>	<b>0.002</b>	<b>0.010</b>
	HDL particles	0.567*	0.897*	0.567*	0.870*	<b>0.003*</b>	<b>0.013*</b>	<b>0.003*</b>	<b>0.013*</b>
	XL-VLDL particles	<b>0.045*</b>	0.464*	<b>0.045*</b>	0.464*	0.229*	0.429*	0.229*	0.437*
	L-VLDL particles	0.312	0.812	0.312	0.792	0.083	0.183	0.092	0.205
	M-VLDL particles	0.403	0.855	0.403	0.806	<b>0.016</b>	<b>0.051</b>	<b>0.015</b>	<b>0.051</b>
	S-VLDL particles	0.516	0.897	0.516	0.870	0.125	0.257	0.124	0.255
	XS-VLDL particles	0.795	0.897	0.795	0.888	0.316	0.508	0.359	0.560
	IDL particles	0.678	0.897	0.659	0.870	<b>0.002</b>	<b>0.010</b>	<b>0.002</b>	<b>0.011</b>
Other metabolites – Fluid balance <sup>b</sup>	L-LDL particles	0.739	0.897	0.739	0.882	<b>0.042</b>	0.114	<b>0.040</b>	0.108
	M-LDL particles	0.574	0.897	0.574	0.870	<b>0.004</b>	<b>0.015</b>	<b>0.005</b>	<b>0.018</b>
	S-LDL particles	0.544	0.897	0.544	0.870	<b>0.001</b>	<b>0.008</b>	<b>0.001</b>	<b>0.007</b>
	XL-HDL particles	0.560	0.897	0.560	0.870	0.497	0.648	0.499	0.657
	L-HDL particles	0.558	0.897	0.558	0.870	0.066	0.155	0.063	0.155
	M-HDL particles	0.644	0.897	0.644	0.870	<b>1.41E-04</b>	<b>0.001</b>	<b>1.00E-06</b>	<b>3.43E-05</b>
	S-HDL particles	0.644	0.897	0.644	0.870	<b>0.016</b>	<b>0.051</b>	<b>0.018</b>	<b>0.057</b>
	Creatinine	0.078	0.640	0.078	0.640	0.382	0.570	0.411	0.605
Albumin		0.370	0.897	0.370	0.806	0.951	0.972	0.951	0.979

Raw P-values were adjusted using an FDR of 10%. Significant raw P-values are indicated in **bold**. Significant FDR-adjusted P-values (Padj < 0.10) are indicated in **underlined bold**. Biomarkers indicated with an asterisk (\*) were analyzed non-parametrically.



# 6

## Mito-nuclear communication and its regulation by B-vitamins

Joëlle J.E. Janssen<sup>1</sup>, Sander Grefte<sup>1</sup>, Jaap Keijer<sup>1</sup>, Vincent C.J. de Boer<sup>1</sup>

<sup>1</sup> *Human and Animal Physiology, Wageningen University and Research,  
P.O. Box 338, 6700 AH, Wageningen, the Netherlands*

**Front Physiol.** 2019; Feb 12;10:78

doi: 10.3389/fphys.2019.00078

## Abstract

Mitochondria are cellular organelles that control metabolic homeostasis and ATP generation, but also play an important role in other processes, like cell death decisions and immune signaling. Mitochondria produce a diverse array of metabolites that act in the mitochondria itself, but also function as signaling molecules to other parts of the cell. Communication of mitochondria with the nucleus by metabolites that are produced by the mitochondria provides the cells with a dynamic regulatory system that is able to respond to changing metabolic conditions. Dysregulation of the interplay between mitochondrial metabolites and the nucleus has been shown to play a role in disease etiology, such as cancer and type 2 diabetes. Multiple recent studies emphasize the crucial role of nutritional cofactors in regulating these metabolic networks. Since B-vitamins directly regulate mitochondrial metabolism, understanding the role of B-vitamins in mito-nuclear communication is relevant for therapeutic applications and optimal dietary lifestyle. In this review, we will highlight emerging concepts in mito-nuclear communication and will describe the role of B-vitamins in mitochondrial metabolite-mediated nuclear signaling.

## Introduction

B-vitamins are water-soluble vitamins (Figure 1) that are essential nutrients in supporting mitochondrial function, predominantly by serving as nutritional cofactors or coenzymes for enzymes that are located in mitochondria (Figure 2, Table 1) (1–3). Five out of the eight B-vitamins are directly involved in functioning of the tricarboxylic acid (TCA) cycle (B1, B2, B3, B5 and B8/B7) (Figure 2). Vitamin B6 is required for iron-sulfur (FeS) biosynthesis, *de novo* synthesis of nicotinamide adenine dinucleotide (NAD<sup>+</sup>) and substrate metabolism, whereas vitamin B11/B9 and B12 are essential in nucleotide biosynthesis and amino acid metabolism (Figure 2). Vitamin B12 is also crucial for the generation of succinyl-CoA from methylmalonyl-CoA in the mitochondria (Figure 2). Since the activity of mitochondrial enzymes is regulated by B-vitamin levels, maintaining a balanced pool of B-vitamins in the mitochondria is essential to support the metabolic and other biochemical reactions that are orchestrated by these mitochondrial enzymes.

In order to maintain a balanced B-vitamin pool, dietary consumption of foods rich in B-vitamins is necessary, as B-vitamins cannot be synthesized by the body and must be derived from the diet. The European Food and Safety Authority (EFSA) has established the daily intake requirement for each B-vitamin (Table 1). Daily intake requirements are expressed as population reference intake (PRI) or adequate intake (AI) and are dependent on population group, age and/or gender. To meet these requirements, it is recommended to have a daily consumption of dietary sources that are rich in B-vitamins (Table 1). Some of these food products contain only one of the B-vitamins, whereas others provide several B-vitamins. For example, dark leafy green vegetables are rich in vitamin B11, whereas eggs contain vitamin B2, B5, B8 as well as B12. In general, a diverse diet will meet the recommended daily intake requirements, but insufficient intake of a food group that exclusively provides a specific B-vitamin requires alternative dietary adjustments. For example, vitamin B12 is mainly provided by animal sources, especially meat, and cannot be derived from plant sources. Individuals who do not consume meat products, such as vegetarian or veganists, should consider the consumption of alternative foods that are fortified with vitamin B12 or should perhaps take supplementation with vitamin B12.

Sufficient B-vitamin intake is essential to maintain mitochondrial function, control levels of mitochondrial metabolites and prevent disease. Evidence is emerging that the wide array of metabolites that are produced in the mitochondria do not only support mitochondrial respiration and adenosine triphosphate (ATP) generation, but can also communicate with other parts of the cell, including the nucleus (4).

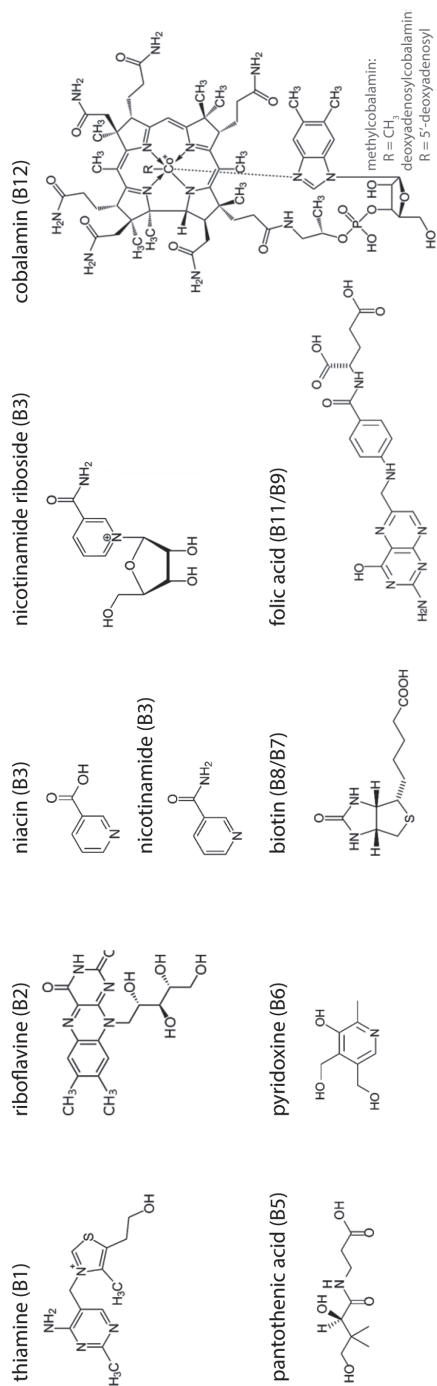


**Figure 1:** Molecular structures of the eight B-vitamins. Three forms are given for vitamin B3: niacin, nicotinamide, and nicotinamide riboside. R-group in vitamin B12 represents a methyl- group (methylcobalamin) or a 5'-deoxyadenosyl-group (deoxyadenosylcobalamin).

**Table 1** B-vitamins and their generic names, bioactive forms, recommended daily intake values and rich dietary sources.

Vitamin	Generic name	Bioactive form	RI/AI <sup>1,2</sup>	Rich dietary sources <sup>1</sup>
B1	Thiamin	Thiamin diphosphate	RI 0.1 mg/MJ/day	Whole grains, legumes, meat, liver, and fish.
B2	Riboflavin	FMN, FAD	RI 1.6 mg/day	Milk, milk products, eggs.
B3	Niacin (nicotinic acid, nicotinamide, nicotinamide riboside, nicotinamide mononucleotide)	NAD <sup>+</sup> , NADP <sup>+</sup>	RI 1.6 mg NE <sup>3</sup> /MJ/ day	Liver, meat, and meat products, fish, peanuts, coffee, and whole grains. Also, in protein-rich foods, such as milk, cheese and eggs (good source of tryptophan = 60 NE)).
B5	Panthothenate	Coenzyme A (CoA)	AI 5 mg/day	Meat products, bread, milk-based products, eggs, nuts and vegetables.
B6	Pyridoxal, pyridoxol or pyridoxamine	Pyridoxalphosphate	RI 1.6-1.7 mg/day	Grains, legumes, nuts, seeds, potatoes, some herbs and spices, meat and meat products, fish.
B8/B7	Biotin	Biotin	AI 40 µg/day	Especially in liver and eggs, but also in mushrooms and some cheeses. Lower amounts in lean meat, fruit, cereals, and bread.
B11/B9	Folate	MTHF, BH4 and others	RI 330 µg DFE <sup>4</sup> /day	Dark green leafy vegetables, legumes, orange, grapefruit, peanuts, and almonds, but also in liver, kidney, and yeast.
B12	Cobalamin	Deoxyadenosylcobalamin, Methylcobalamin	AI 4 µg/day	Meat, liver, milk, eggs.

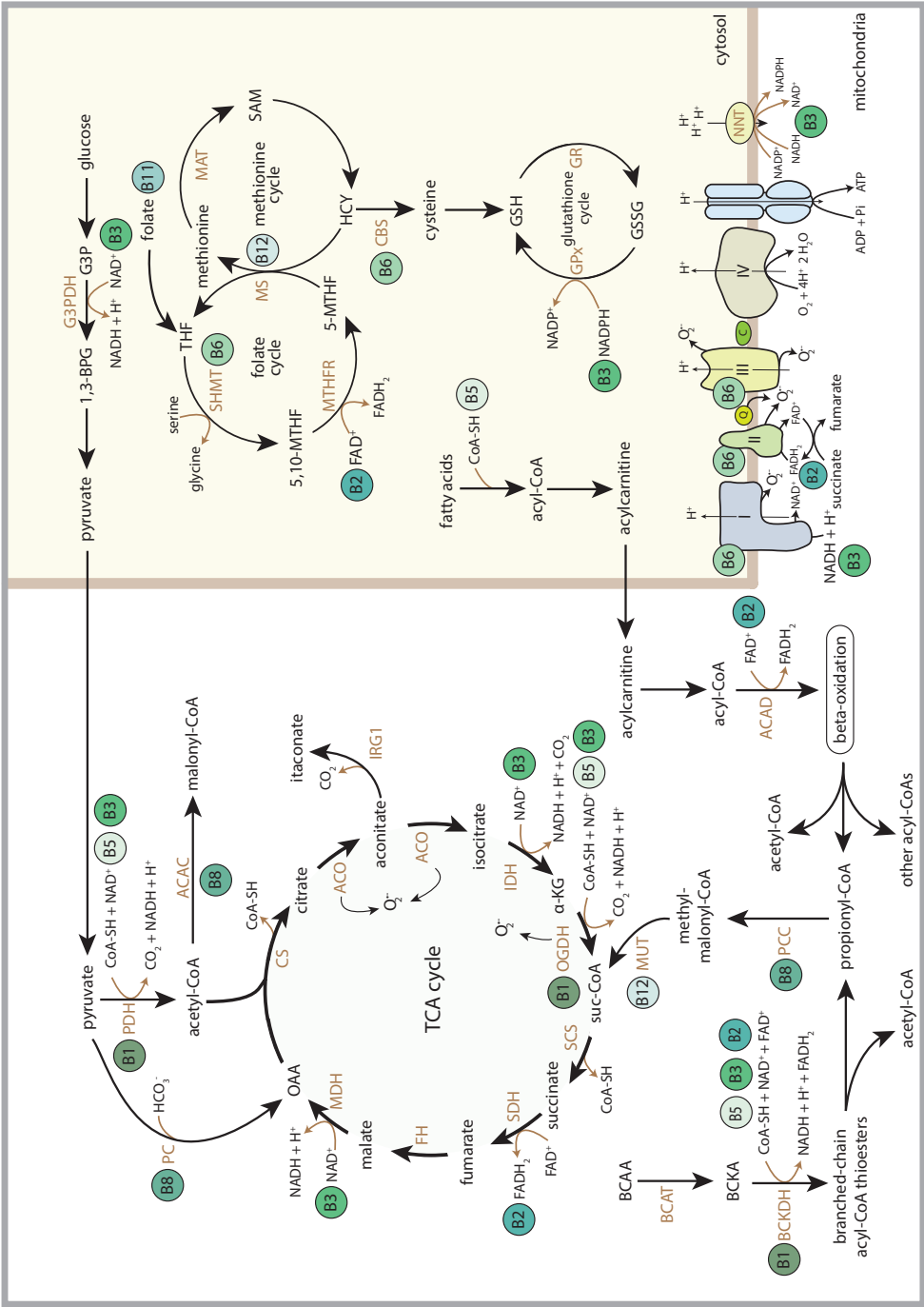


**Figure 2: Schematic overview of the regulatory role of B-vitamins in mitochondrial and cytosolic metabolic reactions.** Abbreviations: FAD = flavin adenine dinucleotide, FADH<sub>2</sub> = hydroquinone form of FAD, NAD<sup>+</sup> = nicotinamide adenine dinucleotide, NADH = reduced form of NAD<sup>+</sup>, CoA-SH = Coenzyme A, PDH = pyruvate dehydrogenase complex, ACAC = acetyl-CoA carboxylase, CS = citrate synthase, ACO = aconitase, IRG1 = immunoresponsive gene 1, IDH = isocitrate dehydrogenase, α-KG = alpha-ketoglutarate, OGDH = 2-oxoglutarate dehydrogenase complex, suc-CoA = succinyl-CoA, SCS = succinyl coenzyme A synthetase, SDH = succinate dehydrogenase, FH = fumarate hydratase, MDH = malate dehydrogenase, OAA = oxaloacetate, BCAA = branched-chain amino acids, BCAT = branched-chain amino acid transaminase, BCKA = branched-chain ketoacids, BCKDH = branched-chain ketoacid dehydrogenase, PCC = propionyl-CoA carboxylase, MUT = methylmalonyl-CoA mutase, ACAD = acyl-CoA dehydrogenase, 1,3-BPG = 1,3-bisphosphoglyceric acid, G3PDH = glyceraldehyde 3-phosphate dehydrogenase, G3p = glyceraldehyde 3-phosphate, THF = tetrahydrofolate, SHMT = serine hydroxymethyltransferase, 5,10-MTHF = 5,10-methylenetetrahydrofolate, MTHFR = methylene tetrahydrofolate reductase, 5-MTHF = 5-methyltetrahydrofolate, MS = methionine synthase, MAT = methionine adenosyltransferase, SAM = S-adenosylmethionine, HCY = homocysteine, CBS = cystathionine-beta-synthase, GSH = glutathione, GSSG = glutathione disulphide, GPx = glutathione peroxidase, GR = glutathione reductase, Q = coenzyme Q, C = cytochrome C, NNT = nicotinamide nucleotide transhydrogenase, OMM = outer mitochondrial membrane, IMM = inner mitochondrial membrane.

This retrograde signaling from mitochondria to the nucleus is called mito-nuclear communication and allows mitochondria to regulate multiple cellular processes, including cell cycle decisions, cell signaling and epigenetic regulation (5,6). Dysregulation of the interplay between mitochondrial metabolites and the nucleus has been established to play a direct role in aging and several disease pathologies (7), including cancer (6,8), inflammation (9), and ischemia/reperfusion (I/R) events (10). Although B-vitamins have direct effects on mitochondrial function, the role of B-vitamins in mito-nuclear communication has been poorly described. Understanding the role of B-vitamins can be relevant for designing novel therapeutic applications or developing new studies that focus on dietary lifestyle changes. Here, we will outline the role of B-vitamins in mitochondrial function, highlight the emerging concepts in the communication between mitochondrial metabolites and the nucleus and identify how B-vitamins can regulate mito-nuclear communication.

## Regulation of mitochondrial metabolism by B-vitamins

### Vitamin B1 – thiamine-diphosphate

Vitamin B1 (thiamine) is highly enriched within the mitochondria, as they contain more than 90% of all cellular thiamine ( $\sim 30 \mu\text{M}$ ) (19). The active form of thiamine, thiamine-diphosphate, is an essential cofactor of multiple mitochondrial dehydrogenase complexes, including the pyruvate dehydrogenase (PDH) complex, the alpha-ketoglutarate (alpha-KG) dehydrogenase (OGDH) complex and branched-chain keto-acid dehydrogenase complex (BCKDH) (Figure 2). Recent analyses also showed that thiamine and its derivatives can allosterically regulate malate dehydrogenase and glutamate dehydrogenase, both involved in the malate-aspartate shuttle, thereby decreasing the efflux of citrate from the mitochondria and increasing citrate flux through the TCA cycle (20).

### Vitamin B2 – FAD and FMN

Vitamin B2 (riboflavin) exists in two bioactive forms, flavin adenine dinucleotide (FAD) and flavin mononucleotide (FMN). Riboflavin is first phosphorylated by riboflavin kinase, generating FMN, which can be further converted into FAD by FAD synthase (FADS) that subsequently transfers an adenosine monophosphate (AMP) unit from ATP to FMN. By acting as electron carriers, FAD and FMN comprise the essential prosthetic groups in flavoproteins. About 90 flavoproteins are identified in humans (21), the majority harboring FAD. They are mainly located in the mitochondria and catalyze a variety of redox reactions, including oxidation, reduction and dehydrogenase reactions (Figure 2). For example, mitochondrial acyl-CoA dehydrogenases, which perform the first step in fatty acid beta-

oxidation, compromise a large group of FAD-dependent flavoproteins. Riboflavin also supports the redox reactions catalyzed by succinate dehydrogenase (SDH) and glutathione reductase (GR) by supplying FAD. Reduction of FAD to FADH<sub>2</sub> is an intermediary step in the oxidation of succinate to fumarate by SDH. Reduction of oxidized glutathione (GSSG) to 2 molecules of glutathione (GSH) by FAD-dependent GR utilizes the reduction of FAD to FADH<sub>2</sub> as an intermediate step, which is also coupled to the reduction of NADPH to NADP<sup>+</sup>. In this way, riboflavin supports anti-oxidant defense mechanisms by serving GSH metabolism (22), but riboflavin is also proposed to act as an anti-oxidant by its own oxidation (23). Riboflavin also supports NADPH-dependent biliverdin reductase B (BLVRB) (24), which is involved in protection against I/R oxidative injuries (22,25).

### Vitamin B3 – NAD<sup>+</sup> and NADP<sup>+</sup>

Vitamin B3 is also referred to as niacin, which comprises the various dietary forms of vitamin B3, nicotinic acid (NA), nicotinamide (NAM), as well as the recently recognized nicotinamide riboside (NR), and nicotinamide mononucleotide (NMN) (26). These forms have different bioactivation routes towards NAD<sup>+</sup>. In addition, NAD<sup>+</sup> can also be synthesized *de novo* from the essential amino acid tryptophan in a ratio of approximately one to 60, meaning that sixty times as much milligrams of tryptophan is needed to generate each gram of NAD<sup>+</sup>, than is generated from each milligram of vitamin B3. As a coenzyme, NAD<sup>+</sup> is principally used as an electron acceptor (Figure 2) (27). Furthermore, NAD<sup>+</sup> can be converted in a second, distinct cofactor form, NADP<sup>+</sup>, with a principal role in lipid metabolism and redox homeostasis. NAD<sup>+</sup> is reduced to NADH by two electrons that are donated mostly by catabolic intermediates in mitochondrial substrate oxidation, especially in the TCA cycle. NADH is primarily used to feed electrons to the electron transport system (ETS) and to provide reduction equivalents to regenerate redox systems, including NADPH. Nicotinamide nucleotide transhydrogenase (NNT) catalyzes NADPH generation from NADH in a proton gradient dependent manner (28). NADPH can also be generated from other sources, including the pentose phosphate pathway, the serine synthesis pathway and glutamate dehydrogenase (29,30).

Apart from mediating mitochondrial metabolic signals via the electron carrier properties, especially NAD<sup>+</sup> is also a direct regulator of protein post-translational acylation and ADP-ribosylation modifications (31). NAD<sup>+</sup> is a co-substrate for three protein modifying enzyme families; the NAD-dependent deacylases (sirtuins, SIRT), poly-ADP ribosylation polymerases (PARPs) and mono-ADP ribosyltransferases (ARTs) (32,33). For each protein modification catalyzed by these enzymes, one NAD<sup>+</sup> molecule is consumed. Recent studies demonstrated that these reactions

account for the use of two-thirds of the total cellular pool of  $\text{NAD}^+$  (34), highlighting the importance of  $\text{NAD}^+$  as precursor for protein modifications in the cell.

### Vitamin B5 – Coenzyme A

Vitamin B5 (pantothenate) is the precursor for biosynthesis of Coenzyme A (CoA). Lipmann et al. (35) were the first to describe CoA as a coenzyme that transfers acyl groups and functions as a carrier of acyl moieties (35). In addition to its role in acyl transferase reactions (**Figure 2**) (36,37), CoA is the balancing factor between carbohydrate and lipid metabolism during glucose oxidation in the TCA cycle vs. fatty acid oxidation (38), and it is a required cofactor for the biosynthesis of ketone bodies (39,40). These metabolic functions explain why CoA is predominantly present in the mitochondria (2.2 mM), with less occurrence in the peroxisomes (20 – 140  $\mu\text{M}$ ) and to some extent in the cytoplasm (less than 15  $\mu\text{M}$ ) (41).

### Vitamin B6 – pyridoxalphosphate

The active form of vitamin B6 (pyridoxalphosphate) is generated by distinct modification pathways that depend on the form of vitamin B6 (pyridoxal, pyridoxol or pyridoxamine) that is available. Pyridoxalphosphate plays a major role in energy metabolism, but is particularly involved in amino acid metabolism, *de novo*  $\text{NAD}^+$  and FeS biosynthesis, and by functioning as a cofactor for several aminotransferases and decarboxylases (**Figure 2**) (2,42). FeS clusters are integral parts of many metabolic protein complexes, such as aconitase and ETS complexes, as well as other cellular protein complexes, such as DNA polymerases and helicases (42). Furthermore, pyridoxalphosphate is the essential coenzyme for mitochondrial aminolevulinate synthase, which is essential for synthesis of heme (43).

### Vitamin B8/B7 - biotin

Vitamin B8/B7 (biotin) is used in organisms without further chemical or enzymatic modification. The cellular localization of biotin is consistent with its function, with enriched fractions in the mitochondria and cytosol (44). Biotin acts as an essential coenzyme for five carboxylases from which four are located within the mitochondria (**Figure 2**). These carboxylases are carboxyl transferases that catalyze the addition of a carboxylic acid group to an organic compound, a reaction that utilizes  $\text{CO}_2$ . Pyruvate carboxylase (PC) converts pyruvate into oxaloacetate (OAA) and functions to resupply the TCA cycle, but also in the initial step of gluconeogenesis (in liver and kidney) and lipogenesis (in adipose tissue, liver, brain). Propionyl-CoA carboxylase (PCC) converts propionyl-CoA to methylmalonyl-CoA with a key role in the catabolism of amino acids (isoleucine, valine, methionine and threonine) and odd-chain fatty acids. Methylcrotonyl-CoA carboxylase (MCCC) converts 3-methylcrotonyl-CoA to 3-methylglutaconyl-CoA, thus having a critical step in leucine

and isovaleric acid catabolism. Acetyl-CoA carboxylase B (ACACB) is a biotin carboxyl carrier protein and can function as a biotin carboxylase and carboxyl-transferase. As carboxyltransferase, it catalyzes the ATP-dependent carboxylation of acetyl-CoA to malonyl-CoA. It is localized in the mitochondrial outer membrane and associates with carnitine palmitoyltransferase 1 (CPT1) allowing it to perform its decisive role in channeling acetyl-CoA towards either lipid synthesis in the cytosol or mitochondrial beta-oxidation. Cytoplasmic biotin containing acetyl-CoA carboxylase (ACACA) has similar metabolic functions and has a key role in long-chain fatty acid biosynthesis.

### Vitamin B11/B9 – folate, methyltetrahydrofolate, and others

Folate is the generic name for various different forms of this vitamin, also being referred to as vitamin B11 or B9. Several key steps of folate metabolism occur in mitochondria, and 30 – 50% of all cellular folate is located within the mitochondria (45,46). Similar to vitamin B3 metabolism, folate metabolism is highly complex, especially because of the wide variety of reactions in which folate is involved (2,47,48). Folate in its various cofactor forms is essential for the synthesis of ADP and GDP, synthesis of purines and thymidylate, providing the methylation donor S-adenosylmethionine (SAM), for cellular GSH metabolism, and for amino acid metabolism, with methionine recycling occurring in the cytoplasm and serine-glycine interconversion taking place in mitochondria (Figure 2) (49,50). The methionine derivative SAM supports more than 100 transmethylation reactions by acting as a universal methyl donor.

### Vitamin B12 – deoxyadenosylcobalamin and methylcobalamin

Vitamin B12 (cobalamin) is structurally the most complex and largest B-vitamin and is required as a coenzyme in both the mitochondria and cytosol. Deoxyadenosylcobalamin is the essential cofactor of methylmalonyl-Coenzyme A mutase (MUT) in mitochondria, which converts methylmalonyl-CoA into succinyl-CoA, and has a role in the degradation of the amino acids and odd-chain fatty acid, just like PCC (Figure 2). Adenosylcobalamin was shown to support the catabolism of branched-chain amino acids (BCAAs) that are utilized for fatty acid synthesis in differentiating adipocytes (51). Adenosylcobalamin deficiency also resulted in accumulation of methyl-malonic acid (MMA), methylmalonyl-CoA, and odd-chain fatty acids, indicating that cobalamin is crucial for MUT function (51). Methylcobalamin is the cofactor for cytosolic 5-methyltetrahydrofolate-homocysteine methyltransferase (MTR), also known as methionine synthase (MS), which catalyzes the transmethylation of homocysteine by methyltetrahydrofolate (MTHF) to methionine (Figure 2) (52,53). The other product of the MS reaction is THF, the fully reduced form of folate, making folate metabolism critically dependent on sufficient availability of

methylcobalamin (54). Furthermore, by acting as coenzyme for MS, methylcobalamin contributes to the synthesis of GSH (55).

## Regulation of mito-nuclear communication by B-vitamins

In the different mitochondrial reactions that are supported by B-vitamins, a diverse array of metabolites are generated. These metabolites are not only drivers of cellular metabolism and respiration, they can also forward metabolic signals to the nucleus. In this way, they maintain metabolic homeostasis, but also facilitate the cell to dynamically respond to environmental stress signals, like nutrient deprivation and oxidative stress (4). Mitochondrial metabolites that perform key signaling roles in mito-nuclear communication are generated in the TCA cycle, in fatty acid and amino acid oxidation pathways, as well as in the ETS. Their signaling roles center mainly around 1) regulating cytosolic and nuclear dioxygenases, hydroxylases and NAD-dependent deacylases, 2) functioning as substrate or precursor for protein post-translational modification (PTM), and 3) acting as electron donor or acceptor for redox reactions. B-vitamins alter the levels of mitochondrial signaling metabolites, and consequently impact their mito-nuclear signaling roles.

Below, we will describe four mito-nuclear communication pathways involving mitochondrial metabolites, and highlight the impact of B-vitamins on these pathways. Firstly, hypoxia-inducible factor 1 (HIF1) signaling is regulated by the TCA cycle intermediates alpha-KG, succinate and fumarate via activating or inhibiting HIF1-regulating hydroxylases. Second, the same TCA cycle intermediates also mediate the regulation of dioxygenases involved in methylation status of DNA and histones in the nucleus. Third, acyl-CoA molecules coming from TCA cycle, fatty acid oxidation and amino acid metabolism, are substrates for acylation modifications of histones. Fourth, antioxidant and redox signaling pathways are altered by TCA cycle intermediates as well as mitochondrial-derived reactive oxygen species (ROS).

### HIF1 signaling

Hypoxia-inducible factor 1 (HIF1) signaling mediates the physiological response to hypoxia. Dimerization of hypoxia-inducible factor 1 alpha (HIF1A) with the aryl hydrocarbon receptor nuclear translocator, ARNT (HIF1B), allows the transcription factor to bind to the hypoxia responsive elements (HRE) in a variety of genes that orchestrate adaptation to hypoxia and restoration of oxygen supply (56) (Figure 3). HIF mediated transcription is dependent on the binding of the co-activators

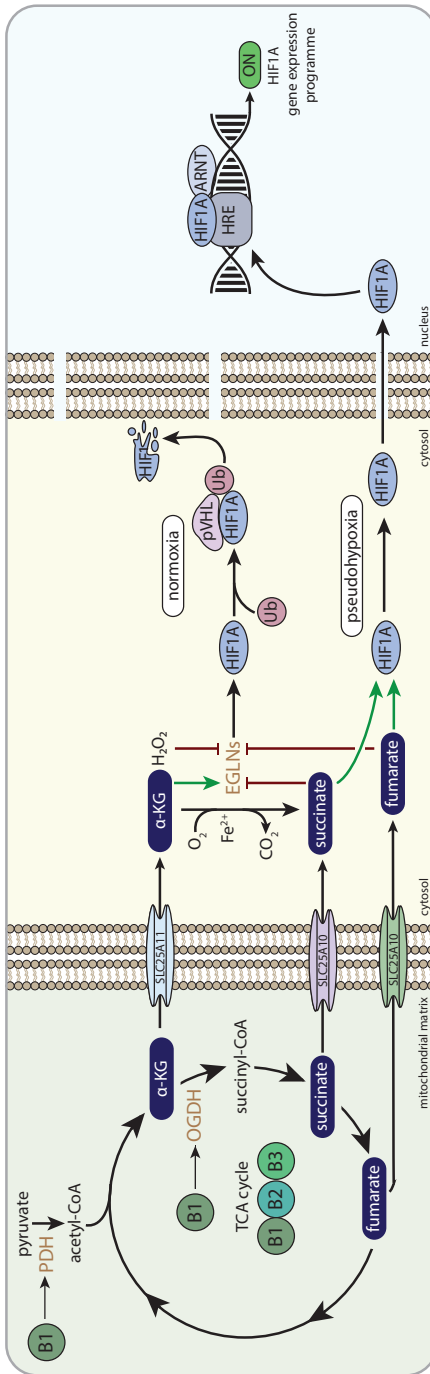


**Figure 3: B-vitamins and HIF1-related mito-nuclear signaling.** Abbreviations: PDH = pyruvate dehydrogenase complex,  $\alpha$ -KG = alpha-ketoglutarate, OGDH = 2-oxoglutarate dehydrogenase complex, SLC25A11 = mitochondrial 2-oxoglutarate/malate carrier protein, SLC25A10 = mitochondrial dicarboxylate carrier, EGLNs = egg-laying-defective nine family or HIF prolyl hydroxylases, Ub = ubiquitin E3 ligase, pVHL = von Hippel–Lindau protein, HIF1A = hypoxia-inducible factor 1 alpha, ARNT = aryl hydrocarbon receptor nuclear translocator, HRE = hypoxia response element, OMM = outer mitochondrial membrane, IMM = inner mitochondrial membrane.

EP300 (E1A binding protein p300) and Creb binding protein (CREBBP). Apart from regulating cellular metabolic pathways in response to hypoxia, HIF1 also regulates red blood cell biosynthesis, iron metabolism and the formation of new blood vessels by coordinating the expression of angiogenic growth factors. In this way it plays a crucial role in regulating the response to hypoxia (57) as well as vascularization of the developing embryo (58). Dysregulation of the HIF1 signaling pathway occurs in multiple pathologies. Cancer cells benefit from altered control of the HIF1 signaling pathway (59), HIF1 is often associated with acute or chronic inflammatory disorders (60), and HIF1 plays a role in the pathology of insulin resistance as well as non-alcoholic fatty liver disease (61).

The oxygen-sensitive HIF1A subunit is regulated by the Egl-Nine (EGLN, also called PHD) prolyl hydroxylase enzymes. EGLNs are part of a large Fe(II)/ $\alpha$ -KG dependent dioxygenase family, that also consists of the ten-eleven translocation (TET) dioxygenases and the Jumonji C-domain-containing histone lysine demethylases (JmJ-KDM). EGLN catalyzes the hydroxylation of prolyl residues on HIF1A, which allows the interaction with von Hippel-Lindau protein (pVHL) that is part of a multimeric protein complex that contains ubiquitin E3 ligase activity. Ubiquitination by the pVHL complex promotes the degradation of HIF1A when normal oxygen levels are present (**Figure 3**) (56). In low oxygen levels (i.e., hypoxia), HIF1A escapes proteosomal degradation, because EGLN cannot hydroxylate HIF1A, which allows HIF1A to bind to ARNT and translocate to the nucleus. Here, the functional HIF1 complex is fully assembled, thereby promoting the expression of multiple genes involved in cellular survival during hypoxia (**Figure 3**) (56,62,63). Assembly of the functional HIF1 complex in the nucleus, i.e., the binding to EP3000 and CREBBP, is also dependent on the absence of HIF asparaginyl hydroxylation by HIF1AN (hypoxia-inducible factor 1,  $\alpha$  subunit inhibitor; also called FIH). Similar to EGLN, HIF1AN is dependent on oxygen, Fe(II), ascorbate and  $\alpha$ -KG (64). EGLNs and HIF1AN use the TCA cycle intermediate  $\alpha$ -KG as co-substrate to catalyze their Fe(II)-dependent hydroxylation reaction (**Figure 3**). One oxygen atom of  $O_2$  is donated to  $CO_2$  when  $\alpha$ -KG is converted to succinate, whereas the other oxygen of  $O_2$  is used for the hydroxylation of the proline residues (63). The direct involvement of  $\alpha$ -KG in the EGLN and HIF1AN reaction connects mitochondrial-derived  $\alpha$ -KG directly to HIF1 signaling. Moreover, both succinate and fumarate have been shown to interfere with the  $\alpha$ -KG dependent EGLN reaction (65–67), whereas citrate was shown to interfere with HIF1AN and EGLN *in vitro* as well (65,68). This links multiple TCA cycle metabolites other than  $\alpha$ -KG to HIF1 signaling. In normal cell physiology it was shown that  $\alpha$ -KG was needed and could be limiting for activation of EGLNs upon reoxygenation after anoxic culturing conditions (66). When cells were cultured in low nutrient

conditions and oxygen deprivation, the EGLN co-substrate alpha-KG was low, whereas the EGLN inhibitor fumarate was normal, indicating that limiting alpha-KG levels could prevent EGLN activation upon reoxygenation and thus prevent the proteasomal breakdown of HIF1 (66).

Since HIF1 signaling is often found to be upregulated in tumors and mutations in the pVHL gene are causing the hereditary cancer syndrome, von Hippel-Lindau disease, HIF1 signaling is studied extensively in the context of cancer (59). The TCA cycle metabolites fumarate and succinate are now known to be able to behave as oncometabolites in cancers. Oncometabolites have been defined as small molecule components of normal metabolism whose accumulation causes cellular dysregulation and consequently primes cells allowing future progression to cancer (69). Since oncometabolites are structurally similar to alpha-KG, they can activate tumorigenic pathways by acting as competitive inhibitors of Fe(II)/alpha-KG-dependent EGLNs, as well as other dioxygenases, to interfere with HIF1 signaling, finally contributing to tumorigenesis (70). Many studies have demonstrated that succinate and fumarate promote tumorigenesis by stabilizing HIF1A via EGLN inhibition (**Figure 3**) (65,71–76), although succinate was also found to alter EGLN activity via a HIF-independent mechanism (77).

In addition to several cancer pathologies, succinate-induced HIF1A stabilization has been demonstrated to play a role in inflammation (78–80) and rheumatoid arthritis (81,82). Activation of macrophages with lipopolysaccharide (LPS) impaired SDH function, thereby boosting the levels of succinate (78), and inducing HIF1-mediated secretion of pro-inflammatory interleukin (IL)1 $\beta$  (78,80). In an *in vivo* model of rheumatoid arthritis, transforming growth factor  $\beta$  (TGF- $\beta$ ) induction also resulted in accumulating succinate levels, which were found to activate the NLRP3 inflammasome in a HIF1A-dependent manner (81). The same authors recently demonstrated that succinate also boosted HIF1A-mediated vascular endothelial growth factor production and angiogenesis (82).

### B-vitamin regulation of HIF1 signaling

Multiple B-vitamins maintain mitochondrial function. Therefore, alterations in the TCA cycle intermediates alpha-KG, succinate and fumarate caused by alterations in B-vitamin levels, likely impact HIF1 signaling through the alpha-KG-dependent EGLNs. Indeed, dysregulation of mitochondrial NAD<sup>+</sup> metabolism by knockdown of the NNT gene in cells, caused accumulation of alpha-KG relative to succinate levels, which lowered HIF1A stability and HIF1A target gene expression (83). HIF1A could be stabilized again by addition of dimethylsuccinate, a cell permeable form of succinate (83). Vitamin B3 supplementation (in the form of NMN) was able to

rescue a pseudo-hypoxic state, characterized by HIF1A stability in muscle during normoxia, that was induced by aging in mice (84). NMN supplementation failed to rescue pseudo-hypoxia in EGLN knockout (KO) mice as well as in SIRT1 KO mice (84), implying either a direct role of NAD<sup>+</sup> availability on SIRT1 activity and HIF1 signaling or an indirect role via regulation of TCA cycle metabolites. This also shows that alterations in TCA cycle metabolites by NMN supplementation could directly impact EGLN activity and thus HIF1 stability. Furthermore, in a glaucoma mouse model, mitochondrial aberrations and low NAD<sup>+</sup> were observed in retina with increasing age, which made mice more vulnerable to high intra-ocular pressure which is an important risk factor for glaucoma (85). Increasing NAD<sup>+</sup> levels by administering vitamin B3 (in the form of nicotinamide), prevented the mice from developing glaucoma. Interestingly, levels of HIF1 were observed to be increased in glaucoma mice, and expression of HIF1 was decreased by vitamin B3 administration (85).

Nicotinamide has also been shown to have a protective role in I/R events. Nicotinamide administration to rats before an experimentally induced ischemic event in the brain, lowered infarct volume, which was attributed to elevated NAD<sup>+</sup> levels in specific brain areas (86). Also, NMN, administered during reperfusion after an ischemic event in mice, reduced hippocampal injury significantly by increasing brain NAD<sup>+</sup> levels (87). Although the mechanisms behind the effects of vitamins or NAD<sup>+</sup> on I/R are not completely clear, both ROS signaling and TCA cycle metabolite signaling to HIF1 could play a role. Activation of HIF1A is generally considered to be protective in I/R, but sustained HIF1A expression could also be detrimental in the long-term (88). Ischemic preconditioning of the heart protects the heart from experimental, otherwise lethal, ischemic events. Mitochondrial ROS generation and stabilization of HIF1A were shown to play a role in the protective effect of ischemic preconditioning (89).

Vitamin B2 generates the necessary FAD for complex (C) II (SDH) to function in the mitochondrial ETS. Mutations in SDH can either cause a hereditary form of cancer or results in a genetic mitochondrial respiratory chain defect, clinically characterized by a mitochondrial encephalomyopathy (90). In fibroblasts derived from patients with a clinical CII deficiency, due to mutations in a SDH assembly protein (SDH assembly factor 1, SDHAF1), HIF1A expression was increased, likely because of accumulation of succinate, that would competitively inhibit EGLNs (91). Interestingly, vitamin B2 supplementation lowered succinate levels, by stabilizing the SDH complex, which concomitantly lowered HIF1A expression (91). This is in line with clinical data showing that patients with SDHAF1 mutations responded positively to oral riboflavin therapy (92), and highlighting that increasing mitochondrial vitamin B2 impacts HIF1 signaling.

Apart from regulating (pseudo)hypoxia by TCA cycle intermediates, also pyruvate and lactate have been shown to induce a pseudo-hypoxic state. Pyruvate has been suggested to bind to EGLNs catalytic site, thereby inhibiting EGLN activity and stabilizing HIF1A (93). Since vitamin B1 (thiamine) is essential for enzymatic activity of PDH and OGDH, thiamine deficiency decreases the activities of both PDH and OGDH (**Figure 3**), which is clinically characterized by increased plasma levels of pyruvate and lactate (94–98). The elevated pyruvate levels observed in B1 deficiency could impact HIF1 signaling. Although increased levels of alpha-KG are expected to induce HIF1A degradation and would thus have opposite effects on HIF1A signaling compared to above described effect, the consequences of increased alpha-KG levels, as reported in thiamine deficiency (99), on alpha-KG-induced nuclear signaling pathways, have not been studied in detail.

Combined, multiple studies point to a role of B-vitamins in regulating HIF1 signaling, but the mechanisms are not sufficiently understood yet. It is likely that B-vitamins could alter the dynamic interplay between TCA cycle metabolites, ROS as well as other metabolites that have been shown to interfere with EGLN activities, which will result in B-vitamin mediated control over the HIF1 signaling pathway.

### Histone and DNA methylation regulation

Apart from regulation of HIF1 signaling by the B-vitamins, other mito-nuclear signaling pathways are also targeted by the B-vitamins. Dioxygenases similar to the EGLN prolyl hydroxylases, regulate demethylation of DNA and histones. The TET dioxygenases catalyze DNA demethylations through 5-methylcytosine (5-mC) hydroxylation (100), and the KDM lysine demethylases catalyze demethylation of histone proteins (101). Again, as is the case for EGLN, these oxidative reactions use O<sub>2</sub> and alpha-KG to generate CO<sub>2</sub> and succinate as co-products, the latter acting also as a competitive inhibitor of the alpha-KG dependent dioxygenases reaction itself (**Figure 4**) (68). Thus, alpha-KG, succinate and fumarate are able to alter the dynamics of DNA and histone methylation through their interaction with TET and KDM demethylation proteins, resulting in the regulation of the epigenetic code and corresponding gene expression programs (102). Several studies have demonstrated that reduced alpha-KG availability drives cancer and stem cell development by lowering dioxygenase activities. For example, reduced levels of alpha-KG due to BCAA transaminase 1 (BCAT1) overexpression in acute myeloid leukemia (AML) cells were found to inhibit TET demethylase activity, thereby inducing DNA hypermethylation, which promoted AML cell survival and lead to decreased clinical outcome (103). Furthermore, exogenous alpha-KG supplementation was found to restore the reduced levels of alpha-KG, increase TET demethylase activity and normalize

methylation patterns that were observed to be hypermethylated in cardiac mesenchymal stem cell (CMSCs) from diabetic individuals (104). Importantly, the functional and clinical outcomes of alpha-KG-induced epigenetic modifications on stem cells have been shown to differ between species and cell types, indicating that the consequences of alpha-KG-induced epigenetic modifications are dependent on its context. alpha-KG supplementation induced maintenance of pluripotency in mouse naive embryonic stem cells (ESC) by upregulating TET and KDM enzymatic activities (105), whereas alpha-KG supplementation was shown to promote differentiation in primed human ESC (106).

Both fumarate and succinate compete with alpha-KG for the binding pocket of the Fe(II)/alpha-KG dependent dioxygenases, including TET and KDM demethylases, thereby altering the epigenetic landscape of several mammalian cells (**Figure 4**). Succinate-induced inhibition of KDMs and TETs was shown to initiate histone and DNA hypermethylation, which had large effects on the expression of genes that regulate cancer cell progression (107–110) and the induction of epithelial-to-mesenchymal transition (EMT) (111). In a similar fashion, accumulating fumarate induced hypermethylation of a class of anti-metastatic miRNAs (miR-200) in fumarate hydratase (FH)-deficient renal cancer cells (112). Whereas miR-200 normally suppressed transcription factors that mediate EMT initiation (113), fumarate-induced hypermethylation of miR-200 prevented this suppression and activated the EMT (112). Combined, mitochondrial-derived alpha-KG, fumarate and succinate have been shown in cancer cells and stem cells to drive the nuclear epigenetic landscape.

### B-vitamin regulation of histone and DNA methylation

Vitamin B2, in the form of FAD, is a co-factor for the lysine demethylase, KDM1, which is an alpha-KG-independent histone demethylase with amine oxidase activity (114). KDM1 lysine demethylases are involved in demethylation of H3K4 and H3K9, which are associated with transcriptional repression and activation, respectively (114,115). One of these KDM1 family members, the lysine demethylase (KDM1A or lysine-specific histone demethylase 1A (LSD1)), is particularly sensitive to FAD availability (**Figure 4**) (116–118). FAD availability was found to alter histone methylation in adipocytes (116). Silencing of riboflavin kinase and FADS inhibited KDM1A demethylase activity, resulting in increased methylation of histones and loss of repression of genes related to energy expenditure and ultimately to increased mitochondrial respiration and the induction of lipolysis (116). Impaired KDM1A demethylase activity due to vitamin B2 deficiency was also found to skew immune cells towards a pro-inflammatory phenotype (118). Vitamin B2 deficiency resulted in an increased methylation of histones on genes encoding pro-inflam-

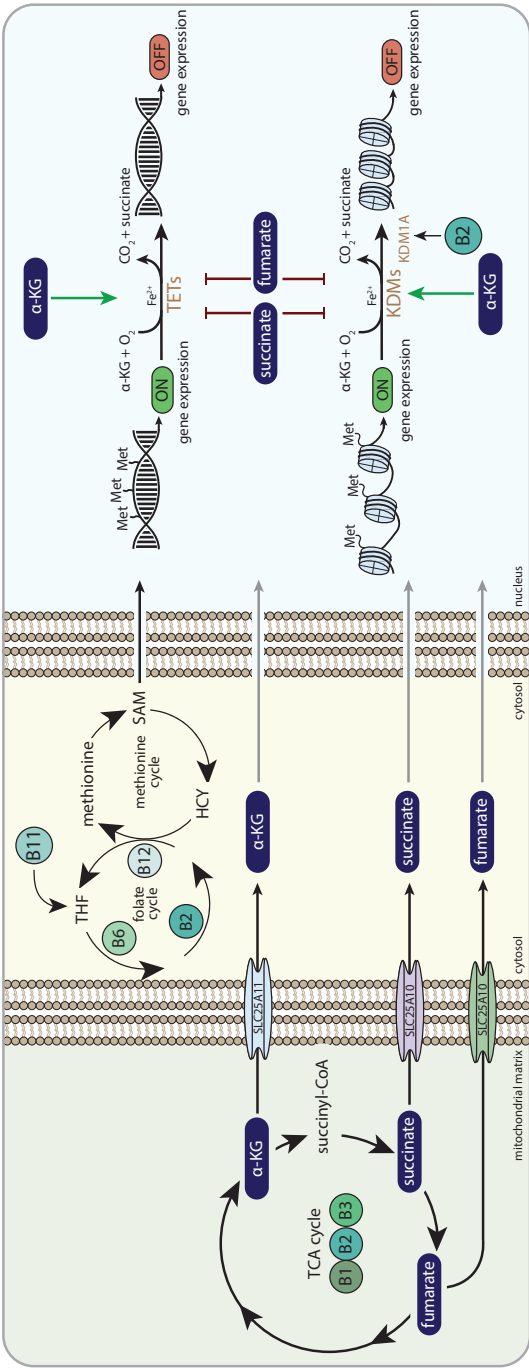


**Figure 4: B-vitamins and DNA and histone methylation.** Abbreviations: α-KG = alpha-ketoglutarate, SLC25A11 = mitochondrial 2-oxoglutarate/malate carrier protein, SLC25A10 = mitochondrial dicarboxylate carrier, THF = tetrahydrofolate, HCY = homocysteine, SAM = S-adenosylmethionine, Met = methyl-group (CH<sub>3</sub>), TETs = ten-eleven translocation family of DNA demethylases, KDMs = histone lysine demethylase family, KDM1A = histone lysine demethylase family 1A (LSD1), OMM = outer mitochondrial membrane, IMM = inner mitochondrial membrane.

matory cytokines, like tumor necrosis factor-alpha and IL-1bèta, highlighting a role for vitamin B2 deficiency in immune signaling (118).

Methylation of histones and DNA requires methyl-donors. The B-vitamins, B2, B6, B11 (folate) and B12 (cobalamin), are necessary to produce the methyl donor SAM from pathways that drive one-carbon metabolism (**Figure 4**). The folate and methionine cycle consist of a complex set of reactions operating in both the mitochondria and the cytosol. Mitochondria-derived serine is the major precursor for the methionine that forms SAM (119). SAM is a substrate for nuclear histone and DNA methylase enzymes that transfer the methyl group of SAM to histone lysines or DNA cytosines. Vitamin B11 (folate) deficiency leads to neural tube defects, which can be attributed to impaired DNA synthesis, but has also been shown to be associated with alterations in the methylation landscape during embryonic development of the brain (120). In adult humans, lowered folate intake was associated with DNA hypomethylation in lymphocytes (121).

In a study using human embryonic stem cells (hESCs), it was shown that nicotinamide-N-methyl transferase (NNMT) expression keeps hESC in a pluripotent state, by consuming methyl donors, lowering SAM levels and concomitantly lowering methylation of H3K27 at specific loci (122). Among the loci affected were the EGLN1 gene as well as genes from the Wnt signaling pathway. Interestingly, the observed mechanism integrates multiple aspects of B-vitamin regulation of mito-nuclear signaling. NNMT not only lowers the availability of the methyl donor SAM, it also lowers the availability of nicotinamide for NAD<sup>+</sup> synthesis. Since NAD<sup>+</sup> availability also impacts histone acylation via SIRT regulation, this could imply that a crosstalk exists between regulation of the synthesis of NAD<sup>+</sup> and SAM, to maintain methylation and acylation epigenetic states in the nucleus. Furthermore, the NNMT mechanism of maintaining pluripotency also demonstrates an interaction between histone methylation status and HIF1 signaling via regulation of the EGLN locus (122). This interaction between nuclear methylation and HIF1 signaling was also demonstrated to occur via FAD (vitamin B2) regulation of KDM1A, where FAD regulated HIF1A stability in a KDM1-dependent fashion in cancer cells (123).

Vitamin B12 (cobalamin) is involved in the methionine cycle through its role as an essential co-factor for the MS protein (**Figure 4**). Maternal cobalamin status has been linked to methylation status at specific loci in the offspring, also a weak association between maternal cobalamin status and child's cognition was observed (124). Furthermore, in a mouse model of reduced cobalamin import into the brain generated by knocking out the CD320 cobalamin receptor, global brain DNA hypomethylation was observed (125,126). Vitamin B6 is mainly shown to

regulate DNA synthesis via its role in one-carbon metabolism (2), but dietary vitamin B6 intake was also shown to be linked to hypermethylation of the MLH1 promotor in colorectal tumors in humans (127).

Similar to the role of the B-vitamins in regulating EGLNs via TCA cycle intermediates in HIF1 signaling, altering TCA cycle intermediates could also impact DNA and histone methylation status via the regulation of the TET and KDM demethylases. Evidence for a direct role of B-vitamins on nuclear methylation via TCA cycle intermediates is lacking. Likely, because both vitamin B1 and vitamin B2 are directly involved in regulating either methyl donor availability or FAD-dependent histone demethylase activity, respectively. However, maintaining TCA cycle function by vitamin B1, B2 and B3 is likely to also play a role in regulating DNA and histone methylation in the nucleus (Figure 4).

### Regulation of histone acylation

Citrate was one of the first mitochondrial metabolites that was shown to serve metabolic, as well as non-metabolic functions outside mitochondria. In the 1950s, it was demonstrated that citrate is not only oxidized for ATP generation in mitochondria, but also stimulates fatty acid synthesis in the cytosol (128,129). Citrate is generated from acetyl-CoA and OAA condensation catalyzed by the mitochondrial enzyme citrate synthase (CS). Mitochondrial-derived citrate can be exported to the cytosol by the citrate carrier (SLC25A1) where citrate can be regenerated to acetyl-CoA and OAA by ATP citrate lyase (ACLY) (Figure 5). Whereas OAA is shuttled back into the mitochondria in the form of malate, citrate-derived acetyl-CoA can subsequently be used to fuel anabolic reactions, such as biosynthesis of fatty acids, amino acids and steroids (36,130).

In addition to serve as an anabolic intermediate and cytosolic signaling molecule, citrate provides a source of nuclear acetyl-CoA for histone acetyltransferase (HAT or lysine acetyltransferase; KAT) activity and promotes acetylation reactions in the nucleus (Figure 5) (131). In histone acetylation, the cleaved acetyl-group from acetyl-CoA is transferred to an  $\epsilon$ -N-lysine residue of histones in chromatin structures to produce  $\epsilon$ -N-acetyllysine residues (132). Histone lysine acetylation plays a pivotal role in nuclear gene expression (133). Addition of negatively charged acetyl-groups neutralizes the positively charged lysine residues on the histone tails. This unlocks the tight interactions between negatively charged DNA and positively charged histones and allows transcription factor binding. Multiple studies have demonstrated that nuclear and cytosolic acetylation is dependent on citrate efflux from the mitochondria, since loss of enzymes that generate, transport or cleave citrate hampers cytosolic acetyl-CoA production and protein

acetylation (131,134–139). For example, ACLY-dependent acetylation was recently found to induce the expression of cell migration and adhesion genes, promoting malignant tumor formation (139). Silencing ACLY was also shown to decrease histone acetylation in several mammalian cell types (131,138), indicating that mitochondrial-derived citrate plays a role in tumorigenesis by indirect alterations in transcriptional programs that dictate cancer cell formation and progression. Acetate-derived acetyl-CoA in the nucleocytoplasmic compartment was found to rescue histone acetylation in ACLY deficient colon cancer cells, also indicating that acetyl-CoA can also be produced from extra-mitochondrial citrate and acetate (131).

Fatty acids are a major source of acetyl-CoA as well as other acyl-CoAs, which form the acyl donors for histone acylation (**Figure 5**). Acyl-CoAs can be generated in different compartments of the cell, and mitochondrial-derived acyl-CoAs have been shown to be a source for histone acylation, allowing for metabolic control of histone acylation and gene transcription by acyl-CoA molecules from inside the mitochondria. Export of acyl-CoAs out of the mitochondria is mediated by reversing parts of the machinery of the carnitine shuttle. Carnitine palmitoyltransferase 2 (CPT2) is able to convert medium and long-chain acyl-CoAs into acylcarnitines (140), whereas an additional enzyme called carnitine acetyl transferase (CRAT) takes care of the conversion of short-chain acyl-CoAs into acylcarnitines (140). Acylcarnitines are likely to be translocated over the mitochondrial inner membrane by carnitine-acylcarnitine translocase (CACT), making them available for the cytosol and the nucleus.

Although histone acetylation is the major contributor to chromatin regulation and is partly regulated by mitochondrial acetyl-CoA levels (141), recent compelling data have shown that histones are modified by a variety of acylation reactions (**Figure 5**) (142). Among them, propionylation, butyrylation, crotonylation, hydroxy-isobutyrylation and succinylation have now been characterized biologically to some extent as well. Propionylation at H3K14 was enriched at transcription start sites and promoters in mouse livers (143). H3K14 propionylation marks overlapped substantially with active H3K9Ac and H3K4me3 marks, providing opportunities for more sophisticated recruitment of transcriptional regulators (143). Interestingly, histone propionylation levels were altered by deleting the mitochondrial propionyl-CoA generating enzyme propionyl-CoA carboxylase, demonstrating that mitochondrial derived propionyl-CoA impacts nuclear histone propionylation (143). In another study, increased H3K14 propionylation induced by elevated propionyl-CoA in nuclear extracts lowered H3K14 acetylation levels (144), highlighting the dynamic interplay between different lysine acylation modifications via acyl-CoA substrate levels.

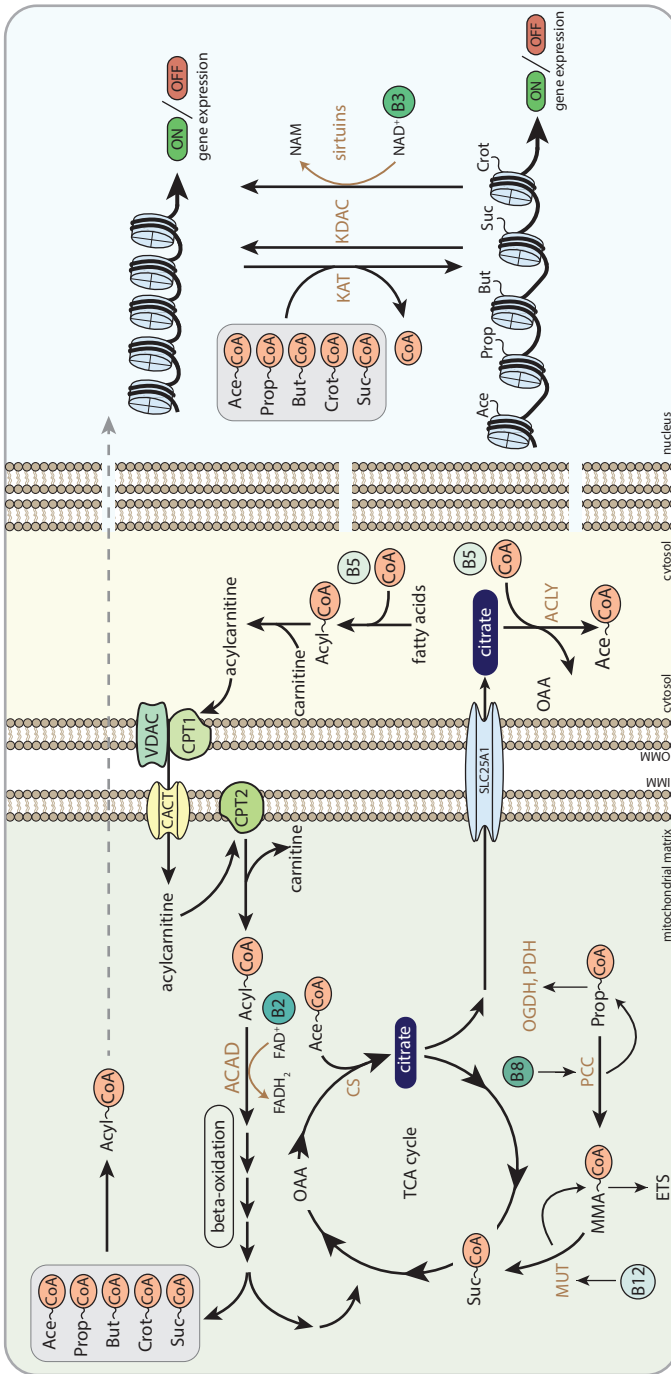


**Figure 5: The role of B-vitamins in Acyl-CoA metabolism and histone acylation.** Acyl-CoA transport from the mitochondria to the nucleus, here depicted as dashed arrow, follows multiple different routes as described in the text. Abbreviations: CoA = Coenzyme A, Ace-CoA = acetyl-CoA, Prop-CoA = propionyl-CoA, But-CoA = butyryl-CoA, Crot-CoA = crotonyl-CoA, Suc-CoA = succinyl-CoA, FAD = flavin adenine dinucleotide, FADH<sub>2</sub> = hydroquinone form of FAD, NAD<sup>+</sup> = nicotinamide adenine dinucleotide, NADH = reduced form of NAD<sup>+</sup>, NAM = nicotinamide, OAA = oxaloacetate, CS = citrate synthase, MUT = methylmalonyl-CoA mutase, MMA-CoA = methylmalonyl-CoA, ETS = electron transfer system, PCC = propionyl-CoA carboxylase, OGDH = 2-oxoglutarate dehydrogenase complex, PDH = pyruvate dehydrogenase complex, SLC25A1 = mitochondrial tricarboxylate transport protein, ACLY = ATP-citrate lyase, ACAD = acyl-CoA dehydrogenase, CPT1 = carnitine palmitoyltransferase 1, CPT2 = carnitine palmitoyltransferase 2, VDAC = voltage-dependent anion channels, CACT = carnitine/acylcarnitine translocase, KAT = lysine acetyltransferase, KDAC = lysine deacetylase, OMM = outer mitochondrial membrane, IMM = inner mitochondrial membrane.

Other histone sites have also been shown to be functionally propionylated. Overexpression of a newly identified propionyltransferase (MOF) increased histone propionylation levels on multiple histone marks, such as H4K16, H4K12, H2Ak5 and H2K9 (145), and H3K23 propionylation levels were lowered upon monocytic differentiation in cultured U937 cells (146). Butyrylation of histones was shown to play a role in dynamically regulating genome organization during spermatogenesis, by mediating Brdt bromodomain binding to histone marks (147). Brdt recognized acetylated H4K5 sites but did not bind to butyrylated sites on the same H3K5 lysines (147), again showing the interplay between different acylations.

Histone crotonylation is different from other short-chain acylation modification in that the crotonyl modification contains an unsaturated bond, making this modification more rigid and thus could exert unique biological functions. Crotonyl-CoA is a mitochondrial fatty acid oxidation intermediate generated in the first step of butyryl-CoA oxidation, which is in turn derived mainly from longer chain fatty acyl-CoAs. Short-chain acyl CoA dehydrogenase (SCAD) catalyzes the reaction making the trans-2-enoyl-CoA from the short-chain fatty acyl-CoA. Moreover, crotonyl-CoA is formed from glutaryl-CoA during tryptophan and lysine degradation by glutaryl-CoA dehydrogenase (GCDH). Although crotonyl-CoA is generally converted by the enoyl-CoA hydratase, crotonase, into 3-hydroxybutyryl-CoA it can also be converted to crotonylcarnitine and/or crotonate. It is likely that mitochondrial crotonyl-CoA can be a source for nuclear histone lysine crotonylation, but it has not been directly established yet. Histone crotonylation was first discovered by the group of Yingming Zhao (142), using sensitive mass spectrometry proteomics techniques and was demonstrated to mark X-linked genes that are post-meiotically expressed in round spermatids (142). In stages of late meiosis during spermatogenesis most of the genes are silenced, but a selection of genes can become activated after meiosis. Mostly the genes associated with the histone crotonylation marks are enriched for escaping chromosome inactivation (142). Again, it has been shown in multiple studies that dynamically regulating the levels of crotonyl-CoA, also regulates the levels of histone crotonylation (148). Incubating cultured cells with high concentrations of short-chain fatty acids, generally increases respective lysine modifications globally in the cell (149,150). In line, incubating RAW264.7 macrophages with crotonate, increased histone crotonylation, and at the same time activated the excretion of cytokines upon LPS stimulation, which differentiates macrophages into a pro-inflammatory state (148). This activation could be turned off when the enzyme that is likely responsible for turning crotonate into crotonyl-CoA (acetyl-CoA synthetase 2, ACS2) was knocked down (148), demonstrating that crotonyl-CoA levels are drivers of the activated gene expression signature in RAW264.7 macrophages. Similar studies have been performed for the

novel histone modification lysine beta-hydroxybutyrylation, where metabolic states of increased beta-hydroxybutyrate were associated with specific increases in histone beta-hydroxybutyrylation marks (151). In an effort to identify novel histone crotonyltransferase enzymes, Liu et al. (152) discovered that the chromodomain protein CDYL lowers histone crotonylation instead of increases it, hinting at a different function for this protein than a histone crotonyltransferase. Intriguingly, the CDYL protein possessed enoyl-CoA hydratase activity, which allowed CDYL to convert crotonyl-CoA into hydroxybutyryl-CoA and thereby lowering the available pool of crotonyl-CoA for histone crotonylation (152). Thus, apart from mitochondrial regulation of acyl-CoA levels, a fine-tuning machinery likely exist inside the nucleus to regulate crotonyl-CoA levels as well as levels of other acyl-CoAs.

Lysine succinylation was first discovered to be primarily a modification that occurs inside the mitochondria (153–155), other studies soon identified lysine succinylation in the cytosol and the nucleus as well (156). The first succinylation on histone peptides in yeast and mammalian cells were discovered by Xie et al. (157) and functional consequences of altering histone lysines with dicarboxylic acid modification, like succinylation, were identified more recently (158,159). H3K122 succinylation was shown to play a role in regulating the DNA-damage response (159). SIRT7, a NAD-dependent deacylase protein from the SIRT family, was identified as histone desuccinylation enzyme (159). SIRT7 was recruited to DNA double-strand breaks, where SIRT7 desuccinylated H3K122, which ultimately promoted DNA damage repair and cell survival (159). SIRT7 has already been shown extensively to have multiple roles in nuclear processes, but it was previously only understood to exert its action by lysine deacetylation, instead of lysine desuccinylation (160).

That mitochondrial alteration of succinate and succinyl-CoA levels could impact nuclear histone succinylation directly, was shown by Smestad et al. (158). Mouse embryonic fibroblasts deficient for SDH accumulated succinate and succinyl-CoA (158). This in turn elevated global lysine succinylation levels and altered histone lysine succinylation distributions (158). Histone succinylation was specifically enriched 600bp from TSS and was abundant at highly expressed genes. Moreover, in line with the observed DNA damage response defect in the SIRT7 deficient cells (159), SDH deficient cells presented with elevated DNA damage, as was shown by analyzing phospho- $\gamma$ H2A.X, making them more sensitive to the genotoxic drugs, etoposide and gemcitabine (158). Although it is currently not precisely known how succinate from the mitochondria is converted into succinyl-CoA in the nucleus, because succinyl-CoA synthetase activities have not been clearly established in nucleocytoplasmic compartments, other succinyl-CoA

generating enzymes are mainly localized in mitochondria and peroxisomes, and succinylcarnitine is not a substrate for nucleo/cytosolic acetyltransferases, this study does highlight the important role of mitochondrial signaling to the nucleus via mitochondrial generated metabolites. An alternative nuclear succinyl-CoA source was shown to be alpha-KG (161). The OGDH complex, which was previously thought to only reside in the mitochondria, was demonstrated to be present in the nucleus of mammalian cells and was bound and recruited by the histone acetyltransferase GCN5 (KAT2A) to histones (161). This mechanism allows for the local production of succinyl-CoA from the mitochondrial-derived metabolite alpha-KG.

### B-vitamin regulation of histone acylation

Already in 1948 it was demonstrated that vitamin B5 (pantothenate) deficiency in rats causes decreased levels of acetylation of p-aminobenzoic acid (PABA) (162), but experimental evidence that vitamin B5 could regulate histone acylation is scarce. In a study using drosophila, histone acetylation has been linked with decreased availability of CoA (163). By interfering with pantothenate kinase activity, either via chemical inhibition or genetic knockdown in drosophila and mammalian cell models, these authors showed that *de novo* CoA biosynthesis is essential to support histone and tubulin acetylation (163). Since other studies have demonstrated that reduced levels of histone and tubulin acetylation are associated with neurodegeneration, it was speculated that at least part of the neurodegeneration observed in pantothenate kinase-associated neurodegeneration (PKAN) might be attributed to altered protein acetylation states that occur as a consequence of impaired CoA metabolism (163). In a follow-up study, addition of extracellular CoA was able to reverse the effects of decreased CoA availability on histone acetylation (164), demonstrating that increasing CoA levels could impact histone acetylation.

Other critical regulators of lysine acylation that are B-vitamin sensitive are the vitamin B3 (NAD<sup>+</sup>)-dependent sirtuins (**Figure 5**), with SIRT3-5 primarily localized in the mitochondria and SIRT1, SIRT2, SIRT6 and SIRT7 primarily localized in the nucleocytoplasmic compartment, although other sirtuins have been proposed to reside in the nucleus as well (165). SIRT1, SIRT6 and SIRT7 have a plethora of nuclear proteins targets, especially those affecting metabolism directly or indirectly (166,167). SIRT1 deacetylates multiple histones directly in a NAD-dependent fashion (168). SIRT1 regulation of histone acetylation could program the epigenetic code and play an important role in chromatin regulation. SIRT1 redistributes to double strand breaks upon DNA damage, promote repair and alter gene expression (169). Interestingly, among its many nuclear targets, SIRT1 also regulates the EP300-acetyltransferase which functions as a general histone acetyltransfer-

ase (168). Also, SIRT6 and SIRT7 are able to deacetylate histone targets making them important regulators of many cellular activities, such as cell proliferation, ribosome biogenesis, metabolic homeostasis, and DNA damage repair (170,171).

Since fatty acid oxidation provides many of the acyl-CoAs needed for histone acylation, B-vitamins involved in regulation of fatty acid oxidation could play a role in regulating acylation in general and histone acylation in specific. Mitochondrial acyl-CoA dehydrogenases, the enzymes that perform the first step in fatty acid beta-oxidation, are flavoproteins that require FAD and thus vitamin B2 (riboflavin) (Figure 5). Levels of multiple acyl-CoA dehydrogenases, mitochondrial CoA pools, as well as the levels of fatty acid derivatives are altered in riboflavin deficiency (172–174). The sensitivity of these metabolic enzymes for FAD deprivation can not only have consequences for mitochondrial lipid metabolism, but are also likely to alter mito-nuclear signaling pathways that are modulated by acyl-CoAs. Using a proteomic approach on livers of Pekin Ducks, Tang et al. (175) identified that especially mitochondrial enzymes involved in lipid metabolism and respiration are sensitive to vitamin B2 deficiency (175), whereas the impact of vitamin B2 deficiency on histone acylation was not studied.

Biotin (vitamin B8/B7) facilitates the metabolic reaction that is catalyzed by propionyl-CoA carboxylase, which converts propionyl-CoA into methylmalonyl-CoA in the mitochondria (Figure 5). Deficiency of biotin leads to elevated levels of mitochondrial CoA intermediates, including 3-methylcrotonyl-CoA and propionyl-CoA (176,177). Accumulating levels of propionyl-CoA can induce mitochondrial toxicity by inhibiting PDH and OGDH and impairing the activity of CIII within the ETS (178) (Figure 5). Although the impact of biotin deficiency on nuclear acylation reactions, such as propionylation, have not been studied so far, alterations in biotin availability are likely to alter cellular protein propionylation levels and could impact the dynamic interplay between multiple acylation reaction on histones, such as histone acetylation and propionylation.

The levels of methylmalonyl-CoA are elevated upon a deficiency in cobalamin (vitamin B12), which is the co-factor for MUT (Figure 5). Cobalamin deficiency is therefore characterized by accumulating levels of MMA in plasma and urine (179). Several studies reported that MMA impairs mitochondrial function by acting as a mitochondrial toxin that inhibits SDH (180,181). Whereas some studies did not find MMA-induced SDH inhibition when MUT was dysfunctional (182), other studies suggested that instead of MMA, alternative metabolites that accumulate upon MUT deficiency (2-methylcitric acid, malonic acid, and propionyl-CoA) synergistically induce mitochondrial dysfunction (183). Other complexes of the ETS were

also reported to be inhibited in MUT deficiency (179,184,185). Interestingly, other new acyl-CoAs were recently also linked to cobalamin and MUT (186). Itaconyl-CoA and citramalyl-CoA both accumulated in cells with a mutation in citrate lyase subunit beta (CLYBL), leading to impaired mitochondrial cobalamin metabolism (186). Mechanistically, itaconyl-CoA and citramalyl-CoA impair MUT activity by poisoning adenosylcobalamin, which cannot be regenerated and induces cobalamin deficiency (186). Again, these acyl-CoAs could also interfere with other more abundant histone acylation marks or could act as novel PTMs on histones, giving that they are able to reach the nucleus. Thus, cobalamin deficiency could affect mito-nuclear communication via regulation of specific acyl-CoA species.

### ROS and redox signaling

ROS are highly reactive biomolecules that are able to react with lipids, DNA and proteins. They are produced as a result of mitochondrial metabolism but also by other enzymes such as NADPH oxidases (Figure 6). Cells also possess powerful anti-oxidant systems to detoxify ROS, and the balance between ROS production and detoxification determines the cellular redox state. It is nowadays known that this cellular redox state plays an important role in cellular (patho)physiology (187). Regulating vascular tonality, enzyme activity, gene expression, cellular proliferation and differentiation are a few physiological examples that can be modulated by ROS (188). Increased ROS production and/or decreased detoxification is linked to aging (189) as well as pathological conditions such as cancer, Alzheimer's disease and diabetes (190–193).

One of the main functions of mitochondria is the production of ATP to drive cellular processes. Mitochondrial ATP generation is ensured by the ETS consisting of 4 multi-protein complexes, which together with the F<sub>1</sub>F<sub>0</sub>-ATP synthase (CV) forms the oxidative phosphorylation (OXPHOS) system (Figure 6). The function of the ETS is to generate an electrochemical gradient over the inner mitochondrial membrane by pumping protons from the matrix to the inter membrane space, which is needed to generate ATP via CV (194). To perform this function, the ETS takes up electrons from NADH at CI or succinate, with FADH<sub>2</sub> as an intermediate, at CII, which are transferred to CIII via ubiquinone (Figure 6). Cytochrome c transfers the electrons from CIII to CIV where they react with oxygen to form water. Most literature states that 0.5 – 2% of the electrons leak out of the ETS and react with oxygen to form ROS (195,196). Superoxide (O<sub>2</sub><sup>-</sup>) and hydrogen peroxide (H<sub>2</sub>O<sub>2</sub>) can be formed at the FMN site in CI (197,198) and CII (199–201) and superoxide is also formed at the quinol-oxidizing site of CI and CIII and the FeS cluster of CIII (Figure 6) (198,202,203). Although ROS production by the ETS is

clearly demonstrated, the ETS is not the only source of ROS in mitochondria. Two other mitochondrial proteins playing an important role in ROS formation are PDH and OGDH, as they both contain a similar flavosubunit that can be a source of superoxide (**Figure 6**) (204–206). Other mitochondrial proteins involved in ROS production are aconitase (207,208), S(n)-glycerol-3-phosphate dehydrogenase dehydrogenase (209), dihydroorotate dehydrogenase (199,210), monoamine oxidases and p66shc/cytochrome-c (211,212). However, how much a protein contributes to the total production of mitochondrial ROS depends on the substrates being used by the mitochondria. Still, in most cases CI, CII, and CIII combined have the highest contribution, varying between 75 – 100% of the total mitochondrial ROS production (213).

To act as a metabolic signal in the nucleus, mitochondrial ROS should travel a certain distance and pass various membranes. Superoxide is negatively charged and is therefore unlikely to pass the (mitochondrial) membranes, although it might use the voltage dependent anion channel to diffuse to the cytoplasm (214). Furthermore, the diffusion capacity of superoxide is affected by superoxide dismutase (SOD) activity, which can reduce the lifetime of superoxide from 100 ms to 35  $\mu$ s (215,216), thereby limiting the traveling distance to 400 nm. Hydrogen peroxide is uncharged and shows physical characteristics similar to water and can therefore freely diffuse through membranes, depending on its form and composition and the presence of aquaporins (217–220). More importantly, many anti-oxidant systems limit the diffusion distance. When taking the cellular concentrations of peroxiredoxin (Prx) 2, glutathione peroxidase (Gpx) 1 and GSH into account, the diffusion distance is estimated to be 4, 6 and 1600  $\mu$ m, respectively (221). Taken together, mitochondrial ROS might not always be able to directly exert nuclear signaling or signaling is limited to perinuclear located mitochondria. Interestingly, it has been proposed that in plant cells, hydrogen peroxide can diffuse over distances up to 10  $\mu$ m at a frequency up to 2 Hz (222), implying that hydrogen peroxide potentially encodes a cellular message depending on amplitude, frequency and localization. The observation that oscillations of the mitochondrial membrane potential are dependent on cellular redox status, suggests that mitochondria could act as relay stations to send out a ROS-mediated message throughout the cell (223). How this eventually is transformed into a cellular response remains unknown.

But how can mitochondria and mitochondrial metabolites affect nuclear signaling via redox balance? One well-described way to affect nuclear signaling is via the stabilization of HIF1A. *In vivo*, the mitochondrial ETS was shown to be essential for HIF1A stabilization and further *in vitro* studies indicated that CIII-derived

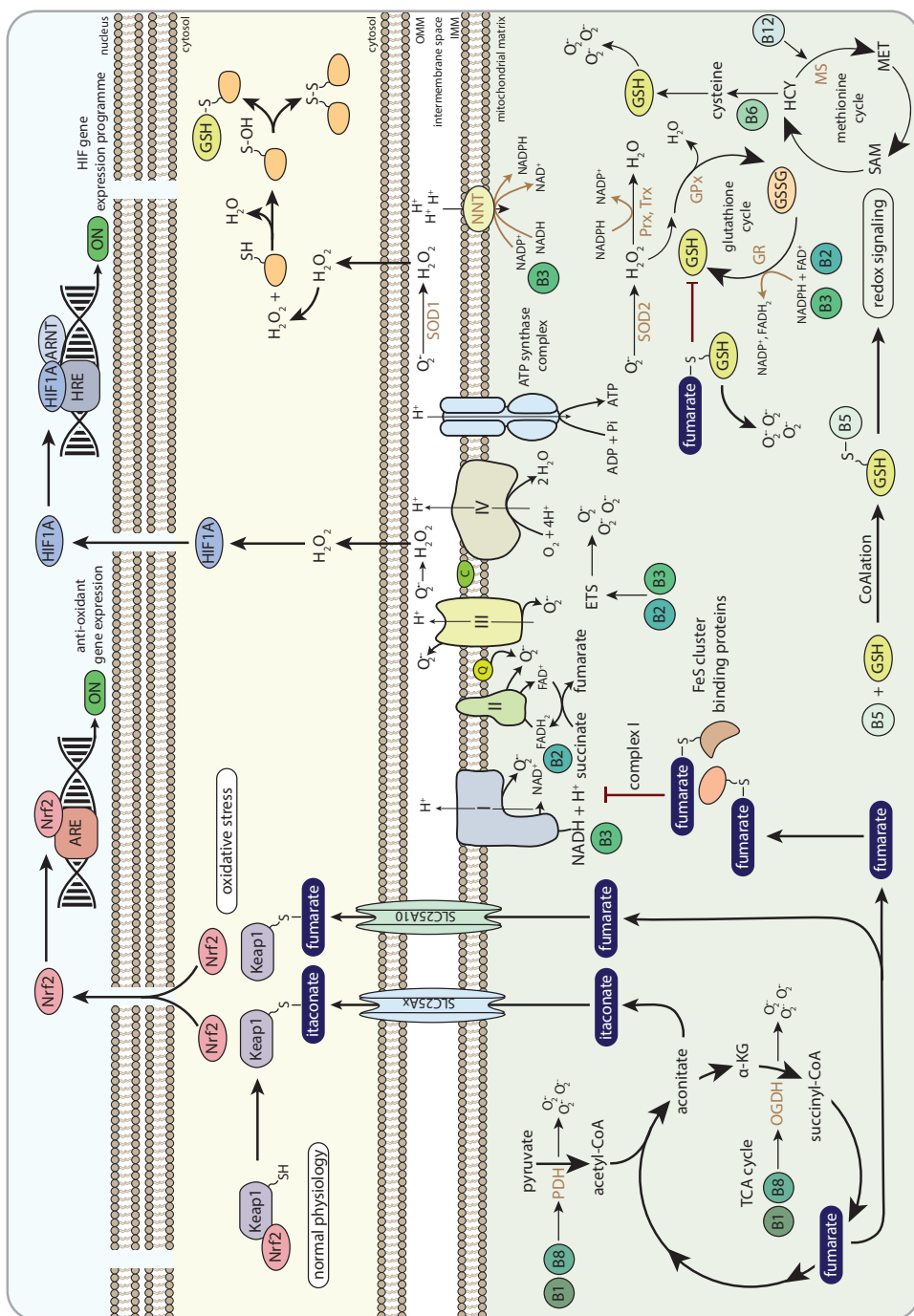


**Figure 6: The role of B-vitamins in redox metabolism and redox-related mito-nuclear communication.** Abbreviations: Keap1 = Kelch-like ECH-associated protein 1, Nrf2 = nuclear factor-like 2, ARE = antioxidant response element,  $H_2O_2$  = hydrogen peroxide, HIF1 $\alpha$  = hypoxia-inducible factor 1  $\alpha$ , ARNT = aryl hydrocarbon receptor nuclear translocator, HRE = hypoxia response element, PDH = pyruvate dehydrogenase,  $\alpha$ -KG =  $\alpha$ -ketoglutarate, OGDH = 2-oxoglutarate dehydrogenase complex, SLC25A1, SLC25A10 or SLC25A11, SLC25A10 = mitochondrial dicarboxylate carrier, FeS cluster = iron-sulfur cluster, FAD = flavin adenine dinucleotide,  $FADH_2$  = hydroquinone form of FAD,  $NAD^+$  = nicotinamide adenine dinucleotide, NADH = reduced form of  $NAD^+$ , Q = coenzyme Q, C = cytochrome C, NNT = nicotinamide nucleotide transhydrogenase,  $NADP^+$  = nicotinamide adenine dinucleotide phosphate, SOD1 = copper-zinc superoxide dismutase, SOD2 = manganese-dependent superoxide dismutase, Prx = peroxiredoxins, Trx = thioredoxins, GPx = glutathione peroxidase, GR = glutathione reductase, GSSG = glutathione disulphide, GSH = glutathione, ETS = electron transfer system, HCY = homocysteine, MS = methionine synthase, MET = methionine, SAM = S-adenosylmethionine, OMM = outer mitochondrial membrane, IMM = inner mitochondrial membrane.

mitochondrial ROS played an important role in stabilizing HIF1A (224). Importantly, these effects can be reversed by overexpressing catalase (CAT) and GPx, but not mitochondrial targeted-CAT, SOD1 and SOD2 (225–227), suggesting that superoxide formed at CIII needs to be converted into hydrogen peroxide in the cytoplasm before it can stabilize HIF1A levels (Figure 6). Although the exact mechanism by which HIF1A is stabilized is still not clear, EGLNs are most likely involved, because ROS competes with oxygen in EGLNs, which stalls the hydroxylation reaction and results in stabilization of HIF1A.

Fumarate is able to regulate ROS levels by interfering with anti-oxidant systems such as GSH (228). Sullivan and colleagues were the first to show that fumarate, which accumulated due to fumarate hydratase deficiency, can induce succination of GSH, generating succinated GSH (succinic-GSH) (Figure 6) (228). Succinic-GSH would support cancer cell proliferation by increasing oxidative stress levels in the mitochondria that subsequently activate HIF1A (228). Mechanistically, succinic-GSH acts as an alternative substrate for GR, thereby lowering NADPH levels, which limits the pool of NADPH that is available to be used as a cofactor for hydrogen peroxide detoxification (228). Two years later, this mechanism was argued by Zheng et al. (229). Although they agreed that succinic-GSH-induced oxidative stress was the leading cause for the clinical manifestations of FH-deficiency, they argued against the mechanism by which succinic-GSH and concurrent NADPH depletion enhanced oxidative stress (229). Instead of detoxification of succinic-GSH by GR as an enhancer of oxidative stress, Zheng et al. (229) demonstrated that succinic-GSH depleted the cells of GSH, and that NADPH requirements were increased to sustain GSH biosynthesis (229). These redox imbalances were not only relevant for anti-oxidative defense, but also for cancer cell fate (229).

Apart from GSH succination, fumarate can also have a signaling role via its ability to act as substrate for succination of other proteins (230–232). Multiple proteins are subjected to succination (Figure 6) (231–233), including Kelch-like ECH-associated protein 1 (KEAP1) (234), aconitase (208), iron regulatory protein 1 (IRP1) (235), FeS cluster binding proteins (236), and glyceraldehyde-3-phosphate dehydrogenase (GAPDH) (237,238). Succination leads to protein dysfunction and disruption of redox homeostasis (228,229) and therefore contributes to the pathology of various chronic diseases, including cancer (228–230,235,239) and diabetes (240–242). In cancer, elevated levels of fumarate increased succination of KEAP1, impairing its function, which induced nuclear translocation of nuclear factor-like 2 (Nrf2) and thereby activating antioxidant response element (ARE)-controlled genes to neutralize oxidative stress and to create an advantageous growth environment for cancer cells (Figure 6) (239,243). Remarkably, although

fumarate-induced Nrf2 stabilization lead to adverse effects in the kidney, the upregulation of ARE-controlled genes exhibits cardioprotective properties in the heart (244). Furthermore, via concurrent activation of Nrf2 and succination of IRP1, fumarate was found to enhance transcription and translation of the ferritin gene, respectively. As a consequence, ferritin levels increased, which promoted the expression of promitotic transcription factor Forkhead box protein M1 (FOXO1), inducing cell cycle progression (235).

Another PTM in the KEAP1-Nrf2 pathway, is also derived from mitochondrial metabolism. Mills et al. (245) demonstrated that itaconate alkylated cysteine residues of KEAP1 in LPS-activated macrophages. Whereas KEAP1 prevents nuclear migration of Nrf2 by forming a cluster under normal physiological conditions, alkylation of KEAP1 by itaconate separates Nrf2 from KEAP1 (Figure 6) (245), liberating Nrf2 for migration to the nucleus, where it activates the transcription of genes involved in anti-oxidant and anti-inflammatory signaling routes (245,246). Bambouskova et al. (247) also identified an anti-inflammatory role of itaconate in cells. Itaconate inhibited the production of a subset of pro-inflammatory cytokines IL6 and IL12 by inhibiting nuclear I $\kappa$ B $\zeta$ , a key player in the secondary transcriptional response upon primary NF- $\kappa$ B activation (247). Although the anti-inflammatory role of itaconate via its nuclear signaling routes have only recently been discovered, these studies highlight the important role of the aconitate-derived itaconate in mito-nuclear communication in immune cells.

### B-vitamin regulation of ROS and redox signaling

Vitamin B2 and B3 act as cofactors for respectively CII and CI, and assist in redox reactions catalysed by GR, in which GSSG is reduced to GSH. Vitamin B2 and B3 are therefore regulators of ROS balance, and dysregulated vitamin B2 or B3 metabolism leads to increased levels of oxidative stress and mitochondrial ROS production (Figure 6) (22,248). Amongst the signaling pathways that are affected by mitochondrial ROS, especially lipid peroxidation and oxidative stress injuries that are caused by I/R, have been found to increase upon vitamin B2 deficiency (22,25). Furthermore, chronic supplementation with the vitamin B3 (in the form of NAM) was shown to reduce hepatic lipid accumulation *in vivo*, which was suggested to ameliorate the oxidative stress response that occurred during liver steatosis (249). Similarly, NR has been shown to lower oxidative stress in mice in an LPS-induced sepsis model, resulting in lower mortality (250). Although multiple studies have shown beneficial effects of NR (26), others have also shown that high doses of NR in mice can be detrimental for mouse metabolic physiology (251), which can possibly be explained by differences in genetic backgrounds or composition of the diets.

High levels of NADH, the reduced form of vitamin B3, drive electron flow through the ETS, while high levels of ATP and low levels of oxygen impede electron flow. Recently it was shown that acute physiological hypoxia increases NADH levels and induces ROS, especially in the intermembrane space (248). At the same time the activity of SDH was inhibited, resulting in increased levels of succinate (248). NADH levels also play a role during I/R, where increased NADH levels drive malate to fumarate conversion during ischemia, and the increased succinate levels at CII that are produced during reperfusion cause increased mitochondrial ROS production, which accounts for the oxidative damage and cell death during I/R (252). Although no studies have been performed that focus on the relation between NADH levels, mitochondrial ROS, succinate and nuclear pathways, it would be interesting to see how succinate communicates with nuclear dioxygenases upon increased mitochondrial ROS. Although this communication remains elusive, a recent study illustrated how vitamin B3 metabolism, anti-oxidant responses and nuclear signaling are connected (253). Wei et al. (253) showed that supplementation of NMN could alter nuclear signaling via modulation of Nrf2 expression and its translocation to the nucleus (253).

In addition to vitamin B2 and B3, vitamin B6 and B12 also play a pivotal role in redox homeostasis as they both operate in GSH metabolism ([Figure 6](#)). So far only a few studies have focused on the possible protective role of vitamin B6 (pyridoxine) or pyridoxine derivatives in amelioration of oxidative stress (254–256). Pyridoxine increased antioxidant responses, possibly via upregulation of nuclear Nrf2 gene expression, and decreased levels of mitochondrial ROS (254). Pyridoxal-5'-phosphate supplementation resulted in reduced NLRP3 inflammasome activation and inflammatory cytokine production in peritoneal macrophages (255), which couples mitochondrial-derived ROS production to nuclear signaling pathways in immune cells. However, Zhang et al. (255) also pointed out that the outcomes for different pyridoxine derivatives are not always similar (255), indicating that more research is needed to elucidate the mechanisms by which pyridoxine potentially prevents ROS-induced oxidative stress, and how these signals are possibly transferred to the nucleus.

Methylcobalamin (vitamin B12) contributes to GSH synthesis by acting as coenzyme for MS. The lack of methylcobalamin that is observed upon cobalamin deficiency is therefore associated with dysregulated GSH metabolism and increased ROS levels ([Figure 6](#)) (55), and cobalamin deficiency is clinically characterized by reduced plasma levels of GSH and impaired anti-oxidant capacity (257). Of note, although adenosylcobalamin is not directly involved in the GSH cycle, a lack of adenosylcobalamin that is observed during MUT dysfunction is also linked to

impaired GSH metabolism and increased ROS levels as it hampers mitochondrial function (179,258).

Although vitamin B1 (thiamine) and vitamin B11 (folate) do not directly assist the ETS or GSH metabolism, both B-vitamins can alter cellular redox states. Thiamine can influence mitochondrial ROS production by acting as a cofactor for PDH and OGDH, two other major sources of mitochondrial superoxide (**Figure 6**). Thiamine deficiency is therefore linked to increased mitochondrial ROS formation (259,260). Since CIII-derived mitochondrial ROS can alter HIF1 signaling (224), the higher levels of ROS that are observed in thiamine deficiency have perhaps also a signaling role towards HIF1. This would also partly explain why thiamine deficiency is associated with HIF1A stabilization (261). Another interesting link between vitamin B1 and redox state was discovered recently (262). Benfotiamine, a synthetic S-acyl derivative of thiamine, was found to induce the expression of Nrf2 and ARE-dependent genes (262). It even restored mitochondrial function in a mouse model of Alzheimer's disease, which indicates that this thiamine derivative can link vitamin B1 metabolism and mitochondrial function to nuclear anti-oxidant defense systems (262). Furthermore, it has also been shown that folate metabolism is linked to cellular redox states, in addition to its predominant role in supporting nucleic acid synthesis (263). Using quantitative flux analyses, the authors observed that oxidation of MTHF to 10-formyl-tetrahydrofolate was coupled to the reduction of NADP<sup>+</sup> to NADPH, which showed that folate metabolism is essential to create reducing power in the cell (263). They also demonstrated that depletion of cytosolic as well as mitochondrial MTHFD resulted in lower NADPH/NADP<sup>+</sup> and GSH/GSSG ratios with concomitant increased sensitivity to oxidative stress. These results showed that folate metabolism contributes to cellular redox states (263).

Recently, it was also identified that vitamin B5 (CoA) has an important role in redox regulation by functioning as a protective thiol (264,265). CoA was covalently linked to cellular proteins of mammalian cells in response to oxidizing agents and metabolic stress and induced a reversible PTM that was identified as protein CoAlation (**Figure 6**) (264,265). Proteins involved in redox homeostasis are particularly sensitive for CoAlation as they exhibit reactive thiol residues that can form homo- and heterodisulphides with CoA, such as GSH (266). Therefore, CoA has now also been implicated as an important regulator of redox homeostasis and could possibly also have nuclear targets.

## Conclusion

Overall, B-vitamins are of critical importance for regulating mitochondria, mitochondrial metabolites and signaling of mitochondrial metabolites to the nucleus. Although B-vitamins are among the oldest studied molecules in relation to health and disease, the revival of studying metabolism in pathologies, which were previously less well understood to be of metabolic origin, like cancer and immunological diseases, makes the B-vitamins highly relevant to be studied in light of novel therapeutic target development. In addition, the role of B-vitamins as essential dietary components makes it important to understand their nutritional role in relation to mito-nuclear signaling. All together this could serve as a proxy for understanding healthy dietary life styles and healthy aging.

### Conflict of interest

The authors declare that the research was conducted in the absence of any commercial or financial relationships that could be construed as a potential conflict of interest.

### Author contributions

JJ reviewed the literature and prepared the first manuscript. SG, JK and VB reviewed the literature, participated in writing and editing of the manuscript. VB supervised the project and compiled the final version of the manuscript.

### Funding

This project (NWO-WIAS Graduate Program 2016 grant) was funded by the Wageningen Institute for Animal Sciences (WIAS) and the Dutch Organization for Scientific Research (NWO).

## References

1. Depeint F, Bruce WR, Shangari N, Mehta R, O'Brien PJ. Mitochondrial function and toxicity: role of the B vitamin family on mitochondrial energy metabolism. *Chem Biol Interact.* 2006 Oct;163(1–2):94–112.
2. Depeint F, Bruce WR, Shangari N, Mehta R, O'Brien PJ. Mitochondrial function and toxicity: role of B vitamins on the one-carbon transfer pathways. *Chem Biol Interact.* 2006 Oct;163(1–2):113–32.
3. Keijer J, Bekkenkamp-Grovenstein M, Venema D, Dommels YEM. Bioactive food components, cancer cell growth limitation and reversal of glycolytic metabolism. *Biochim Biophys Acta - Bioenerg.* 2011;1807(6):697–706.
4. Quirós PM, Mottis A, Auwerx J. Mitonuclear communication in homeostasis and stress. *Nat Rev Mol Cell Biol.* 2016;17(4):213–26.
5. Weinberg SE, Sena LA, Chandel NS. Mitochondria in the Regulation of Innate and Adaptive Immunity. *Immunity.* 2015;42(3):406–17.
6. Vyas S, Zaganjor E, Haigis MC. Mitochondria and Cancer. *Cell.* 2016 Jul 28;166(3):555–66.
7. Nunnari J, Suomalainen A. Mitochondria: In Sickness and in Health. *Cell.* 2012;148(6):1145–59.
8. Cannino G, Ciscato F, Masgras I, Sánchez-Martín C, Rasola A. Metabolic Plasticity of Tumor Cell Mitochondria. Vol. 8, *Frontiers in Oncology*. 2018. p. 333.
9. West AP, Shadel GS, Ghosh S. Mitochondria in innate immune responses. *Nat Rev Immunol.* 2011;11(6):389–402.
10. Murphy MP, Hartley RC. Mitochondria as a therapeutic target for common pathologies. *Nat Rev Drug Discov.* 2018;17(12):865–86.
11. EFSA NDA Panel (EFSA Panel on Dietetic Products N and A. Scientific Opinion on Dietary Reference Values for thiamine. *EFSA J.* 2016;14(12):4653.
12. EFSA NDA Panel (EFSA Panel on Dietetic Products N and A. Scientific Opinion on Dietary Reference Values for riboflavin. *EFSA J.* 2017;15(8):4919.
13. EFSA NDA Panel (EFSA Panel on Dietetic Products N and A. Scientific Opinion on Dietary Reference Values for niacin. *EFSA J.* 2014;12(7):3759.
14. EFSA NDA Panel (EFSA Panel on Dietetic Products N and A. Scientific Opinion on Dietary Reference Values for pantothenic acid. *EFSA J.* 2014;12(2):3581.
15. EFSA NDA Panel (EFSA Panel on Dietetic Products N and A. Scientific Opinion on Dietary Reference Values for vitamin B6. *EFSA Journal.* 2016;14(6):4485.
16. EFSA NDA Panel (EFSA Panel on Dietetic Products N and A. Scientific Opinion on Dietary Reference Values for biotin. *EFSA J.* 2014;12(2):3580.
17. EFSA NDA Panel (EFSA Panel on Dietetic Products N and A. Scientific Opinion on Dietary Reference Values for folate. *EFSA J.* 2014;12(11):3893.
18. EFSA NDA Panel (EFSA Panel on Dietetic Products N and A. Scientific Opinion on Dietary Reference Values for cobalamin (vitamin B12). *EFSA J.* 2015;13(7):4150.
19. Bettendorff L, Wins P, Lesourd M. Subcellular localization and compartmentation of thiamine derivatives in rat brain. *Biochim Biophys Acta - Mol Cell Res.* 1994;1222(1):1–6.
20. Mkrtchyan G, Aleshin V, Parkhomenko Y, Kaehne T, Luigi Di Salvo M, Parroni A, et al. Molecular mechanisms of the non-coenzyme action of thiamin in brain: biochemical, structural and pathway analysis. *Sci Rep.* 2015;5(1):12583.
21. Macheroux P, Kappes B, Ealick SE. Flavogenomics--a genomic and structural view of flavin-dependent proteins. *FEBS J.* 2011 Aug;278(15):2625–34.
22. Ashoori M, Saedisomeolia A. Riboflavin (vitamin B<sub>2</sub>) and oxidative stress: a review. *Br J Nutr.* 2014 Jun 14;111(11):1985–91.
23. Toyosaki T. Antioxidant effect of riboflavin in enzymic lipid peroxidation. *J Agric Food Chem.* 1992 Oct 1;40(10):1727–30.
24. Hultquist DE, Xu F, Quandt KS, Schlafer M, Mack CP, Till GO, et al. Evidence that NADPH-dependent methemoglobin reductase and administered riboflavin protect tissues from oxidative injury. *Am J Hematol.* 1993 Jan 1;42(1):13–8.

25. Sanches SC, Ramalho LNZ, Mendes-Braz M, Terra VA, Cecchini R, Augusto MJ, et al. Riboflavin (vitamin B-2) reduces hepatocellular injury following liver ischaemia and reperfusion in mice. *Food Chem Toxicol.* 2014 May;67:65–71.
26. Yoshino J, Baur JA, Imai S. NAD<sup>+</sup> Intermediates: The Biology and Therapeutic Potential of NMN and NR. *Cell Metab.* 2017;27(3):513–28.
27. Xiao W, Wang R-S, Handy DE, Loscalzo J. NAD(H) and NADP(H) Redox Couples and Cellular Energy Metabolism. *Antioxid Redox Signal.* 2017;28(3):ars.2017.7216.
28. Murphy MP. Redox Modulation by Reversal of the Mitochondrial Nicotinamide Nucleotide Transhydrogenase. *Cell Metab.* 2015 Sep 1;22(3):363–5.
29. Lewis CA, Parker SJ, Fiske BP, McCloskey D, Gui DY, Green CR, et al. Tracing Compartmentalized NADPH Metabolism in the Cytosol and Mitochondria of Mammalian Cells. *Mol Cell.* 2014;55(2):253–63.
30. Ronchi JA, Francisco A, Passos LAC, Figueira TR, Castilho RF. The Contribution of Nicotinamide Nucleotide Transhydrogenase to Peroxide Detoxification Is Dependent on the Respiratory State and Counterbalanced by Other Sources of NADPH in Liver Mitochondria \*. *J Biol Chem.* 2016 Sep 16;291(38):20173–87.
31. Houtkooper RH, Cantó C, Wanders RJ, Auwerx J. The Secret Life of NAD<sup>+</sup>: An Old Metabolite Controlling New Metabolic Signaling Pathways. *Endocr Rev.* 2010 Apr 1;31(2):194–223.
32. Fang EF, Lautrup S, Hou Y, Demarest TG, Croteau DL, Mattson MP, et al. NAD<sup>+</sup> in Aging: Molecular Mechanisms and Translational Implications. *Trends Mol Med.* 2017 Oct 1;23(10):899–916.
33. Ryu KW, Nandu T, Kim J, Challa S, DeBerardinis RJ, Kraus WL. Metabolic regulation of transcription through compartmentalized NAD(+) biosynthesis. *Science (80- ).* 2018 May;360(6389).
34. Liu L, Su X, Quinn WJ, Hui S, Krukenberg K, Frederick DW, et al. Quantitative Analysis of NAD Synthesis-Breakdown Fluxes. *Cell Metab.* 2018;27(5):1067-1080.e5.
35. Lipmann F, Kaplan NO, Novelli GD, Tuttle LC, Guirard BM. Coenzyme for acetylation, a pantothenic acid derivative. *J Biol Chem.* 1947;167(3):869–70.
36. Pietrocola F, Galluzzi L, Bravo-San Pedro JM, Madeo F, Kroemer G. Acetyl coenzyme A: A central metabolite and second messenger. *Cell Metab.* 2015;21(6):805–21.
37. Sabari BR, Zhang D, Allis CD, Zhao Y. Metabolic regulation of gene expression through histone acylations. *Nat Rev Mol Cell Biol.* 2017;18(2):90–101.
38. Leonardi R, Zhang Y-M, Rock CO, Jackowski S. Coenzyme A: Back in action. *Prog Lipid Res.* 2005;44(2):125–53.
39. McGarry JD, Foster DW. Regulation of Hepatic Fatty Acid Oxidation and Ketone Body Production. *Annu Rev Biochem.* 1980 Jun 1;49(1):395–420.
40. Puchalska P, Crawford PA. Multi-dimensional Roles of Ketone Bodies in Fuel Metabolism, Signaling, and Therapeutics. *Cell Metab.* 2017;25(2):262–84.
41. Williamson JR, Corkey BEBT-M in E. Assay of citric acid cycle intermediates and related compounds—Update with tissue metabolite levels and Intracellular Distribution. In: *Methods in Enzymology.* Academic Press; 1979. p. 200–22.
42. Braymer JJ, Lill R. Iron–sulfur cluster biogenesis and trafficking in mitochondria. *J Biol Chem.* 2017;292(31):12754–63.
43. Scholnick PL, Hammaker LE, Marver HS. Soluble d-Aminolevulinic Acid Synthetase of Rat Liver: II. Studies related to the mechanism of enzyme action and hemin inhibition. *J Biol Chem.* 1972 Jul 10;247(13):4132–7.
44. Petrelli F, Moretti P, Paparelli M. Intracellular distribution of biotin-14COOH in rat liver. *Mol Biol Rep.* 1979;4(4):247–52.
45. Appling DR. Compartmentation of folate-mediated one-carbon metabolism in eukaryotes. *FASEB J.* 1991 Sep 1;5(12):2645–51.
46. Tibbetts AS, Appling DR. Compartmentalization of Mammalian Folate-Mediated One-Carbon Metabolism. *Annu Rev Nutr.* 2010 Jul 1;30(1):57–81.
47. Fox JT, Stover PJBT-V& H. Chapter 1 Folate-Mediated One-Carbon Metabolism. In: *Folic Acid and Folates.* Academic Press; 2008. p. 1–44.

48. Nijhout HF, Reed MC, Ulrich CM, BT-V& H. Chapter 2 Mathematical Models of Folate-Mediated One-Carbon Metabolism. In: Folic Acid and Folates. Academic Press; 2008. p. 45–82.
49. Reed MC, Thomas RL, Pavisic J, James SJ, Ulrich CM, Nijhout HF. A mathematical model of glutathione metabolism. *Theor Biol Med Model*. 2008;5(1):8.
50. Ulrich CM, Reed MC, Nijhout HF. Modeling folate, one-carbon metabolism, and DNA methylation. *Nutr Rev*. 2008 Aug 1;66(suppl\_1):S27–30.
51. Green CR, Wallace M, Divakaruni AS, Phillips SA, Murphy AN, Ciaraldi TP, et al. Branched-chain amino acid catabolism fuels adipocyte differentiation and lipogenesis. *Nat Chem Biol*. 2016;12(1):15–21.
52. Ludwig ML, Matthews RG. Structure-based perspectives on B12-dependent enzymes. *Annu Rev Biochem*. 1997 Jun 1;66(1):269–313.
53. Matthews RG, Sheppard C, Goulding C. Methylenetetrahydrofolate reductase and methionine synthase: biochemistry and molecular biology. *Eur J Pediatr*. 1998;157(2):S54–9.
54. Scott JM. Folate and vitamin B12. *Proc Nutr Soc*. 1999 May;58(2):441–8.
55. Pastore A, Martinelli D, Piemonte F, Tozzi G, Boenzi S, Di Giovamberardino G, et al. Glutathione metabolism in cobalamin deficiency type C (cblC). *J Inher Metab Dis*. 2014 Jan 1;37(1):125–9.
56. Schofield CJ, Ratcliffe PJ. Oxygen sensing by HIF hydroxylases. *Nat Rev Mol Cell Biol*. 2004;5(5):343–54.
57. Semenza GL. Hypoxia-inducible factors: coupling glucose metabolism and redox regulation with induction of the breast cancer stem cell phenotype. *EMBO J*. 2017 Feb 1;36(3):252–9.
58. Macklin PS, McAuliffe J, Pugh CW, Yamamoto A. Hypoxia and HIF pathway in cancer and the placenta. *Placenta*. 2017;56:8–13.
59. Schito L, Semenza GL. Hypoxia-Inducible Factors: Master Regulators of Cancer Progression. *Trends in Cancer*. 2016 Dec;2(12):758–70.
60. Imtiyaz HZ, Simon MC. Hypoxia-Inducible Factors as Essential Regulators of Inflammation BT - Diverse Effects of Hypoxia on Tumor Progression. In: Simon MC, editor. Berlin, Heidelberg: Springer Berlin Heidelberg; 2010. p. 105–20.
61. Lefere S, Van Steenkiste C, Verhelst X, Van Vlierberghe H, Devisscher L, Geerts A. Hypoxia-regulated mechanisms in the pathogenesis of obesity and non-alcoholic fatty liver disease. *Cell Mol Life Sci*. 2016;73(18):3419–31.
62. Maxwell PH, Wiesener MS, Chang GW, Clifford SC, Vaux EC, Cockman ME, et al. The tumour suppressor protein VHL targets hypoxia-inducible factors for oxygen-dependent proteolysis. *Nature*. 1999;399(6733):271–5.
63. Aragonés J, Fraisl P, Baes M, Carmeliet P. Oxygen Sensors at the Crossroad of Metabolism. *Cell Metab*. 2009;9(1):11–22.
64. Bishop T, Ratcliffe PJ. HIF hydroxylase pathways in cardiovascular physiology and medicine. *Circ Res*. 2015/06/20. 2015;117(1):65–79.
65. Koivunen P, Hirsilä M, Remes AM, Hassinen IE, Kivirikko KI, Myllyharju J. Inhibition of hypoxia-inducible factor (HIF) hydroxylases by citric acid cycle intermediates: Possible links between cell metabolism and stabilization of HIF. *J Biol Chem*. 2007;282(7):4524–32.
66. Serra-Pérez A, Planas AM, Núñez-O'Mara A, Berra E, García-Villoria J, Ribes A, et al. Extended Ischemia Prevents HIF1α Degradation at Reoxygenation by Impairing Prolyl-hydroxylation: ROLE OF KREBS CYCLE METABOLITES \*. *J Biol Chem*. 2010 Jun 11;285(24):18217–24.
67. Rose NR, McDonough MA, King ONF, Kawamura A, Schofield CJ. Inhibition of 2-oxoglutarate dependent oxygenases. *Chem Soc Rev*. 2011 Aug;40(8):4364–97.
68. Hewitson KS, Lienard BMR, McDonough MA, Clifton IJ, Butler D, Soares AS, et al. Structural and mechanistic studies on the inhibition of the hypoxia-inducible transcription factor hydroxylases by tricarboxylic acid cycle intermediates. *J Biol Chem*. 2007;282(5):3293–301.
69. Yang M, Soga T, Pollard PJ, Adam J. The emerging role of fumarate as an oncometabolite. *Front Oncol*. 2012;2:85.
70. Gottlieb E, Tomlinson IPM. Mitochondrial tumour suppressors: a genetic and biochemical update. *Nat Rev Cancer*. 2005 Nov;5(11):857–66.
71. Gimenez-Roqueplo AP, Favier J, Rustin P, Mourad JJ, Plouin PF, Corvol P, et al. The R22X mutation of the SDHD gene in hereditary paraganglioma abolishes the enzymatic activity of complex II in the

- mitochondrial respiratory chain and activates the hypoxia pathway. *Am J Hum Genet.* 2001; 69(6):1186–97.
72. Brière JJ, Favier J, Bénit P, El Ghouzzi V, Lorenzato A, Rabier D, et al. Mitochondrial succinate is instrumental for HIF1 $\alpha$  nuclear translocation in SDHA-mutant fibroblasts under normoxic conditions. *Hum Mol Genet.* 2005;14(21):3263–9.
  73. Dahia PLM, Ross KN, Wright ME, Hayashida CY, Santagata S, Barontini M, et al. A Hif1 $\alpha$  regulatory loop links hypoxia and mitochondrial signals in pheochromocytomas. *PLoS Genet.* 2005;1(1):0072–80.
  74. Isaacs JS, Jung YJ, Mole DR, Lee S, Torres-Cabala C, Chung Y-L, et al. HIF overexpression correlates with biallelic loss of fumarate hydratase in renal cancer: Novel role of fumarate in regulation of HIF stability. *Cancer Cell.* 2005;8(2):143–53.
  75. Pollard PJ, Brière JJ, Alam NA, Barwell J, Barclay E, Wortham NC, et al. Accumulation of Krebs cycle intermediates and over-expression of HIF1 $\alpha$  in tumours which result from germline FH and SDH mutations. *Hum Mol Genet.* 2005;14(15):2231–9.
  76. Selak MA, Armour SM, MacKenzie ED, Boulahbel H, Watson DG, Mansfield KD, et al. Succinate links TCA cycle dysfunction to oncogenesis by inhibiting HIF- $\alpha$  prolyl hydroxylase. *Cancer Cell.* 2005;7(1):77–85.
  77. Lee S, Nakamura E, Yang H, Wei W, Linggi MS, Sajan MP, et al. Neuronal apoptosis linked to Egln3 prolyl hydroxylase and familial pheochromocytoma genes: Developmental culling and cancer. *Cancer Cell.* 2005;8(2):155–67.
  78. Tannahill GM, Curtis AM, Adamik J, Palsson-McDermott EM, McGettrick AF, Goel G, et al. Succinate is an inflammatory signal that induces IL-1 $\beta$  through HIF-1 $\alpha$ . *Nature.* 2013;496(7444):238–42.
  79. Cordes T, Wallace M, Michelucci A, Divakaruni AS, Sapcariu SC, Sousa C, et al. Immunoresponsive gene 1 and itaconate inhibit succinate dehydrogenase to modulate intracellular succinate levels. *J Biol Chem.* 2016;291(27):14274–84.
  80. Lampropoulou V, Sergushichev A, Bambouskova M, Nair S, Vincent EE, Loginicheva E, et al. Itaconate Links Inhibition of Succinate Dehydrogenase with Macrophage Metabolic Remodeling and Regulation of Inflammation. *Cell Metab.* 2016;24(1):158–66.
  81. Li Y, Zheng JY, Liu JQ, Yang J, Liu Y, Wang C, et al. Succinate/NLRP3 inflammasome induces synovial fibroblast activation: Therapeutic effects of clematichinenoside AR on arthritis. *Front Immunol.* 2016;7(DEC):1–11.
  82. Li Y, Liu Y, Wang C, Xia W-R, Zheng J-Y, Yang J, et al. Succinate induces synovial angiogenesis in rheumatoid arthritis through metabolic remodeling and HIF-1 $\alpha$ /VEGF axis. *Free Radic Biol Med.* 2018;126(February):1–14.
  83. Ho H-Y, Lin Y-T, Lin G, Wu P-R, Cheng M-L. Nicotinamide nucleotide transhydrogenase (NNT) deficiency dysregulates mitochondrial retrograde signaling and impedes proliferation. *Redox Biol.* 2017;12:916–28.
  84. Gomes AP, Price NL, Ling AJY, Moslehi JJ, Montgomery MK, Rajman L, et al. Declining NAD(+) induces a pseudohypoxic state disrupting nuclear-mitochondrial communication during aging. *Cell.* 2013 Dec;155(7):1624–38.
  85. Williams PA, Harder JM, Foxworth NE, Cochran KE, Philip VM, Porciatti V, et al. Vitamin B(3) modulates mitochondrial vulnerability and prevents glaucoma in aged mice. *Science (80- ).* 2017 Feb;355(6326):756–60.
  86. Sadanaga-Akiyoshi F, Yao H, Tanuma S, Nakahara T, Hong JS, Ibayashi S, et al. Nicotinamide attenuates focal ischemic brain injury in rats: with special reference to changes in nicotinamide and NAD<sup>+</sup> levels in ischemic core and penumbra. *Neurochem Res.* 2003 Aug;28(8):1227–34.
  87. Park JH, Long A, Owens K, Kristian T. Nicotinamide mononucleotide inhibits post-ischemic NAD<sup>+</sup> degradation and dramatically ameliorates brain damage following global cerebral ischemia. *Neurobiol Dis.* 2016;95:102–10.
  88. Shoji K, Tanaka T, Nangaku M. Role of hypoxia in progressive chronic kidney disease and implications for therapy. *Curr Opin Nephrol Hypertens.* 2014 Mar;23(2):161–8.
  89. Howell NJ, Tennant DA. The role of HIFs in ischemia-reperfusion injury. *Hypoxia.* 2014 Jul 30;2:107–15.

90. Van Vranken JG, Na U, Winge DR, Rutter J. Protein-mediated assembly of succinate dehydrogenase and its cofactors. *Crit Rev Biochem Mol Biol.* 2015 Mar 4;50(2):168–80.
91. Maio N, Ghezzi D, Verrigni D, Rizza T, Bertini E, Martinelli D, et al. Disease-Causing SDHAF1 Mutations Impair Transfer of Fe-S Clusters to SDHB. *Cell Metab.* 2015/12/31. 2016 Feb 9;23(2):292–302.
92. Bugiani M, Lamantea E, Invernizzi F, Moroni I, Bizzi A, Zeviani M, et al. Effects of riboflavin in children with complex II deficiency. *Brain Dev.* 2006 Oct 1;28(9):576–81.
93. Lu H, Dalgard CL, Mohyeldin A, McFate T, Tait AS, Verma A. Reversible Inactivation of HIF-1 Prolyl Hydroxylases Allows Cell Metabolism to Control Basal HIF-1\*. *J Biol Chem.* 2005;280(51):41928–39.
94. Frohman CE, Day HG. Effect of oxythiamine on blood pyruvate-lactate relationships and the. *J Biol Chem.* 1949 Aug;180(1):93–8.
95. Park DH, Gubler CJ. Studies on the physiological functions of thiamine: V. Effects of thiamine deprivation and thiamine antagonists on blood pyruvate and lactate levels and activity of lactate dehydrogenase and its isozymes in blood and tissues. *Biochim Biophys Acta - Gen Subj.* 1969;177(3):537–43.
96. Falder S, Silla R, Phillips M, Rea S, Gurfinkel R, Baur E, et al. Thiamine supplementation increases serum thiamine and reduces pyruvate and lactate levels in burn patients. *Burns.* 2010;36(2):261–9.
97. Sweet RL, Zastre JA. HIF1- $\alpha$ -Mediated Gene Expression Induced by Vitamin B1 Deficiency. *Int J Vitam Nutr Res.* 2013 Jun 1;83(3):188–97.
98. Hernandez-Vazquez ADJ, Garcia-Sanchez JA, Moreno-Arriola E, Salvador-Adriano A, Ortega-Cuellar D, Velazquez-Arellano A. Thiamine Deprivation Produces a Liver ATP Deficit and Metabolic and Genomic Effects in Mice: Findings Are Parallel to Those of Biotin Deficiency and Have Implications for Energy Disorders. *J Nutrigenet Nutrigenomics.* 2017;9(5–6):287–99.
99. Bettendorff L, Sluse F, Goessens G, Wins P, Grisar T. Thiamine Deficiency-Induced Partial Necrosis and Mitochondrial Uncoupling in Neuroblastoma Cells Are Rapidly Reversed by Addition of Thiamine. *J Neurochem.* 1995 Nov 1;65(5):2178–84.
100. An J, Rao A, Ko M. TET family dioxygenases and DNA demethylation in stem cells and cancers. *Exp Mol Med.* 2017;49(4).
101. Klose RJ, Kallin EM, Zhang Y. JmJc-domain-containing proteins and histone demethylation. *Nat Rev Genet.* 2006;7(9):715–27.
102. Islam S, Leissing TM, Chowdhury R, Hopkinson RJ, Schofield CJ. 2-Oxoglutarate-Dependent Oxygenases. *Annu Rev Biochem.* 2018;87:585–620.
103. Raffel S, Falcone M, Kneisel N, Hansson J, Wang W, Lutiz C, et al. BCAT1 restricts akG levels in AML stem cells leading to IDHmut-like DNA hypermethylation. *Nature.* 2017;551(7680):384–8.
104. Spallotta F, Cencioni C, Atlante S, Garella D, Cocco M, Mori M, et al. Stable Oxidative Cytosine Modifications Accumulate in Cardiac Mesenchymal Cells from Type2 Diabetes Patients: Rescue by  $\alpha$ -Ketoglutarate and TET-TDG Functional Reactivation. *Circ Res.* 2018;122(1):31–46.
105. Carey BW, Finley LWS, Cross JR, Allis CD, Thompson CB. Intracellular  $\alpha$ -ketoglutarate maintains the pluripotency of embryonic stem cells. *Nature.* 2015;518(7539):413–6.
106. TeSlaa T, Chaikovskiy AC, Lipchina I, Escobar SL, Hochedlinger K, Huang J, et al.  $\alpha$ -Ketoglutarate Accelerates the Initial Differentiation of Primed Human Pluripotent Stem Cells. *Cell Metab.* 2016;24(3):485–93.
107. Cervera AM, Bayley JP, Devilee P, McCreath KJ. Inhibition of succinate dehydrogenase dysregulates histone modification in mammalian cells. *Mol Cancer.* 2009;8:89.
108. Killian JK, Kim SY, Miettinen M, Smith C, Merino M, Tsokos M, et al. Succinate dehydrogenase mutation underlies global epigenomic divergence in gastrointestinal stromal tumor. *Cancer Discov.* 2013;3(6):648–57.
109. Letouzé E, Martinelli C, Lorient C, Burnichon N, Abermil N, Ottolenghi C, et al. SDH Mutations Establish a Hypermethylator Phenotype in Paraganglioma. *Cancer Cell.* 2013;23(6):739–52.
110. Mason EF, Hornick JL. Succinate dehydrogenase deficiency is associated with decreased 5-hydroxymethylcytosine production in gastrointestinal stromal tumors: implications for mechanisms of tumorigenesis. *Mod Pathol.* 2013;26(11):1492–7.

111. Aspuria PJP, Lunt SY, Våremo L, Vergnes L, Gozo M, Beach JA, et al. Succinate dehydrogenase inhibition leads to epithelial-mesenchymal transition and reprogrammed carbon metabolism. *Cancer Metab.* 2014;2(1):1–15.
112. Sciacovelli M, Gonçalves E, Johnson TI, Zecchini VR, da Costa ASH, Gaude E, et al. Fumarate is an epigenetic modifier that elicits epithelial-to-mesenchymal transition. *Nature.* 2016;537(7621):544–7.
113. Craene B De, Berx G. Regulatory networks defining EMT during cancer initiation and progression. *Nat Rev Cancer.* 2013;13(2):97–110.
114. Maes T, Mascaró C, Ortega A, Lunardi S, Ciceri F, Somervaille TCP, et al. KDM1 histone lysine demethylases as targets for treatments of oncological and neurodegenerative disease. *Epigenomics.* 2015 Jun 1;7(4):609–26.
115. Shi Y, Lan F, Matson C, Mulligan P, Whetstone JR, Cole PA, et al. Histone demethylation mediated by the nuclear amine oxidase homolog LSD1. *Cell.* 2004 Dec;119(7):941–53.
116. Hino S, Sakamoto A, Nagaoka K, Anan K, Wang Y, Mimasu S, et al. FAD-dependent lysine-specific demethylase-1 regulates cellular energy expenditure. *Nat Commun.* 2012;3(1):758.
117. Liu D, Zemleni J. Transcriptional Regulation of the Albumin Gene Depends on the Removal of Histone Methylation Marks by the FAD-Dependent Monoamine Oxidase Lysine-Specific Demethylase 1 in HepG2 Human Hepatocarcinoma Cells. *J Nutr.* 2014 Jul 1;144(7):997–1001.
118. Liu D, Zemleni J. Low activity of LSD1 elicits a pro-inflammatory gene expression profile in riboflavin-deficient human T Lymphoma Jurkat cells. *Genes Nutr.* 2014/08/08. 2014 Sep;9(5):422.
119. Ducker GS, Rabinowitz JD. One-Carbon Metabolism in Health and Disease. *Cell Metab.* 2017 Jan 10;25(1):27–42.
120. Chang H, Zhang T, Zhang Z, Bao R, Fu C, Wang Z, et al. Tissue-specific distribution of aberrant DNA methylation associated with maternal low-folate status in human neural tube defects. *J Nutr Biochem.* 2011;22(12):1172–7.
121. Jacob RA, Gretz DM, Taylor PC, James SJ, Pogribny IP, Miller BJ, et al. Moderate Folate Depletion Increases Plasma Homocysteine and Decreases Lymphocyte DNA Methylation in Postmenopausal Women. *J Nutr.* 1998 Jul 1;128(7):1204–12.
122. Sperber H, Mathieu J, Wang Y, Ferreccio A, Hesson J, Xu Z, et al. The metabolome regulates the epigenetic landscape during naive-to-primed human embryonic stem cell transition. *Nat Cell Biol.* 2015;17(12):1523–35.
123. Yang S-J, Park YS, Cho JH, Moon B, An H-J, Lee JY, et al. Regulation of hypoxia responses by flavin adenine dinucleotide-dependent modulation of HIF-1 $\alpha$  protein stability. *EMBO J.* 2017 Apr 13;36(8):1011–28.
124. Caramaschi D, Sharp GC, Nohr EA, Berryman K, Lewis SJ, Davey Smith G, et al. Exploring a causal role of DNA methylation in the relationship between maternal vitamin B12 during pregnancy and child's IQ at age 8, cognitive performance and educational attainment: a two-step Mendelian randomization study. *Hum Mol Genet.* 2017 Aug 1;26(15):3001–13.
125. Fernàndez-Roig S, Lai S-C, Murphy MM, Fernandez-Ballart J, Quadros E V. Vitamin B12 deficiency in the brain leads to DNA hypomethylation in the TCbIR/CD320 knockout mouse. *Nutr Metab (Lond).* 2012;9(1):41.
126. Lai S-C, Nakayama Y, Sequeira JM, Wlodarczyk BJ, Cabrera RM, Finnell RH, et al. The transcobalamin receptor knockout mouse: a model for vitamin B12 deficiency in the central nervous system. *FASEB J.* 2013 Jun 1;27(6):2468–75.
127. de Vogel S, Bongaerts BWC, Wouters KAD, Kester ADM, Schouten LJ, de Goeij AFPM, et al. Associations of dietary methyl donor intake with MLH1 promoter hypermethylation and related molecular phenotypes in sporadic colorectal cancer. *Carcinogenesis.* 2008 Sep 1;29(9):1765–73.
128. Brady RO, Gurin S. The biosynthesis of radioactive long-chain fatty acids by homogenized pigeon liver tissue. *Arch Biochem Biophys.* 1951;34(1):221–2.
129. Srere PA. The Molecular Physiology of Citrate. *Nature.* 1965;205(4973):766–70.
130. Iacobazzi V, Infantino V. Citrate--new functions for an old metabolite. *Biol Chem.* 2014 Apr;395(4):387–99.
131. Wellen KE, Hatzivassiliou G, Sachdeva UM, Bui T V, Cross JR, Thompson CB. ATP-Citrate Lyase Links Cellular Metabolism to Histone Acetylation. *Science (80- ).* 2009;324(2009):0–4.

132. Montgomery DC, Sorum AW, Guasch L, Nicklaus MC, Meier JL. Metabolic Regulation of Histone Acetyltransferases by Endogenous Acyl-CoA Cofactors. *Chem Biol.* 2015;22(8):1030–9.
133. Verdin E, Ott M. 50 years of protein acetylation: from gene regulation to epigenetics, metabolism and beyond. *Nat Rev Mol Cell Biol.* 2015;16(4):258–64.
134. Morciano P, Carrisi C, Capobianco L, Mannini L, Burgio G, Cestra G, et al. A conserved role for the mitochondrial citrate transporter Sea/SLC25A1 in the maintenance of chromosome integrity. *Hum Mol Genet.* 2009;18(21):4180–8.
135. Yi CH, Pan H, Seebacher J, Jang IH, Hyberts SG, Heffron GJ, et al. Metabolic regulation of protein N-alpha-acetylation by Bcl-xL promotes cell survival. *Cell.* 2011;146(4):607–20.
136. Tatiana LG, Chao L, M. LP, Sarah T, H. OS, S. WE, et al. DNMT1 Is Regulated by ATP-Citrate Lyase and Maintains Methylation Patterns during Adipocyte Differentiation. *Mol Cell Biol.* 2013 Oct 1;33(19):3864–78.
137. Ashbrook MJ, McDonough KL, Pituch JJ, Christopherson PL, Cornell TT, Selewski DT, et al. Citrate modulates lipopolysaccharide-induced monocyte inflammatory responses. *Clin Exp Immunol.* 2015;180(3):520–30.
138. Sivanand S, Rhoades S, Jiang Q, Lee J V., Benci J, Zhang J, et al. Nuclear Acetyl-CoA Production by ACLY Promotes Homologous Recombination. *Mol Cell.* 2017;67(2):252-265.e6.
139. Lee JV, Berry CT, Kim K, Sen P, Kim T, Carrer A, et al. Acetyl-CoA promotes glioblastoma cell adhesion and migration through Ca<sup>2+</sup>-NFAT signaling. *Genes Dev.* 2018;32(7–8):1–15.
140. Violante S, IJlst L, Ruiter J, Koster J, van Lenthe H, Duran M, et al. Substrate specificity of human carnitine acetyltransferase: Implications for fatty acid and branched-chain amino acid metabolism. *Biochim Biophys Acta - Mol Basis Dis.* 2013;1832(6):773–9.
141. Moussaieff A, Rouleau M, Kitsberg D, Cohen M, Levy G, Barasch D, et al. Glycolysis-Mediated Changes in Acetyl-CoA and Histone Acetylation Control the Early Differentiation of Embryonic Stem Cells. *Cell Metab.* 2015 Mar 3;21(3):392–402.
142. Tan M, Luo H, Lee S, Jin F, Yang JS, Montellier E, et al. Identification of 67 Histone Marks and Histone Lysine Crotonylation as a New Type of Histone Modification. *Cell.* 2011 Sep 16;146(6):1016–28.
143. Kebede AF, Nieborak A, Shahidian LZ, Le Gras S, Richter F, Gómez DA, et al. Histone propionylation is a mark of active chromatin. *Nat Struct Mol Biol.* 2017;24(12):1048–56.
144. Simithy J, Sidoli S, Yuan Z-F, Coradin M, Bhanu N V, Marchione DM, et al. Characterization of histone acylations links chromatin modifications with metabolism. *Nat Commun.* 2017;8(1):1141.
145. Han Z, Wu H, Kim S, Yang X, Li Q, Huang H, et al. Revealing the protein propionylation activity of the histone acetyltransferase MOF (males absent on the first). *J Biol Chem.* 2018;293(9):3410–20.
146. Liu B, Lin Y, Darwanto A, Song X, Xu G, Zhang K. Identification and Characterization of Propionylation at Histone H3 Lysine 23 in Mammalian Cells. *J Biol Chem.* 2009 Nov 20;284(47):32288–95.
147. Goudarzi A, Zhang D, Huang H, Barral S, Kwon OK, Qi S, et al. Dynamic Competing Histone H4 K5K8 Acetylation and Butyrylation Are Hallmarks of Highly Active Gene Promoters. *Mol Cell.* 2016 Apr;62(2):169–80.
148. Sabari BR, Tang Z, Huang H, Yong-Gonzalez V, Molina H, Kong HE, et al. Intracellular crotonyl-CoA stimulates transcription through p300-catalyzed histone crotonylation. *Mol Cell.* 2015 Apr;58(2):203–15.
149. Pougovkina O, te Brinke H, Wanders RJA, Houten SM, de Boer VCJ. Aberrant protein acylation is a common observation in inborn errors of acyl-CoA metabolism. *J Inherit Metab Dis.* 2014;37(5):709–14.
150. Colak G, Pougovkina O, Dai L, Tan M, te Brinke H, Huang H, et al. Proteomic and Biochemical Studies of Lysine Malonylation Suggest Its Malonic Aciduria-associated Regulatory Role in Mitochondrial Function and Fatty Acid Oxidation. *Mol Cell Proteomics.* 2015;14(11):3056–71.
151. Xie Z, Zhang D, Chung D, Tang Z, Huang H, Dai L, et al. Metabolic Regulation of Gene Expression by Histone Lysine Beta-Hydroxybutyrylation. *Mol Cell.* 2016 Apr 21;62(2):194–206.
152. Liu S, Yu H, Liu Y, Liu X, Zhang Y, Bu C, et al. Chromodomain Protein CDYL Acts as a Crotonyl-CoA Hydratase to Regulate Histone Crotonylation and Spermatogenesis. *Mol Cell.* 2017;67(5):853-866.e5.
153. Du J, Zhou Y, Su X, Yu JJ, Khan S, Jiang H, et al. Sirt5 Is a NAD-Dependent Protein Lysine Demalonylase and Desuccinylase. *Science (80- ).* 2011;334(6057):806–9.

154. Park J, Chen Y, Tishkoff DX, Peng C, Tan M, Dai L, et al. SIRT5-Mediated Lysine Desuccinylation Impacts Diverse Metabolic Pathways. *Mol Cell*. 2013;50(6):919–30.
155. Rardin MJ, He W, Nishida Y, Newman JC, Carrico C, Danielson SR, et al. SIRT5 regulates the mitochondrial lysine succinylome and metabolic networks. *Cell Metab*. 2013 Dec;18(6):920–33.
156. Kumar S, Lombard DB. Functions of the sirtuin deacylase SIRT5 in normal physiology and pathobiology. *Crit Rev Biochem Mol Biol*. 2018 May 4;53(3):311–34.
157. Xie Z, Dai J, Dai L, Tan M, Cheng Z, Wu Y, et al. Lysine Succinylation and Lysine Malonylation in Histones \*. *Mol Cell Proteomics*. 2012 May 1;11(5):100–7.
158. Smestad J, Erber L, Chen Y, Maher LJ 3rd. Chromatin Succinylation Correlates with Active Gene Expression and Is Perturbed by Defective TCA Cycle Metabolism. *iScience*. 2018 Apr;2:63–75.
159. Li L, Shi L, Yang S, Yan R, Zhang D, Yang J, et al. SIRT7 is a histone desuccinylase that functionally links to chromatin compaction and genome stability. *Nat Commun*. 2016;7(1):12235.
160. Chalkiadaki A, Guarente L. The multifaceted functions of sirtuins in cancer. *Nat Rev Cancer*. 2015;15(10):608–24.
161. Wang Y, Guo YR, Liu K, Yin Z, Liu R, Xia Y, et al. KAT2A coupled with the  $\alpha$ -KGDH complex acts as a histone H3 succinyltransferase. *Nature*. 2017;552(7684):273–7.
162. Riggs TR, Hegsted DM. The effect of pantothenic acid deficiency on acetylation in rats. *Fed Proc*. 1948 Mar;7(1):297.
163. Siudeja K, Srinivasan B, Xu L, Rana A, de Jong J, Nollen EAA, et al. Impaired Coenzyme A metabolism affects histone and tubulin acetylation in *Drosophila* and human cell models of pantothenate kinase associated neurodegeneration. *EMBO Mol Med*. 2011 Dec;3(12):755–66.
164. Srinivasan B, Baratashvili M, van der Zwaag M, Kanon B, Colombelli C, Lambrechts RA, et al. Extracellular 4'-phosphopantetheine is a source for intracellular coenzyme A synthesis. *Nat Chem Biol*. 2015;11(10):784–92.
165. Iwahara T, Bonasio R, Narendra V, Reinberg D. SIRT3 Functions in the Nucleus in the Control of Stress-Related Gene Expression. *Mol Cell Biol*. 2012 Dec 15;32(24):5022 LP – 5034.
166. Haigis MC, Sinclair DA. Mammalian sirtuins: biological insights and disease relevance. *Annu Rev Pathol*. 2010;5:253–95.
167. Chalkiadaki A, Guarente L. Sirtuins mediate mammalian metabolic responses to nutrient availability. *Nat Rev Endocrinol*. 2012;8(5):287–96.
168. Zhang T, Kraus WL. SIRT1-dependent regulation of chromatin and transcription: Linking NAD<sup>+</sup> metabolism and signaling to the control of cellular functions. *Biochim Biophys Acta - Proteins Proteomics*. 2010;1804(8):1666–75.
169. Oberdoerffer P, Michan S, McVay M, Mostoslavsky R, Vann J, Park S-K, et al. SIRT1 Redistribution on Chromatin Promotes Genomic Stability but Alters Gene Expression during Aging. *Cell*. 2008 Nov 28;135(5):907–18.
170. Blank MF, Grummt I. The seven faces of SIRT7. *Transcription*. 2017/01/10. 2017;8(2):67–74.
171. Tasselli L, Zheng W, Chua KF. SIRT6: Novel Mechanisms and Links to Aging and Disease. *Trends Endocrinol Metab*. 2017 Mar 1;28(3):168–85.
172. Olpin SE, Bates CJ. Lipid metabolism in riboflavin-deficient rats: 2. Mitochondrial fatty acid oxidation and the microsomal desaturation pathway. *Br J Nutr*. 2007/03/09. 1982;47(3):589–96.
173. Veitch K, Draye JP, Van Hoof F, Sherratt HSA. Effects of riboflavin deficiency and clofibrate treatment on the five acyl-CoA dehydrogenases in rat liver mitochondria. *Biochem J*. 1988 Sep 1;254(2):477–81.
174. Nagao M, Tanaka K. FAD-dependent regulation of transcription, translation, post-translational processing, and post-processing stability of various mitochondrial acyl-CoA dehydrogenases and of electron transfer flavoprotein and the site of holoenzyme formation. *J Biol Chem*. 1992;267(25):17925–32.
175. Tang J, Hegeman MA, Hu J, Xie M, Shi W, Jiang Y, et al. Severe riboflavin deficiency induces alterations in the hepatic proteome of starter Pekin ducks. *Br J Nutr*. 2017/11/29. 2017;118(9):641–50.
176. Liu Y-Y, Shigematsu Y, Nakai A, Kikawa Y, Saito M, Fukui T, et al. The effects of biotin deficiency on organic acid metabolism: Increase in propionyl coenzyme A-related organic acids in biotin-deficient rats. *Metabolism*. 1993;42(11):1392–7.

177. Hernández-Vázquez A, Wolf B, Pindolia K, Ortega-Cuellar D, Hernández-González R, Heredia-Antúnez A, et al. Biotinidase knockout mice show cellular energy deficit and altered carbon metabolism gene expression similar to that of nutritional biotin deprivation: Clues for the pathogenesis in the human inherited disorder. *Mol Genet Metab*. 2013;110(3):248–54.
178. Schwab MA, Sauer SW, Okun JG, Nijtmans LG, Rodenburg RJ, van den Heuvel LP, et al. Secondary mitochondrial dysfunction in propionic aciduria: a pathogenic role for endogenous mitochondrial toxins. *Biochem J*. 2006;05/12. 2006;398(1):107–12.
179. Chandler RJ, Zerfas PM, Shanske S, Sloan J, Hoffmann V, DiMauro S, et al. Mitochondrial dysfunction in mut methylmalonic acidemia. *FASEB J*. 2009 Apr 1;23(4):1252–61.
180. Toyoshima S, Watanabe F, Saido H, Miyatake K, Nakano Y. Methylmalonic Acid Inhibits Respiration in Rat Liver Mitochondria. *J Nutr*. 1995 Nov 1;125(11):2846–50.
181. Narasimhan P, Sklar R, Murrell M, Swanson RA, Sharp FR. Methylmalonyl-CoA Mutase Induction by Cerebral Ischemia and Neurotoxicity of the Mitochondrial Toxin Methylmalonic Acid. *J Neurosci*. 1996 Nov 15;16(22):7336 LP – 7346.
182. Krahenbuhl S, Ray DB, Stabler SP, Allen RH, Brass EP. Increased hepatic mitochondrial capacity in rats with hydroxy-cobalamin[c-lactam]-induced methylmalonic aciduria. *J Clin Invest*. 1990/12/01. 1990;86(6):2054–61.
183. Kölker S, Schwab M, Hörster F, Sauer S, Hinz A, Wolf NI, et al. Methylmalonic Acid, a Biochemical Hallmark of Methylmalonic Acidurias but No Inhibitor of Mitochondrial Respiratory Chain\*. *J Biol Chem*. 2003;278(48):47388–93.
184. Krahenbuhl S, Chang M, Brass EP, Hoppel CL. Decreased activities of ubiquinol:ferricytochrome c oxidoreductase (complex III) and ferrocyclochrome c: oxygen oxidoreductase (complex IV) in liver mitochondria from rats with hydroxycobalamin[c-lactam]-induced methylmalonic aciduria. *J Biol Chem*. 1991;266(31):20998–1003.
185. Brusque AM, Borba Rosa R, Chuck PF, Dalcin KB, Ribeiro CAJ, Silva CG, et al. Inhibition of the mitochondrial respiratory chain complex activities in rat cerebral cortex by methylmalonic acid. *Neurochem Int*. 2002;40(7):593–601.
186. Shen H, Campanello GC, Flicker D, Grabarek Z, Hu J, Luo C, et al. The Human Knockout Gene CLYBL Connects Itaconate to Vitamin B 12. *Cell*. 2017;106(0):21317–22.
187. Holmström KM, Finkel T. Cellular mechanisms and physiological consequences of redox-dependent signalling. *Nat Rev Mol Cell Biol*. 2014;15(6):411–21.
188. McDonald LJ, Murad F. Nitric Oxide and cGMP Signaling. In: Ignarro L, Murad FBT-A in P, editors. *Advances in Pharmacology*. Academic Press; 1995. p. 263–75.
189. Finkel T, Holbrook NJ. Oxidants, oxidative stress and the biology of ageing. *Nature*. 2000;408(6809):239–47.
190. Freeman H, Shimomura K, Cox RD, Ashcroft FM. Nicotinamide nucleotide transhydrogenase: a link between insulin secretion, glucose metabolism and oxidative stress. *Biochem Soc Trans*. 2006 Nov;34(Pt 5):806–10.
191. Kumar B, Koul S, Khandrika L, Meacham RB, Koul HK. Oxidative Stress Is Inherent in Prostate Cancer Cells and Is Required for Aggressive Phenotype. *Cancer Res*. 2008 Mar 15;68(6):1777 LP – 1785.
192. Pi J, Collins S. Reactive oxygen species and uncoupling protein 2 in pancreatic  $\beta$ -cell function. *Diabetes, Obes Metab*. 2010 Oct 1;12(s2):141–8.
193. Sabens Liedhegner EA, Gao X-H, Mיעאל JJ. Mechanisms of altered redox regulation in neurodegenerative diseases—focus on S--glutathionylation. *Antioxid Redox Signal*. 2012 Mar;16(6):543–66.
194. Mitchell P. Coupling of Phosphorylation to Electron and Hydrogen Transfer by a Chemi-Osmotic type of Mechanism. *Nature*. 1961;191(4784):144–8.
195. Boveris A. Mitochondrial Production of Superoxide Radical and Hydrogen Peroxide BT - Tissue Hypoxia and Ischemia. In: Reivich M, Coburn R, Lahiri S, Chance B, editors. *Advances in Experimental Medicine and Biology*. Boston, MA: Springer US; 1977. p. 67–82.
196. Gonçalves RLS, Quinlan CL, Perevoshchikova IV, Hey-Mogensen M, Brand MD. Sites of Superoxide and Hydrogen Peroxide Production by Muscle Mitochondria Assessed ex Vivo under Conditions Mimicking Rest and Exercise \*. *J Biol Chem*. 2015 Jan 2;290(1):209–27.

197. Kussmaul L, Hirst J. The mechanism of superoxide production by NADH:ubiquinone oxidoreductase (complex I) from bovine heart mitochondria. *Proc Natl Acad Sci*. 2006 May 16;103(20):7607 LP – 7612.
198. Grivennikova VG, Vinogradov AD. Partitioning of superoxide and hydrogen peroxide production by mitochondrial respiratory complex I. *Biochim Biophys Acta - Bioenerg*. 2013;1827(3):446–54.
199. Quinlan CL, Orr AL, Perevoshchikova I V, Treberg JR, Ackrell BA, Brand MD. Mitochondrial Complex II Can Generate Reactive Oxygen Species at High Rates in Both the Forward and Reverse Reactions\*. *J Biol Chem*. 2012;287(32):27255–64.
200. Siebels I, Dröse S. Q-site inhibitor induced ROS production of mitochondrial complex II is attenuated by TCA cycle dicarboxylates. *Biochim Biophys Acta - Bioenerg*. 2013;1827(10):1156–64.
201. Jardim-Messeder D, Caverzan A, Rauber R, de Souza Ferreira E, Margis-Pinheiro M, Galina A. Succinate dehydrogenase (mitochondrial complex II) is a source of reactive oxygen species in plants and regulates development and stress responses. *New Phytol*. 2015 Nov;208(3):776–89.
202. Lambert AJ, Brand MD. Inhibitors of the Quinone-binding Site Allow Rapid Superoxide Production from Mitochondrial NADH:Ubiquinone Oxidoreductase (Complex I)\*. *J Biol Chem*. 2004;279(38):39414–20.
203. Muller FL, Roberts AG, Bowman MK, Kramer DM. Architecture of the Qo Site of the Cytochrome bc<sub>1</sub> Complex Probed by Superoxide Production. *Biochemistry*. 2003 Jun 1;42(21):6493–9.
204. Starkov AA, Fiskum G, Chinopoulos C, Lorenzo BJ, Browne SE, Patel MS, et al. Mitochondrial alpha-ketoglutarate dehydrogenase complex generates reactive oxygen species. *J Neurosci*. 2004 Sep;24(36):7779–88.
205. Fisher-Wellman KH, Gilliam LAA, Lin C-T, Cathey BL, Lark DS, Darrell Neuffer P. Mitochondrial glutathione depletion reveals a novel role for the pyruvate dehydrogenase complex as a key H<sub>2</sub>O<sub>2</sub>-emitting source under conditions of nutrient overload. *Free Radic Biol Med*. 2013 Dec;65:1201–8.
206. Quinlan CL, Goncalves RLS, Hey-Mogensen M, Yadava N, Bunik VI, Brand MD. The 2-Oxoacid Dehydrogenase Complexes in Mitochondria Can Produce Superoxide/Hydrogen Peroxide at Much Higher Rates Than Complex I\*. *J Biol Chem*. 2014;289(12):8312–25.
207. Gardner PR. Aconitase: sensitive target and measure of superoxide. *Methods Enzymol*. 2002;349:9–23.
208. Ternette N, Yang M, Laroya M, Kitagawa M, O'Flaherty L, Wolhuter K, et al. Inhibition of Mitochondrial Aconitase by Succination in Fumarate Hydratase Deficiency. *Cell Rep*. 2013 Mar 28;3(3):689–700.
209. Orr AL, Quinlan CL, Perevoshchikova I V, Brand MD. A Refined Analysis of Superoxide Production by Mitochondrial sn-Glycerol 3-Phosphate Dehydrogenase \*. *J Biol Chem*. 2012 Dec 14;287(51):42921–35.
210. Forman JH, Kennedy J. Superoxide production and electron transport in mitochondrial oxidation of dihydroorotic acid. *J Biol Chem*. 1975 Jun 10;250(11):4322–6.
211. Giorgio M, Migliaccio E, Orsini F, Paolucci D, Moroni M, Contursi C, et al. Electron transfer between cytochrome c and p66Shc generates reactive oxygen species that trigger mitochondrial apoptosis. *Cell*. 2005 Jul;122(2):221–33.
212. Di Lisa F, Kaludercic N, Carpi A, Menabò R, Giorgio M. Mitochondrial pathways for ROS formation and myocardial injury: the relevance of p66Shc and monoamine oxidase. *Basic Res Cardiol*. 2009;104(2):131–9.
213. Quinlan CL, Perevoshchikova I V, Hey-Mogensen M, Orr AL, Brand MD. Sites of reactive oxygen species generation by mitochondria oxidizing different substrates. *Redox Biol*. 2013;1(1):304–12.
214. Han D, Antunes F, Canali R, Rettori D, Cadenas E. Voltage-dependent Anion Channels Control the Release of the Superoxide Anion from Mitochondria to Cytosol\*. *J Biol Chem*. 2003;278(8):5557–63.
215. Mikkelsen RB, Wardman P. Biological chemistry of reactive oxygen and nitrogen and radiation-induced signal transduction mechanisms. *Oncogene*. 2003;22(37):5734–54.
216. Cardoso AR, Chausse B, da Cunha FM, Luevano-Martinez LA, Marazzi TB, Pessoa PS, et al. Mitochondrial compartmentalization of redox processes. *Free Radic Biol Med*. 2012/05/09. 2012;52(11–12):2201–8.
217. Mathai JC, Sitaramam V. Stretch sensitivity of transmembrane mobility of hydrogen peroxide through voids in the bilayer. Role of cardiolipin. *J Biol Chem*. 1994 Jul;269(27):17784–93.

218. Antunes F, Cadenas E. Estimation of H<sub>2</sub>O<sub>2</sub> gradients across biomembranes. *FEBS Lett.* 2000 Jun 16;475(2):121–6.
219. Sousa-Lopes A, Antunes F, Cyrne L, Marinho HS. Decreased cellular permeability to H<sub>2</sub>O<sub>2</sub> protects *Saccharomyces cerevisiae* cells in stationary phase against oxidative stress. *FEBS Lett.* 2004 Dec;578(1–2):152–6.
220. Bienert GP, Møller ALB, Kristiansen KA, Schulz A, Møller IM, Schjoerring JK, et al. Specific Aquaporins Facilitate the Diffusion of Hydrogen Peroxide across Membranes \*. *J Biol Chem.* 2007 Jan 12;282(2):1183–92.
221. Winterbourn CC, Hampton MB. Thiol chemistry and specificity in redox signaling. *Free Radic Biol Med.* 2008;45(5):549–61.
222. Vestergaard C, Flyvbjerg H, Møller I. Intracellular Signaling by Diffusion: Can Waves of Hydrogen Peroxide Transmit Intracellular Information in Plant Cells? Vol. 3, *Frontiers in Plant Science.* 2012.
223. Schwarzländer M, Logan DC, Johnston IG, Jones NS, Meyer AJ, Fricker MD, et al. Pulsing of membrane potential in individual mitochondria: a stress-induced mechanism to regulate respiratory bioenergetics in *Arabidopsis*. *Plant Cell.* 2012 Mar;24(3):1188–201.
224. Hamanaka RB, Weinberg SE, Reczek CR, Chandel NS. The Mitochondrial Respiratory Chain Is Required for Organismal Adaptation to Hypoxia. *Cell Rep.* 2016/04/14. 2016;15(3):451–9.
225. Chandel NS, McClintock DS, Feliciano CE, Wood TM, Melendez JA, Rodriguez AM, et al. Reactive Oxygen Species Generated at Mitochondrial Complex III Stabilize Hypoxia-inducible Factor-1α during Hypoxia. *J Biol Chem.* 2000 Aug 18;275(33):25130–8.
226. Brunelle JK, Bell EL, Quesada NM, Vercauteren K, Tiranti V, Zeviani M, et al. Oxygen sensing requires mitochondrial ROS but not oxidative phosphorylation. *Cell Metab.* 2005 Jun 1;1(6):409–14.
227. Guzy RD, Hoyos B, Robin E, Chen H, Liu L, Mansfield KD, et al. Mitochondrial complex III is required for hypoxia-induced ROS production and cellular oxygen sensing. *Cell Metab.* 2005 Jun;1(6):401–8.
228. Sullivan LB, Martinez-Garcia E, Nguyen H, Mullen AR, Dufour E, Sudarshan S, et al. The proto-oncometabolite fumarate binds glutathione to amplify ROS-dependent signaling. *Mol Cell.* 2013 Jul;51(2):236–48.
229. Zheng L, Cardaci S, Jerby L, MacKenzie ED, Sciacovelli M, Johnson TI, et al. Fumarate induces redox-dependent senescence by modifying glutathione metabolism. *Nat Commun.* 2015;6(1):6001.
230. Adam J, Hatipoglu E, O'Flaherty L, Ternette N, Sahgal N, Lockstone H, et al. Renal Cyst Formation in Fh1-Deficient Mice Is Independent of the Hif/Phd Pathway: Roles for Fumarate in KEAP1 Succination and Nrf2 Signaling. *Cancer Cell.* 2011 Oct 18;20(4):524–37.
231. Merkley ED, Metz TO, Smith RD, Baynes JW, Frizzell N. The succinated proteome. *Mass Spectrom Rev.* 2014;33(2):98–109.
232. Yang M, Ternette N, Su H, Dabiri R, Kessler BM, Adam J, et al. The Succinated Proteome of FH-Mutant Tumours. Vol. 4, *Metabolites* . 2014.
233. Bardella C, El-Bahrawy M, Frizzell N, Adam J, Ternette N, Hatipoglu E, et al. Aberrant succination of proteins in fumarate hydratase-deficient mice and HLRCC patients is a robust biomarker of mutation status. *J Pathol.* 2011 Sep 1;225(1):4–11.
234. Kaspar JW, Niture SK, Jaiswal AK. Nrf2:Inrf2 (Keap1) signaling in oxidative stress. *Free Radic Biol Med.* 2009/08/07. 2009 Nov 1;47(9):1304–9.
235. Kerins MJ, Vashisht AA, Liang BX-T, Duckworth SJ, Praslicka BJ, Wohlschlegel JA, et al. Fumarate Mediates a Chronic Proliferative Signal in Fumarate Hydratase-Inactivated Cancer Cells by Increasing Transcription and Translation of Ferritin Genes. *Mol Cell Biol.* 2017 Jun 1;37(11):e00079-17.
236. Tyrakis PA, Yurkovich ME, Sciacovelli M, Papachristou EK, Bridges HR, Gaude E, et al. Fumarate Hydratase Loss Causes Combined Respiratory Chain Defects. *Cell Rep.* 2017/10/27. 2017;21(4):1036–47.
237. Blatnik M, Frizzell N, Thorpe SR, Baynes JW. Inactivation of Glyceraldehyde-3-Phosphate Dehydrogenase by Fumarate in Diabetes. *Diabetes.* 2008 Jan 1;57(1):41 LP – 49.
238. Kornberg MD, Bhargava P, Kim PM, Putluri V, Snowman AM, Putluri N, et al. Dimethyl fumarate targets GAPDH and aerobic glycolysis to modulate immunity. *Science (80- )*. 2018 Apr 27;360(6387):449 LP – 453.
239. Menegon S, Columbano A, Giordano S. The Dual Roles of NRF2 in Cancer. *Trends Mol Med.* 2016;22(7):578–93.

240. Alderson NL, Wang Y, Blatnik M, Frizzell N, Walla MD, Lyons TJ, et al. S-(2-Succinyl)cysteine: A novel chemical modification of tissue proteins by a Krebs cycle intermediate. *Arch Biochem Biophys*. 2006;450(1):1–8.
241. Frizzell N, Rajesh M, Jepson MJ, Nagai R, Carson JA, Thorpe SR, et al. Succination of thiol groups in adipose tissue proteins in diabetes: succination inhibits polymerization and secretion of adiponectin. *J Biol Chem*. 2009 Sep;284(38):25772–81.
242. Adam J, Ramracheya R, Chibalina M V, Ternette N, Hamilton A, Tarasov AI, et al. Fumarate Hydratase Deletion in Pancreatic  $\beta$ 2 Cells Leads to Progressive Diabetes. *Cell Rep*. 2017 Sep 26;20(13):3135–48.
243. Ooi A, Wong J-C, Petillo D, Roossien D, Perrier-Trudova V, Whitten D, et al. An Antioxidant Response Phenotype Shared between Hereditary and Sporadic Type 2 Papillary Renal Cell Carcinoma. *Cancer Cell*. 2011 Oct 18;20(4):511–23.
244. Ashrafiyan H, Czibik G, Bellahcene M, Aksentijević D, Smith AC, Mitchell SJ, et al. Fumarate Is Cardioprotective via Activation of the Nrf2 Antioxidant Pathway. *Cell Metab*. 2012 Mar 7;15(3):361–71.
245. Mills EL, Ryan DG, Prag HA, Dikovskaya D, Menon D, Zaslona Z, et al. Itaconate is an anti-inflammatory metabolite that activates Nrf2 via alkylation of KEAP1. *Nature*. 2018;556(7699):113–7.
246. Hayes JD, Dinkova-Kostova AT. The Nrf2 regulatory network provides an interface between redox and intermediary metabolism. *Trends Biochem Sci*. 2014;39(4):199–218.
247. Bambouskova M, Gorvel L, Lampropoulou V, Sergushichev A, Loginicheva E, Johnson K, et al. Electrophilic properties of itaconate and derivatives regulate the I $\kappa$ B $\zeta$ –ATF3 inflammatory axis. *Nature*. 2018;556(7702):501–4.
248. Arias-Mayenco I, González-Rodríguez P, Torres-Torrel H, Gao L, Fernández-Agüera MC, Bonilla-Henao V, et al. Acute O<sub>2</sub> Sensing: Role of Coenzyme QH<sub>2</sub>/Q Ratio and Mitochondrial ROS Compartmentalization. *Cell Metab*. 2018 Jul 3;28(1):145–158.e4.
249. Mitchell SJ, Bernier M, Aon MA, Cortassa S, Kim EY, Fang EF, et al. Nicotinamide Improves Aspects of Healthspan, but Not Lifespan, in Mice. *Cell Metab*. 2018 Mar 6;27(3):667–676.e4.
250. Hong G, Zheng D, Zhang L, Ni R, Wang G, Fan G-C, et al. Administration of nicotinamide riboside prevents oxidative stress and organ injury in sepsis. *Free Radic Biol Med*. 2018;123:125–37.
251. Shi W, Hegeman MA, van Dartel DAM, Tang J, Suarez M, Swarts H, et al. Effects of a wide range of dietary nicotinamide riboside (NR) concentrations on metabolic flexibility and white adipose tissue (WAT) of mice fed a mildly obesogenic diet. *Mol Nutr Food Res*. 2017 Aug;61(8).
252. Chouchani ET, Pell VR, Gaude E, Aksentijević D, Sundier SY, Robb EL, et al. Ischaemic accumulation of succinate controls reperfusion injury through mitochondrial ROS. *Nature*. 2014;515(7527):431–5.
253. Wei C-C, Kong Y-Y, Li G-Q, Guan Y-F, Wang P, Miao C-Y. Nicotinamide mononucleotide attenuates brain injury after intracerebral hemorrhage by activating Nrf2/HO-1 signaling pathway. *Sci Rep*. 2017;7(1):717.
254. Ren X, Sun H, Zhang C, Li C, Wang J, Shen J, et al. Protective function of pyridoxamine on retinal photoreceptor cells via activation of the p-Erk1/2/Nrf2/Trx/ASK1 signalling pathway in diabetic mice. *Mol Med Rep*. 2016;14(1):420–4.
255. Zhang P, Tsuchiya K, Kinoshita T, Kushiya H, Suidasari S, Hatakeyama M, et al. Vitamin B6 Prevents IL-1 $\beta$  Protein Production by Inhibiting NLRP3 Inflammasome Activation. *J Biol Chem*. 2016 Nov 1;291(47):24517–27.
256. Roh T, De U, Lim SK, Kim MK, Choi SM, Lim DS, et al. Detoxifying effect of pyridoxine on acetaminophen-induced hepatotoxicity via suppressing oxidative stress injury. *Food Chem Toxicol*. 2018 Apr;114:11–22.
257. Misra UK, Kalita J, Singh SK, Rahi SK. Oxidative Stress Markers in Vitamin B12 Deficiency. *Mol Neurobiol*. 2017 Mar;54(2):1278–84.
258. Richard E, Jorge-Finnigan A, Garcia-Villoria J, Merinero B, Desviat LR, Gort L, et al. Genetic and cellular studies of oxidative stress in methylmalonic aciduria (MMA) cobalamin deficiency type C (cblC) with homocystinuria (MMACHC). *Hum Mutat*. 2009 Nov 1;30(11):1558–66.

259. Bunik VI, Fernie AR. Metabolic control exerted by the 2-oxoglutarate dehydrogenase reaction: a cross-kingdom comparison of the crossroad between energy production and nitrogen assimilation. *Biochem J.* 2009;422(3):405–21.
260. Ambrus A, Nemeria NS, Torocsik B, Tretter L, Nilsson M, Jordan F, et al. Formation of reactive oxygen species by human and bacterial pyruvate and 2-oxoglutarate dehydrogenase multienzyme complexes reconstituted from recombinant components. *Free Radic Biol Med.* 2015;89:642–50.
261. Zera K, Zastre J. Stabilization of the hypoxia-inducible transcription Factor-1 alpha (HIF-1α) in thiamine deficiency is mediated by pyruvate accumulation. *Toxicol Appl Pharmacol.* 2018;355:180–8.
262. Tapias V, Jainuddin S, Ahuja M, Stack C, Elipenahli C, Vignisse J, et al. Benfotiamine treatment activates the Nrf2/ARE pathway and is neuroprotective in a transgenic mouse model of tauopathy. *Hum Mol Genet.* 2018 Aug 15;27(16):2874–92.
263. Fan J, Ye J, Kamphorst JJ, Shlomi T, Thompson CB, Rabinowitz JD. Quantitative flux analysis reveals folate-dependent NADPH production. *Nature.* 2014;510(7504):298–302.
264. Tsuchiya Y, Zhyvoloup A, Baković J, Thomas N, Yu BYK, Das S, et al. Protein CoAlation and antioxidant function of coenzyme A in prokaryotic cells. *Biochem J.* 2018 Jun 6;475(11):1909–37.
265. Tsuchiya Y, Peak-Chew SY, Newell C, Miller-Aidoo S, Mangal S, Zhyvoloup A, et al. Protein CoAlation: a redox-regulated protein modification by coenzyme A in mammalian cells. *Biochem J.* 2017 Jul 11;474(14):2489–508.
266. Luo J, Jankowski V, Henning L, Schlüter H, Zidek W, Jankowski J. Endogenous coenzyme A glutathione disulfide in human myocardial tissue. *J Endocrinol Invest.* 2006;29(8):688–93.



# 7

## The effect of a single bout of exercise on vitamin B2 status is not different between high-fit and low-fit females

Joëlle J.E. Janssen<sup>1,2</sup>, Bart Lagerwaard<sup>1,3</sup>, Arie G. Nieuwenhuizen<sup>1</sup>,  
Silvie Timmers<sup>1</sup>, Vincent C.J. de Boer<sup>1</sup>, Jaap Keijer<sup>1</sup>

<sup>1</sup> *Human and Animal Physiology, Wageningen University and Research,  
P.O. Box 338, 6700 AH, Wageningen, the Netherlands*

<sup>2</sup> *Cell Biology and Immunology, Wageningen University and Research,  
P.O. Box 338, 6700 AH, Wageningen, the Netherlands*

<sup>3</sup> *TI Food and Nutrition, P.O. Box 557, 6700 AN, Wageningen, the Netherlands*

**Nutrients** 2021; Nov 16;13(11):4097

doi: 10.3390/nu13114097

## Abstract

High-fitness individuals have been suggested to be at risk of a poor vitamin B2 (riboflavin) status due to a potentially higher vitamin B2 demand, as measured by the erythrocyte glutathione reductase (EGR) activation coefficient (EGRAC). Longer-term exercise interventions have been shown to result in a lower vitamin B2 status, but studies are contradictory. Short-term exercise effects potentially contribute to discrepancies between studies but have only been tested in limited study populations. This study investigated if vitamin B2 status, measured by EGRAC, is affected by a single exercise bout in females who differ in fitness levels, representing a difference in long-term physical activity. At baseline and overnight after a 60-minute cycling bout at 70%  $\dot{V}O_{2\text{peak}}$ , EGR activity and EGRAC were measured in 31 young female adults, divided into a high-fit ( $\dot{V}O_{2\text{peak}} \geq 47$  mL/kg/min, N = 15) and low-fit ( $\dot{V}O_{2\text{peak}} \leq 37$  mL/kg/min, N = 16) group. A single exercise bout significantly increased EGR activity in high-fit and low-fit females ( $P_{\text{exercise}} = 0.006$ ). This response was not affected by fitness level ( $P_{\text{exercise} \times \text{group}} = 0.256$ ). The effect of exercise on EGRAC was not significant ( $P_{\text{exercise}} = 0.079$ ) and not influenced by EGR activity. The exercise response of EGRAC was not significantly different between high-fit and low-fit females ( $P_{\text{exercise} \times \text{group}} = 0.141$ ). Thus, a single exercise bout increased EGR activity, but did not affect EGRAC, indicating that vitamin B2 status was not affected. The exercise response on EGRAC and EGR did not differ between high-fit and low-fit females.

## Introduction

Exercise requires chemical energy (adenosine triphosphate, ATP) to enable muscle contractions and relaxations (1). At the same time, exercise generates reactive oxygen species (ROS) as a by-product, which enhance antioxidant defense systems (2–4), including those that depend on glutathione (3). One essential gatekeeper of energy and redox metabolism is vitamin B2 (riboflavin) (5). Vitamin B2 acts as a precursor for the electron carriers flavin mononucleotide (FMN) and flavin adenine dinucleotide (FAD), which are both essential mitochondrial cofactors of oxidative phosphorylation (OXPHOS) complexes I and II, respectively (6,7). In addition, FAD is an essential cofactor for the antioxidant enzyme glutathione reductase (GR) (6,8) that catalyzes the conversion of oxidized glutathione (GSSG) to reduced glutathione (GSH), thereby clearing ROS and supporting redox homeostasis. Since aerobic exercise puts a high demand on processes that are essentially dependent on the vitamin B2-derived cofactors FMN and FAD, especially athletes and recreationally active individuals, i.e., high-fitness (high-fit) individuals, are thought to benefit from an optimal vitamin B2 status (9).

In exercise studies, systemic vitamin B2 status is commonly assessed by the erythrocyte glutathione reductase activation coefficient (EGRAC) biomarker (9,10). This coefficient represents the ratio between erythrocyte GR (EGR) activity in the absence and presence of its cofactor FAD (11,12). Higher GR activity in the presence of FAD compared to the activity in its absence reflects the incomplete occupancy of GR by FAD and therefore a lower vitamin B2 status (13). Using this EGRAC assay, studies have demonstrated that longer-term exercise interventions of three weeks up to three months resulted in a lower vitamin B2 status (14–19). However, not all exercise studies confirm these findings (20,21); one study failed to show a change in vitamin B2 status (20), whereas another study even showed an improved vitamin B2 status following a longer-term exercise intervention (21). Large observational studies comparing the vitamin B2 status in athletes and recreationally active individuals also show inconsistent results (22–27). Differences in experimental set-up, including the selection of the study population (14,15,24,26–28,16–23) and the assessment of subjects' fitness levels (24,27) could be of importance. However, the inconsistent findings could also be related to alterations in the EGR enzymatic activity itself. EGR enzymatic activity was shown to increase upon a longer-term exercise intervention (21), but has also been found to alter upon a single bout of exercise (21,28–30) and importantly, this has been linked to a lower EGRAC (21,28). This implies that the long- and short-term effects of exercise on vitamin B2 status parameters could differ, but this has not yet been investigated, nor has the effect of long-term exercise on the EGRAC response to short-term exercise.

This study investigates the effect of a single bout of exercise, i.e., short-term exercise, on EGRAC and EGR activity in high-fit compared to low-fit females, i.e., females that differ in long-term physical activity. We chose to study females, because females have been shown to be at risk for a poor vitamin B2 status (31), especially upon exercise (14,16). We hypothesize that a single bout of exercise affects these vitamin B2 status parameters, and that the longer-term physiological adaptations to regular aerobic exercise will increase vitamin B2 demand, resulting in a higher EGRAC and lower vitamin B2 status in high-fit females as compared to low-fit females in response to a single bout of exercise.

## Materials and Methods

### Ethical approval

The protocol for collection and handling of human samples was ethically approved by the medical ethical committee of Wageningen University and Research with reference number NL70136.081.19 and registered in the Dutch Trial Register (NL7891). All procedures performed were in accordance with the ethical standards of the institutional and/or national research committee and with the 1964 Helsinki Declaration. Written informed consent was obtained from all individual subjects included in the study.

### Study subjects

Healthy young females (18–28 years of age, BMI 18.5–25 kg/m<sup>2</sup>) were recruited from the local university and community population. Exclusion criteria were: history of cardiovascular, respiratory, hematological or metabolic disease; use of prescribed chronic medication; anemia (hemoglobin concentration < 12 g/dL); blood donation within two months before the start of the study; smoking (> 5 cigarettes per week); veganism; recreational drug use or over-the-counter drug use during the study; supplement use (performance enhancers or supplements containing vitamin B2); pregnancy or lactating. Subjects were selected if they had a  $\dot{V}O_{2\text{peak}} \geq 47$  mL/kg/min (high-fit group) or  $\leq 37$  mL/kg/min (low-fit group). This was determined using a maximal exercise test on a bicycle ergometer (Corival CPET, Lode, the Netherlands), and measured using the screening protocol of Lagerwaard et al. (2019) (32). The power analysis was based on findings from previous studies that examined the effect of exercise interventions on vitamin B2 status (14,16,17). This yielded a sample size of N = 14 per group using the G\*power software program with 90% power ( $\beta$ ), 0.05 level of significance ( $\alpha$ ), a two-tailed confidence interval, and comparing two dependent (paired) means. Taking a 10% drop-out rate into account, this resulted in a sample size of N = 16 per group.

Sixteen high-fit subjects (representing physically active, trained individuals) and sixteen low-fit subjects (representing untrained individuals) were included. The  $\dot{V}O_{2\text{peak}}$  data and results of the skeletal muscle mitochondrial capacity of these included subjects have been published previously by our group (33). A total of 111 maximal exercise tests were conducted to result in the desired sample size of 32 ( $N = 16$  per group), i.e., 79 subjects had a  $\dot{V}O_{2\text{peak}} \geq 37$  and  $\leq 47$  mL/kg/min. The use of oral contraceptives (OC) was not excluded; only the use of monophasic OC containing low synthetic estradiol and progesterone was allowed and was controlled for ( $N = 7$  in the high-fit and  $N = 6$  in the low-fit group). The 17 $\beta$ -estradiol levels were measured using a chemiluminescent immunoassay on a Lumipulse G1200 analyzer (Fujirebio Inc) at the Erasmus Medical Centre (NL) and were not significantly different between those high-fit and low-fit females that did not use OC (Table 1) and were not correlated with basal EGRAC (Supplementary Figure S1).

### Study design

Subjects refrained from heavy physical exercise 48 hours prior to the first study day and from any physical exercise and consumption of alcohol 24 hours prior to the first study day. Subjects adhered to dietary guidelines 24 hours before each study day, which included a list of product choices containing low levels of vitamin B2, and recorded their food intake in a food diary. They also consumed a standardized evening meal (73% carbohydrates/16% protein/11% fat, 1818 kJ) before 8:00 PM.; subjects were not allowed to eat after 8:00 PM. After the overnight fast, blood was collected on the morning of the first study day (baseline) and overnight after a single bout of exercise, i.e., the morning of the second study day (21 hours post-exercise). Subjects received breakfast and after two hours, subjects completed an individualized exercise protocol consisting of 60 minutes cycling on an electrically braked bicycle ergometer (Corival CPET, Lode, the Netherlands) at a workload aiming to equal 70% of their individual  $\dot{V}O_{2\text{peak}}$  that was determined during the maximal exercise test. Oxygen consumption, carbon dioxide production, and air flow were measured using the MAX-II metabolic cart (AEI technologies, Landivisiau, France). Exhaled air was continuously sampled from a mixing chamber and averaged over 15 second time windows. Oxygen consumption was measured the first and last 15 minutes of the exercise test and used to confirm the relative workload. Body fat percentage was measured according to the four-site method by Durnin–Womersley using the skinfold measurements of the triceps, biceps, sub scapula, and supra iliac, measured using a skinfold calliper (Harpenden, UK). After the exercise, the protocol subjects went home and refrained from moderate to heavy physical activity, kept low levels of light physical activity, and refrained from alcohol consumption until blood collection

on the second study day. Physical activity was monitored using a wearable accelerometer (wGT3X-BT, Actigraph, FL, USA) during this period. Habitual vitamin B2 intake was determined via a food frequency questionnaire (FFQ) that assessed dietary intake in the past four weeks (34).

### Blood sampling and hemolysate preparation

Blood samples (1 x 6 mL) were collected from the subjects by venapuncture in vacutainers containing dipotassium (K<sub>2</sub>-) ethylenediaminetetraacetic acid (EDTA) (K<sub>2</sub>-EDTA, BD Biosciences, Vianen, the Netherlands), kept on ice-water, and processed within 30 minutes. Blood was centrifugated for 10 minutes at 1200g at 4°C. Plasma and buffy coat were removed and 2 mL of erythrocytes were collected and transferred to a new sample tube. Erythrocytes were washed twice in 10 mL of 1X Dulbecco's phosphate-buffered saline (DPBS, Thermo Fisher Scientific, Pittsburgh, PA, USA) and centrifugated for 5 minutes at 2000g at 4°C. The supernatant was discarded, and the erythrocyte pellet was gently resuspended in sterile Milli-Q (MQ) to induce an osmotic burst. Hemolysates were stored at -20°C for 30 minutes and transferred to -80°C afterwards. EGRAC assays were performed within six months after blood collection. For the EGRAC assay, hemolysates were thawed on ice, 10x diluted with MQ, and centrifugated for 2 minutes at 13,000g at 4°C to remove cellular debris. The supernatant was transferred to a new vial and protein content was determined. Thawed hemolysates and samples were kept on ice and protected from light.

### Protein content determination

The hemolysate protein content was determined in 100x diluted samples using the DC Protein Assay kit (Bio-Rad, Hercules, CA, USA) according to the manufacturer's protocol and a standard curve of bovine serum albumin (BSA, Sigma-Aldrich, St. Louis, MO, USA) in MQ. Absorbance was measured using a BioTek Synergy HT plate reader. Hemolysate protein content was optimized (0 – 300 µg) to achieve linearity of the EGR enzymatic reaction within the 30-minute measurement period and the absorbance detection limit. The final protein input was set to 112.5 µg.

### Erythrocyte glutathione reductase activity coefficient (EGRAC) assay

The EGRAC assay quantifies the reduction of oxidized glutathione (GSSG) to reduced glutathione (GSH) with the concomitant oxidation of NADPH to NADP<sup>+</sup> in the presence and absence of its essential cofactor FAD (11,12). The assay was based on the method of Hill et al. (2009) (35) and optimized for the in-house analysis. All reagents were prepared fresh daily. Samples were diluted to 5 µg/µL protein and a 270 µL sample was incubated for 30 minutes at 37°C in the presence of 30 µL 15 µM FAD (final concentration 1.5 µM, Sigma-Aldrich, St. Louis, MO, USA)

dissolved in 100 mM/3.4 mM H<sub>2</sub>KPO<sub>4</sub>/EDTA buffer pH 7.6 (for FAD-stimulated EGR activity) or with 30 µL H<sub>2</sub>KPO<sub>4</sub>/EDTA buffer only (for unstimulated EGR activity). After incubation, a 25 µL sample was aliquoted in octuplicate in a 96-well microplate (final protein input 112.5 µg). To each sample, 125 µL of the cofactor 0.33 mM beta-nicotinamide adenine dinucleotide (NADPH, final concentration 0.16 mM, Sigma-Aldrich) in H<sub>2</sub>KPO<sub>4</sub>/EDTA buffer (NADPH mix, 37°C) and 50 µL MQ (37°C) was added. Absorbance was measured every minute for 5 minutes at 340 nm at 37°C using a BioTek Synergy HT plate reader. The enzymatic reaction was started by adding 50 µL 5 mM oxidized glutathione (GSSG, final concentration 1 mM, Sigma-Aldrich, 37°C) as a substrate. The reaction was monitored every 30 seconds for 30 minutes at 340 nm at 37°C. Reaction slopes (0 - 30 minutes) were calculated using a linear regression analysis. Each assay included a reference blood sample to assess intra-assay variation, a positive control (GR from baker's yeast (6.25 units/µg protein, Sigma-Aldrich) in 1% BSA in H<sub>2</sub>KPO<sub>4</sub>/EDTA buffer), and negative controls for the background, substrate, cofactor, and enzyme. EGR enzymatic activity was calculated using the Beer–Lambert law:

$$C = \frac{\Delta A}{\epsilon \times \lambda}$$

where *c* is the concentration of NADPH (mM),  $\Delta A$  is the decrease in NADPH absorbance per minute,  $\epsilon$  is the molecular absorbance of NADPH at 340 nm ( $6.22 \times 10^3$  mmol/L/cm), and  $\lambda$  is the optical pathlength (0.69 cm). Activity was expressed as nmol NADPH oxidized per minute after adjustment for well volume (250 µL). The EGRAC ratio was calculated as FAD-stimulated EGR activity/unstimulated EGR activity using the reaction slopes (all  $R^2 > 0.99$ ). An EGRAC of 1.0 reflects complete FAD saturation and an EGRAC of  $> 1.3$  was used as a cut-off for suboptimal vitamin B2 status (10). The intra-assay coefficient of variation (CV) for EGR activity was 3.7%; the inter-assay CV was 2.8% for EGRAC and 12.3% for EGR activity.

### Statistical analyses

Statistical analyses were performed using IBM SPSS Statistics for Windows (Version 25.0, IBM Corp, Armonk, NY, USA). Graphs were created using GraphPad Prism (Version 8.0, Graphpad Software, CA, USA). Data were presented as mean  $\pm$  standard deviation (SD) or as median  $\pm$  interquartile range [IQR]. Normality was checked using Shapiro–Wilk normality tests. A repeated-measures ANOVA (RM-ANOVA) was used to study the effect of a single exercise bout on the response of EGRAC and EGRAC-related parameters, with the exercise bout as the within-subjects factor (time) and fitness level as the between-subjects factor (group). All assumptions for the RM-ANOVA analysis were met. Pearson correlation coefficients (*r*) were used to compare associations between variables, and *p*-values  $< 0.05$  were considered as statistically significant.

## Results

In total, 31 of the 32 subjects finished the study protocol. One subject was excluded due to protocol violation (i.e., medication intake). The conducted  $\dot{V}O_{2\text{peak}}$  measurements were considered valid on the posed criteria. Subject characteristics are shown in **Table 1**. All submaximal exercise tests were performed at a workload corresponding to approximately 70%  $\dot{V}O_{2\text{peak}}$  ( $67.2 \pm 8.1\%$  in high-fit and  $71.8 \pm 5.7\%$  in low-fit females). Average group values from the exercise test are shown in **Supplementary Figure S2**. Two subjects from the low-fit group terminated the submaximal exercise test prematurely due to feelings of presyncope and exhaustion; one subject cycled for 40 minutes at an intensity of 71% and one subject cycled for 48 minutes and at an intensity of 71.9%. Average habitual vitamin B2 intake was not significantly different between high-fit ( $1.40 \pm 0.35$  mg/day) and low-fit ( $1.32 \pm 0.46$  mg/day) females ( $P = 0.595$ ).

**Table 1.** Subject characteristics.

	Low-fit (N = 16)	High-fit (N = 15)
Age (years)	24.0 [21.3 – 25.5]	21.8 [21.6 – 23.7]
Weight (kg)	$59.2 \pm 7.2$	$61.2 \pm 7.0$
Height (m)	$1.63 \pm 0.08$	$1.68 \pm 0.05$ *
Fat mass (% of weight)	$28.9 \pm 3.9$	$25.1 \pm 4.4$ *
$\dot{V}O_{2\text{peak}}$ ( $\text{mL} \cdot \text{kg}^{-1} \cdot \text{min}^{-1}$ )	35.1 [32.2 – 35.7]	50.4 [49.0 – 54.0] ****
Baecke total score	$7.3 \pm 1.0$	$9.5 \pm 0.8$ ****
Hemoglobin (mM)	$8.4 \pm 0.6$	$8.5 \pm 0.6$
Use of birth control pill	6/16	7/15
If not; 17 $\beta$ -estradiol (pmol/L)	470.9 (337.2 – 590.1)	217.4 (109.1 – 895.2)

$\dot{V}O_{2\text{peak}}$  = maximal oxygen consumption values. Values are mean  $\pm$  SD for normally distributed data, and median [IQR] for not normally distributed data. \* $P < 0.05$ , \*\*\*\* $P < 0.0001$ .

### EGR enzymatic activities were increased after a single bout of exercise, but were not significantly different in high-fit compared to low-fit females

Compared to baseline, a single bout of exercise significantly increased unstimulated EGR activity ( $P_{\text{exercise}} = 0.006$ ), but fitness level did not influence this outcome ( $P_{\text{group}} = 0.163$ ) (**Figure 1A**). The exercise-induced increase ( $0.260 \pm 0.031$  to  $0.273 \pm 0.060$  nmol NADPH per minute) in unstimulated EGR activity in low-fit females was not significantly different from the increase ( $0.282 \pm 0.063$  to  $0.309 \pm 0.079$  nmol NADPH per minute) in high-fit females ( $P_{\text{exercise*group}} = 0.256$ ). FAD-stimulated

EGR activity increased after the exercise bout, but this did not reach statistical significance ( $P_{\text{exercise}} = 0.056$ ) (Figure 1B). Again here, fitness level had no influence on this finding ( $P_{\text{group}} = 0.619$ ). The exercise-induced increase in FAD-stimulated EGR activity in low-fit females ( $0.397 \pm 0.046$  to  $0.401 \pm 0.096$  nmol NADPH per minute) was not significantly different from the increase ( $0.393 \pm 0.078$  to  $0.427 \pm 0.100$  nmol NADPH per minute) in high-fit females ( $P_{\text{exercise*group}} = 0.126$ ).

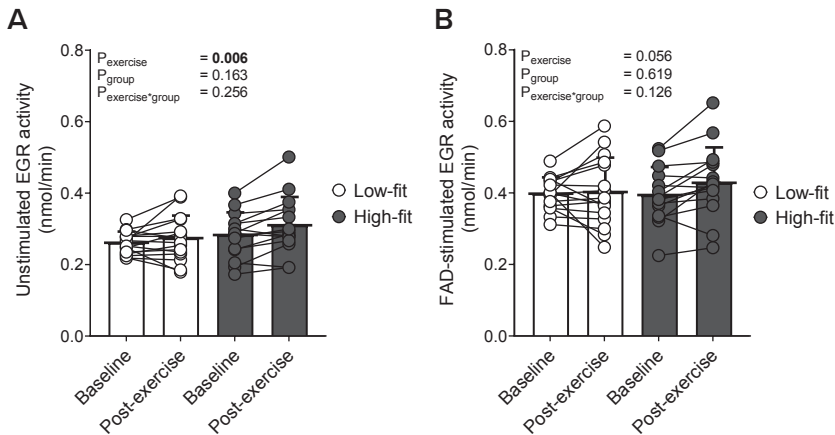


**Figure 1: The effect of a single exercise bout on unstimulated and FAD-stimulated EGR activity in high-fit and low-fit females.** Baseline and post-exercise unstimulated EGR activity (expressed as nmol NADPH converted per minute (A), and FAD-stimulated EGR activity (expressed as nmol NADPH converted per minute (B), in low-fit (N = 16, white) and high-fit (N = 15, grey) females.

### The EGRAC response to a single bout of exercise is not different between high-fit and low-fit females and not related to the EGR response

A single bout of exercise did not affect the vitamin B2 status as reflected by EGRAC ( $P_{\text{exercise}} = 0.079$ ), and fitness level did not have a significant effect ( $P_{\text{group}} = 0.057$ ) (Figure 2A). The exercise-induced decrease ( $1.54 \pm 0.14$  to  $1.47 \pm 0.17$ ) in EGRAC in low-fit females was not significantly different from the decrease ( $1.41 \pm 0.14$  to  $1.40 \pm 0.15$ ) in high-fit females ( $P_{\text{exercise*group}} = 0.141$ ). The individual exercise responses of EGRAC and unstimulated EGR activity were analyzed per subject and plotted against each other with the two groups combined. The change in unstimulated EGR activity after exercise ( $\Delta$  unstimulated EGR activity) was not correlated ( $r = 0.06$ ,  $P = 0.74$ ) to the change in EGRAC after exercise ( $\Delta$  EGRAC) (Figure 2B).

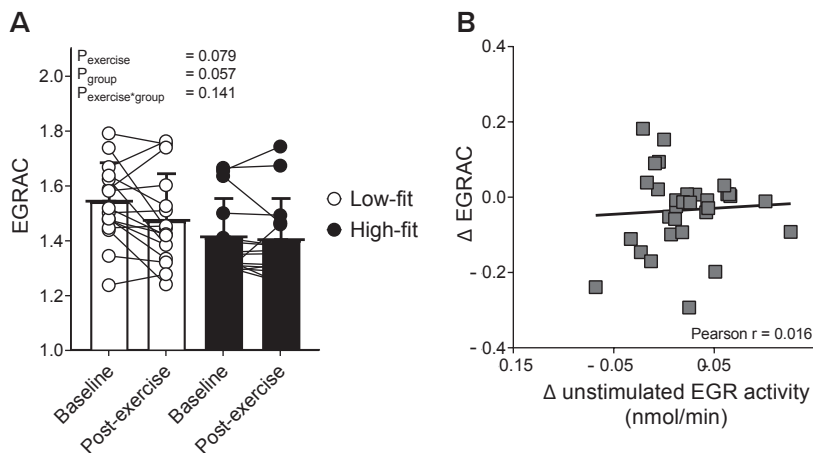


**Figure 2: The effect of a single exercise bout on vitamin B2 status (EGRAC) in high-fit and low-fit females.** Baseline and post-exercise EGRAC in low-fit ( $N = 16$ , white) and high-fit ( $N = 15$ , grey) females (**A**). Correlation between the individual exercise response of unstimulated EGR activity ( $\Delta$  unstimulated EGR activity, expressed as nmol NADPH per minute) and the exercise response of EGRAC ( $\Delta$  EGRAC); the high-fit and low-fit groups are plotted together (**B**).

## Discussion

Our results indicate that the effect of a single bout of exercise on EGRAC and EGR was not different between high- and low-fit females. The exercise bout significantly increased unstimulated EGR activity and tended to increase FAD-stimulated EGR activity, yet this exercise response was not different between high-fit and low-fit females. The decrease in EGRAC in response to a bout of exercise was not significant; neither was this response significantly different between high-fit and low-fit females. There was a lack of association between the change in EGR and EGRAC in response to a bout of exercise.

We hypothesized that the single bout of exercise could affect vitamin B2 status as determined by EGRAC, as the short-term effects ( $< 24$  hours) of exercise on EGR activity have been reported by previous studies (21,28,30). We also hypothesized that the EGRAC values after the single bout of exercise would be higher, i.e., vitamin B2 status would be lower in high-fit compared to low-fit individuals, as regular aerobic exercise enhances vitamin B2-dependent processes that could increase vitamin B2 demand. Indeed, we observed that EGR activity was significantly increased after the single bout of exercise, but EGRAC was not

significantly affected, neither was the change in unstimulated EGR activity related to the change in EGRAC. The first finding implies that a short-term exercise intervention on the day prior to blood sampling does not affect the reliability of using EGRAC for vitamin B2 status determination. Moreover, our observations are similar to previous findings (21,28,30). Ohno et al. (30) demonstrated in 11 untrained males (age  $20.3 \pm 0.3$  years) that a single bout of exercise (30-minute cycling test at  $75\% \dot{V}O_{2\text{peak}}$ ) significantly increased FAD-stimulated EGR activity and non-significantly increased unstimulated EGR activity (30), but EGRAC values were lacking. Evelo et al. (21) observed significantly higher EGR activity and significantly decreased EGRAC in trained males and females ( $N = 23$  and  $18$ , age  $18-41$  years) one day after running a 15-km contest or a half marathon. Similar effects of exercise on EGR activity and EGRAC were found by Frank et al. (28) in females ( $N = 5$ ) and males ( $N = 5$  and  $55$ , age  $25-65$  years) that participated in a 100-km walking contest and showed a non-significantly increased EGR activity and a significantly decreased EGRAC. These two studies cited above (21,28) used longer-duration exercises, i.e., a 15-km running contest or 100-km walking contest, which may explain why they found a significant effect on EGRAC, while our results were not significant. Despite this, previous studies have thus also consistently shown that short-term exercise elevated EGR activity (21,28,30) and decreased EGRAC (21,28), yet we are the first study that examined this effect in both high-fit and low-fit individuals. High-fit and low-fit individuals could have responded differently to the single bout of exercise, as the redox metabolism can adapt in response to regular aerobic training (2,36). That is, the increase in exercise-induced oxidative damage seems higher in untrained compared to trained individuals (36). Consequently, a single bout of exercise could have resulted in different redox enzyme activity between high-fit and low-fit females; however, our study indicated that the response of EGR activity and EGRAC to a single bout of exercise did not significantly differ between the two groups. Furthermore, our study demonstrates that the change in EGR activity was not correlated to the change in EGRAC after exercise. Apparently, short-term exercise could influence EGR activity without affecting EGR saturation with FAD in the short-term. Fitness level does not seem to be important, indicating that other factors, such as vitamin B2 intake (28,37,38), could be more important determining factors for short-term EGRAC responses. In our study, the habitual vitamin B2 intake was not different between high-fit and low-fit females; therefore, this may have resulted in similar EGRAC responses between the two groups.

Our results indicated that fitness level did not significantly affect EGRAC. Studies have described that vitamin B2-dependent processes can adapt in response to training, including an increased mitochondrial number and function (39,40) and an

increased production of FAD- and FMN-dependent enzymes, such as succinate dehydrogenase and long-chain acyl-CoA dehydrogenase, but also GR (41–43), which could increase vitamin B2 flux. Several longer-term exercise intervention studies have translated this into an increased vitamin B2 requirement for athletes and physically active individuals in response to regular aerobic exercise (14–18). This was supported by increased EGRAC after regular aerobic exercise while vitamin B2 intake was controlled (14–18), but was not confirmed by other intervention studies (20,21,28). Observational studies also did not find EGRAC differences between trained and untrained subjects (23–25), which is similar to the lack of a fitness level effect in our study. Based on the results of our study, we suggest that regular aerobic training could possibly change vitamin B2 status, but that the training adaptations in high-fit individuals do not necessarily result in an increased vitamin B2 requirement during exercise; if this was the case, we would likely have found a difference in the EGRAC response to the single exercise bout between high-fit and low-fit females, as well as increased rather than decreased EGRAC after exercise. We cannot exclude that EGRAC may change following more strenuous exercise performed over a longer period of time, since EGRAC was found to be significantly decreased following a 15-km running contest or 100-km walking contest (21,28). However, in those cases a decrease rather than an increase in EGRAC was observed.

Our findings suggest that vitamin B2 status was suboptimal ( $\text{EGRAC} > 1.3$ ) in almost all females (15 out of 16 low-fit and 13 out of 15 high-fit females). The risks of vitamin B2 deficiency have been observed in other exercise studies (14–16,18–20,44,45), but also in other study populations, including adolescents, young women, adults, and the elderly from developed countries such as the United Kingdom, Spain, and France (31,46–49). In the Netherlands, vitamin B2 status studies are scarce; one cross-sectional study from 1989 showed that the mean EGRAC in adult (18–64 years) females was 1.11 (50), and the first Dutch food consumption survey from 1987–1988 showed that the average vitamin B2 intake among females aged 22–49 years was 1.49 mg/day (51). The mean habitual vitamin B2 intake across subjects in our study was close to the RDA of 1.4 mg (10,52), and it is thus remarkable that we found a suboptimal vitamin B2 status. The controlled, low vitamin B2 intake during the study could possibly play a role, although we deem this unlikely since EGRAC is considered a vitamin B2 status rather than a vitamin B2 intake marker (10). Furthermore, an  $\text{EGRAC} > 1.3$  is generally accepted as a cut-off point for a suboptimal vitamin B2 status (10), but cut-off points of 1.2 to 1.4 have also been used (13,46,48). Details in experimental protocols between studies differ (11,12,53), which are unlikely to affect relative EGRAC outcomes, but may impact absolute EGRAC values. This has been proposed earlier by Hill et al. (35), who indicated

that details of the EGRAC method should be standardized and the EGRAC cut-off point should be re-evaluated. Although this was not the focus of our study, we recommend future studies to focus on validation of the EGRAC cut-off point to better understand the consequences of a suboptimal vitamin B2 status, especially since it may dispose a person to enhanced (metabolic) disease susceptibility.

The strength of our study is the use of a well-characterized study population including high-fit and low-fit individuals with a validated difference in  $\dot{V}O_{2\text{peak}}$ , while previous studies included only a high-fit or low-fit group that received exercise interventions (14–17,21,28,30) or selected their study population by exercise routines or physical activity questionnaires (20,24,27,44). Another strength of our study is that we sampled blood the day after the exercise intervention to mimic a situation that allowed us to examine if the recent effects of exercise could interfere with the EGRAC determination on the next day. A limitation is that we only sampled at one timepoint, while more insight may have been obtained by a time-course since the effects of exercise on EGR can be maintained up to 24 hours after exercise (21) and the kinetics may differ between individuals. Another limitation is the assessment of habitual vitamin B2 intake using the FFQ, which is based on selected foods from the food consumption data of the Dutch National Food Consumption Survey of 1998 (34), but may be influenced by the inter-individual variation in the relatively small population used in our study. Lastly, our data did not show a significant effect of fitness level on EGRAC. The relatively small sample size of our study may have contributed to this. Vitamin B2 status tended to be better rather than worse in high-fit females, which would possibly have statistically been confirmed with a larger sample size.

In conclusion, the effect of a single bout of exercise on EGRAC and EGR was not different between high-fit and low-fit females. A single bout of exercise significantly increased EGR activity, but did not affect EGRAC values, indicating that a single bout of exercise did not affect vitamin B2 status. Our findings help to better understand the influence of short-term exercise on vitamin B2 status and contribute to the interpretation of EGRAC as a vitamin B2 status parameter.

### Author contributions

Investigation: J.J.E.J., B.L.; Validation: J.J.E.J.; Data analysis: J.J.E.J.; Data interpretation: J.J.E.J., S.T., V.C.J.d.B., J.K.; Writing—original draft preparation: J.J.E.J.; review and editing: J.J.E.J., B.L., A.G.N., S.T., V.C.J.d.B., J.K.; Funding acquisition: J.J.E.J., J.K., V.C.J.d.B. All authors have read and agreed to the published version of the manuscript.

### **Funding**

J.J.E.J. was supported by the NWO-WIAS Graduate Program grant 2016, B.L. was supported by NWO-TIFN (ALWTF.2015.5); J.K and B.L. were supported by H2020-EU 3.2.2.1/2 PREVENTOMICS GA 818318.

### **Institutional Review Board statement**

The study was conducted according to the guidelines of the Declaration of Helsinki, and approved by the Declaration of Helsinki, and approved by the Ethics Committee of Wageningen University and Research (protocol code NL70136.081.19, date of approval 05 August 2019).

### **Informed consent**

Written informed consent was obtained from all individual subjects involved in the study.

### **Data availability statement**

The data presented in this study are available in this article and its supplementary material.

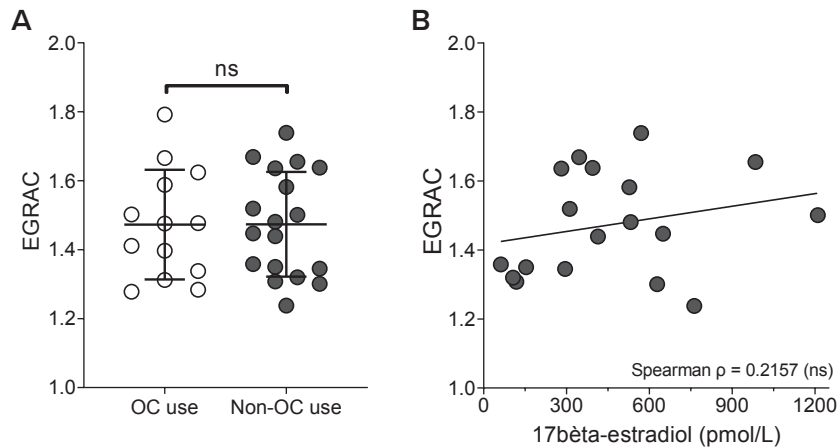
## References

1. Hargreaves M, Spriet LL. Skeletal muscle energy metabolism during exercise. *Nat Metab.* 2020;2(9):817–28.
2. He F, Li J, Liu Z, Chuang C-C, Yang W, Zuo L. Redox Mechanism of Reactive Oxygen Species in Exercise. *Front Physiol.* 2016 Nov 7;7:486.
3. Sen CK. Oxidants and antioxidants in exercise. *J Appl Physiol.* 1995;79(3):675–86.
4. Jackson MJ. Control of Reactive Oxygen Species Production in Contracting Skeletal Muscle. *Antioxid Redox Signal.* 2011 Jun 23;15(9):2477–86.
5. Depeint F, Bruce WR, Shangari N, Mehta R, O'Brien PJ. Mitochondrial function and toxicity: role of the B vitamin family on mitochondrial energy metabolism. *Chem Biol Interact.* 2006 Oct;163(1–2):94–112.
6. Lienhart WD, Gudipati V, MacHeroux P. The human flavoproteome. *Arch Biochem Biophys.* 2013;535(2):150–62.
7. Joosten V, van Berkel WJ. Flavoenzymes. *Curr Opin Chem Biol.* 2007;11(2):195–202.
8. Schulz GE, Schirmer RH, Sachsenheimer W, Pai EF. The structure of the flavoenzyme glutathione reductase. *Nature.* 1978;273(5658):120–4.
9. Woolf K, Manore MM. B-vitamins and exercise: Does exercise alter requirements? *Int J Sport Nutr Exerc Metab.* 2006;16(5):453–84.
10. EFSA NDA Panel (EFSA Panel on Dietetic Products N and A. Scientific Opinion on Dietary Reference Values for riboflavin. *EFSA J.* 2017;15(8):4919.
11. Bayoumi RA, Rosalki SB. Evaluation of methods of coenzyme activation of erythrocyte enzymes for detection of deficiency of vitamins B1, B2, and B6. *Clin Chem.* 1976 Mar;22(3):327–35.
12. Sauberlich HE, Judd Jr. JH, Nichoalds GE, Broquist HP, Darby WJ. Application of the erythrocyte glutathione reductase assay in evaluating riboflavin nutritional status in a high school student population. *Am J Clin Nutr.* 1972 Aug 1;25(8):756–62.
13. Hoey L, McNulty H, Strain JJ. Studies of biomarker responses to intervention with riboflavin: a systematic review. *Am J Clin Nutr.* 2009 Jun;89(6):1960S-1980S.
14. Belko AZ, Meredith MP, Kalkwarf HJ, Obarzanek E, Weinberg S, Roach R, et al. Effects of exercise on riboflavin requirements: biological validation in weight reducing women. *Am J Clin Nutr.* 1985 Feb 1;41(2):270–7.
15. Belko AZ, Obarzanek E, Kalkwarf HJ, Rotter MA, Bogusz S, Miller D, et al. Effects of exercise on riboflavin requirements of young women. *Am J Clin Nutr.* 1983 Apr;37(4):509–17.
16. Belko AZ, Obarzanek PE, Roach R. Effects of aerobic exercise and weight loss on riboflavin requirements of moderately obese, marginally deficient young women. *Am J Clin Nutr.* 1984;40(3):553–61.
17. Winters LR, Yoon JS, Kalkwarf HJ, Davies JC, Berkowitz MG, Haas J, et al. Riboflavin requirements and exercise adaptation in older women. *Am J Clin Nutr.* 1992 Sep;56(3):526–32.
18. Soares MJ, Satyanarayana K, Bamji MS, Jacob CM, Ramana Y V, Rao SS. The effect of exercise on the riboflavin status of adult men. *Br J Nutr.* 1993 Mar;69(2):541–51.
19. Ohno H, Yahata T, Sato Y, Yamamura K, Taniguchi N. Physical training and fasting erythrocyte activities of free radical scavenging enzyme systems in sedentary men. *Eur J Appl Physiol Occup Physiol.* 1988;57(2):173–6.
20. Fogelholm M. Micronutrient status in females during a 24-week fitness-type exercise program. *Ann Nutr Metab.* 1992;36(4):209–18.
21. Evelo CTA, Palmen NGM, Artur Y, Janssen GME. Changes in blood glutathione concentrations, and in erythrocyte glutathione reductase and glutathione S-transferase activity after running training and after participation in contests. *Eur J Appl Physiol Occup Physiol.* 1992;64(4):354–8.
22. Weight LM, Noakes TD, Labadarios D, Graves J, Jacobs P, Berman PA. Vitamin and mineral status of trained athletes including the effects of supplementation. *Am J Clin Nutr.* 1988 Feb 1;47(2):186–91.
23. Guillaud JC, Penaranda T, Gallet C, Boggio V, Fuchs F, Klepping J. Vitamin status of young athletes including the effects of supplementation. *Med Sci Sport Exerc.* 1989 Aug;21(4):441–9.

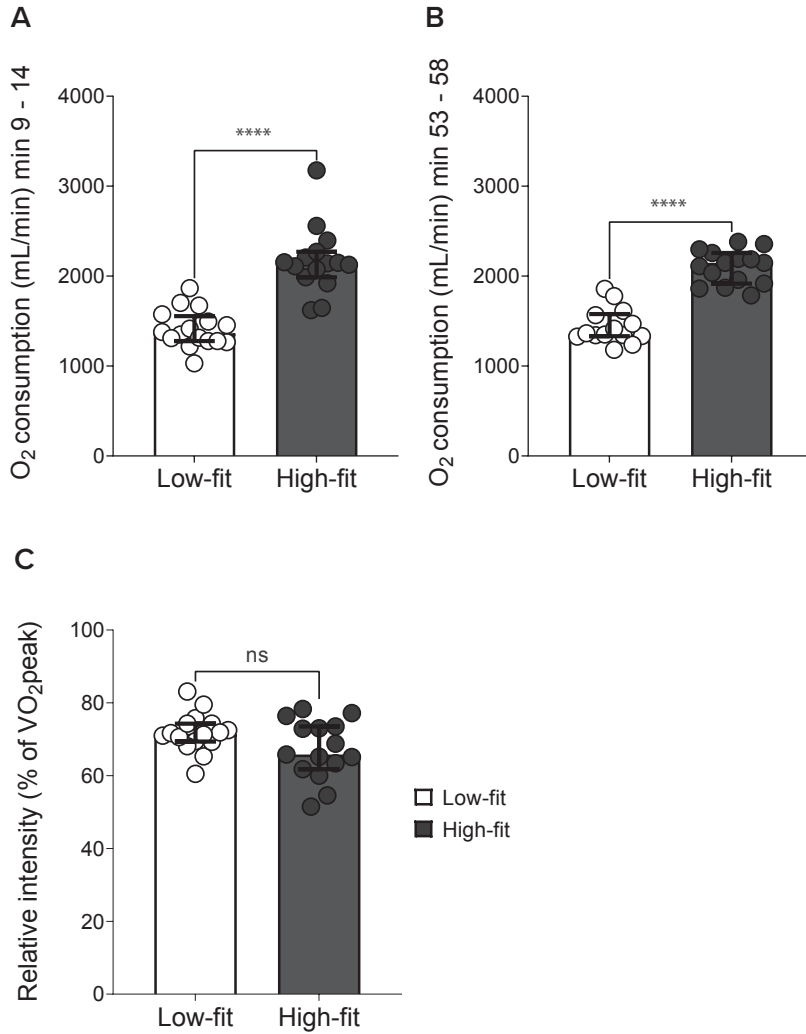
24. Keith RE, Alt LA. Riboflavin status of female athletes consuming normal diets. *Nutr Res.* 1991;11(7):727–34.
25. Malara M, Hübner-Wozniak E, Lewandowska I. Assessment of intake and nutritional status of vitamin b1, b2, and b6 in men and women with different physical activity levels. *Biol Sport.* 2013/04/11. 2013 Jun;30(2):117–23.
26. Tremblay A, Boilard F, Breton M-F, Bessette H, Roberge AG. The effects of a riboflavin supplementation on the nutritional status and performance of elite swimmers. *Nutr Res.* 1984;4(2):201–8.
27. Rokitzki L, Sagredos A, Keck E, Sauer B, Keul J. Assessment of vitamin B2 status in performance athletes of various types of sports. *J Nutr Sci Vitaminol.* 1994 Feb;40(1):11–22.
28. Frank T, Kuhl M, Makowski B, Bitsch R, Jahreis G, Hubscher J. Does a 100-km walking affect indicators of vitamin status? *Int J Vitam Nutr Res.* 2000 Sep;70(5):238–50.
29. Tauler P, Aguiló A, Guix P, Jiménez F, Villa G, Tur JA, et al. Pre-exercise antioxidant enzyme activities determine the antioxidant enzyme erythrocyte response to exercise. *J Sports Sci.* 2005 Jan 1;23(1):5–13.
30. Ohno H, Sato Y, Yamashita K, Doi R, Arai K, Kondo T, et al. The effect of brief physical exercise on free radical scavenging enzyme systems in human red blood cells. *Can J Physiol Pharmacol.* 1986 Sep;64(9):1263–1265.
31. Powers HJ, Hill MH, Mushtaq S, Dainty JR, Majsak-Newman G, Williams EA. Correcting a marginal riboflavin deficiency improves hematologic status in young women in the United Kingdom (RIBOFEM). *Am J Clin Nutr.* 2011;93(6):1274–84.
32. Lagerwaard B, Keijer J, McCully KK, de Boer VCJ, Nieuwenhuizen AG. In vivo assessment of muscle mitochondrial function in healthy, young males in relation to parameters of aerobic fitness. *Eur J Appl Physiol.* 2019;
33. Lagerwaard B, Janssen JJE, Cuijpers I, Keijer J, de Boer VCJ, Nieuwenhuizen AG. Muscle mitochondrial capacity in high- and low-fitness females using near-infrared spectroscopy. *Physiol Rep.* 2021;9(9):1–10.
34. Streppel MT, de Vries JHM, Meijboom S, Beekman M, de Craen AJM, Slagboom PE, et al. Relative validity of the food frequency questionnaire used to assess dietary intake in the Leiden Longevity Study. *Nutr J.* 2013;12(1):75.
35. Hill MHE, Bradley A, Mushtaq S, Williams EA, Powers HJ. Effects of methodological variation on assessment of riboflavin status using the erythrocyte glutathione reductase activation coefficient assay. *Br J Nutr.* 2008/12/23. 2008;102(2):273–8.
36. Radak Z, Zhao Z, Koltai E, Ohno H, Atalay M. Oxygen consumption and usage during physical exercise: the balance between oxidative stress and ROS-dependent adaptive signaling. *Antioxid Redox Signal.* 2012/11/16. 2013 Apr 1;18(10):1208–46.
37. Suboticanec K, Stavljenic A, Schalch W, Buzina R. Effects of pyridoxine and riboflavin supplementation on physical fitness in young adolescents. *Int J Vitam Nutr Res.* 1990;60(1):81–8.
38. Boisvert WA, Castañeda C, Mendoza I, Langeloh G, Solomons NW, Gershoff SN, et al. Prevalence of riboflavin deficiency among Guatemalan elderly people and its relationship to milk intake. *Am J Clin Nutr.* 1993 Jul 1;58(1):85–90.
39. Conley KE. Mitochondria to motion: optimizing oxidative phosphorylation to improve exercise performance. *J Exp Biol.* 2016 Jan 1;219(2):243 LP – 249.
40. Lanza IR, Nair KS. Muscle mitochondrial changes with aging and exercise. *Am J Clin Nutr.* 2009 Jan 1;89(1):467S–471S.
41. Gollnick PD, Armstrong RB, Saubert CW, Piehl K, Saltin B. Enzyme activity and fiber composition in skeletal muscle of untrained and trained men. *J Appl Physiol.* 1972 Sep 1;33(3):312–9.
42. Molé PA, Oscai LB, Holloszy JO. Adaptation of muscle to exercise: Increase in levels of palmityl CoA synthetase, carnitine palmyltransferase, and palmityl CoA dehydrogenase, and in the capacity to oxidize fatty acids. *J Clin Invest.* 1971 Nov 1;50(11):2323–30.
43. Powers SK, Jackson MJ. Exercise-induced oxidative stress: cellular mechanisms and impact on muscle force production. *Physiol Rev.* 2008 Oct;88(4):1243–76.
44. Fogelholm M, Ruokonen I, Laakso JT, Vuorimaa T, Himberg JJ. Lack of association between indices of vitamin B1, B2, and B6 status and exercise-induced blood lactate in young adults. *Int J Sport Nutr.* 1993 Jun;3(2):165–76.

45. Haralambie G. Vitamin B2 status in athletes and the influence of riboflavin administration on neuromuscular irritability. *Nutr Metab.* 1976;20(1):1–8.
46. Jungert A, McNulty H, Hoey L, Ward M, Strain JJ, Hughes CF, et al. Riboflavin Is an Important Determinant of Vitamin B-6 Status in Healthy Adults. *J Nutr.* 2020 Aug;(10):2699–2706.
47. Aljaadi AM, How RE, Loh SP, Hunt SE, Karakochuk CD, Barr SI, et al. Suboptimal Biochemical Riboflavin Status Is Associated with Lower Hemoglobin and Higher Rates of Anemia in a Sample of Canadian and Malaysian Women of Reproductive Age. *J Nutr.* 2019;149(11):1952–9.
48. Mataix J, Aranda P, Sánchez C, Montellano MA, Planells E, Llopis J. Assessment of thiamin (vitamin B1) and riboflavin (vitamin B2) status in an adult Mediterranean population. *Br J Nutr.* 2003;90(3):661–6.
49. Preziosi P, Galan P, Deheeger M, Yacoub N, Hercberg S, Drewnowski A. Breakfast Type, Daily Nutrient Intakes and Vitamin and Mineral Status of French Children, Adolescents and Adults. *J Am Coll Nutr.* 1999;18(2):171–8.
50. Löwik MR, Schrijver J, Odink J, van den Berg H, Wedel M, Hermus RJ. Nutrition and aging: nutritional status of “apparently healthy” elderly (Dutch nutrition surveillance system). *J Am Coll Nutr.* 1990 Feb;9(1):18–27.
51. Hulshof KFAM, Van Staveren WA. The Dutch National Food Consumption Survey: design, methods and first results. *Food Policy.* 1991;16(3):257–60.
52. Health Council of the Netherlands. Voedingsnormen voor vitamines en mineralen voor volwassenen. The Hague; 2018.
53. Glatzle D, Körner WF, Christeller S, Wiss O. Method for the detection of a biochemical riboflavin deficiency. Stimulation of NADPH2-dependent glutathione reductase from human erythrocytes by FAD in vitro. Investigations on the vitamin B2 status in healthy people and geriatric patients. *Int J Vitam Res.* 1970;40(2):166–83.

# Supplementary materials



**Supplementary Figure S1: The effect of oral contraceptives (OC) use and 17β-estradiol levels on vitamin B2 status. (A)** Baseline EGRAC in OC users (N = 13, white) and non-OC users (N = 18, dark grey). **(B)** Correlation between levels of 17β-estradiol and baseline EGRAC in non-OC users (N = 18). ns = not significant.



**Supplementary Figure S2: Submaximal exercise test characteristics.** The average oxygen consumption (mL / min) was calculated between 9 - 14 minutes in low-fit (N = 16, white) and high-fit (N = 15, dark grey) females (A) and between 53 - 58 minutes in low-fit (N = 14, white) and high-fit (N = 15, dark grey) females (B) of the 60-minutes exercise protocol. (C) The mean intensity of the exercise test as a percentage to an individual's  $\dot{V}O_{2\text{peak}}$ . ns = not significant; \*\*\*\*P < 0.0001.



# 8

## General Discussion





The research presented in this thesis was performed to develop concepts and tools that allow for a better understanding of human physiological health. Physiological health was not considered as the absence of disease but rather described as a continuum that includes different health states and the transition from optimal health to disease. This allows for quantification of health states and evaluation of the trajectory from health to disease, which may translate into strategies to improve health and prevent disease. Since differences in health states are likely more subtle than differences between a healthy and disease state, health biomarkers should allow for the detection of small but physiologically relevant differences between health states, and could possibly serve, after future validation, as prognostic disease markers. Sufficient detection resolution may not be achieved by analyzing individual levels of classical clinical diagnostic markers that are mainly used for detecting differences between health and disease, since a functional, even suboptimal homeostasis tends to maintain these biomarkers within a certain range of values. These diagnostic biomarkers will thus have difficulty capturing early deviations in the trajectory from a healthy toward an unhealthier state, unless the individual is acutely challenged. This is inherent to these markers' short lifetime and acute signaling role. Therefore, in this thesis, I studied functional readouts in healthy individuals as potential health biomarkers, and focused on metabolism as a key aspect of physiological health. I used two innovative approaches with a potential for robust and sensitive physiological health quantification: 1) examining metabolic function in cells and tissues that have a longer lifespan and may thus imprint physiologically relevant health differences, and 2) investigating the behavior of multiple classical clinical diagnostic metabolic biomarkers simultaneously and evaluate their joined response in the context of physiological health processes. These concepts were studied in healthy, young, adult females with high and low levels of aerobic fitness. High aerobic fitness levels, compared to low aerobic fitness levels, represents a healthier state due to its association with improved health outcomes, such as lower blood pressure and visceral fat levels (1,2), and a reduced risk for the development of later life disease, including cardiovascular disease (CVD) and type 2 diabetes (1,3). Therefore, the overall aim of this thesis was to study how metabolic measurements in healthy females with high and low levels of aerobic fitness can contribute to a better understanding of human physiological health.

## Main findings

The **first aim** of this thesis was to study the link between skeletal muscle mitochondrial capacity and aerobic fitness level. In **Chapter 2** we demonstrated that mitochondrial capacity was significantly higher in the *gastrocnemius* muscle of high aerobically fit (high-fit) compared to low aerobically fit (low-fit) females. The **second aim** was to evaluate the potential of PBMC metabolism as a health biomarker by 1) developing a normalization method for PBMC metabolic XF analysis, and 2) evaluating the link between PBMC metabolism and aerobic fitness level. In **Chapter 3** we developed a brightfield imaging method for normalization of PBMC metabolic XF analysis that improved the reliable measurement, comparison, and extrapolation of XF assay results in PBMCs. **Chapter 4** showed that mitochondrial PBMC metabolism was significantly higher in high-fit compared to low-fit females and that this effect was unrelated to PBMC subset composition and not affected by a recent bout of exercise. The **third aim** was to explore the relationship between systemic metabolism biomarkers and aerobic fitness level. In **Chapter 5** we found that the levels of these systemic biomarkers were similar between high-fit and low-fit females, but that a recent exercise bout significantly changed the levels of biomarkers, mainly those that are related to inflammation and lipid metabolism. We also showed that linking each biomarker to a physiological health process resulted in functional biomarker categories that could be relevant for characterization of human physiological health, and that there was a considerable level of interindividual variation in biomarker responses. The **fourth aim** was to describe the state-of-the-art on the role of B-vitamins in mitochondrial metabolism and the communication with the nucleus. **Chapter 6** showed how B-vitamins could modulate the signaling of mitochondria-derived metabolites to the nucleus and highlighted the crucial importance of B-vitamins for maintaining physiological health. The **final aim** of this thesis was to study the link between vitamin B2 status parameters and aerobic fitness level, because regular exercise may alter the use and need of vitamin B2. In **Chapter 7** we demonstrated that vitamin B2 status was not different between high-fit and low-fit females, indicating that there was no link between vitamin B2 status and aerobic fitness level. Recent exercise did also not impact vitamin B2 status, although the activity of the metabolic enzyme that is used for vitamin B2 status assessment was increased after exercise.

## The way ahead for PBMC metabolism as a biomarker in health and disease

### Levels of aerobic fitness are imprinted in mitochondrial PBMC metabolism

In this thesis, a link between mitochondrial PBMC metabolism and aerobic fitness level was revealed ([Chapter 4](#)). This novel finding strongly increased the potential for using PBMC metabolism as a health biomarker, as it showed that PBMC metabolism can imprint a physiological health difference. Since PBMCs circulate through the body and infiltrate into various tissues, the physiological alterations driven by regular exercise may not only induce molecular changes into the key tissues, such as skeletal muscle (4) ([Chapter 2](#)) and liver (5), but also in the blood cells that interact with them. We proposed in [Chapter 4](#) that several physiological factors could possibly underlie our observation that PBMC metabolism responds to a difference in aerobic fitness level, such as the systemic release of biologically active proteins from skeletal muscle, also defined as myokines (6), and alterations in the metabolic makeup of the blood plasma (7,8). With respect to this metabolic makeup, systemic levels of several lipid metabolites, such as several triglycerides, fatty acids, glycoproteins, and cholesterol markers, are examples of metabolites that have been shown to differ between high-fit and low-fit individuals (7,8). Interestingly, plasma or serum levels of the myocytokines IL6 and IL10 as well as multiple lipid metabolites, such as fatty acids, cholesterol markers, and acylcarnitines were analyzed in [Chapter 5](#). Here, we found that baseline plasma levels of IL6, IL10 and lipid metabolites were not significantly different between high-fit and low-fit females, but that particularly these biomarker categories significantly responded to the recent bout of exercise ([Chapter 5](#)). Exercise-induced responses of cytokines and lipid metabolites have been demonstrated previously, with different responses with time after exercise (9–13). For example, the fall in skeletal muscle glycogen content acts as a major stimulus for IL6 release by skeletal muscle, resulting in a manifold increase in plasma IL6 (14). Subsequently, the rise in circulating IL6 promotes an increase in the plasma levels of IL10 and IL1 receptor alpha, which are anti-inflammatory cytokines that counterbalance exercise-induced inflammatory responses and prevent high systemic inflammation (14). Hence, the time-dependent release of pro- and anti-inflammatory cytokines restores the immunological equilibrium to maintain physiological homeostasis. Although immediate and short-term (< 12 hours) post-exercise responses have been often investigated, late (> 20 hours) post-exercise responses have been little studied. However, they are highly relevant in view of biomarker analysis because it implies that the physical activity status of the study subject prior to the analysis should be controlled.

everal systemic biomarkers significantly changed in response to the recent bout of exercise, mitochondrial and glycolytic PBMC metabolic values did not, and resulted in similar baseline as well as post-exercise values and a consistent elevation of mitochondrial PBMC metabolism in high-fit compared to low-fit females (Chapter 4). To examine whether short-term cytokine and metabolite release could possibly program PBMC metabolic responses, I studied whether these responses were correlated. No strongly significant correlations between mitochondrial PBMC metabolism (represented here as basal OCR) and plasma levels of IL6, IL10, or total fatty acids were observed (Figure 1), which could be due to the timepoints that were analyzed. IL6, IL10 and various metabolites could have been acutely released upon exercise with manifold increased levels, as have been observed before in other studies (10,12,13,15). However, since in our study we did not sample blood and cells immediately after the single exercise bout, but

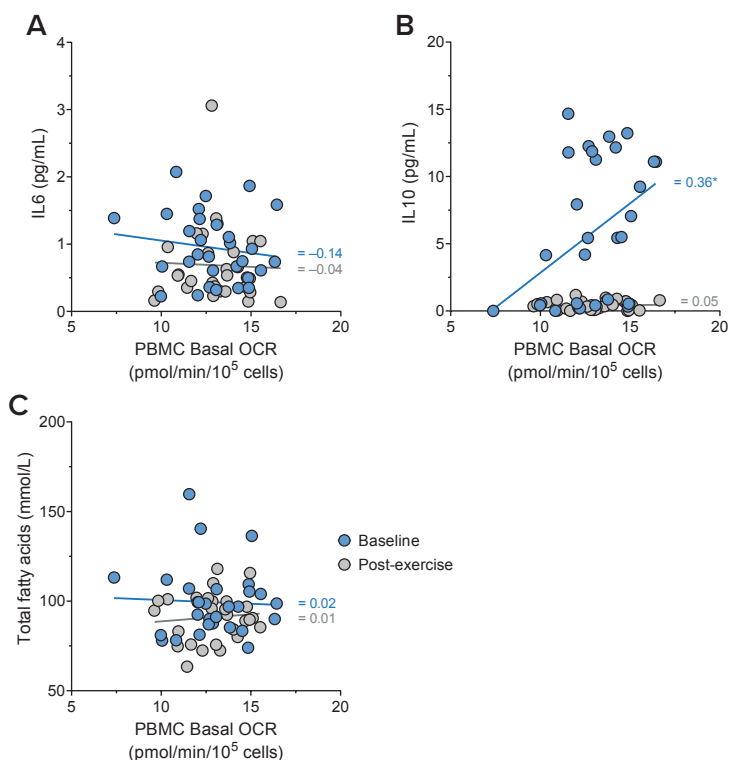


**Figure 1: Correlations between mitochondrial PBMC metabolism and circulating biomarkers.** Correlations of basal OCR and IL6 (A), IL10 (B) and total fatty acids (C) at baseline (blue) or post-exercise (grey). Spearman rank correlation coefficients ( $\rho$ ) were calculated. \* $P < 0.05$ .

rather after 21 hours, the levels of IL6, IL10 and various metabolites levels could have been already normalized (16–18), which could also explain why they were decreased rather than increased 21 hours post-exercise (Chapter 5). It can thus not be excluded that IL6, IL10, or total fatty acids induced longer-term metabolic reprogramming in PBMCs. However, also other myokines and metabolites may have been involved (6,13), as well as other physiological factors, such as changes in blood flow and endothelial function (19) or ROS release by skeletal muscle (20). To study how metabolic alterations in PBMCs arise is of interest, not only scientifically, but also to better understand their value as a biomarker.

### Systemic release of exercise-induced signals may underlie metabolic changes in PBMCs from high-fit females

Metabolic programming is not an unlikely event and there are indications for several possibilities how myokines and plasma metabolites could impact mitochondrial PBMC metabolism. Recently, it has been demonstrated that IL10 exposure improved mitochondrial fitness, i.e., mitochondrial function and quality, in bone marrow-derived macrophages (21). This IL10-enhanced oxidative program could act as a potential driver behind anti-inflammatory macrophage responses (21). Although the capacity of IL10 to modify cellular metabolism was only studied in macrophages, the differentiated monocyte population, IL10 has also been demonstrated to limit the pro-inflammatory cytokine production in activated PBMCs (22). Since pro-inflammatory immune responses are often accompanied by upregulation of glycolytic programs, while anti-inflammatory immune responses enhance oxidative metabolism (23), these findings could indicate that IL10 release could impact PBMC metabolism by specifically enhancing mitochondrial metabolism in monocytes. Similar to IL10, IL6 has also been reported to impact mitochondrial metabolism in immune cells. IL6 improved the motility fitness of activated CD4<sup>+</sup> T cells by enhancing and sustaining mitochondrial calcium levels, which mediates the migration of CD4<sup>+</sup> T cells to the sites of infection or inflammation to reach their cell targets (24). Of note, IL6 only functioned in the presence of T cell activators, but enhanced CD4<sup>+</sup> T cell motility and migration even in the absence of chemokines such as the chemokine (C-C motif) ligand 19 (CCL19), indicating that the IL6-mediated trigger on mitochondrial calcium can improve the motility fitness of CD4<sup>+</sup> T cells independently of chemokines (24).

Besides IL6 and IL10, other myokines that may program mitochondrial PBMC metabolism are IL15 (25,26) and growth differentiation factor 15 (GDF15) (27). IL15 has been shown to promote mitochondrial biogenesis and expression of carnitine palmitoyl transferase (CPT1A), a metabolic enzyme that regulates import of fatty acids into the mitochondria, in CD8<sup>+</sup> memory T cells (25). In addition, acute IL15

exposure to skeletal muscle cells was found to enhance basal mitochondrial respiration (26) and promote activation of the AMP-dependent protein kinase (AMPK), which is one of the cellular nutrient sensors that promotes glucose transport, mitochondrial function, and mitochondrial biogenesis when the cellular adenosine monophosphate (AMP) and adenosine triphosphate (ADP) to ATP ratios increases, as typically occurs during exercise in muscle (28). GDF15 is also acutely released upon exercise (29) and has been particularly associated with the integrated mitochondrial-induced stress responses (30). GDF15 was found to increase mitochondrial capacity and promoted an anti-inflammatory, fatty acid oxidizing phenotype in adipose-tissue macrophages (31), which acts as a signal to dampen the inflammatory activation during exercise, therewith driving the inflammation-immunosuppression axis (32). Of note, the receptor for GDF15, glial cell-derived neurotrophic family receptor alpha-like (GFRAL), is not expressed on immune cells, yet the evidence for immunosuppressive effects exists (32). Although studies that investigate the direct impact of exercise-induced myokine release on the collective PBMC pool are scarce, it was recently shown that mitochondrial metabolism was enhanced in PBMCs after an acute bout of exercise (33,34). These observations may be linked to the above-described ability of myokines to reprogram cellular metabolism. However, since our study did not find differences in mitochondrial PBMC metabolism 21 hours post-exercise ([Chapter 4](#)), the systemic release of myokines during each bout of exercise may not only acutely reprogram PBMC metabolism via the mobilization of nutrients and switch in metabolic fuels, but may also induce long-lasting metabolic adaptations, and epigenetic modifications could play a role in this.

For example, it has been recently demonstrated that histone deacetylases (HDACs) in PBMC nuclear fractions respond to exercise-induced systemic signals, thereby altering histone acetylation patterns that regulate transcription levels of inflammatory genes in PBMCs (35). Furthermore, acute exercise has been shown to alter DNA methylation patterns and microRNA expression that promote cell signaling pathways involved in cell growth, proliferation, and differentiation in PBMCs from healthy young adults (36,37). Interestingly, it has recently been demonstrated that exercise-regulated plasma metabolites could act as epigenetic programmers (38). Lactate, the well-known muscle-derived “waste” product that accumulates during exercise in both muscle and blood (39), which has also recently been shown to act as an important metabolic substrate for several tissues in humans (40), has now been proposed as a novel epigenetic modifier of immune cells (38). Lactate was found to promote anti-inflammatory gene expression in macrophages, via so-called *lactylation* of histones (38,41). Although lactylation has not yet been described in monocytes, earlier it has been demonstrated that

lactate promoted an anti-inflammatory phenotype in monocytes (42), which suggest that lactate may also affect unpolarized monocytes. Importantly, this phenotypic shift was accompanied by an increase in mitochondrial metabolism and a decrease in glycolysis (42). Although in this thesis glycolytic PBMC metabolism was not affected, the study from Ratter et al. (42) indicates that this exercise-associated metabolite is indeed able to modify the metabolism of a specific PBMC subset. Interestingly, studies have suggested that HDACs can also be modulated by gut-derived short-chain fatty acids (SCFA), i.e., acetate, propionate, and butyrate, which can promote anti-inflammatory responses by inhibiting HDAC activity (43). Since recent studies have indicated that systemic levels of SCFA, particularly butyrate, are increased in regularly exercising individuals (44,45), exercise-associated SCFA release may also affect PBMC metabolic programs via modulating HDAC activities. Furthermore, in addition to lactate or SCFA, other exercise-induced changes in mitochondrial substrates and ROS may also induce alterations in the level of mitochondrial acyl-CoAs that could be forwarded to the cell nucleus, which may also contribute to the observed epigenetic changes (Chapter 6).

Thus, the release of systemic signals during each bout of exercise may impact the epigenetic machinery and subsequent up- and downregulation of transcriptional programs in PBMCs. This potential mechanism is supported by recent studies that show increased protein and gene expression levels of mitochondrial markers in PBMCs in response to aerobic exercise training (46,47) and increased gene expression levels of mitochondrial OXPHOS and biogenesis in endurance-trained athletes as compared to sedentary controls (48). Because the different cell types present in the PBMCs have different lifespans, with monocytes, and effector T- and B-lymphocytes being relatively short-lived (lifespan up to ~7 days) (49) compared to long-lived naïve T lymphocytes (lifespan ~months to years) (50), it is likely that such epigenetic modifications do not only impact the established PBMC population, but also affect the PBMC progenitor cells in lymphoid tissues that give rise to the next generation of PBMCs. Whether muscle-derived lactate and myokines, as well as gut-derived SCFA that are produced during regular exercise could thus impact circulating PBMC epigenetics and, in this way affect PBMC mitochondrial metabolism, is an interesting avenue for future studies. Scientists begin to understand the exercise-induced epigenetic modifications in skeletal muscle (51), yet the role of epigenetics in PBMC metabolic responses is still in its infancy (52). Considering the intimate crosstalk between systemic signals, intracellular signaling pathways, epigenetic modifications, and metabolic reprogramming, studying transcriptomic, proteomic, and metabolomic PBMC patterns in relation to PBMC metabolism in the context of aerobic exercise is of great relevance to better

understand which molecular pathways could mediate our observed alterations in PBMC metabolism.

### Understanding PBMC metabolism as a biomarker in health and disease

In this thesis, the link between PBMC metabolism and aerobic fitness level was unrelated to the composition of PBMCs for specific immune subsets ([Chapter 4](#)), which indicates that PBMC metabolism could capture early deviations from steady-state physiology and underpins the suitability of PBMC metabolism as an early health biomarker. Yet, to date, PBMC metabolism has been mainly studied as a biomarker in disease pathologies, such as type 2 diabetes (53,54), obesity (55,56), CVD (57,58), inherited metabolic diseases (59,60), autoimmune disease (61,62) and recently also in coronavirus disease 19 (COVID19) (63). These studies often conclude that PBMC metabolic function has the potential to act as a disease-specific biomarker. However, in those studies, it is challenging to establish whether the outcomes are primarily related to centralized metabolic adaptations within PBMC subsets, or whether they are more likely to reflect differences in metabolic phenotypes between different PBMC subsets particularly because PBMC subset composition often changes in disease pathologies. For example, in type 2 diabetes (64,65), the number of T-helper 17 (Th17) lymphocytes, which typically display a glycolytic profile, increases (66), and the number of regulatory T (Treg) lymphocytes, that typically rely heavily on fatty acid oxidation, decreases (67). Thus, shifts in the overall PBMC bioenergetic profile may at least be a partial reflection of a shift in PBMC subsets. When scientists and clinicians are aware that the observed metabolic differences likely result from distinct levels of specialized PBMC subsets, it does not necessarily have to impair the biological interpretation. However, PBMC subset transitions may become a disrupting factor when the effect of lifestyle interventions or health promotion strategies are evaluated across the complete health to disease window. For example, exercise interventions and weight-loss strategies have been shown to be effective in type 2 diabetes management (68). In [Chapter 4](#) we showed that improved cardiorespiratory fitness, a plausible consequence of such exercise interventions, drive PBMCs to a more oxidative state. These interventions are also associated with improved metabolic health (69) and alleviated inflammation (14), which may induce a shift in PBMC subset composition back to pre-disease levels, becoming more comparable to healthy controls. Consequently, exercise-induced PBMC metabolic changes will in the case of disease-related biomarker studies not only reflect exercise-induced physiological adaptations, but also a shift in PBMC subset composition, thereby lowering its predictive value. Hence, for the development of PBMC metabolism as a biomarker across the full health to disease trajectory, a better understanding of the dynamics between PBMC metabolism and PBMC subset composition in physiology and pathophysiology is needed.

Although respirometric analysis has been applied to understand the metabolic preference of individual PBMC subtypes (70), this has not yet been longitudinally studied from physiological to pathophysiological health conditions. Recent advances in single cell multiomics technologies have now enabled large-scale metabolic characterization of specialized PBMC subtypes, to study the contribution of different metabolic pathways to the overarching cellular metabolism (71,72). Interestingly, using single-cell transcriptomics combined with plasma metabolomics and proteomics, metabolic changes in PBMCs during coronavirus disease 19 (COVID19) development have been monitored (72). PBMC metabolism was strikingly different between healthy controls and COVID19 patients, and the degree of COVID19 severity was driven by small, metabolically hyperactive subpopulations (72). Therefore, to study the dynamics between PBMC metabolism and PBMC subset composition from the health to disease window, and for a better understanding of the molecular mechanisms that underlie our observations, such multiomics technologies are of high interest for underpinning XF metabolic PBMC analysis in future studies. In the end, analysis of PBMCs as a biomarker for the health to disease trajectory may consist of metabolic flux analysis and complementary PBMC subset phenotyping. Furthermore, although many studies have demonstrated that distinct metabolic pathways in specialized PBMC subsets are the drivers behind their pro- or anti-inflammatory effector functions (23,73), it is not yet clear how the total metabolic function of the overall PBMC pool affects immune system functioning. Therefore, it is also relevant to study the contribution of PBMC immunometabolic pathways to immune-related health and disease processes.

### **Moving the use of PBMCs as a future health biomarker forward**

Besides imprinting aerobic fitness levels, it is also interesting to speculate whether other physiological health differences could also induce metabolic alterations in PBMCs, such as lifestyle-related differences in body weight or dietary intake. At the gene expression level, studies have shown that PBMCs can reflect differences in body weight and body composition (74). In rodents, the expression levels of genes involved in lipid metabolism were significantly different between normal weight and obese rats (75,76) and these findings have been recently confirmed in humans (77). The latter study is of special interest, since here it was found that PBMC transcripts could reflect impaired metabolic health in overweight-obese individuals who did not yet develop pathological alterations in clinical biomarkers (e.g., levels of fasting plasma glucose and triglycerides) and reinforces the use of PBMCs as an early biomarker of metabolic health (77). Furthermore, PBMC antioxidant enzyme levels and activity have recently been shown to increase progressively with body mass index (BMI), which likely results from the oxidative

stress that is related to body fat accumulation (56). Next to the reflection of metabolic changes associated with increased body fat percentage, PBMCs could also be useful to monitor diet-induced metabolic changes (78–82) or nutrient status (83). For example, supplementation of polyunsaturated fatty acids (PUFA), polyphenols and L-carnitine has been demonstrated to increase the expression of fatty oxidation genes in PBMCs from obese adults (79), thus showing that PBMC lipid metabolism could also reflect diet-induced alterations in metabolic health. Furthermore, the consumption of a Mediterranean (80) or Nordic (81) diet, which has beneficial effects on metabolic and cardiovascular health, has been found to lower the expression of mitochondrial OXPHOS genes in PBMCs from obese (81) or overweight (80) adults. Lower mitochondrial OXPHOS gene expression was suggested to be associated with diet-induced alleviation of the oxidative stress that was induced by mitochondrial ROS (80,81). Of note, at the cellular level, lower mitochondrial respiration through OXPHOS has been linked to increased cardio-metabolic risk factors (57,84), suggesting mixed findings on the regulation of PBMC mitochondrial metabolism, although there seems sufficient evidence that PBMCs could reflect diet-induced alterations.

Emerging evidence thus suggest that PBMC metabolic readouts may act as a novel biomarker for human physiological health. At this moment, PBMC-based biomarker profiling is still largely in the research domain, principally because the mechanisms how PBMC readouts underpin physiological health status are not yet fully understood. The rapid advancement of state-of-the-art technologies and the development of computational methods to analyze high-throughput omics data, such as transcriptomics, proteomics, and metabolomics, could mechanistically relate PBMC metabolic function to PBMC transcripts, proteins, metabolites, as well as to classical biomarkers, which may unveil the underlying physiological processes and provide a link with whole-body physiology. There are already some notable studies that have linked the PBMC transcriptome, proteome or metabolome to whole-body health status (72,77,85). Although studies that recommend analyzing PBMCs at the subset level (70,86) or the single-cell level (71,72) are gaining traction, here we show that the collective PBMC pool, which is easier to obtain and isolate than single PBMC subsets, can also act as a highly informatic metabolic pick-up line.

## Measuring skeletal muscle mitochondrial capacity for human physiological health

The differences in skeletal muscle mitochondrial capacity between high-fit and low-fit females, as detected by NIRS ([Chapter 2](#)), were of similar magnitude as previously demonstrated by our group in males (87). This highlights that NIRS can detect similar differences in mitochondrial capacity in both males and females ([Figure 2A](#)). However, two data sets from low-fit individuals that were amongst the highest in adipose tissue thickness (ATT) thickness ([Figure 2B](#)) were excluded from this study due to low curve fitting. A proper  $\dot{V}O_2$  vs. time during the recovery phase after occlusion with  $R^2 > 0.95$  is a technical quality control for calculation of the recovery rate constant  $k$ . It remains unknown whether the low curve fitting was related to the ATT or to other factors, especially since other NIRS measurements with higher ATT were successful. Of note, subcutaneous adiposity, but not BMI seem to be important for NIRS assessment ([Figure 2C, 2D](#)). The healthy females in our study and the healthy males in our previous study had healthy body fat percentage (24.6% for high-fit, 28.9% for low-fit females, and 18.7% for high-fit, 12.5% for low-fit males) (88) but the two unsuccessful NIRS measurements at the upper adiposity limit indicate that unhealthy body fat percentages may hamper reliable NIRS assessment. Since females have a relatively higher level of subcutaneous adipose tissue, NIRS measurements may be impaired in slightly overweight (BMI 25-30 kg/m<sup>2</sup>) females (generally showing body fat percentages >35%) but not in overweight males (generally showing body fat percentages >24%) (88). In fact, in males NIRS may even generate reliable results in obese subjects (BMI > 30 kg/m<sup>2</sup>) as adiposity levels can still be at 28% (88). Since overweight and obesity have also been associated with impaired skeletal muscle mitochondrial function (89), NIRS is a highly attractive tool to better understand the effect of weight loss or physical activity interventions on mitochondrial function in skeletal muscle. Yet at this point, this may be best achieved in male individuals. Thus, the limitation of ATT must be overcome before NIRS can be widely applied in all study populations, including overweight and obese females (90,91).

In [Chapter 2](#), we demonstrated that skeletal muscle mitochondrial capacity was significantly higher in high-fit than low-fit females, which further confirms the association between aerobic capacity at the level of skeletal muscle ( $m\dot{V}O_2$ ) with whole-body aerobic capacity (92,93). Aerobic fitness level is an important determinant of physiological health status (1), and peak oxygen uptake ( $\dot{V}O_{2peak}$ ) tests are currently the golden standard for aerobic fitness level determination, yet it is demanding for the subjects. We show that NIRS can also reflect aerobic capacity but with much less demand, which makes NIRS a promising tool to

monitor physiological health. Importantly, NIRS can even be used in a lying position to reliably measure mitochondrial capacity, which thus also enables the assessment of skeletal muscle mitochondrial capacity in individuals with disabilities, elderly subjects or community-dwelling individuals. Furthermore, its portability and the low costs of NIRS over other non-invasive techniques such as magnetic resonance spectroscopy ( $^3\text{P}$ -MRS) (94) makes NIRS highly relevant for monitoring physiological health differences in response to lifestyle interventions.

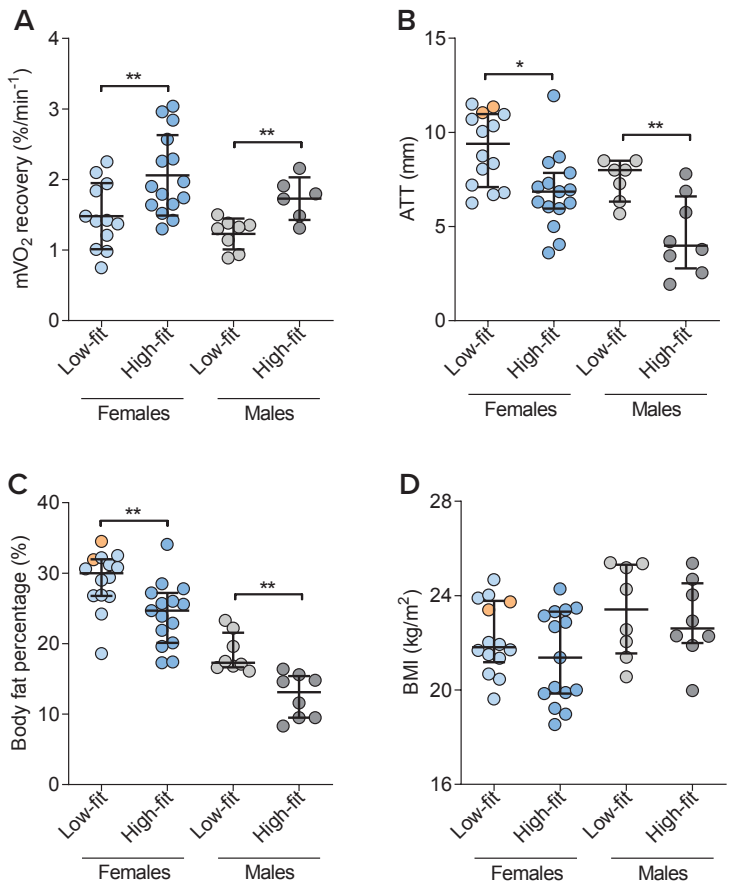


**Figure 2:** Comparison of skeletal muscle mitochondrial capacity and body composition between high-fit and low-fit males and females. (A – D): Muscle oxygen consumption recovery constant ( $\dot{m}\text{VO}_2$ ) measured using NIRS in *gastrocnemius* (A), adipose tissue thickness (ATT) in *gastrocnemius* (B), body fat percentage (C) and body mass index (BMI) (D) in high-fit and low-fit females (blue) and males (grey). The datasets that were excluded due to low curve fitting ( $R^2 < 0.95$ ) are indicated in orange. \* $P < 0.05$ , \*\* $P < 0.01$ .

By operating at the level of skeletal muscle, NIRS is obviously relevant for interventions that directly target skeletal muscle mitochondria, such as endurance exercise (95). However, besides being useful for studying exercise-induced improvements in skeletal muscle mitochondrial capacity, NIRS may also be relevant for monitoring effects of nutrient (96) or pharmaceutical interventions (97) and to study the decline in skeletal muscle mitochondrial capacity in response to alternative physiological factors, such as physical inactivity (98) or ageing (99,100), as well as to disease pathologies (90), such as type 2 diabetes (101) and COPD (102). Thus, NIRS is a relevant technique to monitor skeletal muscle mitochondrial function as a biomarker in the trajectory from optimal healthy physiologies to impaired physiologies, and ultimately to disease.

## Vitamin B2 status determination in exercise studies

In this thesis, we demonstrated that vitamin B2 status, as determined by the erythrocyte glutathione reductase coefficient (EGRAC), was not different between high-fit and low-fit females and was not impacted by a single recent bout of exercise ([Chapter 7](#)). Although the EGRAC remained unchanged after exercise, we showed that EGR enzymatic activity increased post-exercise, suggesting that short-term exercise could influence EGR activity without affecting its saturation with FAD. From the biomarker perspective, the latter finding could call into question whether vitamin B2 status was truly unaffected in our study population, or whether we were not able to detect a potential change in vitamin B2 demand using the EGRAC. In general, FAD and FMN are not covalently bound to flavoproteins (103). Nevertheless, their anchoring into flavoproteins to support redox reactions is strong (103). This also holds for EGR; FAD is not dissociated from EGR after each GSSG oxidation cycle, but remains tightly bound (104–106). Therefore, temporal upregulation of EGR activity, which can occur during exercise-induced ROS production (107) may accelerate FAD recycling without necessarily increasing FAD usage. This mechanism could possibly explain why we observed increased EGR activity, but a similar EGRAC after the recent exercise bout in our study ([Chapter 7](#)).

On the other hand, increased FAD usage, i.e., FAD consumption, may be a consequence of regular aerobic exercise performance, since this can enhance *de novo* flavoprotein synthesis (108,109). For example, increased levels of succinate dehydrogenase (complex II), alpha-ketoglutarate dehydrogenase, and acyl-CoA dehydrogenase have been found in skeletal muscle mitochondria after aerobic exercise training (108,109). Since these flavoproteins must incorporate FAD to

increase their catalytic activity, extracellular FAD levels will decrease if FAD is not synthesized *de novo*, which could in turn decrease plasma FAD levels and ultimately lower vitamin B2 status. Thus, due to the assumed difference between short- and long-term exercise effects on EGR and FAD physiologies, the EGRAC was hypothesized to respond to regular exercise training. Yet, reported in this thesis ([Chapter 7](#)), and in other studies in young healthy adults, no link between fitness level and EGRAC was found. Currently, we still do not completely understand whether there is truly no effect of exercise on FAD/FMN levels and vitamin B2 status, or whether there is an effect, but it is difficult to detect in healthy individuals with the EGRAC method. This could be because the EGRAC has some technical limitations (110) that may impact its sensitivity to detect small differences in vitamin B2 status, such as differences induced by regular exercise. Therefore, to study exercise-induced differences on vitamin B2 status, although the EGRAC is considered the golden standard for long-term vitamin B2 status (111), alternative methods may be more appropriate.

The currently suggested alternative vitamin B2 status biomarker includes determination of vitamin B2 levels in 24-hour urine, which is more demanding than a single blood sample, and requires estimation of vitamin B2 intake because urinary vitamin B2 excretion levels are based on vitamin B2 intake minus use (111). Recently, the pyridoxamine phosphate oxidase (PPO) activation coefficient (PPOAC) has been proposed as an alternative enzymatic determination of vitamin B2 status (112). PPO is a FMN-dependent flavoenzyme that converts pyridoxine and pyridoxamine (vitamin B6) to the bioactive form of vitamin B6, pyridoxal phosphate (PLP) (112). PLP is required as a cofactor for enzymes that are involved in protein metabolism and glycogen breakdown, metabolic processes that are also enhanced during exercise (113,114). Although it is interesting to study whether the PPOAC can detect exercise-induced alterations in vitamin B2 status, it seems to respond like EGRAC (112). Furthermore, the PPOAC may partially depend on vitamin B6 status, since the plasma PLP level is the recommended vitamin B6 status biomarker (115). Therefore, it is relevant to consider alternative approaches that may be more suitable for detecting small differences in vitamin B2 status between healthy individuals.

As a starting point, it would be interesting to identify the metabolic enzymes that are the first being affected by subtle alterations in vitamin B2 availability, since these enzymes will likely also be the first to be affected by exercise-induced changes in FAD consumption. Currently, most available studies have focused on severe vitamin B2 deficiency, yet they demonstrate that vitamin B2 can act as a regulator of tissue protein abundancies (116). For example, vitamin B2 deficiency

has been linked to a significant reduced abundance of multiple flavoproteins, especially some involved in fatty acid  $\beta$ -oxidation, the TCA cycle, the mitochondrial ETS, and iron metabolism in the human liver cell line HepG2 (117), like what has been demonstrated in the liver proteome of Pekin ducks (118) and rats (119). Hence, it is of interest to study which flavoenzymes are most sensitive to a marginal vitamin B2 deficiency in red blood cells, PBMCs, platelets or whole blood. Once the most sensitive flavoenzymes have been identified, the protein expression of these enzymes in blood cells should be measured, followed by studies that investigate whether these enzymes could be useful biomarkers to predict vitamin B2 status. These studies may ultimately lead to the development of a biomarker that is suitable to study small, but physiologically relevant changes in vitamin B2 status in healthy individuals.

## Functional mapping of human physiological health

### Alternative blood-based biomarker tissues for characterizing human physiological health

In this thesis, PBMCs were studied as a non-invasive blood-based biomarker tissue, but alternative circulating blood components, such as red blood cells, platelets, and extracellular vesicles (EVs), also carry relevant information on human physiological health. For example, platelets have received special interest in biomarker research in disease conditions (84,120). Platelets are the tiny, anucleated blood cells that contain a relatively small number of mitochondria, yet these mitochondria are fully operational and show high rates of ATP turnover (84,121). Indeed, platelet mitochondrial function has been studied as a biomarker in multiple disease pathologies (120), although they are of particular interest for monitoring CVD management due to their primary role in blood coagulation (84). Interestingly, studies have demonstrated that platelet mitochondria also respond to exercise in healthy individuals (122,123) as well as patients suffering from various CVDs (124–126). Platelet mitochondrial respiration and function were enhanced after regular exercise training (122,124–126) as well as after short-term, yet extreme (duration ~12 hours) exercise (123). Mechanistically, exercise has been suggested to blunt the oxidative stress and ameliorate the hypoxia-induced mitochondrial dysfunction in platelets, which may contribute to a lower risk of developing CVD-related events such as thrombosis (122,125). Although both platelets and PBMCs ([Chapter 4](#)) could thus be useful biomarkers to monitor exercise interventions, the mechanisms that underpin the exercise-induced alterations are likely different. Platelets do not contain cell nuclei; hence the exercise-induced alterations cannot be established via epigenetic modifications as we described

above for PBMCs. In this regard, it has been suggested that the exercise-induced metabolic alterations in platelets are probably linked to improved ETS efficiency rather than increased mitochondrial biogenesis (122). Furthermore, platelets have a lifespan of approximately 10 days (127) and PBMCs include different immune cell subsets with lifespans ranging from one day to years (49,50). Hence, the way how platelet and PBMCs react to exercise may differ, depending on the (patho) physiological context. Examining whether platelet mitochondrial function could also be used to monitor other lifestyle interventions is therefore also of interest for future research.

Red blood cells have been extensively used for biomarker analysis in relation to disease but can also be relevant for health biomarker analysis. They are now mainly used for the determination of micronutrient status (111,115,128,129), including vitamin B2 status ([Chapter 7](#)). Recently the red blood cell (erythrocyte) plasma lipidome was also shown to reflect health status (130–133) and to be amendable to exercise (134) and dietary (135) lifestyle interventions. For example, higher erythrocyte levels of omega-6 PUFAs, which mediate pro-inflammatory responses, have been found in children with overweight and obesity as compared to their normal weight peers (130) as well as in sedentary as compared to exercise-trained rodents (134). This shows that erythrocytes can reflect metabolic signatures that are associated with inflammation, and is further supported by studies that have linked high omega-3 PUFA erythrocyte levels to improved metabolic health outcomes (132,133). Thus, although red blood cells lack mitochondria and a nucleus, they can reflect metabolic changes that are associated with improved or impaired physiological health.

Circulating EVs are another emerging option as blood-based biomarker source (136,137). They are shed from cells and have a role in intercellular communication (138). EVs can carry nucleic acids, (including RNAs, microRNAs, and DNA sequences), proteins, lipids, metabolites, and cell organelles that can stimulate signaling pathways or provide nutritional support to recipient cells (138). They are an emerging tool to follow the progression of multiple disease pathologies (136), and have been suggested as a promising source to monitor dietary intake (137) or exercise interventions (139). It has been suggested that unbalanced diets (e.g., high-fat diets) drive EV shedding to convey pro-inflammatory or pro-atherogenic signals, which may ultimately contribute to the increased risk for metabolic diseases such as type 2 diabetes and obesity (137). Indeed, overweight, obese and type 2 diabetic individuals display enhanced levels of multiple pro-inflammatory and pro-atherogenic EVs as compared to normal weight individuals (140–142), which can be lowered via dietary modifications, such as caloric restriction (141) or

increased intake of complex carbohydrates (143). Furthermore, EV shedding may also be triggered by exercise (144,145). For example, a single bout of exercise was shown to promote the release of EV from platelets, endothelial cells, and leukocytes (145). This exercise-induced EV release has been suggested to provide the multisystemic signalling between different tissues and cells, which subsequently mediates the acute physiological alterations to exercise, such as an increase in oxidative stress (145). Although the use of EV as a biomarker is currently in its infancy, its gaining traction because they provide a novel way of conveying fundamental information between cells and tissues. In the future, platelets, red blood cells, and EVs, may thus serve as novel biomarkers, or may serve to underpin health status and substantiate the health relevance of circulating metabolite and protein biomarkers.

### How circulating biomarkers can discriminate differences in health states

The data from [Chapter 5](#) offered valuable insights in the levels of multiple circulating metabolite and protein biomarkers in the context of physiological processes. Since these biomarkers, except for leptin, were similar between healthy females and multiple of these biomarkers are dysregulated during disease, our findings imply that this biomarker set is promising to monitor the trajectory from a healthy to an unhealthier or disease state. The functional classification of these biomarkers and the computation of an integrated biomarker score (also called multibiomarker panels (146)) may increase their predictive value. Still, the fact that these biomarkers were not linked to aerobic fitness level, while we have demonstrated in [Chapter 2](#) and [Chapter 4](#) that high-fit and low-fit females display physiologically relevant differences, may thus indicate that these biomarkers have difficulty in capturing early deviations from health, possibly unless the individual is challenged (147). Challenge tests can induce acute physiological perturbations, which could reveal differences that may be obscured during the steady state. They are especially attractive to monitor physiological responses in time, thereby measuring the capacity of physiological processes to return to homeostasis after a short-term perturbation, also called metabolic flexibility (148–151). Interestingly, it has recently been demonstrated that a standardized nutritional challenge, the phenotypic flexibility (“PhenFlex”) test, allowed for the discrimination of metabolic health levels of healthy individuals (148). Markedly different physiological responses in phenotypic flexibility between young individuals with low and normal body fat percentages and also between older individuals with normal to high body fat percentages were observed (148). Furthermore, similar nutritional challenges have also allowed for the discrimination of type 2 diabetic subjects from healthy individuals (149,151). Here, it was shown that the circulating biomarker levels after the nutritional challenge displayed a higher sensitivity as compared to fasting

circulating biomarker levels, which stressed the relevance of the challenge test (149). In addition to nutritional challenges, other challenge tests, such as acute physical exercise or cold stress are also relevant to consider, especially because these have also shown to increase metabolite variability in healthy individuals (150). Thus, challenge tests may provide additional insight in the interindividual variation in biomarker responses. It is unclear whether acute challenges would have revealed differences in biomarker responses between the high-fit and low-fit females in our study. Although the differences in body fat percentage between the high-fit and low-fit females in our study are very small as compared to the individuals in the study that showed differences in phenotypic flexibility between young individuals with low and normal body fat percentages (148), it cannot be excluded that the nutritional PhenFlex test would have revealed a difference, especially since we observed metabolic differences in the basal state in PBMCs (Chapter 4) and 21 hours post-exercise in lipid metabolic parameters (Chapter 5). Challenge test could thus help to provide a better discrimination of metabolic health in healthy individuals (147). To further advance the development of health-related biomarkers, it has been suggested to measure them longitudinally and on a regular basis. This would generate a timeline of an individual's health trajectory, and create a so-called 'biopassport' (146). The increased possibilities of self-sampling and digital monitoring during remote clinical trials and the increased use of smartphones and smartwatches during remote clinical trials could play a major role in accelerating such developments.

### Considering sex as a biological variable in scientific research

The research in this thesis was conducted in females, because females are under-represented in biomedical and exercise research (152,153), but are important to study because they represent 50% of the human population and may differ from males because of their differences in body composition (154) and metabolic health (155). We showed that NIRS was able to detect a similar physiological difference in skeletal muscle mitochondrial capacity between high-fit and low-fit females (Chapter 2) as was previously demonstrated in males (87) (Figure 2A). Furthermore, the differences in mitochondrial PBMC metabolism between high-fit and low-fit females (Chapter 4) were similar to the differences that we previously observed in our lab between high-fit and low-fit males (unpublished findings). The relative difference between high-fit and low-fit individuals in skeletal muscle mitochondrial capacity and PBMC mitochondrial function was thus highly similar between males and females, although the absolute values differed. It has been suggested to normalize  $\dot{V}O_{2\text{peak}}$  to lean body mass to account for the sex-associated difference in skeletal muscle metabolism (93,156). Although females indeed show proportionally higher adiposity levels than males of similar BMI (154) (Figure 2C, 2D), correcting

$\dot{V}O_{2\text{peak}}$  for lean body mass would likely have removed part of the aerobic fitness level effect, because the body fat percentages were also significantly different between high-fit and low-fit males and females (Figure 2C, 2D). Therefore, due to the primary interest of our study in the link between mitochondrial function and aerobic fitness,  $\dot{V}O_{2\text{peak}}$  was normalized to body weight rather than to lean body mass in our studies.

Sex-associated differences are not only important for the interpretation, validation, and generalizability of research findings, but should also be considered in the study design and data analysis (153,157). For example, in the 55 – 64 age range, men have more than double the rate of coronary heart disease (CHD) than women, while in the 85 – 94 age range, male CHD rates are only 10% higher than those in females (158). Thus, when researchers aim to study the incidence of CHD in a cohort of males and females aged 50, they should include more females to achieve equivalent statistical power in both sexes. Currently, most studies are underpowered to examine associations separately for males and females (157). This is particularly true for studies that were not powered to examine subgroup differences with sex as a biological variable, but analyze their data by sex in secondary analyses, which could result in false-negative results. Therefore, it is recommended to include both males and females and consider sex as a separate biological variable in the power calculation of studies (153,157). When the current scientific evidence primarily focuses on one sex and there is a lack of research in the other sex, researchers can also include either males or females to further substantiate the current findings, as shown in this thesis.

## Conclusions

Overall, the research conducted in this thesis showed that metabolic readouts in cells, tissues and blood can act as potential biomarkers of human physiological health. Mitochondrial metabolism in PBMCs was significantly higher in healthy females with high levels of aerobic fitness (high-fit females) than in healthy females with low levels of aerobic fitness (low-fit females), an effect that was unrelated to PBMC subset composition. Although the molecular mechanisms underpinning this effect must be identified, our findings imply that PBMC metabolism can imprint a physiologically relevant health difference. We also developed a novel normalization method that allowed for a more reliable estimation of metabolic PBMC function. Together these findings offer opportunities for the further development and validation of PBMC metabolism as a health biomarker. Besides PBMCs, skeletal muscle was also shown to reflect a difference in aerobic fitness level. NIRS-derived

mitochondrial capacity was significantly higher in the *gastrocnemius* muscle of high-fit compared to low-fit females, which indicates that measuring skeletal muscle mitochondrial capacity using NIRS could be also a relevant technique for monitoring human physiological health. Yet, at this point, the technical limitation of ATT must be overcome before NIRS can be widely applied in all study populations, including metabolically impaired females with higher body fat percentages. This thesis also demonstrated that the levels of multiple classical metabolite and protein biomarkers in plasma and serum were not significantly different between high-fit and low-fit females, but that evaluation of these biomarkers in the context of functional physiological health processes, i.e., a more integrated biomarker analysis, could be relevant for the characterization of human physiological health. Thus, mitochondrial PBMC metabolism, skeletal muscle mitochondrial capacity, and the integrated analysis of circulating biomarkers may act as potential novel biomarkers that reflect human physiological health (Figure 3). This thesis also described the relevance of B-vitamins in the signalling of mitochondria-derived metabolites to the cell nucleus, which further highlighted the crucial importance of B-vitamins for maintaining physiological health. In addition, we showed that vitamin B2 status was not different between high-fit and low-fit females, and we discussed the challenges for studying differences in vitamin B2 status between healthy individuals. Overall, this thesis contributed to a better understanding of human physiological health by functional metabolic mapping of healthy individuals with high and low levels of aerobic fitness. Metabolic readouts can allow for the quantification of physiological health states, and may be of great relevance for monitoring health improvement strategies in the future.

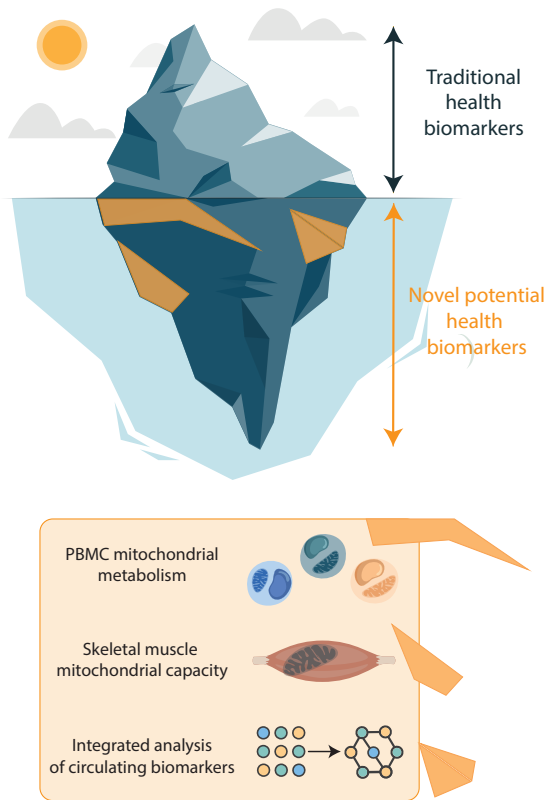


**Figure 3:** The concept of physiological health assessment that was studied in this thesis and that revealed PBMC mitochondrial metabolism, skeletal muscle mitochondrial capacity, and the integrated analysis of circulating biomarkers as new biomarkers for human physiological health.

## References

1. Ross R, Blair SN, Arena R, Church TS, Després J-P, Franklin BA, et al. Importance of Assessing Cardiorespiratory Fitness in Clinical Practice: A Case for Fitness as a Clinical Vital Sign: A Scientific Statement From the American Heart Association. *Circulation*. 2016 Dec;134(24):e653–99.
2. Arsenault BJ, Lachance D, Lemieux I, Alméras N, Tremblay A, Bouchard C, et al. Visceral adipose tissue accumulation, cardiorespiratory fitness, and features of the metabolic syndrome. *Arch Intern Med*. 2007 Jul;167(14):1518–25.
3. Kodama S, Saito K, Tanaka S, Maki M, Yachi Y, Asumi M, et al. Cardiorespiratory fitness as a quantitative predictor of all-cause mortality and cardiovascular events in healthy men and women: a meta-analysis. *JAMA*. 2009 May;301(19):2024–35.
4. Hargreaves M, Spriet LL. Skeletal muscle energy metabolism during exercise. *Nat Metab*. 2020;2(9):817–28.
5. McGee SL, Hargreaves M. Exercise adaptations: molecular mechanisms and potential targets for therapeutic benefit. *Nat Rev Endocrinol*. 2020;16(9):495–505.
6. Pedersen BK, Febbraio MA. Muscles, exercise and obesity: skeletal muscle as a secretory organ. *Nat Rev Endocrinol*. 2012;8(8):457–65.
7. Kujala UM, Vaara JP, Kainulainen H, Vasankari T, Vaara E, Kyröläinen H. Associations of Aerobic Fitness and Maximal Muscular Strength With Metabolites in Young Men. *JAMA Netw Open*. 2019 Aug 23;2(8):e198265–e198265.
8. Carrard J, Guerini C, Appenzeller-Herzog C, Infanger D, Königstein K, Streese L, et al. The Metabolic Signature of Cardiorespiratory Fitness: A Systematic Review. *Sports Medicine*. New Zealand; 2021.
9. Calder PC, Ahluwalia N, Albers R, Bosco N, Bourdet-Sicard R, Haller D, et al. A Consideration of Biomarkers to be Used for Evaluation of Inflammation in Human Nutritional Studies. *Br J Nutr*. 2013/01/23. 2013;109(S1):S1–34.
10. Garneau L, Parsons SA, Smith SR, Mulvihill EE, Sparks LM, Aguer C. Plasma Myokine Concentrations After Acute Exercise in Non-obese and Obese Sedentary Women. *Front Physiol*. 2020;11(February):1–8.
11. Jürimäe J, Vaiksaar S, Purge P. Circulating Inflammatory Cytokine Responses to Endurance Exercise in Female Rowers. *Int J Sports Med*. 2018 Dec;39(14):1041–8.
12. Ostrowski K, Rohde T, Asp S, Schjerling P, Pedersen BK. Pro- and anti-inflammatory cytokine balance in strenuous exercise in humans. *J Physiol*. 1999 Feb;515(Pt 1):287–91.
13. Schraner D, Kastenmüller G, Schönfelder M, Römisch-Margl W, Wackerhage H. Metabolite Concentration Changes in Humans After a Bout of Exercise: a Systematic Review of Exercise Metabolomics Studies. *Sport Med - Open*. 2020;6(1):11.
14. Gleeson M, Bishop NC, Stensel DJ, Lindley MR, Mastana SS, Nimmo MA. The anti-inflammatory effects of exercise: Mechanisms and implications for the prevention and treatment of disease. *Nat Rev Immunol*. 2011;11(9):607–10.
15. Schild M, Eichner G, Beiter T, Zügel M, Krumholz-Wagner I, Hudemann J, et al. Effects of Acute Endurance Exercise on Plasma Protein Profiles of Endurance-Trained and Untrained Individuals over Time. Galvez J, editor. *Mediators Inflamm*. 2016;2016:4851935.
16. Pournot H, Bieuzen F, Louis J, Fillard J-R, Barbiche E, Hausswirth C. Time-Course of Changes in Inflammatory Response after Whole-Body Cryotherapy Multi Exposures following Severe Exercise. *PLoS One*. 2011 Jul 28;6(7):e22748.
17. Stander Z, Luies L, Mienie LJ, Van Reenen M, Howatson G, Keane KM, et al. The unaided recovery of marathon-induced serum metabolome alterations. *Sci Rep*. 2020;10(1):11060.
18. Lehmann R, Zhao X, Weigert C, Simon P, Fehrenbach E, Fritsche J, et al. Medium Chain Acylcarnitines Dominate the Metabolite Pattern in Humans under Moderate Intensity Exercise and Support Lipid Oxidation. *PLoS One*. 2010 Jul 12;5(7):e11519.
19. Fiura-Luces C, Santos-Lozano A, Joyner M, Carrera-Bastos P, Picazo O, Zugaza JL, et al. Exercise benefits in cardiovascular disease: beyond attenuation of traditional risk factors. *Nat Rev Cardiol*. 2018;15(12):731–43.

20. He F, Li J, Liu Z, Chuang C-C, Yang W, Zuo L. Redox Mechanism of Reactive Oxygen Species in Exercise. *Front Physiol.* 2016 Nov 7;7:486.
21. Ip WKE, Hoshi N, Shouval DS, Snapper S, Medzhitov R. Anti-inflammatory effect of IL-10 mediated by metabolic reprogramming of macrophages. *Science.* 2017 May 5;356(6337):513–9.
22. Wang P, Wu P, Siegel MI, Egan RW, Billah MM. IL-10 inhibits transcription of cytokine genes in human peripheral blood mononuclear cells. *J Immunol.* 1994 Jul;153(2):811–6.
23. O'Neill LAJ, Kishton RJ, Rathmell J. A guide to immunometabolism for immunologists. *Nat Rev Immunol.* 2016;16(9):553–65.
24. Felipe V-P, Qian F, J. MI, L. GE, A. FK, Rui Y, et al. IL-6 enhances CD4 cell motility by sustaining mitochondrial Ca<sup>2+</sup> through the noncanonical STAT3 pathway. *Proc Natl Acad Sci.* 2021 Sep 14;118(37):e2103444118.
25. van der Windt GJW, Everts B, Chang C-H, Curtis JD, Freitas TC, Amiel E, et al. Mitochondrial Respiratory Capacity Is a Critical Regulator of CD8<sup>+</sup> T Cell Memory Development. *Immunity.* 2012; 36(1):68–78.
26. Nadeau L, Patten DA, Caron A, Garneau L, Pinault-Masson E, Foretz M, et al. IL-15 improves skeletal muscle oxidative metabolism and glucose uptake in association with increased respiratory chain supercomplex formation and AMPK pathway activation. *Biochim Biophys Acta - Gen Subj.* 2019; 1863(2):395–407.
27. Aguilar-Recarte D, Barroso E, Gumà A, Pizarro-Delgado J, Peña L, Ruart M, et al. GDF15 mediates the metabolic effects of PPAR $\beta$ / $\delta$  by activating AMPK. *Cell Rep.* 2021;36(6):109501.
28. Lantier L, Fentz J, Mounier R, Leclerc J, Treebak JT, Pehmøller C, et al. AMPK controls exercise endurance, mitochondrial oxidative capacity, and skeletal muscle integrity. *FASEB J.* 2014;28(7):3211–24.
29. Kleinert M, Clemmensen C, Sjøberg KA, Carl CS, Jeppesen JF, Wojtaszewski JFP, et al. Exercise increases circulating GDF15 in humans. *Mol Metab.* 2018;9:187–91.
30. Ost M, Igual Gil C, Coleman V, Keipert S, Efstathiou S, Vidic V, et al. Muscle-derived GDF15 drives diurnal anorexia and systemic metabolic remodeling during mitochondrial stress. *EMBO Rep.* 2020 Mar 4;21(3):e48804.
31. Jung S-B, Choi MJ, Ryu D, Yi H-S, Lee SE, Chang JY, et al. Reduced oxidative capacity in macrophages results in systemic insulin resistance. *Nat Commun.* 2018;9(1):1551.
32. Wischhusen J, Melero I, Fridman WH. Growth/Differentiation Factor-15 (GDF-15): From Biomarker to Novel Targetable Immune Checkpoint. Vol. 11, *Frontiers in Immunology.* 2020.
33. Liepinsh E, Makarova E, Plakane L, Konrade I, Liepins K, Videja M, et al. Low-intensity exercise stimulates bioenergetics and increases fat oxidation in mitochondria of blood mononuclear cells from sedentary adults. *Physiol Rep.* 2020 Jun;8(12):e14489.
34. Theall B, Stampley J, Cho E, Granger J, Johannsen NM, Irving BA, et al. Impact of acute exercise on peripheral blood mononuclear cells nutrient sensing and mitochondrial oxidative capacity in healthy young adults. *Physiol Rep.* 2021 Dec;9(23):166.
35. Dorneles GP, da Silva IM, Santos MA, Elsner VR, Fonseca SG, Peres A, et al. Immunoregulation induced by autologous serum collected after acute exercise in obese men: a randomized cross-over trial. *Sci Rep.* 2020;10(1):21735.
36. Radom-Aizik S, Zaldivar FJ, Leu S-Y, Adams GR, Oliver S, Cooper DM. Effects of exercise on microRNA expression in young males peripheral blood mononuclear cells. *Clin Transl Sci.* 2012 Feb;5(1):32–8.
37. Denham J, O'Brien BJ, Marques FZ, Charchar FJ. Changes in the leukocyte methylome and its effect on cardiovascular-related genes after exercise. *J Appl Physiol.* 2015 Feb;118(4):475–88.
38. Zhang D, Tang Z, Huang H, Zhou G, Cui C, Weng Y, et al. Metabolic regulation of gene expression by histone lactylation. *Nature.* 2019;574(7779):575–80.
39. Tesch PA, Daniels WL, Sharp DS. Lactate accumulation in muscle and blood during submaximal exercise. *Acta Physiol Scand.* 1982 Mar;114(3):441–6.
40. Hui S, Ghergurovich JM, Morscher RJ, Jang C, Teng X, Lu W, et al. Glucose feeds the TCA cycle via circulating lactate. *Nature.* 2017;551(7678):115–8.

41. Jin F, Li J, Guo J, Doeppner TR, Hermann DM, Yao G, et al. Targeting epigenetic modifiers to reprogramme macrophages in non-resolving inflammation-driven atherosclerosis. *Eur Hear J Open*. 2021 Sep 1;1(2):oeab022.
42. Ratter JM, Rooijackers HMM, Hooiveld GJ, Hijmans AGM, de Galan BE, Tack CJ, et al. In vitro and in vivo Effects of Lactate on Metabolism and Cytokine Production of Human Primary PBMCs and Monocytes. Vol. 9, *Frontiers in Immunology*. 2018.
43. Meijer K, de Vos P, Priebe MG. Butyrate and other short-chain fatty acids as modulators of immunity: what relevance for health? *Curr Opin Clin Nutr Metab Care*. 2010;13(6).
44. Mailing LJ, Allen JM, Buford TW, Fields CJ, Woods JA. Exercise and the Gut Microbiome: A Review of the Evidence, Potential Mechanisms, and Implications for Human Health. *Exerc Sport Sci Rev*. 2019 Apr;47(2):75–85.
45. Estaki M, Pither J, Baumeister P, Little JP, Gill SK, Ghosh S, et al. Cardiorespiratory fitness as a predictor of intestinal microbial diversity and distinct metagenomic functions. *Microbiome*. 2016;4(1):42.
46. Busquets-Cortés C, Capó X, Martorell M, Tur JA, Sureda A, Pons A. Training Enhances Immune Cells Mitochondrial Biosynthesis, Fission, Fusion, and Their Antioxidant Capabilities Synergistically with Dietary Docosahexaenoic Supplementation. *Oxid Med Cell Longev*. 2016;2016.
47. Busquets-Cortés C, Capó X, Martorell M, Tur JA, Sureda A, Pons A. Training and acute exercise modulates mitochondrial dynamics in football players' blood mononuclear cells. *Eur J Appl Physiol*. 2017 Oct;117(10):1977–87.
48. Liu D, Wang R, Grant AR, Zhang J, Gordon PM, Wei Y, et al. Immune adaptation to chronic intense exercise training: new microarray evidence. *BMC Genomics*. 2017 Jan 5;18(1):29.
49. Patel AA, Zhang Y, Fullerton JN, Boelen L, Rongvaux A, Maini AA, et al. The fate and lifespan of human monocyte subsets in steady state and systemic inflammation. *J Exp Med*. 2017/06/12. 2017 Jul 3;214(7):1913–23.
50. Sprent J. Lifespans of naive, memory and effector lymphocytes. *Curr Opin Immunol*. 1993;5(3):433–8.
51. McGee SL, Hargreaves M. Epigenetics and Exercise. *Trends Endocrinol Metab*. 2019;30(9):636–45.
52. Tarnowski M, Kopytko P, Piotrowska K. Epigenetic Regulation of Inflammatory Responses in the Context of Physical Activity. *Genes (Basel)*. 2021 Aug 25;12(9):1313.
53. Hartman M-L, Shirihaï OS, Holbrook M, Xu G, Kocherla M, Shah A, et al. Relation of mitochondrial oxygen consumption in peripheral blood mononuclear cells to vascular function in type 2 diabetes mellitus. *Vasc Med*. 2014 Feb;19(1):67–74.
54. Widlansky ME, Wang J, Shenouda SM, Hagen TM, Smith AR, Kizhakekuttu TJ, et al. Altered mitochondrial membrane potential, mass, and morphology in the mononuclear cells of humans with type 2 diabetes. *Transl Res*. 2010;156(1):15–25.
55. Tyrrell DJ, Bharadwaj MS, Van Horn CG, Marsh AP, Nicklas BJ, Molina AJA. Blood-cell bioenergetics are associated with physical function and inflammation in overweight/obese older adults. *Exp Gerontol*. 2015 Oct;70:84–91.
56. Monserrat-Mesquida M, Quetglas-Llabrés M, Bouzas C, Capó X, Mateos D, Ugarriza L, et al. Peripheral Blood Mononuclear Cells Oxidative Stress and Plasma Inflammatory Biomarkers in Adults with Normal Weight, Overweight and Obesity. *Antioxidants (Basel, Switzerland)*. 2021 May;10(5).
57. DeConne TM, Muñoz ER, Sanjana F, Hobson JC, Martens CR. Cardiometabolic risk factors are associated with immune cell mitochondrial respiration in humans. *Am J Physiol Circ Physiol*. 2020 Jul 17;319:H481–487.
58. Li P, Wang B, Sun F, Li Y, Li Q, Lang H, et al. Mitochondrial respiratory dysfunctions of blood mononuclear cells link with cardiac disturbance in patients with early-stage heart failure. *Sci Rep*. 2015;5(1):10229.
59. Stenlid R, Olsson D, Cen J, Manell H, Haglind C, Chowdhury AI, et al. Altered mitochondrial metabolism in peripheral blood cells from patients with inborn errors of  $\beta$ -oxidation. *Clin Transl Sci*. 2021 Aug;00:1–13.
60. Audano M, Pedretti S, Cermenati G, Brioschi E, Diaferia GR, Ghisletti S, et al. Zc3h10 is a novel mitochondrial regulator. *EMBO Rep*. 2018 Apr 1;19(4):e45531.

61. Lee H-T, Lin C-S, Pan S-C, Wu T-H, Lee C-S, Chang D-M, et al. Alterations of oxygen consumption and extracellular acidification rates by glutamine in PBMCs of SLE patients. *Mitochondrion*. 2019;44:65–74.
62. Araujo BG, Souza E Silva LF, de Barros Torresi JL, Siena A, Valerio BCO, Brito MD, et al. Decreased Mitochondrial Function, Biogenesis, and Degradation in Peripheral Blood Mononuclear Cells from Amyotrophic Lateral Sclerosis Patients as a Potential Tool for Biomarker Research. *Mol Neurobiol*. 2020 Dec;57(12):5084–102.
63. Ajaz S, McPhail MJ, Singh KK, Mujib S, Trovato FM, Napoli S, et al. Mitochondrial metabolic manipulation by SARS-CoV-2 in peripheral blood mononuclear cells of patients with COVID-19. *Am J Physiol Cell Physiol*. 2021 Jan;320(1):C57–65.
64. Grossmann V, Schmitt VH, Zeller T, Panova-Noeva M, Schulz A, Laubert-Reh D, et al. Profile of the Immune and Inflammatory Response in Individuals With Prediabetes and Type 2 Diabetes. *Diabetes Care*. 2015 Apr 15;38(7):1356–64.
65. Jagannathan-Bogdan M, McDonnell ME, Shin H, Rehman Q, Hasturk H, Apovian CM, et al. Elevated Proinflammatory Cytokine Production by a Skewed T Cell Compartment Requires Monocytes and Promotes Inflammation in Type 2 Diabetes. *J Immunol*. 2011;186(2):1162–72.
66. Shi LZ, Wang R, Huang G, Vogel P, Neale G, Green DR, et al. HIF1 $\alpha$ -dependent glycolytic pathway orchestrates a metabolic checkpoint for the differentiation of TH17 and Treg cells. *J Exp Med*. 2011 Jul;208(7):1367–76.
67. Michalek RD, Gerriets VA, Jacobs SR, Macintyre AN, MacIver NJ, Mason EF, et al. Cutting Edge: Distinct Glycolytic and Lipid Oxidative Metabolic Programs Are Essential for Effector and Regulatory CD4 + T Cell Subsets. *J Immunol*. 2011;186(6):3299–303.
68. Magkos F, Hjorth MF, Astrup A. Diet and exercise in the prevention and treatment of type 2 diabetes mellitus. *Nat Rev Endocrinol*. 2020;16(10):545–55.
69. Thyfault JP, Bergouignan A. Exercise and metabolic health: beyond skeletal muscle. *Diabetologia*. 2020;63(8):1464–74.
70. Chacko BK, Kramer PA, Ravi S, Johnson MS, Hardy RW, Ballinger SW, et al. Methods for defining distinct bioenergetic profiles in platelets, lymphocytes, monocytes, and neutrophils, and the oxidative burst from human blood. *Lab Invest*. 2013;93(6):690–700.
71. Ahl PJ, Hopkins RA, Xiang WW, Au B, Kaliaperumal N, Fairhurst A-M, et al. Met-Flow, a strategy for single-cell metabolic analysis highlights dynamic changes in immune subpopulations. *Commun Biol*. 2020;3(1):305.
72. Lee JW, Su Y, Baloni P, Chen D, Pavlovitch-Bedzyk AJ, Yuan D, et al. Integrated analysis of plasma and single immune cells uncovers metabolic changes in individuals with COVID-19. *Nat Biotechnol*. 2022;40(1):110–20.
73. Buck MD, Sowell RT, Kaech SM, Pearce EL. Metabolic Instruction of Immunity. *Cell*. 2017;169(4):570–86.
74. Reynés B, Priego T, Cifre M, Oliver P, Palou A. Peripheral Blood Cells, a Transcriptomic Tool in Nutrigenomic and Obesity Studies: Current State of the Art. *Compr Rev Food Sci Food Saf*. 2018 Jul;17(4):1006–20.
75. Caimari A, Oliver P, Rodenburg W, Keijer J, Palou A. Slc27a2 expression in peripheral blood mononuclear cells as a molecular marker for overweight development. *Int J Obes*. 2010;34(5):831–9.
76. Reynés B, García-Ruiz E, Palou A, Oliver P. The intake of high-fat diets induces an obesogenic-like gene expression profile in peripheral blood mononuclear cells, which is reverted by dieting. *Br J Nutr*. 2016 Jun;115(11):1887–95.
77. Costa A, Reynés B, Konieczna J, Martín M, Fiol M, Palou A, et al. Use of human PBMC to analyse the impact of obesity on lipid metabolism and metabolic status: a proof-of-concept pilot study. *Sci Rep*. 2021 Sep;11(1):18329.
78. de Mello VDF, Kolehmanien M, Schwab U, Pulkkinen L, Uusitupa M. Gene expression of peripheral blood mononuclear cells as a tool in dietary intervention studies: What do we know so far? *Mol Nutr Food Res*. 2012 Jul;56(7):1160–72.

79. Radler U, Stangl H, Lechner S, Lienbacher G, Krepp R, Zeller E, et al. A combination of ( $\omega$ -3) polyunsaturated fatty acids, polyphenols and L-carnitine reduces the plasma lipid levels and increases the expression of genes involved in fatty acid oxidation in human peripheral blood mononuclear cells and HepG2 cells. *Ann Nutr Metab.* 2011;58(2):133–40.
80. van Dijk SJ, Feskens EJM, Bos MB, de Groot LCPGM, de Vries JHM, Müller M, et al. Consumption of a high monounsaturated fat diet reduces oxidative phosphorylation gene expression in peripheral blood mononuclear cells of abdominally overweight men and women. *J Nutr.* 2012 Jul;142(7):1219–25.
81. Myhrstad MCW, de Mello VD, Dahlman I, Kolehmainen M, Paananen J, Rundblad A, et al. Healthy Nordic Diet Modulates the Expression of Genes Related to Mitochondrial Function and Immune Response in Peripheral Blood Mononuclear Cells from Subjects with Metabolic Syndrome-A SYSDIET Sub-Study. *Mol Nutr Food Res.* 2019 Apr;e1801405.
82. Kim M, Song G, Kang M, Yoo HJ, Jeong T-S, Lee S-H, et al. Replacing carbohydrate with protein and fat in prediabetes or type-2 diabetes: greater effect on metabolites in PBMC than plasma. *Nutr Metab (Lond).* 2016;13(1):3.
83. Calton EK, Keane KN, Soares MJ, Rowlands J, Newsholme P. Prevailing vitamin D status influences mitochondrial and glycolytic bioenergetics in peripheral blood mononuclear cells obtained from adults. *Redox Biol.* 2016;10:243–50.
84. Alfadni A, Riou M, Charles A-L, Meyer A, Barnig C, Andres E, et al. Peripheral Blood Mononuclear Cells and Platelets Mitochondrial Dysfunction, Oxidative Stress, and Circulating mtDNA in Cardiovascular Diseases. *J Clin Med.* 2020 Jan 22;9(2):311.
85. Li S, Sullivan NL, Roupheal N, Yu T, Banton S, Maddur MS, et al. Metabolic Phenotypes of Response to Vaccination in Humans. *Cell.* 2017;169(5):862–877.e17.
86. Rausser S, Trumpff C, McGill MA, Junker A, Wang W, Ho S-H, et al. Mitochondrial phenotypes in purified human immune cell subtypes and cell mixtures. Johnson SC, Akhmanova A, editors. *Elife.* 2021;10:e70899.
87. Lagerwaard B, Keijer J, McCully KK, de Boer VCJ, Nieuwenhuizen AG. In vivo assessment of muscle mitochondrial function in healthy, young males in relation to parameters of aerobic fitness. *Eur J Appl Physiol.* 2019;
88. Gallagher D, Heymsfield SB, Heo M, Jebb SA, Murgatroyd PR, Sakamoto Y. Healthy percentage body fat ranges: an approach for developing guidelines based on body mass index. *Am J Clin Nutr.* 2000 Sep;72(3):694–701.
89. Hesselink MKC, Schrauwen-Hinderling V, Schrauwen P. Skeletal muscle mitochondria as a target to prevent or treat type 2 diabetes mellitus. *Nat Rev Endocrinol.* 2016;12(11):633–45.
90. Adami A, Rossiter HB. Principles, insights, and potential pitfalls of the noninvasive determination of muscle oxidative capacity by near-infrared spectroscopy. *J Appl Physiol.* 2017 Jul 5;124(1):245–8.
91. van Beekvelt MC, Borghuis MS, van Engelen BG, Wevers RA, Colier WN. Adipose tissue thickness affects in vivo quantitative near-IR spectroscopy in human skeletal muscle. *Clin Sci (London, England).* 2001 Jul;101(1):21–8.
92. Guzman S, Ramirez J, Keslacy S, de Leon R, Yamazaki K, Dy C. Association between muscle aerobic capacity and whole-body peak oxygen uptake. *Eur J Appl Physiol.* 2020;120(9):2029–36.
93. Beever AT, Tripp TR, Zhang J, MacInnis MJ. NIRS-derived skeletal muscle oxidative capacity is correlated with aerobic fitness and independent of sex. *J Appl Physiol.* 2020 Sep;129(3):558–68.
94. McCully KK, Fielding RA, Evans WJ, Leigh JS, Posner JD. Relationships between in vivo and in vitro measurements of metabolism in young and old human calf muscles. *J Appl Physiol.* 1993 Aug 1;75(2):813–9.
95. Tonkonogi M, Sahlin K. Physical exercise and mitochondrial function in human skeletal muscle. *Exerc Sport Sci Rev.* 2002 Jul;30(3):129–37.
96. Grootswagers P, Smeets E, Oteng A-B, Groot L de. A novel oral nutritional supplement improves gait speed and mitochondrial functioning compared to standard care in older adults with (or at risk of) undernutrition: results from a randomized controlled trial. *Aging (Albany NY).* 2021 Apr;13(7):9398–418.

97. A.E. AN, Lando J, Thorben A, A.F. SA, J. RR, J.J. AW, et al. Moderate Intensity Exercise Training Improves Skeletal Muscle Performance in Symptomatic and Asymptomatic Statin Users. *J Am Coll Cardiol*. 2021 Nov 23;78(21):2023–37.
98. Ryan TE, Southern WM, Brizendine JT, McCully KK. Activity-induced changes in skeletal muscle metabolism measured with optical spectroscopy. *Med Sci Sports Exerc*. 2013 Dec;45(12):2346–52.
99. Lagerwaard B, Nieuwenhuizen AG, de Boer VCJ, Keijer J. In vivo assessment of mitochondrial capacity using NIRS in locomotor muscles of young and elderly males with similar physical activity levels. *GeroScience*. 2020;42(1):299–310.
100. Chung S, Rosenberry R, Ryan TE, Munson M, Dombrowsky T, Park S, et al. Near-infrared spectroscopy detects age-related differences in skeletal muscle oxidative function: promising implications for geroscience. *Physiol Rep*. 2018 Feb;6(3).
101. Pedersen BL, Bækgaard N, Quistorff B. Muscle Mitochondrial Function in Patients with Type 2 Diabetes Mellitus and Peripheral Arterial Disease: Implications in Vascular Surgery. *Eur J Vasc Endovasc Surg*. 2009 Sep 1;38(3):356–64.
102. Adami A, Corvino RB, Calmelat RA, Porszasz J, Casaburi R, Rossiter HB. Muscle Oxidative Capacity Is Reduced in Both Upper and Lower Limbs in COPD. *Med Sci Sport Exerc*. 2020 Oct;52(10):2061–8.
103. Martin C, Binda C, Fraaije MW, Mattevi A. Chapter Three - The multipurpose family of flavoprotein oxidases. In: Chaiyen P, Tamanoi FBT-TE, editors. *Flavin-Dependent Enzymes: Mechanisms, Structures and Applications*. Academic Press; 2020. p. 63–86.
104. Decker KF. Biosynthesis and Function of Enzymes with Covalently Bound Flavin. *Annu Rev Nutr*. 1993 Jul 1;13(1):17–41.
105. Schulz GE, Schirmer RH, Pai EF. FAD-binding site of glutathione reductase. *J Mol Biol*. 1982;160(2):287–308.
106. Berkholz DS, Faber HR, Savvides SN, Karplus PA. Catalytic cycle of human glutathione reductase near 1 Å resolution. *J Mol Biol*. 2008/07/07. 2008 Oct 3;382(2):371–84.
107. Ohno H, Sato Y, Yamashita K, Doi R, Arai K, Kondo T, et al. The effect of brief physical exercise on free radical scavenging enzyme systems in human red blood cells. *Can J Physiol Pharmacol*. 1986 Sep;64(9):1263–1265.
108. Holloszy JO. Biochemical Adaptations in Muscle: EFFECTS OF EXERCISE ON MITOCHONDRIAL OXYGEN UPTAKE AND RESPIRATORY ENZYME ACTIVITY IN SKELETAL MUSCLE. *J Biol Chem*. 1967 May 10;242(9):2278–82.
109. Holloszy JO, Oscai LB, Don LJ, Molé PA. Mitochondrial citric acid cycle and related enzymes: Adaptive response to exercise. *Biochem Biophys Res Commun*. 1970;40(6):1368–73.
110. Hill MHE, Bradley A, Mushtaq S, Williams EA, Powers HJ. Effects of methodological variation on assessment of riboflavin status using the erythrocyte glutathione reductase activation coefficient assay. *Br J Nutr*. 2008/12/23. 2008;102(2):273–8.
111. EFSA NDA Panel (EFSA Panel on Dietetic Products N and A. Scientific Opinion on Dietary Reference Values for riboflavin. *EFSA J*. 2017;15(8):4919.
112. Mushtaq S, Su H, Hill MHE, Powers HJ. Erythrocyte pyridoxamine phosphate oxidase activity: a potential biomarker of riboflavin status? *Am J Clin Nutr*. 2009 Nov 1;90(5):1151–9.
113. Depeint F, Bruce WR, Shangari N, Mehta R, O'Brien PJ. Mitochondrial function and toxicity: role of the B vitamin family on mitochondrial energy metabolism. *Chem Biol Interact*. 2006 Oct;163(1–2):94–112.
114. Manore MM. Vitamin B6 and exercise. *Int J Sport Nutr*. 1994 Jun;4(2):89–103.
115. EFSA NDA Panel (EFSA Panel on Dietetic Products N and A. Scientific Opinion on Dietary Reference Values for vitamin B6. *EFSA Journal*. 2016;14(6):4485.
116. Jeong H, Vacanti NM. Systemic vitamin intake impacting tissue proteomes. *Nutr Metab (Lond)*. 2020;17(1):73.
117. Xin Z, Pu L, Gao W, Wang Y, Wei J, Shi T, et al. Riboflavin deficiency induces a significant change in proteomic profiles in HepG2 cells. *Sci Rep*. 2017;7(45861):1–10.

118. Tang J, Hegeman MA, Hu J, Xie M, Shi W, Jiang Y, et al. Severe riboflavin deficiency induces alterations in the hepatic proteome of starter Pekin ducks. *Br J Nutr.* 2017;118(9):641–50.
119. Olpin SE, Bates CJ. Lipid metabolism in riboflavin-deficient rats: 2. Mitochondrial fatty acid oxidation and the microsomal desaturation pathway. *Br J Nutr.* 2007;03/09. 1982;47(3):589–96.
120. Zharikov S, Shiva S. Platelet mitochondrial function: from regulation of thrombosis to biomarker of disease. *Biochem Soc Trans.* 2013 Jan 29;41(1):118–23.
121. Garcia-Souza LF, Oliveira MF. Mitochondria: Biological roles in platelet physiology and pathology. *Int J Biochem Cell Biol.* 2014;50:156–60.
122. Wu LH, Chang SC, Fu TC, Huang CH, Wang JS. High-intensity Interval Training Improves Mitochondrial Function and Suppresses Thrombin Generation in Platelets undergoing Hypoxic Stress. *Sci Rep.* 2017;7(1):1–14.
123. Hoppel F, Calabria E, Pesta DH, Kantner-Rumplmair W, Gnaiger E, Bartscher M. Effects of Ultramarathon Running on Mitochondrial Function of Platelets and Oxidative Stress Parameters: A Pilot Study. Vol. 12, *Frontiers in Physiology.* 2021.
124. Chou C-H, Fu T-C, Tsai H-H, Hsu C-C, Wang C-H, Wang J-S. High-intensity interval training enhances mitochondrial bioenergetics of platelets in patients with heart failure. *Int J Cardiol.* 2019;274:214–20.
125. Hsu C-C, Tsai H-H, Fu T-C, Wang J-S. Exercise Training Enhances Platelet Mitochondrial Bioenergetics in Stroke Patients: A Randomized Controlled Trial. Vol. 8, *Journal of Clinical Medicine.* 2019.
126. Lin ML, Fu TC, Hsu CC, Huang SC, Lin YT, Wang JS. Cycling Exercise Training Enhances Platelet Mitochondrial Bioenergetics in Patients with Peripheral Arterial Disease: A Randomized Controlled Trial. *Thromb Haemost.* 2021;121(7):900–12.
127. LEEKSMA CHW, COHEN JA. Determination of the Life of Human Blood Platelets using Labelled Di-isopropylfluorophosphonate. *Nature.* 1955;175(4456):552–3.
128. EFSA NDA Panel (EFSA Panel on Dietetic Products N and A. Scientific Opinion on Dietary Reference Values for iron. *EFSA J.* 2015;13(10).
129. EFSA NDA Panel (EFSA Panel on Dietetic Products N and A. Scientific Opinion on Dietary Reference Values for cobalamin (vitamin B12). *EFSA J.* 2015;13(7):4150.
130. Jauregibeitia I, Portune K, Rica I, Tueros I, Velasco O, Grau G, et al. Fatty Acid Profile of Mature Red Blood Cell Membranes and Dietary Intake as a New Approach to Characterize Children with Overweight and Obesity. *Nutrients.* 2020 Nov;12(11).
131. Jauregibeitia I, Portune K, Rica I, Tueros I, Velasco O, Grau G, et al. Potential of Erythrocyte Membrane Lipid Profile as a Novel Inflammatory Biomarker to Distinguish Metabolically Healthy Obesity in Children. Vol. 11, *Journal of Personalized Medicine.* 2021.
132. Harris WS, Tintle NL, Etherton MR, Vasan RS. Erythrocyte long-chain omega-3 fatty acid levels are inversely associated with mortality and with incident cardiovascular disease: The Framingham Heart Study. *J Clin Lipidol.* 2018;12(3):718-727.e6.
133. Fontes JD, Rahman F, Lacey S, Larson MG, Vasan RS, Benjamin EJ, et al. Red blood cell fatty acids and biomarkers of inflammation: A cross-sectional study in a community-based cohort. *Atherosclerosis.* 2015;240(2):431–6.
134. Marini M, Abruzzo PM, Bolotta A, Veicsteinas A, Ferreri C. Aerobic training affects fatty acid composition of erythrocyte membranes. *Lipids Health Dis.* 2011;10(1):188.
135. Hodson L, Eyles HC, McLachlan KJ, Bell ML, Green TJ, Skeaff CM. Plasma and Erythrocyte Fatty Acids Reflect Intakes of Saturated and n–6 PUFA within a Similar Time Frame. *J Nutr.* 2014 Jan 1;144(1):33–41.
136. Mallocci M, Perdomo L, Veerasamy M, Andriantsitohaina R, Simard G, Martínez MC. Extracellular Vesicles: Mechanisms in Human Health and Disease. *Antioxid Redox Signal.* 2018 Mar 14;30(6):813–56.
137. Monfoulet L-E, Martinez MC. Dietary modulation of large extracellular vesicles: the good and the bad for human health. *Nutr Rev.* 2022 May 1;80(5):1274–93.
138. van Niel G, D'Angelo G, Raposo G. Shedding light on the cell biology of extracellular vesicles. *Nat Rev Mol Cell Biol.* 2018;19(4):213–28.

139. Denham J, Spencer SJ. Emerging roles of extracellular vesicles in the intercellular communication for exercise-induced adaptations. *Am J Physiol Metab.* 2020 Jun 30;319(2):E320–9.
140. Campello E, Zabeo E, Radu CM, Spiezia L, Gavasso S, Fadin M, et al. Hypercoagulability in overweight and obese subjects who are asymptomatic for thrombotic events. *Thromb Haemost.* 2015 Jan;113(1):85–96.
141. Murakami T, Horigome H, Tanaka K, Nakata Y, Ohkawara K, Katayama Y, et al. Impact of weight reduction on production of platelet-derived microparticles and fibrinolytic parameters in obesity. *Thromb Res.* 2007;119(1):45–53.
142. Li S, Wei J, Zhang C, Li X, Meng W, Mo X, et al. Cell-Derived Microparticles in Patients with Type 2 Diabetes Mellitus: a Systematic Review and Meta-Analysis. *Cell Physiol Biochem.* 2016;39(6):2439–50.
143. Zhang X, McGeoch SC, Megson IL, MacRury SM, Johnstone AM, Abraham P, et al. Oat-enriched diet reduces inflammatory status assessed by circulating cell-derived microparticle concentrations in type 2 diabetes. *Mol Nutr Food Res.* 2014 Jun;58(6):1322–32.
144. Frühbeis C, Helmig S, Tug S, Simon P, Krämer-Albers E-M. Physical exercise induces rapid release of small extracellular vesicles into the circulation. *J Extracell Vesicles.* 2015;4:28239.
145. Brahmner A, Neuberger E, Esch-Heisser L, Haller N, Jorgensen MM, Baek R, et al. Platelets, endothelial cells and leukocytes contribute to the exercise-triggered release of extracellular vesicles into the circulation. *J Extracell Vesicles.* 2019;8(1):1615820.
146. van Ommen B, Wopereis S. Next-Generation Biomarkers of Health. In: Nestlé Nutrition Institute Workshop Series. 2016. p. 25–33.
147. van Ommen B, Keijer J, Heil SG, Kaput J. Challenging homeostasis to define biomarkers for nutrition related health. *Mol Nutr Food Res.* 2009;53(7):795–804.
148. van den Broek TJ, Bakker GCM, Rubingh CM, Bijlsma S, Stroeve JHM, van Ommen B, et al. Ranges of phenotypic flexibility in healthy subjects. *Genes Nutr.* 2017;12:32.
149. Wopereis S, Stroeve JHM, Stafleu A, Bakker GCM, Burggraaf J, van Erk MJ, et al. Multi-parameter comparison of a standardized mixed meal tolerance test in healthy and type 2 diabetic subjects: the PhenFlex challenge. *Genes Nutr.* 2017;12:21.
150. Krug S, Kastenmüller G, Stücker F, Rist MJ, Skurk T, Sailer M, et al. The dynamic range of the human metabolome revealed by challenges. *FASEB J.* 2012;26(6):2607–19.
151. Agueusop I, Musholt PB, Klaus B, Hightower K, Kannt A. Short-term variability of the human serum metabolome depending on nutritional and metabolic health status. *Sci Rep.* 2020;10(1):16310.
152. Costello JT, Bieuzen F, Bleakley CM. Where are all the female participants in Sports and Exercise Medicine research? *Eur J Sport Sci.* 2014;14(8):847–51.
153. Clayton JA, Tannenbaum C. Reporting Sex, Gender, or Both in Clinical Research? *JAMA.* 2016 Nov 8;316(18):1863–4.
154. Wells JCK. Sexual dimorphism of body composition. *Best Pract Res Clin Endocrinol Metab.* 2007;21(3):415–30.
155. Pradhan AD. Sex Differences in the Metabolic Syndrome: Implications for Cardiovascular Health in Women. *Clin Chem.* 2014 Jan 1;60(1):44–52.
156. Cureton KJ. Matching of Male and Female Subjects Using VO2 max. *Res Q Exerc Sport.* 1981 May 1;52(2):264–8.
157. Rich-Edwards JW, Kaiser UB, Chen GL, Manson JE, Goldstein JM. Sex and Gender Differences Research Design for Basic, Clinical, and Population Studies: Essentials for Investigators. *Endocr Rev.* 2018 Aug 1;39(4):424–39.
158. Mosca L, Barrett-Connor E, Wenger NK. Sex/gender differences in cardiovascular disease prevention: what a difference a decade makes. *Circulation.* 2011 Nov;124(19):2145–54.





# APPENDICES

**Summary of main findings**

**Acknowledgements**

**About the author**

- Curriculum vitae
- List of publications
- Education and training activities



## Summary

Health optimization strategies aim to achieve or improve health. To monitor their effectiveness, we should be able to quantify physiological health using tools (biomarkers) that reflect different states of health. Health biomarkers should therefore allow for the detection of small but physiologically relevant health differences. Yet, the classical clinical diagnostic markers that are used to assess health have been extensively studied for detecting the difference between health and disease but are very limited in detecting differences between health states, since a functional, even suboptimal homeostasis tends to maintain these biomarkers within a certain range of values. These biomarkers will thus have difficulty capturing early deviations in the trajectory from a healthy toward an unhealthier state. Thus, to monitor the progression from health to optimized health conditions in humans and *vice versa*, biomarkers that respond to physiological differences in healthy individuals are needed. Metabolism is the fundament to all physiological processes in the human body and provides several readily measurable parameters that can be used for characterization of a healthy physiology. Therefore, in this thesis, the potential of metabolic readouts for the quantification of human physiological health was studied. These metabolic readouts were measured in healthy, young, adult females with high and low levels of aerobic fitness. A high aerobic fitness level, compared to a low aerobic fitness level, is associated with improved health outcomes and a reduced risk for the development of later life disease and can thus represent a healthier state. Females were studied because they are largely underrepresented in scientific research and may respond differently from males. Therefore, the **overall aim** of this thesis was to study how metabolic measurements in healthy females with high and low levels of aerobic fitness can contribute to a better understanding of human physiological health.

Since mitochondria are cellular organelles with a key role in energy metabolism, studying mitochondrial function parameters is of great relevance for characterization of human physiological health. Mitochondrial function is classically analyzed via *ex vivo* respirometry of tissues biopsies, but this is invasive and a burden for study subjects, and it requires fresh tissue and technical expertise. A technique that can assess mitochondrial function non-invasively is based on near-infrared spectroscopy (NIRS). It indirectly quantifies *in vivo* skeletal muscle mitochondrial capacity. Therefore, the **first aim** of this thesis was to study the link between skeletal muscle mitochondrial capacity and aerobic fitness level. In **Chapter 2** we demonstrated that mitochondrial capacity was significantly higher in the *gastrocnemius* muscle of high aerobically fit (high-fit) than low aerobically fit (low-fit)

females. NIRS can thus detect a physiologically relevant difference between healthy individuals with different aerobic capacities, hence NIRS is a relevant technique to monitor skeletal muscle mitochondrial function as a biomarker for human physiological health.

In addition to measuring mitochondrial capacity *in vivo* using NIRS, emerging evidence suggests that mitochondrial function of peripheral blood mononuclear cells (PBMC) may act as a novel health biomarker. Mitochondrial PBMC function can be analyzed *ex vivo* in a Seahorse extracellular flux (XF) analyzer, which concomitantly measures glycolysis and thus provides a proxy for total PBMC metabolic profiles. The **second aim** was to evaluate the potential of PBMC metabolism as a health biomarker. In **Chapter 3** we developed a normalization method based on brightfield imaging that improved the measurement, comparison, and extrapolation of PBMC metabolic XF analysis. **Chapter 4** showed that mitochondrial PBMC metabolism was higher in high-fit than low-fit females. Importantly, it was also demonstrated that these observations were unrelated to alterations in the PBMC subset composition, which was important due to the heterogeneity of PBMCs. Although the molecular mechanisms underpinning this effect have yet to be identified, our findings imply that PBMCs can imprint a physiologically relevant metabolic difference and are promising to monitor as a biomarker for human physiological health.

The **third aim** was to explore the relationship between systemic metabolism biomarkers and aerobic fitness level. Although these biomarkers will likely have difficulty capturing early deviations from a healthy state because a functional, even suboptimal homeostasis tends to maintain their levels within a certain range, most of these biomarkers have not been examined for their discriminative potential between different health states. We hypothesized that their sensitivity may increase if the joined response of multiple biomarkers is evaluated in the context of overarching physiological processes. In **Chapter 5** we found that the levels of these systemic biomarkers were similar between high-fit and low-fit females and that analyzing joined biomarker responses in the context of functional physiological processes could be relevant for the characterization of human physiological health. Moreover, we observed that a recent exercise bout significantly changed the levels of inflammatory and lipid-related biomarkers, indicating that exercise performance on the day prior to blood sampling should be prevented when aiming to study baseline biomarker levels.

B-vitamins are essential nutrients that support many metabolic enzymes, including the ones located in mitochondria. Importantly, mitochondria-derived metabolic

signals can actively communicate with the cell nucleus. In view of the essential role of B-vitamins in mitochondrial function, B-vitamins may also play a role in this mitochondria-to-nucleus communication, but an overview is lacking. The **fourth aim** was to describe the state-of-the-art on the role of B-vitamins in mitochondrial metabolism and the communication with the nucleus. **Chapter 6** described how B-vitamins could modulate the signaling of mitochondria-derived metabolites to the nucleus, further highlighting the crucial importance of B-vitamins for maintaining physiological health.

To maintain the cellular pool of B-vitamins and prevent deficiencies, sufficient intake of B-vitamins is important. However, it has been suggested that lifestyle activities, including regular exercise, may also affect the need and use of B-vitamins, particularly vitamin B2. Vitamin B2 status may thus change in regular exercising individuals with high levels of aerobic fitness. Therefore, the **final aim** of this thesis was to study the link between vitamin B2 status parameters and aerobic fitness level. **Chapter 7** demonstrated that vitamin B2 status was not different between high-fit and low-fit females. However, the metabolic enzyme that is used for this 'golden standard' vitamin B2 status determination was increased after a recent exercise bout. This sheds some doubt on whether this is the best manner to determine vitamin B2 status, at least to study exercise effects, and alternative measures may need to be developed to reliably determine exercise-induced vitamin B2 status in healthy individuals.

In **Chapter 8**, the main findings of the thesis, perspectives, and recommendations for future research are discussed. The main conclusion is that PBMC mitochondrial metabolism, skeletal muscle mitochondrial capacity, and the integrated analysis of systemic metabolic biomarkers are promising metabolic readouts to quantify physiological health states, and may be of great relevance for monitoring health improvement strategies in the future.



## Acknowledgements

This is it, the end of my thesis! After working on this thesis for almost five years, it was a great moment to finally hand in my thesis. A lot of people have been involved to get to this achievement, and I am grateful for everyone who supported me through the years of blood, sweat, tears and PBMCs. In this chapter I would like to give my gratitude to all of you.

Allereerst wil ik graag mijn (co-)promotoren bedanken: Jaap, Vincent, Huub en Joost. **Jaap**, bedankt voor al het vertrouwen dat je van begin af aan in mij hebt gehad. Samen met jouw creatieve ideeën en je kritische, maar constructieve feedback, heb je me geleerd om *out of the box* te denken en te groeien als wetenschapper. Ik waardeer alle tijd die je hebt vrijgemaakt om met me te sparren over wetenschappelijke vraagstukken en persoonlijke struikelblokken. **Vincent**, bedankt voor de mogelijkheden die jij mij hebt gegeven om dit PhD project op poten te zetten en alle steun tijdens de afgelopen jaren. Ik kijk met veel plezier terug op onze brainstormsessies! Jouw kritische blik op mijn onderzoeksresultaten, manuscripten, posters en presentaties hebben de kwaliteit ervan altijd weer naar een hoger niveau getild. Bedankt dat ik altijd bij je terecht kon met mijn vragen, en dat je me hebt laten uitgroeien van masterstudent naar wetenschapper. **Huub**, jouw immunologische kennis en input zijn ontzettend waardevol geweest voor de invulling van mijn project. Bedankt voor al jouw nieuwe ideeën en het enthousiasme waarmee je in dit gezamenlijk project bent gestapt. **Joost**, ik wil je bedanken voor alle ideeën die je hebt aangedragen en je waardevolle feedback. Met behulp van jouw input wist ik net wat beter de vertaalslag te maken naar de maatschappelijke impact van mijn onderzoek; iets wat ik graag meeneem naar de toekomst.

Furthermore, I would like to thank my PhD thesis committee: **Prof. Dr Renger Witkamp**, **Dr Jan van den Bossche**, **Dr Suzan Wopereis**, and **Prof. Dr Francisca Serra Vich**. Thank you for your time and effort to read my thesis and travel to Wageningen to discuss it with me. I would also like to thank WIAS, NWO and Human and Animal Physiology (H2020-EU 3.2.2.1/2 Preventomics GA 818318 grant) for the financial contribution that allowed me to conduct this research.

Ik wil alle BSc- en MSc studenten bedanken die onder mijn begeleiding aan hun thesis hebben gewerkt: **Martijn**, **Myrthe**, **Boudewijn**, **Rick**, **Maud**, **Camiel**, **Danny** en **Iduna**. Mijn humane studie had ik niet uit kunnen voeren zonder hulp van de B-MCORE squad! **Maud** en **Camiel**, bedankt voor de tientallen PBMC-isolaties, honderden celtellingen en eindeloze wachtstappen. Ik heb ontzettend genoten

van onze momenten in het celkweeklab en daarbuiten! **Rosanne**, bedankt voor jouw inzet tijdens het optimaliseren van de vitamine B2 status bepaling van de deelnemers, het vele pipetteren van monsters en de gastvrijheid waarmee je de deelnemers hebt ontvangen. **Iris**, **Sophie** en **Laura**: jullie werden dagelijks begeleid door Bart, maar de hoeveelheid VO<sub>2</sub>max testen die jullie hebben uitgevoerd, het aantal menstruatiecycli die jullie hebben geteld en de studiedagen die jullie soepel hebben laten verlopen zijn voor mij enorm waardevol geweest! Bedankt voor al jullie enthousiasme en inzet. Ik wens jullie allemaal veel geluk voor de toekomst! Ook wil ik **Henriëtte** en **Diana** van Humane Voeding bedanken voor het uitvoeren van alle bloedafnames van de deelnemers. Ik ben enorm dankbaar dat jullie zo flexibel waren en jullie uiterste best deden om te zorgen dat er op de juiste momenten geprikt werd!

Next, I would like to express my gratitude to my colleagues at HAP. **Irene** en **Corine**, bedankt dat jullie er altijd voor mij waren! Ik kon met elke vraag bij jullie terecht en jullie deur stond altijd open! De M&Ms, pepernoten en paaseieren maakten het ook wel lastig om níet binnen te lopen 😊. **Annelies**, jij stond altijd klaar om te helpen met (spoed)problemen op het lab! Dankzij jou heeft mijn humane studie op tijd kunnen starten en zijn er veel ad hoc problemen snel opgelost, dankjewel! En onze gezamenlijke liefde voor stroopwafelcake was toch wel een genietmoment tijdens de koffiepauzes. **Inge**, bedankt voor alle gezellige momenten binnen en buiten het lab! Ook was het fijn dat ik altijd bij je terecht kon om even te sparren over wetenschappelijke en niet-wetenschappelijke vragen, dankjewel daarvoor! **Jur**, het was leuk om mijn kennis over PBMCs met jou te delen, en ik hoop dat je de PBMC-lijn op het lab door blijft zetten! In addition, many thanks to **Marcel**, **Mel**, and **Melissa**, for always being available for technical questions, lab support, or just nice conversations during our coffee- and lunch breaks!

**Arie**, bedankt voor het meedenken over de opzet van mijn humane studie en de interpretatie van de resultaten. Jouw waardevolle feedback hebben me regelmatig een andere kijk op mijn resultaten of stukken gegeven, wat tot nieuwe inzichten heeft geleid. Hier heb ik veel van geleerd! **Silvie**, bedankt voor jouw luisterend oor, je adviezen, en het meedenken over mijn humane studie! Je hebt me ontzettend veel geleerd over het opzetten, uitvoeren en opschrijven van humaan onderzoek. **Katja**, bedankt voor het meedenken over de aanpak van vrouwen en hun hormonen in mijn onderzoek, en alle tips die je me hebt gegeven over het begeleiden van studenten. I also want to thank **Claudia**, **Deli**, **Evert**, **Gerwin**, **Sander**, **Sandra**, **Sarah**, **Werner**, and **Zhuohui** for your valuable questions and input during the Tuesday Morning presentations and of course all the nice coffee- and lunch breaks we shared together!

I would like to give a special thanks to my (former) PhD colleagues at HAP: **Andrea, Anna, Alexia, Bart, Cresci-Anna, Chris, Evelien, Eveline, Ferran, Jelle, Jeske, Jingyi, José, Liangyu, Lianne, Lonneke, Marjanne, Melissa, Natasja, Peixin, Qi, Sarmad, Taolin, Xi, Wenbiao**. I always enjoyed our coffee breaks, lunch breaks, campus walks, HAPpy dinners, and HAPpy (Sinterklaas) activities! You all made my time at HAP much more fun and were of great support during (sometimes) difficult periods. Thank you for that.

A special thanks to **Taolin, Bart**, and **Anna**: the Mito-crew! **Taolin**, you are one of the most dedicated researchers I have ever met. I enjoyed all moments we shared together! **Bart**, bedankt voor alle ins- en outs die je mij hebt geleerd over het uitvoeren van een humane studie en natuurlijk het gezamenlijk runnen van de B-MCORE studie! In tegenstelling tot jou ga ik het tellen van menstruatiecycli en onze vrijdagavond telefoontjes over ongestelde deelnemers wél heel erg missen; je gekookte eieren in Tupperware daarentegen minder 😊. **Anna**, mijn sparringsmaatje bij HAP: bedankt voor je luisterend oor en goede adviezen tijdens onze vele wandelingen, stikstofmomenten, Whatsapp-memes en bureaustoelgesprekken. Juist door onze totaal verschillende persoonlijkheden konden we elkaar denk ik goed aanvullen! Ik waardeer al die keren dat je me dwong om mijn perfectionisme los te laten. Voor mij was dat ontzettend moeilijk, maar zonder jouw adviezen was ik denk ik nog steeds bezig geweest met het uitlijnen van mijn grafieken 😊. Ook jouw lesjes Engels (ik kan niet beloven dat ik *signals* ooit correct ga uitspreken) kwamen goed van pas 😊. Ik voel me vereerd dat jij één van mijn paranimfen wilt zijn, en ik hoop dat we na onze PhD's lekker blijven afspreken!

**Mojtaba**, my closest PhD colleague at CBI: thank you for the opportunity to work together and for your valuable support during my PhD. I really enjoyed the nice coffee breaks and chats we had in- and outside the human lab! **Agustí**, I enjoyed your stay at HAP and thank you for your contribution to my research project. In addition, I want to thank **Klaas** from ADP for all his statistical advice and assistance with the data analysis of my human study.

Ik had mijn PhD niet kunnen volbrengen zonder de steun van mijn vrienden en alle leuke momenten die ik met hen heb beleefd. Zij hebben ervoor gezorgd dat ik even kon loskomen van mijn PhD, om vervolgens weer met frisse moed verder te gaan!

Allereerst wil ik mijn allerliefste vriendin **Lisanne** bedanken voor haar onvoorwaardelijke steun en vriendschap. Wat ben ik blij dat wij elkaar na de middelbare school weer hebben gevonden! Één blik is voor ons genoeg om elkaar te begrijpen en ik

geniet elke dag weer van onze (bel)wandelingen, koffie- en sportmomenten. Jouw glas is altijd halfvol en je denkt altijd in oplossingen, wat me enorm heeft geholpen, met name tijdens de laatste fase! Bedankt dat jij er áltijd voor me bent. Het was een enorme eer om bij de meest bijzondere momenten in jouw leven een speciaal plekje te hebben, en ik ben dan ook enorm trots dat jij vandaag mijn paranif bent! Lieve **Huub**, ik kan niet beloven dat het e-mailverkeer tussen mij en Lisanne zal afnemen 😊, maar ik hoop dat onze altijd gezellige borrels en etentjes het ruimschoots goedmaken! Ik ben ontzettend blij dat we in jouw Arend mijn promotie mogen vieren!

Lieve **Irini**, **Carmelita** en **Danitsja**, dank jullie wel voor de heerlijke weekenddagen waarin er veel te weinig tijd is om helemaal bij te kletsen met altijd lekker eten! Onze momenten samen voelen nog steeds als vanouds, ook al zijn we na onze bachelor Farmacie allemaal onze eigen weg ingeslagen. Jullie blijven voor altijd mijn lieve Utrecht vriendinnen en ik hoop dat we nog heel veel mooie momenten uit ons leven met elkaar gaan delen!

Lieve **Marlou**, wat ben ik blij dat wij elkaar hebben ontmoet tijdens onze thesis periode bij HAP. Vanaf het begin af aan hadden wij een klik en inmiddels begrijpen we elkaar als geen ander. Ik heb bewondering voor jouw doorzettingsvermogen om voor die PhD positie te blijven vechten, en jouw moed om je spullen te pakken en naar Zweden te verhuizen. Onze maandelijkse telefoontjes zijn inmiddels vaste prik, en ik hoop dat dat nog heel lang zo blijft!

Lieve **Christy**, bedankt voor de heerlijke lunchmomenten rondom Nijmegen, dagjes uit, weekendjes Maastricht en natuurlijk de FaceTime avonden als we elkaar al een tijd niet hebben gezien! Ik denk dat onze (semi) traumatiserende ervaring bij FA305 ons voor het leven verbonden heeft 😊. Dit heeft geresulteerd in vele leuke herinneringen in Utrecht, Wageningen, Nijmegen en Maastricht. Het maakt niet uit hoe vaak we elkaar zien, wij kunnen uren met elkaar kletsen zonder dat we er genoeg van krijgen. Dit is wat onze vriendschap zo bijzonder maakt, en ik geniet er elke keer weer van!

Lieve **Anne**, het moment dat wij elkaar ontmoeten bij de Introductieweek, tijdens dat hoorcollege over hoe een Nederlandse kringverjaardag in zijn werk gaat, zal ik nooit meer vergeten. Al gauw besloten we om dit te ontvluchten en samen op pad te gaan om Wageningen te verkennen. Bij jou op de Molenstraat was ik altijd welkom, voor een lach en een traan. Jij hebt mijn tijd in Wageningen extra bijzonder gemaakt en ik ben dan ook blij dat we elkaar jaarlijks blijven zien! Dan hebben we enorm veel bij te kletsen, en vooral ook bij te lachen, maar daar

kunnen we dan ook weer even op teren. Ik hoop dat we dit nog heel lang blijven doen!

Lieve **Schuumkes**, lieve **Anne G, Anne L, Iris, Mayke, Milou, Minou, Nienke, Lieke, Lotte H, Lotte J, Lynn** en **Tessa**. Dank jullie wel voor alle gezellige borrels, etentjes, kermissen en feestjes, en natuurlijk jullie interesse in mijn PhD leven! Ik geniet altijd van onze avonden samen en hoop dat ons nog vele mooie momenten staan te wachten! **Demi**, ik kijk met veel plezier terug op onze avonden samen koken, eten en cocktails drinken en hoop dat er nog vele zullen volgen samen met de mannen!

**Roland** en **Sabine**, bedankt voor jullie medeleven en bovenal begrip dat een PhD soms eindeloos lijkt te duren. Tijdens onze borrels en etentjes konden we het PhD leven altijd goed relativeren, en ik heb veel respect voor de manier waarop jullie beiden je promotie succesvol hebben afgerond! Onze momenten samen zijn soms schaars maar nóóit minder gezellig. Sabine, hoe is het mogelijk dat we exact op dezelfde datum en tijd aan het promoveren zijn?! Helaas kunnen we niet bij elkaars promotie aanwezig zijn, maar ik verheug me op het moment dat we onze mijlpalen gaan vieren! Ook kijk ik nu alweer uit naar ons volgend diner (zonder apenkoppenijs 😊), rijsttafels, of whiskey & gin avonden!

Ook wil ik graag **Pierre** en **Dorothe** bedanken voor jullie interesse in mijn onderzoek, de lieve kaartjes en berichtjes, en dat jullie altijd voor mij klaarstaan. Dit waardeer ik enorm! **Herman** en **Ankie**, bedankt dat ik altijd welkom ben ik Breda en me meteen onderdeel heb gevoeld van de RaLi's! Ik heb intens genoten van alle gezellige RaLi activiteiten waarbij zo veel gelachen en gekletst wordt dat ik überhaupt niet aan PhD problemen kon denken. Deze momenten zijn goud waard, en ik hoop dat er nog vele mogen volgen!

Ook de steun, interesse en liefde vanuit mijn familie is voor mij van onschatbare waarde geweest.

Lieve oom **Gerard**, bedankt dat u altijd het vertrouwen in mij en mijn wetenschappelijke carrière heeft gehad. Ik vind het een eer dat u vandaag samen met **Iselle** aanwezig bent om deze mooie dag met mij te vieren. Helaas kan mijn lieve peettante **Marga** dit niet meer meemaken, maar ik prijs me gelukkig dat ze samen met u aanwezig was op de dag dat ik mijn scriptieprijs ontving. Dit was een belangrijk opstapje richting deze PhD. Marga heeft mij het vertrouwen, de liefde en de kracht gegeven om voor deze promotie te vechten. Ook wil ik mijn allerleukste neven en nichten 'Janssen' bedanken: **Milou, Claire, Justin, Maxime,**

**Carlo, Bram** en **Arthur**: ik hoop dat er nog vele familiedagen zullen volgen waarbij we samen met alle partners het leven kunnen vieren!

Lieve peetoom **Hans**, bedankt dat je altijd meeleeft met mij en mijn onderzoek, en altijd voor me klaarstaat! Ik kijk uit naar vele kopjes koffie die we samen gaan drinken en bijzondere momenten die we met elkaar mogen vieren! Lieve **Sonja** en **Adriaan**, ik geniet altijd enorm van onze koffie- en theemomentjes, altijd met een heerlijk stukje gebak. Samen met **Alex** kunnen we uitgebreid bijkletsen en elkaar een dikke knuffel geven. Bedankt dat jullie deur altijd voor mij en Pim openstaat! **Peggy**, elke periode in mijn studietijd heb je erg met me meegeleefd en me regelmatig een hart onder de riem gestoken. Dankjewel daarvoor, ik hoop dat we elkaar na mijn PhD weer wat vaker gaan zien! Ook een shout-out naar **Ron, Frank** en **Twan**: het was en is altijd feest met jullie, en ik hoop dat we nog vele leuke feestjes met elkaar mogen meemaken!

Lieve **Ruud** en **Irma**, bij jullie heb ik me vanaf het allereerste moment enorm welkom gevoeld. Ik had me geen leukere en lievere schoonouders kunnen wensen! Bedankt voor jullie interesse in mijn onderzoek, steun en gezelligheid. Met heel veel plezier kijk ik terug op onze familiemomenten in Eindhoven, Zwolle, Ewijk, Limburg en Frankrijk. Jullie staan altijd voor ons klaar en wisten mijn gedachten altijd mooi af te leiden van mijn onderzoek. Ik kijk uit naar de nieuwe fase die komen gaat!

Lieve **Milou** en **Bart**, ook jullie hebben de afgelopen 4,5 jaar een plekje in mijn hart veroverd! Jullie lieve berichtjes, steun en gezellige familiemomenten hebben me geholpen om de boel wat vaker te relativeren! De komst van **Bram** heeft onze band extra bijzonder gemaakt. Ik ben vanaf nu een super trotse tante Jo en kan niet wachten op alle weekendjes weg, vakanties en feestdagen die we samen nog mogen vieren!

Lieve **Jules**, bedankt voor jouw onvoorwaardelijke steun (ook al ben je het niet altijd met me eens 😊) en dat ik altijd jouw kleine zus mag zijn. Jij hebt me regelmatig een terechte spiegel voorgehouden en geholpen om lastige momenten of gesprekken aan te gaan. Ik ben enorm trots dat jij mijn broer bent! Lieve **Ellis**, ik ben ontzettend blij dat jij Jules' leven bent ingestapt – ik had me geen leukere schoonzus kunnen wensen! Bedankt voor jouw interesse in mijn onderzoek en de leuke dingen die we samen al hebben ondernomen. Ik hoop dat we nog vele mooie momenten gaan beleven samen!

Lieve **mama** en **papa**, jullie onvoorwaardelijke liefde heeft mij door vele lastige periodes heen geholpen. Ook tijdens mijn PhD boden jullie áltijd een luisterend oor en vele knuffels, en lekker eten om weer op te laden voor nieuwe uitdagingen! Bedankt voor alles wat jullie voor ons doen en jullie onvoorwaardelijke steun en vertrouwen. Zonder jullie had ik dit niet kunnen bereiken! Samen met **Beau** gaan we nog vele mooie momenten beleven, en ik kijk uit naar de herinneringen die we als familie gaan maken.

Ik had deze PhD nooit succesvol kunnen afronden zonder de liefde van mijn leven: **Pim**. Bedankt voor jouw onvoorwaardelijke liefde en steun, en al jouw knuffels en geduld de afgelopen jaren! Jij was er om de pieken te vieren en de dalen te relativeren. Jij stimuleert me altijd om mijn ambities na te jagen en (soms moeilijke) keuzes te durven maken. Ik ben enorm dankbaar voor al het vertrouwen dat je altijd in mij hebt gehad! Jij bent de liefste en leukste vriend die ik me kan wensen en ik ben enorm trots dat ik jou straks de papa van ons aapje mag noemen! Ons veelbesproken 'leven na mijn PhD' gaat dan nu éindelijk beginnen 😊. Ik kijk uit naar een hele mooie toekomst samen en ik kan niet wachten om samen met jou een gezin te mogen vormen. Ik houd van jou! ❤️

Bedankt allemaal, *Hora est!*



## Curriculum vitae



Joëlle Jeanine Elise Janssen was born on the 12<sup>th</sup> of November 1992 in Nijmegen, the Netherlands. In 2011, she completed her pre-university education at the Stedelijk Gymnasium Nijmegen. Pursuing her interest for human health and disease, she started the BSc program Pharmacy at Utrecht University, with a minor in Nutrition and Pharma. She received her BSc diploma in 2014. Joëlle followed her passion for the role of nutrition in health optimization and disease prevention, and in 2015 she enrolled in the MSc program Nutrition and Health at Wageningen University, with a specialization in Molecular Nutrition and Toxicology. She conducted her MSc thesis in the Human and Animal Physiology chair group at Wageningen University in 2016 under the supervision of Dr Vincent de Boer and studied the role of essential amino acids in immune system regulation. Her MSc thesis was awarded with the Wageningen University Life Sciences Thesis Award 2016. Joëlle also enrolled in the Research Master Cluster and wrote a PhD proposal. She participated in the NWO-WIAS graduate program competition in 2016. She was the winner of this competition, which resulted in funding of her proposed PhD project. In 2017, she concluded her studies with an internship at the MRC Cancer Unit at Cambridge University in the United Kingdom under the supervision of Dr Christian Frezza and Dr Vincent Zecchini. During her intership, she studied the metabolic adaptations that occur during renal cancer. She graduated with a *cum laude* MSc degree in 2017.

Joëlle started her PhD project at Wageningen University in 2017. This PhD project was a collaboration between the Human and Animal Physiology and the Cell Biology and Immunology chair group and performed under the supervision of Prof. Dr Jaap Keijer, Prof. Dr Huub Savelkoul, Dr Vincent de Boer, and Prof. Dr Joost van Neerven. Her work focused on metabolic measurements in healthy individuals for a better understanding of human physiological health. During her PhD, Joëlle successfully participated in the educational program of the Graduate School WIAS and presented her results at national and international meetings. Next to her PhD research, Joëlle was an active member of the WIAS PhD council to represent the interests and concerns of PhD students. She was also actively involved in the teaching activities of the chair group and supervised several MSc and BSc students.



## List of publications

### Peer-reviewed publications

**Joëlle J.E. Janssen**, Sander Grefte, Jaap Keijer, Vincent C.J. de Boer. (2019). Mito-nuclear communication and its regulation by B-vitamins. *Front. Physiol*, 10:78. doi: 10.3389/fphys.2019.00078.

Annelieke S. Wentzel, **Joëlle J.E. Janssen**, Vincent C.J. de Boer, Wouter G. van Veen, Maria Forlenza, Geert F. Wiegertjes. (2020). Fish macrophages show distinct metabolic signatures upon polarization. *Front Immunol*, 11:152. doi: 10.3389/fimmu.2020.00152.

**Joëlle J.E. Janssen**, Bart Lagerwaard, Annelies Bunschoten, Huub F.J. Savelkoul, R.J. Joost van Neerven, Jaap Keijer, Vincent C.J. de Boer. (2021). Novel standardized method for extracellular flux analysis of oxidative and glycolytic metabolism in peripheral blood mononuclear cells. *Sci Rep*, 11(1):1662. doi: 10.1038/s41598-021-81217-4.

Bart Lagerwaard, **Joëlle J.E. Janssen**, Iris Cuijpers, Jaap Keijer, Vincent C.J. de Boer, Arie G. Nieuwenhuizen. (2021). Muscle mitochondrial capacity in high- and low-fitness females using near-infrared spectroscopy. *Physiol Rep*, 9(9):e14838. doi: 10.14814/phy2.14838.

**Joëlle J.E. Janssen**, Bart Lagerwaard, Arie G. Nieuwenhuizen, Silvie Timmers, Vincent C.J. de Boer, Jaap Keijer. (2021). The effect of a single bout of exercise on vitamin B2 status is not different between high-fit and low-fit females. *Nutrients*, 13(11):4097. doi: 10.3390/nu13114097.

**Joëlle J.E. Janssen**, Bart Lagerwaard, Mojtaba Porbahaie, Arie G. Nieuwenhuizen, Huub F.J. Savelkoul, R.J. Joost van Neerven, Jaap Keijer, Vincent C.J. de Boer. (2022). Extracellular flux analyses reveal differences in mitochondrial PBMC metabolism between high-fit and low-fit females. *Am J Physiol Endocrinol Met*, 322(2):E141-E153. doi:10.1152/ajpendo.00365.2021.

### Expected publications

**Joëlle J.E. Janssen**, Bart Lagerwaard, Arie G Nieuwenhuizen, Xavier Escoté, Núria Canela, Josep M. del Bas, Vincent C.J. de Boer, Jaap Keijer. Single and joined behaviour of circulating biomarkers in high-fit and low-fit healthy females. *Submitted*.



## Education and training activities

### The Basic Package – 3.0 ECTS

WIAS Introduction Day	Wageningen, NL
Course on philosophy of science and/or ethics	Wageningen, NL
Course on essential skills	Wageningen, NL

### Disciplinary Competences – 12.0 ECTS

Writing a PhD proposal	Wageningen, NL
Laboratory Animal Sciences	Wageningen, NL
Agilent Seahorse XF Users' Group Meeting:	
Measure What is Important to Your Cell	Freiburg, DE
Mitochondrial Physiology, from Organelle to Organism	Copenhagen, DK
Mechanisms of Metabolic Signaling	New York, USA (virtual)

### Presentation Skills – 4.0 ECTS

WIAS Science Day 2018, poster presentation	Wageningen, NL
Mitochondrial Physiology, from Organelle to Organism, oral presentation	Copenhagen, DK
WIAS Annual Conference 2020, poster presentation	Lunteren, NL
Mechanisms of Metabolic Signaling, poster presentation	New York, USA (virtual)

### Teaching Competences – 6.0 ECTS

Supervision practicals Nutritional Aspects of Food (FCH-11306)	
Supervision practicals Human and Animal Biology 2 (HAP-20306)	
Supervision practicals Integrated Human Physiology (HAP-21303)	
Tutoring course Research Methodology for Nutrition and Health I (HNE-25806)	
Tutoring course Research Methodology for Nutrition and Health II (HNE-26206)	
Supervising MSc and BSc thesis students	

## Colophon

The Netherlands Organization for Scientific Research (NWO) and the Wageningen Institute for Animal Sciences (WIAS) are acknowledged for providing the NWO-WIAS Graduate Program grant 2016 for financial contribution to the author of this thesis. Financial support from Human and Animal Physiology, Agilent and BioSPX for printing this thesis is gratefully acknowledged.

### **Cover design, lay-out and print**

Promotie in Zicht ([www.promotie-inzicht.nl](http://www.promotie-inzicht.nl))



